

**IMPROVING THE SYNTHETIC COEFFICIENT OF
VARIATION CHART BY INCORPORATING SIDE
SENSITIVITY**

LEE PING YIN

**SCHOOL OF MATHEMATICAL SCIENCES
SUNWAY UNIVERSITY
MALAYSIA**

2024

**IMPROVING THE SYNTHETIC COEFFICIENT OF
VARIATION CHART BY INCORPORATING SIDE
SENSITIVITY**

LEE PING YIN

**THESIS SUBMITTED IN FULFILMENT OF
THE REQUIREMENTS FOR THE DEGREE OF
DOCTOR OF PHILOSOPHY IN MATHEMATICAL
SCIENCES**

**SCHOOL OF MATHEMATICAL SCIENCES
SUNWAY UNIVERSITY
MALAYSIA**

2024

ORIGINAL LITERARY WORK DECLARATION

Name of Candidate : **Lee Ping Yin**

IC / Passport No : **850903-14-5448**

Student ID : **19117886**

Name of Degree : **PHD in Mathematical Sciences**

Title of Project Paper/Research Report/Dissertation/Thesis ("this Work"):

Improving The Synthetic Coefficient of Variation Chart By Incorporating Side Sensitivity

I do solemnly and sincerely declare that:

1. I am the sole author/writer of this Work;
2. This Work is original;
3. Any use of any work in which copyright exists was done by way of fair dealing and for permitted purposes and any excerpt or extract from, or reference to or reproduction of any copyright work has been disclosed expressly and sufficiently and the title of the Work and its authorship have been acknowledged in this Work;
4. I do not have any actual knowledge nor do I ought reasonably to know that the making of this work constitutes an infringement of any copyright work;
5. I hereby assign all and every right in the copyright to this Work to the Sunway University (SunU), who henceforth shall be owner of the copyright in this Work and that any reproduction or use in any form or by any means whatsoever is prohibited without the written consent of Sunway University having been first had and obtained;
6. I am fully aware that if in the course of making this Work I have infringed any copyright whether intentionally or otherwise, I may be subject to legal action or any other action as may be determined by Sunway University.



Candidate's Signature

Date: 2/5/2024

Subscribed and solemnly declared before,



Witness's Signature

Date: 3/5/2024

Name : **Yeong Wai Chung**
Designation : **Associate Professor**

**Witness will be the supervisor*

(This form to be attached together with the final hardbound thesis)

IMPROVING THE SYNTHETIC COEFFICIENT OF VARIATION CHART BY INCORPORATING SIDE SENSITIVITY

ABSTRACT

The control chart is recognized as a crucial technique in Statistical Process Control. However, due to inconsistencies in the mean (μ) and/or standard deviation (σ) of some processes, traditional control charts monitoring the mean or standard deviation become inappropriate in such situations. Therefore, monitoring the coefficient of variation (γ) is selected as an alternative and it has been implemented in numerous industries, for example, in human and public sciences, environmental research, agricultural sciences, engineering, technology, finance and education. The synthetic chart that monitors the coefficient of variation, namely the synthetic- γ chart, is a widely used control chart. Unlike the Shewhart- γ chart, the synthetic- γ chart does not immediately signal an out-of-control condition when a sample coefficient of variation ($\hat{\gamma}$) appears in the non-conforming region, i.e. the region below the lower control limit (LCL) or the region above the upper control limit (UCL). Instead, it waits until a second sample coefficient of variation to appear in the non-conforming region, and if these successive points are close to each other, it generates an out-of-control signal. In the existing literature, the synthetic- γ chart performs better than the Shewhart- γ chart at the same rate of false alarms, as waiting for the second sample coefficient of variation to appear in the non-conforming region allows for the adoption of tighter control limits without increasing the false alarm rate. However, the existing synthetic- γ chart treats all points falling below the LCL or above the UCL as non-conforming samples. A side-sensitive synthetic- γ chart is proposed in this thesis in order to monitor the coefficient of variation, where the non-conforming samples must appear in the same non-conforming region, for instance, either

both samples must fall in the region above the UCL or both must fall in the region below the LCL , resulting in faster detection of out-of-control conditions. Markov chains are applied to compute various performance measures, for example, the Average Run Length (ARL), Standard Deviation of the Run Length ($SDRL$) and Expected Average Run Length ($EARL$). In order to evaluate the performance of the proposed chart accurately due to run lengths that may be skewed, the analysis of the entire run length distribution was conducted, together with the Median Run Length (MRL) and Expected Median Run Length ($EMRL$). Algorithms to obtain optimal chart parameters are also formulated. Based on the results obtained which had been validated using simulations, the proposed side-sensitive synthetic- γ chart outperformed the Shewhart- γ chart, the EWMA- γ^2 chart and the existing synthetic- γ chart without the side sensitivity feature for most cases and displayed a significant improvement. For instance, when $n=5$, $\tau=1.3$ and $\gamma_0=0.05$, the values of the ARL_1 and MRL_1 for the proposed chart were 10.18 and 4, respectively, whereas the values of the ARL_1 and MRL_1 were 30.61 and 14, respectively, for the Shewhart- γ chart, 11.80 and 9, respectively, for the EWMA- γ^2 chart, and 16.38 and 5, respectively, for the existing synthetic- γ chart. The proposed chart was further implemented on actual industrial data and compared with the same existing coefficient of variation charts, showed better efficiency in detecting out-of-control conditions.

Keywords – Average run length, Coefficient of variation, Median run length, Side-sensitive, Synthetic chart

(498 words)

ACKNOWLEDGEMENTS

First of all, I would like to thank God for giving me the strengths to complete this thesis within four and a half years as a part time student. It is truly a great blessing. Besides, I would like to extend my appreciation to my main supervisor, Associate Professor Dr Yeong Wai Chung and my co-supervisor, Associate Professor Leow Soo Kar. They have given me countless guidance and support throughout the journey. Whenever I face any difficulty in my study, either in writing the thesis or generating data using the software, ScicosLab, my supervisors are always there to help me. In addition, I also want to thank Sunway Education Group for providing full scholarship to me. Without this fund, I am not able to stand a chance to pursue my study for Phd in Mathematical Sciences. Lastly, I am deeply grateful to my husband, Chan Jin Swan, my son, Chan Kai Le, my immediate family, my in-law family, my director of programme, Ms Ruth Cheah, my subject leader, Mr Yong Yau, my colleagues and close friends who have encouraged and prayed for me since I enroll to this programme in January 2020. With all supports I receive, I manage to complete my thesis finally.

TABLE OF CONTENTS

Original Literary Work Declaration.....	ii
Abstract.....	iii
Acknowledgements.....	v
Table of Contents.....	vi
List of Tables.....	viii
List of Figures.....	xiv
List of Symbols and Abbreviations.....	xv
List of Appendices.....	xviii
CHAPTER 1: INTRODUCTION.....	1
1.0 Introduction.....	1
1.1 Background of the Thesis.....	1
1.2 Problem Statement.....	7
1.3 Scope of the Thesis.....	9
1.4 Research Questions.....	9
1.5 Research Objectives.....	10
1.6 Significance of the Thesis.....	10
1.7 Organization of the Thesis.....	11
CHAPTER 2: LITERATURE REVIEW.....	13
2.0 Introduction.....	13
2.1 Coefficient of Variation and Its Applications.....	13
2.2 Control Charts on Monitoring the Coefficient of Variation.....	18
2.3 Development of Synthetic Charts.....	31
2.4 Performance Measures of Control Charts.....	40

CHAPTER 3: METHODOLOGY	44
3.0 Introduction.....	44
3.1 Sample Coefficient of Variation's Distribution Properties	46
3.2 Shewhart- γ and EWMA- γ^2 Charts.....	49
3.3 Side-sensitive Synthetic- γ Chart.....	50
3.4 Performance Measures.....	55
3.5 Markov Chain Approach	56
3.6 <i>ARL</i> and <i>EARL</i> -based Designs	62
3.7 Run Length Distribution's Percentiles	67
3.8 <i>MRL</i> and <i>EMRL</i> -based Designs.....	69
CHAPTER 4: ANALYSIS AND INTERPRETATION OF RESULT	74
4.0 Introduction.....	74
4.1 <i>ARL</i> and <i>EARL</i> -based Designs	74
4.2 Analysis of Run Length Distribution's Percentiles	81
4.3 <i>MRL</i> and <i>EMRL</i> -based Designs.....	97
4.4 Comparison with Other Coefficient of Variation Charts.....	106
4.5 Implementation Based on Real Industrial Example	128
CHAPTER 5: CONCLUSION.....	135
5.0 Introduction.....	135
5.1 Discussion and Summary	135
5.2 Limitation of Research and Future Recommendation	138
References	140
List of Publications	151
Appendix	152

LIST OF TABLES

Table 2.1 Meta-analysis of coefficient of variation in different fields	16
Table 2.2 Meta-analysis of control chart monitoring coefficient of variation	28
Table 2.3 Classification of synthetic charts according to their use.....	39
Table 2.4 Usage of performance measures for control chart.....	43
Table 4.1 The optimal chart parameters (L , LCL , UCL) of the side-sensitive synthetic- γ chart and the corresponding ARL_1 and $SDRL_1$ for $n \in \{5, 7, 10, 15, 20\}$, $\tau \in \{1.1, 1.2, 1.3, 1.4, 1.5, 1.6, 1.7, 1.8, 1.9, 2.0\}$ and $\gamma_0 \in \{0.05, 0.10\}$	76
Table 4.2 The optimal chart parameters (L , LCL , UCL) of the side-sensitive synthetic- γ chart and the corresponding ARL_1 and $SDRL_1$ for $n \in \{5, 7, 10, 15, 20\}$, $\tau \in \{1.1, 1.2, 1.3, 1.4, 1.5, 1.6, 1.7, 1.8, 1.9, 2.0\}$ and $\gamma_0 \in \{0.15, 0.20\}$	77
Table 4.3 Optimal chart parameters (L , LCL , UCL) of the side-sensitive synthetic- γ chart and the corresponding $EARL_1$ for $n \in \{5, 7, 10, 15, 20\}$, $\gamma_0 \in \{0.05, 0.10, 0.15, 0.20\}$ and $(\tau_{\min}, \tau_{\max}) = (1, 2]$	80
Table 4.4 In-control percentiles of the run length distribution for the ARL -based side-sensitive synthetic- γ chart for $n \in \{5, 7, 10, 15, 20\}$, $\tau \in \{1.1, 1.2, 1.3, 1.4, 1.5, 1.6, 1.7, 1.8, 1.9, 2.0\}$ and $\gamma_0 = 0.05$	82
Table 4.5 In-control percentiles of the run length distribution for the ARL -based side-sensitive synthetic- γ chart for $n \in \{5, 7, 10, 15, 20\}$, $\tau \in \{1.1, 1.2, 1.3, 1.4, 1.5, 1.6, 1.7, 1.8, 1.9, 2.0\}$ and $\gamma_0 = 0.10$	84
Table 4.6 In-control percentiles of the run length distribution for the ARL -based side-sensitive synthetic- γ chart for $n \in \{5, 7, 10, 15, 20\}$, $\tau \in \{1.1, 1.2, 1.3, 1.4, 1.5, 1.6, 1.7, 1.8, 1.9, 2.0\}$ and $\gamma_0 = 0.15$	85

Table 4.7 In-control percentiles of the run length distribution for the *ARL*-based side-sensitive synthetic- γ chart for $n \in \{5, 7, 10, 15, 20\}$, $\tau \in \{1.1, 1.2, 1.3, 1.4, 1.5, 1.6, 1.7, 1.8, 1.9, 2.0\}$ and $\gamma_0 = 0.20$ 86

Table 4.8 Out-of-control percentiles of the run length distribution for the *ARL*-based side-sensitive synthetic- γ chart for $n \in \{5, 7, 10, 15, 20\}$, $\tau \in \{1.1, 1.2, 1.3, 1.4, 1.5, 1.6, 1.7, 1.8, 1.9, 2.0\}$ and $\gamma_0 = 0.05$ 87

Table 4.9 Out-of-control percentiles of the run length distribution for the *ARL*-based side-sensitive synthetic- γ chart for $n \in \{5, 7, 10, 15, 20\}$, $\tau \in \{1.1, 1.2, 1.3, 1.4, 1.5, 1.6, 1.7, 1.8, 1.9, 2.0\}$ and $\gamma_0 = 0.10$ 88

Table 4.10 Out-of-control percentiles of the run length distribution for the *ARL*-based side-sensitive synthetic- γ chart for $n \in \{5, 7, 10, 15, 20\}$, $\tau \in \{1.1, 1.2, 1.3, 1.4, 1.5, 1.6, 1.7, 1.8, 1.9, 2.0\}$ and $\gamma_0 = 0.15$ 89

Table 4.11 Out-of-control percentiles of the run length distribution for the *ARL*-based side-sensitive synthetic- γ chart for $n \in \{5, 7, 10, 15, 20\}$, $\tau \in \{1.1, 1.2, 1.3, 1.4, 1.5, 1.6, 1.7, 1.8, 1.9, 2.0\}$ and $\gamma_0 = 0.20$ 90

Table 4.12 In-control expected percentile of the run length distribution for the *EARL*-based side-sensitive synthetic- γ chart for $n \in \{5, 7, 10, 15, 20\}$, $\gamma_0 \in \{0.05, 0.10, 0.15, 0.20\}$ and $(\tau_{\min}, \tau_{\max}) = (1, 2]$ 95

Table 4.13 Out-of-control expected percentile of the run length distribution for the *EARL*-based side-sensitive synthetic- γ chart for $n \in \{5, 7, 10, 15, 20\}$, $\gamma_0 \in \{0.05, 0.10, 0.15, 0.20\}$ and $(\tau_{\min}, \tau_{\max}) = (1, 2]$ 95

Table 4.14 Optimal chart parameters and the corresponding l_{05} , MRL_1 , l_{95} , ARL_1 and ARL_0 for the *MRL*-based side-sensitive synthetic- γ chart for

$n \in \{5, 7, 10, 15, 20\}$, $\tau \in \{1.1, 1.2, 1.3, 1.4, 1.5, 1.6, 1.7, 1.8, 1.9, 2.0\}$ and $\gamma_0 = 0.05$ 99

Table 4.15 Optimal chart parameters and the corresponding l_{05} , MRL_1 , l_{95} , ARL_1 and ARL_0 for the *MRL*-based side-sensitive synthetic- γ chart for $n \in \{5, 7, 10, 15, 20\}$, $\tau \in \{1.1, 1.2, 1.3, 1.4, 1.5, 1.6, 1.7, 1.8, 1.9, 2.0\}$ and $\gamma_0 = 0.10$ 100

Table 4.16 Optimal chart parameters and the corresponding l_{05} , MRL_1 , l_{95} , ARL_1 and ARL_0 for the *MRL*-based side-sensitive synthetic- γ chart for $n \in \{5, 7, 10, 15, 20\}$, $\tau \in \{1.1, 1.2, 1.3, 1.4, 1.5, 1.6, 1.7, 1.8, 1.9, 2.0\}$ and $\gamma_0 = 0.15$ 101

Table 4.17 Optimal chart parameters and the corresponding l_{05} , MRL_1 , l_{95} , ARL_1 and ARL_0 for the *MRL*-based side-sensitive synthetic- γ chart for $n \in \{5, 7, 10, 15, 20\}$, $\tau \in \{1.1, 1.2, 1.3, 1.4, 1.5, 1.6, 1.7, 1.8, 1.9, 2.0\}$ and $\gamma_0 = 0.20$ 102

Table 4.18 Optimal chart parameters and the corresponding $E(l_{05})$, $EMRL_1$, $E(l_{95})$, $EARL$ and ARL_0 for the *EMRL*-based side-sensitive synthetic- γ chart for $n \in \{5, 7, 10, 15, 20\}$, $\gamma_0 \in \{0.05, 0.10, 0.15, 0.20\}$ and $(\tau_{\min}, \tau_{\max}) = (1, 2]$ 105

Table 4.19 Comparison of the optimal chart parameters (L , LCL , UCL) of the *ARL*-based design of the side-sensitive synthetic- γ (SS Syn) and non-side-sensitive synthetic- γ charts (NSS Syn) for $n \in \{5, 7, 10, 15, 20\}$, $\tau \in \{1.1, 1.2, 1.3, 1.4, 1.5, 1.6, 1.7, 1.8, 1.9, 2.0\}$ and $\gamma_0 = 0.05$ 107

Table 4.20 Comparison of the optimal chart parameters (L , LCL , UCL) of the ARL -based design of the side-sensitive synthetic- γ (SS Syn) and non-side-sensitive synthetic- γ charts (NSS Syn) for $n \in \{5, 7, 10, 15, 20\}$, $\tau \in \{1.1, 1.2, 1.3, 1.4, 1.5, 1.6, 1.7, 1.8, 1.9, 2.0\}$ and $\gamma_0 = 0.10$ 109

Table 4.21 Comparison of the optimal chart parameters (L , LCL , UCL) of the ARL -based design of the side-sensitive synthetic- γ (SS Syn) and non-side-sensitive synthetic- γ charts (NSS Syn) for $n \in \{5, 7, 10, 15, 20\}$, $\tau \in \{1.1, 1.2, 1.3, 1.4, 1.5, 1.6, 1.7, 1.8, 1.9, 2.0\}$ and $\gamma_0 = 0.15$ 110

Table 4.22 Comparison of the optimal chart parameters (L , LCL , UCL) of the ARL -based design of the side-sensitive synthetic- γ (SS Syn) and non-side-sensitive synthetic- γ charts (NSS Syn) for $n \in \{5, 7, 10, 15, 20\}$, $\tau \in \{1.1, 1.2, 1.3, 1.4, 1.5, 1.6, 1.7, 1.8, 1.9, 2.0\}$ and $\gamma_0 = 0.20$ 111

Table 4.23 The ARL_1 and $SDRL_1$ of the ARL -based design of the Shewhart- γ , EWMA- γ^2 , non-side-sensitive synthetic- γ (NSS Syn) and side-sensitive synthetic- γ (SS Syn) charts for $n \in \{5, 7, 10, 15, 20\}$, $\tau \in \{1.1, 1.2, 1.3, 1.4, 1.5, 1.6, 1.7, 1.8, 1.9, 2.0\}$ and $\gamma_0 = 0.05$ 113

Table 4.24 The ARL_1 and $SDRL_1$ of the ARL -based design of the Shewhart- γ , EWMA- γ^2 , non-side-sensitive synthetic- γ (NSS Syn) and side-sensitive synthetic- γ (SS Syn) charts for $n \in \{5, 7, 10, 15, 20\}$, $\tau \in \{1.1, 1.2, 1.3, 1.4, 1.5, 1.6, 1.7, 1.8, 1.9, 2.0\}$ and $\gamma_0 = 0.10$ 114

Table 4.25 The ARL_1 and $SDRL_1$ of the ARL -based design of the Shewhart- γ , EWMA- γ^2 , non-side-sensitive synthetic- γ (NSS Syn) and side-sensitive synthetic-

γ (SS Syn) charts for $n \in \{5, 7, 10, 15, 20\}$,
 $\tau \in \{1.1, 1.2, 1.3, 1.4, 1.5, 1.6, 1.7, 1.8, 1.9, 2.0\}$ and $\gamma_0 = 0.15$ 115

Table 4.26 The ARL_1 and $SDRL_1$ of the ARL -based design of the Shewhart- γ , EWMA- γ^2 , non-side-sensitive synthetic- γ (NSS Syn) and side-sensitive synthetic-

γ (SS Syn) charts for $n \in \{5, 7, 10, 15, 20\}$,
 $\tau \in \{1.1, 1.2, 1.3, 1.4, 1.5, 1.6, 1.7, 1.8, 1.9, 2.0\}$ and $\gamma_0 = 0.20$ 116

Table 4.27 The $EARL_1$ values of the $EARL$ -based design of the Shewhart- γ , EWMA- γ^2 , non-side-sensitive synthetic- γ (NSS Syn) and side-sensitive synthetic- γ

(SS Syn) charts for $n \in \{5, 7, 10, 15, 20\}$, $\gamma_0 \in \{0.05, 0.10, 0.15, 0.20\}$ and
 $(\tau_{\min}, \tau_{\max}) = (1, 2]$ 119

Table 4.28 The l_{05} , MRL_1 and l_{95} values of the MRL -based Shewhart- γ , EWMA- γ^2 , non-side-sensitive synthetic- γ (NSS Syn) and side-sensitive synthetic- γ (SS

Syn) charts for $n \in \{5, 7, 10, 15, 20\}$,
 $\tau \in \{1.1, 1.2, 1.3, 1.4, 1.5, 1.6, 1.7, 1.8, 1.9, 2.0\}$ and $\gamma_0 = 0.05$ 121

Table 4.29 The l_{05} , MRL_1 and l_{95} values of the MRL -based Shewhart- γ , EWMA- γ^2 , non-side-sensitive synthetic- γ (NSS Syn) and side-sensitive synthetic- γ (SS

Syn) charts for $n \in \{5, 7, 10, 15, 20\}$,
 $\tau \in \{1.1, 1.2, 1.3, 1.4, 1.5, 1.6, 1.7, 1.8, 1.9, 2.0\}$ and $\gamma_0 = 0.10$ 122

Table.4.30 The l_{05} , MRL_1 and l_{95} values of the MRL -based Shewhart- γ , EWMA- γ^2 , non-side-sensitive synthetic- γ (NSS Syn) and side-sensitive synthetic- γ (SS

Syn) charts for $n \in \{5, 7, 10, 15, 20\}$,
 $\tau \in \{1.1, 1.2, 1.3, 1.4, 1.5, 1.6, 1.7, 1.8, 1.9, 2.0\}$ and $\gamma_0 = 0.15$ 123

Table 4.31 The l_{05} , MRL_1 and l_{95} values of the *MRL*-based Shewhart- γ , EWMA- γ^2 , non-side-sensitive synthetic- γ (NSS Syn) and side-sensitive synthetic- γ (SS Syn) charts for $n \in \{5, 7, 10, 15, 20\}$, $\tau \in \{1.1, 1.2, 1.3, 1.4, 1.5, 1.6, 1.7, 1.8, 1.9, 2.0\}$ and $\gamma_0 = 0.20$ 124

Table 4.32 The $E(l_{05})$, $EMRL_1$ and $E(l_{95})$ values of the *EMRL*-based of the Shewhart- γ , EWMA- γ^2 , non-side-sensitive synthetic- γ (NSS Syn) and side-sensitive synthetic- γ (SS Syn) charts for $n \in \{5, 7, 10, 15, 20\}$, $\gamma_0 \in \{0.05, 0.10, 0.15, 0.20\}$ and $(\tau_{\min}, \tau_{\max}) = (1, 2]$ 127

Table 4.33 Phase I dataset from a sintering process 129

Table 4.34 Phase II dataset from a sintering process 130

LIST OF FIGURES

Figure 1.1 Feature of non-side-sensitivity	4
Figure 1.2 Feature of side-sensitivity	5
Figure 2.1 Feature of side-sensitivity with five regions.....	34
Figure 2.2 Feature of side-sensitivity with four regions	35
Figure 3.1 Flow chart of the methodology of the side-sensitive synthetic- γ chart.....	45
Figure 3.2 <i>CRL</i> sub-chart of the existing synthetic- γ chart.....	52
Figure 3.3 <i>CRL</i> sub-chart of the side-sensitive synthetic- γ chart.....	54
Figure 4.1 The γ sub-chart of the <i>ARL</i> -based design of the side-sensitive synthetic- γ chart	131
Figure 4.2 The <i>ARL</i> -based design of the EWMA- γ^2 chart	132
Figure 4.3 The γ sub-chart of the <i>ARL</i> -based design of the non-side-sensitive synthetic- γ chart	132
Figure 4.4 The <i>ARL</i> -based design of the Shewhart- γ chart	132
Figure 4.5 The γ sub-chart of the <i>MRL</i> -based design of the side-sensitive synthetic- γ chart	134

LIST OF SYMBOLS AND ABBREVIATIONS

Symbols

γ	: Coefficient of variation
γ^2	: Coefficient of variation squared
K	: Control limit coefficient
F	: Cumulative distribution function
$E(l_\theta)$: Expected percentile of the run length distribution
X	: Independent positive random variable
λ	: Lambda
μ	: Mean
T	: Non-central t -distribution
l	: Percentile of the run length distribution
T_{pd}	: Pressure test drop time
f	: Probability density function
θ	: Probability of run length distribution
α	: Quantile of sample coefficient of variation
m	: Sample
$\hat{\gamma}$: Sample coefficient of variation
\bar{X}	: Sample mean
n	: Sample size
S	: Sample standard deviation
k	: Sequence of sample
τ	: Shift size
σ	: Standard deviation

Z_k : Test statistic of EWMA chart
 L : Threshold
 ξ : Value for in-control

Abbreviations

AEWMA : Adaptive exponentially weighted moving average
arg min : Algorithm for minimization
 ARL : Average run length
 ASS : Average sample size
 ATS : Average time to signal
 CL : Centre line
 A : Conforming region
 CRL : Conforming run length
c.d.f : Cumulative density function
CUSUM : Cumulative sum-type
DEWMA : Double exponentially weighted moving average
 $EARL$: Expected average run length
 $EATS$: Expected average time to signal
 $EMRL$: Expected median run length
 $ESDRL$: Expected standard deviation of the run length
EWMA : Exponentially weighted moving average
FSI : Fixed sampling interval
HEWMA : Hybrid exponentially weighted moving average
 LCL : Lower control limit
 LWL : Lower warning limit

<i>MRL</i>	: Median run length
<i>MCV</i>	: Multivariate coefficient of variation
<i>B</i>	: Non-conforming region
<i>NSS Syn</i>	: Non-side-sensitive synthetic
<i>p.d.f</i>	: Probability density function
<i>p.m.f</i>	: Probability mass function
<i>REARL</i>	: Relative expected average run length
<i>RL</i>	: Run length
<i>SS Syn</i>	: Side-sensitive synthetic
<i>SDRL</i>	: Standard deviation of the run length
<i>SDTS</i>	: Standard deviation of the time to signal
<i>TEWMA</i>	: Triple exponentially weighted moving average
<i>UCL</i>	: Upper control limit
<i>UWL</i>	: Upper warning limit
<i>VSSI</i>	: Variable sample size and sampling interval
<i>VSS</i>	: Variable sample size
<i>VSI</i>	: Variable sampling interval

LIST OF APPENDICES

Appendix A: Computer programming for <i>ARL</i> and <i>EARL</i> -based designs of side-sensitive synthetic- γ chart	152
Appendix B: Computer programming for <i>MRL</i> and <i>EMRL</i> -based designs of side-sensitive synthetic- γ chart.....	159
Appendix C: Computer programming for <i>ARL</i> and <i>EARL</i> -based designs of non-side-sensitive synthetic- γ chart.....	167
Appendix D: Computer programming for <i>MRL</i> and <i>EMRL</i> -based designs of non-side-sensitive synthetic- γ chart	172
Appendix E: Computer programming for <i>ARL</i> and <i>EARL</i> -based designs of Shewhart- γ chart.....	181
Appendix F: Computer programming for <i>MRL</i> and <i>EMRL</i> -based designs of Shewhart- γ chart.....	184
Appendix G: Computer programming for <i>ARL</i> and <i>EARL</i> -based designs of EWMA- γ^2 chart.....	190
Appendix H: Computer programming for <i>MRL</i> and <i>EMRL</i> -based designs of EWMA- γ^2 chart.....	196

CHAPTER 1: INTRODUCTION

1.0 Introduction

This chapter begins with the background of thesis that describes the types of control charts for monitoring the coefficient of variation, γ , which are available in the literature, followed by the problem statement of the thesis. Next, it continues with the scope of the thesis and the research questions. Subsequently, all the research objectives are stated in Section 1.5. The significances of the thesis are explained in the next subsection. Lastly, the organization of the thesis according to each chapter is listed down as the final subsection of this chapter.

1.1 Background of the Thesis

According to Montgomery et al. (2009), statistical process control is one of the major areas in quality improvement which is useful in detecting quality problems and improving the performance of processes at the same time. In statistical process control, control charts are widely recognized as a useful tool to monitor product quality. An effective control chart should be capable of detecting assignable cause(s) with a small quantity of samples and producing few false alarms. The occurrence of assignable cause(s) indicates that the process is an out-of-control. Typically, a conventional control chart monitors the mean, μ and/or standard deviation, σ , where changes in these parameters signal the existence of assignable cause(s). Nevertheless, in certain procedures, the mean is predicted to fluctuate, with a proportional change in the standard deviation. For example, Lynn et al. (1996) conducted a study of enzyme-linked immunosorbent assays (ELISA) which were used for measuring human antibodies to Bordetella pertussis Antigens. It was found that the mean values of the repeated trials varied. In fact, the increase or decrease of the mean was also associated with an increase or decrease in the standard deviation. Therefore, for such processes, traditional mean and/or standard deviation charts are not recommended

as they require constant values of mean and standard deviation. In order to resolve this issue, monitoring the coefficient of variation, γ is suggested as an alternative method. The coefficient of variation is the ratio of the standard deviation over the mean, i.e. $\gamma = \frac{\sigma}{\mu}$. Other than manufacturing industries, and human and public sciences, control charts monitoring the coefficient of variation are popular in many different industries such as engineering (Jiang et al., 2020) , technology (Singh and Singh, 2019), education (P Obite et al., 2020) and pollution control (Sun et al., 2019). Yeong et al. (2018a) have reviewed several fields where monitoring the coefficient of variation is important. The importance of the coefficient of variation to the industries is described further in the next chapter of this thesis.

Kang et al. (2007) proposed the Shewhart coefficient of variation chart, i.e. the Shewhart- γ chart, as the first control chart to monitor the coefficient of variation. This chart used the present sample coefficient of variation, $\hat{\gamma}$, to determine if the process is in-control or out-of-control. However, it only considers the present sample, which requires many samples to detect small or moderate shifts. Therefore, several improvements are proposed. One of the popular coefficient of variation charts is the Exponentially Weighted Moving Average (EWMA) chart. Studies on the EWMA- γ chart was carried out by Hong et al. (2008), Castagliola et al. (2011), Yeong et al. (2017b), Zhang et al. (2018), Muhammad et al. (2018) and Giner-Bosch et al. (2019). Other studies on the coefficient of variation chart are the Hybrid Exponentially Weighted Moving Average (HEWMA) chart by Aslam et al. (2019); Adaptive Exponentially Weighted Moving Average (AEWMA) chart by Haq and Khoo (2019); Double Exponentially Weighted Moving Average (DEWMA) chart by Hu et al. (2022a); run rules chart by Castagliola et al. (2013a); run sum chart by Teoh et al. (2017); side-sensitive group runs

chart by You et al. (2016) and Saha et al. (2021); cumulative sum-type chart by Tran and Tran (2016); charts with variable chart parameters by Castagliola et al. (2013b), Castagliola et al. (2015), Khaw et al. (2017), Yeong et al. (2018a), Chew et al. (2019), Chew et al. (2022), Tran and Heuchenne (2021) and Yeong et al. (2023); charts with measurement errors by Yeong et al. (2017a) and Tran et al. (2019); charts with joint monitoring of mean and coefficient of variation by Noor-ul-Amin et al. (2019); and the γ -type charts based on Phase-I performance by Dawod et al. (2018).

The synthetic- γ chart was introduced by Calzada and Scariano (2013) as an alternative to the Shewhart- γ chart. This chart defines a sample as a conforming sample if the sample coefficient of variation, is between the upper and lower control limits (*UCL* and *LCL*), and non-conforming sample if the sample coefficient of variation falls below the *LCL* or above the *UCL*. When the quantity of conforming samples between two consecutive non-conforming samples is fewer than a predetermined threshold value, the chart produces an out-of-control signal. The outcomes show that the synthetic- γ chart has demonstrated superior performance over the Shewhart- γ chart which is created by Kang et al. (2007) but it is not as effective as the EWMA- γ^2 chart which is developed by Castagliola et al. (2011) in detecting small to moderate shift sizes. However, for large shift sizes, the synthetic- γ chart outperforms the EWMA- γ^2 chart.

The current synthetic- γ chart is not restricted to have two consecutive non-conforming samples appearing in the same region, since both the regions above the *UCL* and below the *LCL* are classified as non-conforming. As an example, if the first non-conforming sample appears in the region below the *LCL*, the second non-conforming sample can either appear in the region below the *LCL* or the region above the *UCL* for

the sample to be considered non-conforming. This is referred to as non-side-sensitivity. An illustration of this feature is shown in Figure 1.1.

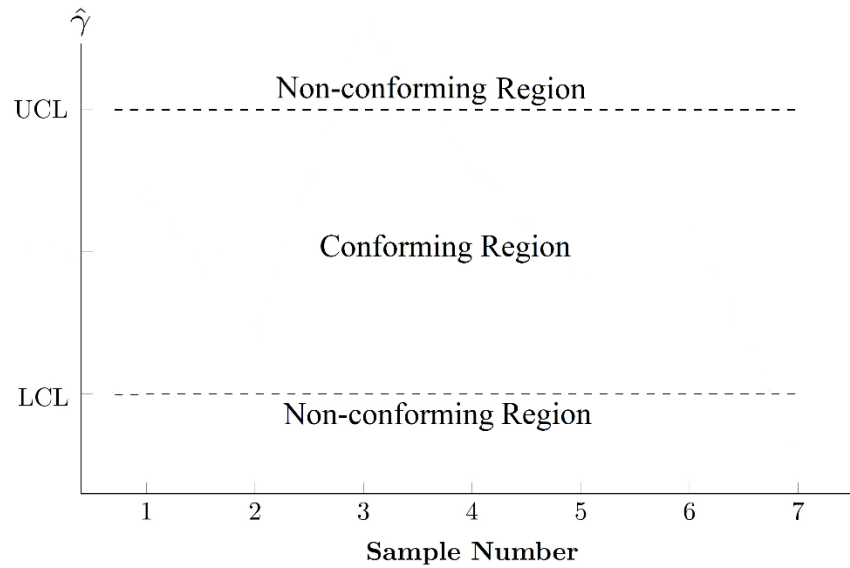


Figure 1.1 Feature of non-side-sensitivity

However, the drawback of this non-side-sensitivity is that it requires a narrower non-conforming region in order to control the false alarm rate. As a result of a narrower non-conforming region, the sensitivity of the chart towards shifts in the coefficient of variation will be reduced. In addition, when shifts happen, it will usually result in successive non-conforming samples that fall in the same region, for instance, either both non-conforming samples will fall above the *UCL* or both will fall below the *LCL*, thus reducing the width of the non-conforming region so that successive samples that fall on opposite sides of the centerline can be considered non-conforming samples is less meaningful. Consequently, the goal of this thesis is to enhance the synthetic- γ chart's effectiveness by incorporating side sensitivity where the region above the *UCL* is classified as upper non-conforming and the region below the *LCL* is classified as lower non-conforming. An illustration of the feature of side-sensitivity is shown in Figure 1.2.

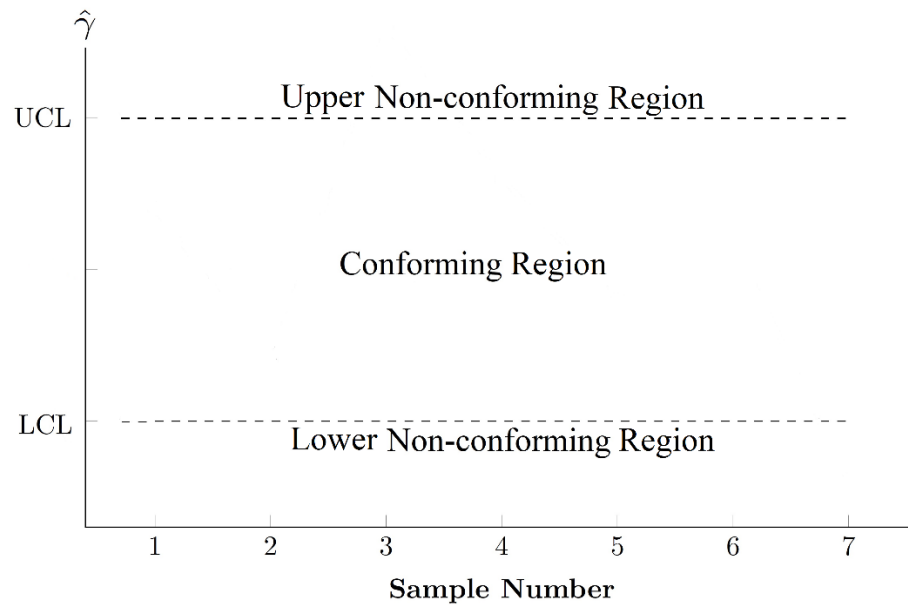


Figure 1.2 Feature of side-sensitivity

The side-sensitive synthetic- $\hat{\gamma}$ chart requires the two consecutive non-conforming samples to appear in the same non-conforming region for these samples to be classified as non-conforming samples. If the first non-conforming sample appears in the region above the UCL , then the second non-conforming sample must also appear in the region above the UCL , and vice versa. If the subsequent sample falls below the LCL , this sample is considered as a conforming sample since it does not fall in the same non-conforming region. This proposed chart is able to enhance the existing synthetic- $\hat{\gamma}$ chart's performance by enabling stricter control limits without raising the quantity of false alarms. This, in turn, allows for quicker detection of shifts in the coefficient of variation, and appropriate measures can be taken to eliminate the assignable cause(s) sooner, thereby decreasing the amount of time the process remains out-of-control and the quantity of faulty products or unsatisfactory service produced by the process. The suggested chart can be utilized to monitor any processes that require monitoring of the coefficient of variation.

In this thesis, a Markov chain approach is adopted for the development of the formulae to evaluate the Average Run Length (ARL), Standard Deviation of the Run Length ($SDRL$), Median Run Length (MRL), Expected Average Run Length ($EARL$), Expected Median Run Length ($EMRL$) and run length distribution of the side-sensitive synthetic- γ chart. ARL measures the average quantity of samples needed by the chart to produce an out-of-control signal, whereas $SDRL$ measures the variability in the quantity of samples required to generate an out-of-control signal. As for MRL , it is defined as the median quantity of samples needed by the chart to generate an out-of-control signal (Gan, 1993).

However, relying solely on the ARL to evaluate the performance of a control chart can lead to a misinterpretation of its actual performance. Gan (1993) pointed out that for small shift sizes, the distribution of run length is likely to be positively skewed for both in-control and out-of-control processes. When the distribution is positively skewed, the mean is always greater than the median, which means the ARL is greater than the MRL . In cases where the in-control MRL (MRL_0) is less than the in-control ARL (ARL_0), greater than half of the in-control run lengths will be less than the ARL_0 , resulting in false alarms occurring before the ARL_0 more than 50% of the time. Thus, this thesis assesses the proposed side-sensitive synthetic- γ chart's performance based on the entire run length distribution to gain a better understanding of its real performance. Additionally, MRL is chosen as the alternative performance measure as it is not affected by the skewness of the distribution.

The ARL , $SDRL$ and MRL require an exact value for the shift size. However, it is not always possible in most practical scenarios because of insufficient data, especially for out-of-control data since assignable cause(s) are usually quickly removed as soon as they

are detected. Besides, shift size may vary according to some unknown stochastic models and may not be deterministic (Castagliola et al., 2011). Hence, in this thesis, the *EARL* and *EMRL* are selected as the performance measures for the proposed chart when the shift size is unknown and specific values of the shift size could not be determined. In fact, they only require the shift size to be stated as a possible range of values like $(\tau_{\min}, \tau_{\max})$. Subsequently, optimization algorithms are proposed to obtain the optimal chart parameters. The optimal chart parameters refer to the chart parameters which optimize the performance measures. Next, a comparison was made between the performance of the proposed side-sensitive synthetic- γ chart with existing coefficient of variation charts in the literature. Finally, the proposed chart was implemented on an actual industrial example and compared with the same existing coefficient of variation charts.

1.2 Problem Statement

The synthetic- γ chart is attractive to practitioners as it waits until the second sample to fall beyond the control limits before determining whether to produce an out-of-control signal. This enables tighter control limits to be adopted without increasing the false alarm rate. Calzada and Scariano (2013) proved that the synthetic- γ chart showed better performance compared to the Shewhart- γ chart for all shift sizes and EWMA- γ^2 chart for large shift sizes. The synthetic- γ chart showed inferior performance compared to the EWMA- γ^2 chart for small and moderate shift sizes.

However, the existing synthetic- γ chart does not have the feature of side sensitivity and this drawback has affected the chart in terms of controlling the false alarm rate as a narrower non-conforming region is required. The sensitivity of the chart towards shifts in the coefficient of variation will be reduced due to the outcome of a narrower non-

conforming region. Machado and Costa (2014a) developed a side-sensitive synthetic- \bar{X} chart and compared the performance with the existing synthetic- \bar{X} chart. The result showed that the proposed chart gave a quicker out-of-control signal than the existing synthetic- \bar{X} chart with 23% lesser samples on average to spot the out-of-control condition. Therefore, this thesis would like to improve the performance of the existing synthetic- γ chart by incorporating side sensitivity as it is expected to show better performance than the existing synthetic- γ chart by providing an earlier out-of-control signal due to more stringent control limits being adopted, without resulting in an increase in the number of false alarms.

For studying the performance of the proposed side-sensitive synthetic- γ chart, suitable performance measures to evaluate the sensitivity of the chart towards shifts in the coefficient of variation are needed. In this thesis, formulae to assess the *ARL*, *SDRL*, *MRL*, *EARL* and *EMRL* were developed, where these measures are based on the quantity of samples required to signal an out-of-control condition. Furthermore, to enhance the performance of the proposed chart, this thesis also developed the algorithms to obtain the optimal chart parameters of the proposed side-sensitive synthetic- γ chart.

As the skewness of the run length distribution will have an impact on the accuracy of the proposed performance measures, this thesis also studied the run length distribution of the proposed chart. It is important for practitioners to know how the proposed chart performs relative to the existing coefficient of variation charts, so that practitioners can decide whether to adopt the proposed chart. Thus, this thesis compared the performance of the proposed chart with existing coefficient of variation charts in the literature. Furthermore, this thesis also shows how the proposed chart was implemented to monitor

an actual industrial process, to guide practitioners to adopt the proposed chart for process monitoring.

1.3 Scope of the Thesis

The main scope of this thesis is to incorporate the feature of side-sensitivity into the existing synthetic- γ chart. This thesis studied the side-sensitive synthetic- γ chart's operation, developed the respective formulae based on Markov chain approach in assessing the *ARL*, *SDRL*, *MRL*, *EARL* and *EMRL* of the proposed chart, and developed algorithms to enhance its' performance. This thesis considered both known and unknown shift sizes as well as the designs for skewed run length distributions.

1.4 Research Questions

The research questions of this thesis are as follows:

1. Does the proposed side-sensitive synthetic- γ chart provides more stringent control limits and shows better performance?
2. Is the run length distribution of the proposed side-sensitive synthetic- γ chart skewed?
3. Does the proposed side-sensitive synthetic- γ chart outperforms the other existing coefficient of variation charts in terms of all performance measures?
4. Does the proposed side-sensitive synthetic- γ chart generates a quicker out-of-control signal compared to existing coefficient of variation charts based on a real industrial example from an Italian company which manufactures sintered mechanical parts?

1.5 Research Objectives

The goal of this thesis is to improve the existing synthetic- γ chart by incorporating side sensitivity. The following are the research objectives:

1. To evaluate whether the proposed side-sensitive synthetic- γ chart adopts stricter control limits and shows better performance.
2. To analyze the run length distribution of the proposed side-sensitive synthetic- γ chart.
3. To compare the proposed side-sensitive synthetic- γ chart with existing coefficient of variation charts based on all performance measures.
4. To apply the proposed side-sensitive synthetic- γ chart on a practical scenario using actual industrial data from an Italian company which manufactures sintered mechanical parts.

1.6 Significance of the Thesis

Incorporating the feature of side sensitivity on the existing synthetic- γ chart is believed to provide significant contributions to the industries as it allows practitioners to adopt more stringent control limits, which results in a smaller difference between the *UCL* and *LCL* of the chart and hence improves the sensitivity of the chart in detecting shifts, without increasing the quantity of false alarms. Thus, the proposed side-sensitive synthetic- γ chart is able to detect an out-of-control condition more rapidly than the existing synthetic- γ chart.

The study of the proposed side-sensitive synthetic- γ chart's run length distribution in this thesis offers practitioners enough insights on the skewness of the distribution. By doing so, they can select appropriate performance measures for the control chart. If the

run length distribution is shown to follow a right-skewed distribution, for instance, they can opt for *MRL* as the performance measure instead of *ARL*.

One of the challenges that is usually faced by practitioners is to implement the synthetic- γ chart on real industry examples because the shift sizes are difficult to be specified as specific values, which is required for performance measures like the *ARL*, *SDRL* and *MRL*. Therefore, the development of the *EARL* and *EMRL* formulae using Markov chain approach in this thesis has resolved the issue where the shift size need not be a specific value as it is only referred to as a possible range of values such as $(\tau_{\min}, \tau_{\max})$. This will help the industry to quickly detect out-of-control conditions, thereby reducing wastage due to defective products and ensuring the quality of the products produced. In addition, the proposed side-sensitive synthetic- γ chart's operation is not complicated compared to the existing synthetic- γ and other coefficient of variation charts and it can be easily implemented and understood by practitioners, including those with little or no experience. Hence, it is believed that the proposed side-sensitive synthetic- γ chart is able to provide numerous significant contributions to industries.

1.7 Organization of the Thesis

In this thesis, there will be a total of five chapters which starts with this current chapter, which describes the introduction, background of the thesis, problem statement, scope of the thesis, research questions, research objectives and significance of the thesis. The second chapter is the literature review. Next, the methodology will be explained in Chapter 3, where the operation of the proposed chart and the development of the formulae for the *ARL*, *SDRL*, *MRL*, *EARL* and *EMRL* based on Markov chain approach is explained. Subsequently, the next chapter shows the results for the optimal chart parameters and the corresponding *ARL*, *SDRL*, *MRL*, *EARL* and *EMRL* of the proposed

side-sensitive synthetic- γ chart using the chosen sample sizes (n), in-control coefficient of variation (γ_0) and shift sizes (τ). The run length distribution's percentiles of the proposed chart will also be analyzed in this chapter. Besides, a discussion will be carried out based on the comparison with the existing synthetic- γ and other coefficient of variation charts. Furthermore, the proposed chart will be applied to a real life example and its performance will be compared with the same coefficient of variation charts. Finally, the last chapter is the conclusion of this thesis and suggestions for further studies are given.

CHAPTER 2: LITERATURE REVIEW

2.0 Introduction

As mentioned in the background of thesis in Chapter 1, this chapter starts with a detailed explanation on coefficient of variation and its applications in various fields. Next, a review of developments on charts monitoring the coefficient of variation is elaborated in the second subsection. Subsequently, the following subsection reviews the development of the synthetic chart. Lastly, the importance of the chosen performance measures in evaluating the control chart is described in the last subsection of this thesis.

2.1 Coefficient of Variation and Its Applications

The coefficient of variation (γ) was proposed by Pearson (1896). It is the ratio of the standard deviation over the mean, i.e. $\gamma = \frac{\sigma}{\mu}$. It is known as one of the commonly chosen measures of dispersion particularly for a distribution of repetitive measurements. According to Shechtman (2013), if the value of the coefficient of variation is large, it indicates greater variability between the recurring measures whereas a small value of the coefficient of variation shows the consistency of the measurements.

The coefficient of variation has been widely used in inferential statistics. Banik and Kibria (2011) focused on the estimation of confidence intervals of the population coefficient of variation for symmetric and skewed distributions. They claimed that the main reason for them to choose the coefficient of variation was that the standard deviation is not an appropriate measure for comparing the variations of several variables with different units of measurement. Another study on the confidence intervals for the estimation of population coefficient of variation was conducted by Gulhar et al. (2012) based on parametric, nonparametric and modified methods using generated data with

$\gamma \in \{0.1, 0.3 \text{ and } 0.5\}$ and two real data sets from health sciences, for instance, child birth weight and cigarette smoking prevalence. Another study on the coefficient of variation was done by El-Din et al. (2019) who studied the estimation of the coefficient of variation using progressive first failure censored data for Lindley distribution with Bayesian and non-Bayesian approaches.

Apart from inferential statistics, the coefficient of variation is also applied regularly in the field of human and public sciences. Babu and Sudha (2016) studied the speckle noise reduction in ultrasound images by applying an adaptive fuzzy logic approach on the coefficient of variation obtained from the noisy image. Tuovinen et al. (2017) focused on the effect of mapping blood oxygenation level dependent (BOLD) data using the coefficient of variation and the gray matter internal carotid artery (ICA) in order to detect the functional connectivity changes in Alzheimer's disease and behavioral variant frontotemporal dementia (bvFTD). Rangasamy et al. (2020) compared the variability of blood glucose using two measurements, the coefficient of variation and blood glucose risk index based on the patients who undergo cardiac surgery. Kong et al. (2022) studied the coefficient of variation of children's blood pressure and heart rate for the purpose of identifying those children with suspected orthostatic intolerance in a rapid way.

In the field of environment research and public health, Zhao et al. (2017) explored the variability of particle grain size as it is a significant indicator for physical features and pollutants composition of road-deposited sediments by using the coefficient of variation of the particle size compositions, metal concentration, metal loads and grain size fraction load (GSF_{Load}) values. Sun et al. (2019) used the coefficient of variation to assess the influence of land use on groundwater pollution in Shuangliao City.

The coefficient of variation is adopted in many different fields as well. In the field of agricultural sciences, Doring and Reckling (2018) applied the coefficient of variation in detecting the global trend of cereal yield stability as it is the main objective in crop production and breeding, especially under the situations of climate change. Lopes et al. (2021) referred to a few experiments of eucalyptus growth and analyzed the distributions of coefficient of variation in order to identify the more appropriate classification ranges for eucalyptus seedlings cultures in either protected cultivation or greenhouses, compared to existing classification ranges. Xu et al. (2021) studied the contribution of features and selected the optimal features using a maximum feature tree embedded with the coefficient of variation and mutual information for the classification of bird sound. England et al. (2022) used the coefficient of variation to assess the performance response of the broilers that were being reared as mixed or single-sex to standard and reduced crude protein diet. At the same time, the authors also examined the uniformity of the broilers.

In the field of engineering, Jiang et al. (2020) proposed an approach to detect the built-up land change based on a single-channel synthetic aperture radar (SAR) by analyzing the coefficient of variation. In terms of technology, Singh and Singh (2019) introduced a submissive blind scheme that consisted of two different algorithms for detecting the video frame and regions of duplication forgery based on the coefficient of variation and correlation coefficient. In education, P Obite et al. (2020) used the coefficient of variation to assess the disparities in the applications of Higher Education, the Joint Admissions and Matriculation board in Nigeria. In the field of finance, Ma et al. (2021) chose the coefficient of variation to determine the time and the reason of a risk-averse firm for implementing the program of advance booking discount in the presence of a spot market. In the field of investment, Chaudhari and Thakkar (2023) applied the coefficient of variation on several selected features such as backpropagation neural network (BPNN),

long short-term memory (LSTM), gated recurrent unit (GRU), and convolutional neural network (CNN) for the stock price and trend prediction.

The literature on the application of the coefficient of variation in numerous industries stated earlier is summarized in Table 2.1 below.

Table 2.1 Meta-analysis of coefficient of variation in different fields

Author(s) and Year	Field	Title of Article
Banik and Kibria (2011)	Inferential Statistics	Estimating the population coefficient of variation by confidence intervals
Gulhar et al. (2012)		A comparison of some confidence intervals for estimating the population coefficient of variation: a simulation study
El-Din et al. (2019)		Estimation of the coefficient of variation for Lindley distribution based on progressive first failure censored data
Babu and Sudha (2016)		Adaptive speckle reduction in ultrasound images using fuzzy logic on the coefficient of variation
Tuovinen et al. (2017)	Human and Public Sciences	The effect of gray matter ICA and coefficient of variation mapping of BOLD data on the detection of functional connectivity changes in Alzheimer's disease and bvFTD
Rangasamy et al. (2020)		Comparison of glycemic variability indices blood glucose risk index and coefficient of variation in predicting adverse outcomes for patients undergoing cardiac surgery
Kong et al. (2022)		Coefficient of variation of heart rate and blood pressure in rapid identification of children with suspected orthostatic intolerance
Zhao et al. (2017)		Environment Research and Public Health

Table 2.1, continued

Author(s) and Year	Field	Title of Article
Sun et al. (2019)	Environment Research and Public Health	Assessing the influence of land use on groundwater pollution based on the coefficient of variation weight method: a case study of shuangliao city
Doring and Reckling (2018)		Detecting global trends of cereal yield stability by adjusting the coefficient of variation
Lopes et al. (2021)		Classification of the coefficient of variation for experiments with eucalyptus seedlings in greenhouse
Xu et al. (2021)	Agricultural Sciences	Feature selection using maximum feature tree embedded with mutual information and coefficient of variation for bird sound classification
England et al. (2022)		Rearing broilers as mixed or single-sex: relevance to performance, coefficient of variation, and flock uniformity
Jiang et al. (2020)	Engineering	Delineation of built-up land change from SAR stack by analysing the coefficient of variation
Singh and Singh (2019)	Technology	Video frame and region duplication forgery detection based on correlation coefficient and coefficient of variation
P Obite et al. (2020)	Education	Assessment of the disparities in the applications to higher education in Nigeria: a coefficient of variation approach
Ma et al. (2021)	Finance	Advance booking discount for risk-averse firms in the presence of spot market
Chaudhari and Thakkar (2023)	Investment	Neural network systems with an integrated coefficient of variation-based feature selection for stock price and trend prediction

Considering the importance of the coefficient of variation in numerous industries that are elaborated above, a tool to monitor the stability of the coefficient of variation is needed. This results in the development of control charts to monitor the coefficient of

variation. The next subsection reviews existing control charts for monitoring the coefficient of variation.

2.2 Control Charts on Monitoring the Coefficient of Variation

The first coefficient of variation chart was a Shewhart-type chart. This chart was proposed by Kang et al. (2007) when the standard \bar{X} , S and R charts could not be used due to inconsistent mean in some circumstances such as clinical chemistry. Rational subgroups of patients who were undergoing immunosuppressive treatment were taken as the samples for the development of the Shewhart- γ chart. The performance of the proposed Shewhart- γ chart was evaluated in terms of the ARL obtained for sample sizes, $n \in \{5, 10, 15\}$, in-control coefficient of variation, $\gamma_0 \in \{0.05, 0.10, 0.15\}$ and shift sizes, $\tau \in \{1, 1.25, 1.5, 2.0\}$. The Shewhart- γ chart does not demonstrate good performance for small and moderate shift sizes because it only considers the present sample coefficient of variation. As a result, the chart requires a larger size of sample for better performance.

Another commonly used control chart for monitoring the coefficient of variation is called the EWMA chart. EWMA- γ chart was developed by Hong et al. (2008) to improve the performance of the Shewhart- γ chart by Kang et al. (2007) in detecting small and moderate shift sizes. The EWMA- γ chart takes the weighted average of all past and present samples. The ARL of the EWMA- γ chart for $n \in \{5, 10, 15\}$, $\gamma_0 \in \{0.05, 0.10, 0.15\}$ and $\tau \in \{1.00, 1.25, 1.50\}$ are shown. When a comparison was done between the proposed EWMA- γ and the Shewhart- γ charts, the results showed that the EWMA- γ chart outperformed the Shewhart- γ charts, where smaller out-of-control ARL (ARL_1) were shown for all cases.

Castagliola et al. (2011) proposed two one-sided EWMA charts by monitoring the coefficient of variation squared, i.e. the EWMA- γ^2 chart, and proposed the algorithm to obtain the optimal λ and L , which is not available in Hong et al. (2008). The investigation on unknown shift size was conducted in the study as well through the *EARL*. The outcomes showed that the proposed two one-sided EWMA- γ^2 charts outperform the Shewhart- γ charts in all cases by producing much smaller ARL_1 and out-of-control *EARL* ($EARL_1$), while compared to the EWMA- γ chart, the proposed charts performed slightly better, although the difference between the two is small.

Apart from the Shewhart- γ and EWMA- γ charts, there are many studies on other control charts monitoring the coefficient of variation. Castagliola et al. (2013a) introduced the run rules chart to monitor the coefficient of variation using three run rules strategies, which were the 2-out-of-3, 3-out-of-4 and 4-out-of-5 run rules. The performance of all three run rules charts was evaluated in terms of ARL_1 and out-of-control standard deviation of the run length ($SDRL_1$) for $n \in \{5, 7, 10, 15\}$, $\gamma_0 \in \{0.05, 0.10, 0.15, 0.20\}$ and $\tau \in \{0.5, 0.6, 0.7, 0.8, 0.9, 1.1, 1.2, 1.5, 2.0, 2.5\}$. It can be observed that the three proposed run rules charts outperformed the Shewhart- γ chart for small and moderate shift sizes whereas the Shewhart- γ chart showed better performance for larger shift sizes.

Nevertheless, the EWMA- γ chart still performs better than the run rules chart for small and moderate shift sizes. This is proven by Zhang et al. (2014), who modified the existing two one-sided EWMA- γ^2 charts by Castagliola et al. (2011) by using the information for all the former and current samples. The performance of the modified two one-sided EWMA- γ^2 charts was compared with the Shewhart- γ chart with

supplementary run rules by Castagliola et al. (2013a), synthetic- γ chart by Calzada and Scariano (2013) and the existing two one-sided EWMA- γ^2 charts by Castagliola et al. (2011). The outcomes showed that the proposed charts outperformed these charts for small and moderate shift sizes but not for large shift sizes.

You et al. (2016) proposed the side-sensitive group runs chart to monitor the coefficient of variation. The proposed chart was evaluated in terms of the ARL_1 , $SDRL_1$ and $EARL_1$ for $n \in \{5, 10, 15\}$, $\gamma_0 \in \{0.05, 0.10, 0.15, 0.20\}$, downward shift, $\tau \in \{0.10, 0.25, 0.50, 0.80\}$ and upward shift, $\tau \in \{1.25, 1.50, 2.00, 2.50, 3.00, 4.00\}$ followed by comparison with the Shewhart- γ , 2-out-of-3 run rules, 4-out-of-5 run rules, synthetic- γ and EWMA- γ charts. Generally, the side-sensitive group runs- γ chart outperformed all other charts in most cases excluding the small downward shift where the EWMA- γ chart has the best performance.

Tran and Tran (2016) presented two one-sided cumulative sum-type control charts that monitors the squared coefficient of variation (CUSUM- γ^2 chart) based on fixed and random shift sizes under zero-state assumptions. The performance of the proposed chart was compared with the EWMA- γ^2 chart by Castagliola et al. (2011) and the modified EWMA- γ^2 chart by Zhang et al. (2014) for $n \in \{5, 7, 10, 15\}$, $\gamma_0 \in \{0.05, 0.10, 0.15, 0.20\}$ and $\tau \in \{0.50, 0.65, 0.80, 0.90, 1.10, 1.25, 1.50, 2.00\}$. Overall, the proposed two one-sided CUSUM- γ^2 charts outperformed the EWMA- γ^2 chart for most cases and the modified EWMA- γ^2 chart for $\tau \in \{0.50, 0.65, 1.50, 2.00\}$. Furthermore, it was able to detect the assignable cause(s) quicker than the other two charts except for $\tau \in \{0.65, 0.90, 1.50, 2.00\}$.

Run sum chart is known as one of the recent control charts to monitor the coefficient of variation which was established by Teoh et al. (2017). In the study, the authors considered four and seven regions run sum- γ charts under both zero-state and steady-state for $n = 5$, $\gamma_0 \in \{0.05, 0.10, 0.15, 0.20\}$ and $\tau \in \{0.50, 0.65, 0.80, 0.90, 1.25, 1.50, 1.75, 2.00\}$. Based on the performance of ARL_1 , $SDRL_1$ and $EARL_1$, the seven regions run sum- γ chart was also compared with the Shewhart- γ and EWMA- γ charts under zero-state and steady-state for the same values of n , γ_0 and τ . The results of the ARL_1 and $SDRL_1$ showed that both run sum- γ charts performed better than the Shewhart- γ chart for all cases under both states. However, EWMA- γ chart has the best performance compared to the two proposed run sum- γ charts in most cases except for $\tau = 0.50$ under both states and $\tau = 2.00$ under steady-state. For the performance of $EARL_1$, EWMA- γ chart outperformed all three charts for all cases under both states.

However, the study that was conducted by Zhang et al. (2018) showed different outcomes when EWMA- γ chart was compared with the side-sensitive group runs- γ chart. The authors proposed a new two one-sided EWMA- γ^2 charts by resetting the negative normalized observations to zero for the purpose of overcoming the inertia issue of the traditional EWMA- γ chart. These two one-sided EWMA- γ^2 charts were compared with the modified two one-sided EWMA- γ^2 charts by Zhang et al. (2014), existing two one-sided EWMA- γ^2 charts by Castagliola et al. (2011), Shewhart- γ chart with supplementary run rules by Castagliola et al. (2013a), synthetic- γ chart by Calzada and Scariano (2013) and side-sensitive group runs- γ chart by You et al. (2016) in terms

of the ARL_1 performance. The outcomes showed that the proposed two one-sided EWMA- γ^2 charts outperformed the other four control charts for most cases.

The attention to EWMA- γ chart is continued with another new control chart, namely the HEWMA chart monitoring the coefficient of variation which is proposed by Aslam et al. (2019) using two EWMA statistics. The authors evaluated the performance of the proposed chart and compared it with the EWMA- γ^2 chart by Castagliola et al. (2011) and the modified EWMA- γ^2 chart by Zhang et al. (2014) for $n \in \{5, 7, 10, 15\}$, $\gamma_0 \in \{0.05, 0.10, 0.15, 0.20\}$ and $\lambda_1, \lambda_2 \in \{0.05, 0.10, 0.20, 0.30, 0.50\}$. The outcomes showed that the proposed chart outperformed the other two charts in most cases. Besides that, the proposed chart showed greater efficiency in perceiving the process shift for both simulated and real industry data.

In the following year, Haq and Khoo (2019) introduced the AEWMA chart which is focused on infrequent changes in the coefficient of variation and compared it with the EWMA- γ^2 chart by Castagliola et al. (2011), the modified EWMA- γ^2 chart by Zhang et al. (2014) and CUSUM- γ^2 chart by Tran and Tran (2016) for $n \in \{5, 7, 10, 15\}$, $\gamma_0 \in \{0.05, 0.10, 0.15, 0.20\}$ and $\tau \in \{0.50, 0.65, 0.80, 0.90, 1.10, 1.25, 1.50, 2.00\}$. It can be observed that the proposed chart outperformed the other three charts for moderate to large shift sizes. Similar results were obtained based on real industry data.

Saha et al. (2021) introduced a side-sensitive modified group runs chart to monitor the coefficient of variation and compared it with the existing EWMA- γ , run sum- γ and side-sensitive group runs- γ charts in terms of the ARL and $SDRL$ performance for

$n \in \{5, 7, 10\}$, $\gamma_0 \in \{0.05, 0.10, 0.15, 0.20\}$ and $\tau \in \{0.25, 0.50, 0.75, 1.25, 1.50, 2.00\}$.

It is found that the proposed chart outperformed the other three control charts for increasing shift size, where $\tau > 1$. However, for decreasing shift size, $\tau < 1$, EWMA- γ and run sum- γ charts still performed better.

Hu et al. (2022a) developed two one-sided DEWMA charts for monitoring the coefficient of variation squared in order to improve the performance of the existing EWMA- γ^2 chart which was proposed by Castagliola et al. (2011). Monte Carlo simulations were chosen as the method to assess the performance of the proposed chart based on ARL for $n = 5$, $\lambda = 0.1$, $\gamma_0 \in \{0.10, 0.20\}$, downward shift, $\tau \in \{0.50, 0.65, 0.75, 0.80, 0.90, 0.95\}$ and upward shift, $\tau \in \{1.05, 1.10, 1.20, 1.25, 1.50, 2.00\}$. A comparison between these two charts was conducted and it is observed that the proposed DEWMA- γ^2 chart outperformed the EWMA- γ^2 chart for small shift sizes. Besides, the advantage of the proposed chart showed significant improvement over the EWMA- γ^2 chart when λ increases. However, EWMA- γ^2 chart still outperformed DEWMA- γ^2 chart for large shift sizes.

Hu et al. (2022b) proposed three one-sided DEWMA chart in monitoring the squared coefficient of variation, namely the DEWMA1- γ^2 , DEWMA2- γ^2 , and DEWMA3- γ^2 charts. The proposed charts were assessed based on the ARL performance, where the ARL was obtained through Monte Carlo simulations, and compared among themselves as well as with the existing EWMA- γ^2 chart. It can be observed that DEWMA1- γ^2 outperformed the other two proposed charts for small shift sizes whereas DEWMA2- γ^2 performed the best for large shift sizes. For the comparison between the proposed charts

and the EWMA- γ^2 chart, the results showed that the proposed charts outperformed the existing EWMA- γ^2 chart for small shift sizes. However, for large shift sizes, the EWMA- γ^2 chart performed the best.

Besides those coefficient of variation charts mentioned earlier, there are several studies regarding charts with variable chart parameters. Castagliola et al. (2013b) proposed an Adaptive Shewhart- γ chart by implementing the strategy of the variable sampling interval (VSI). It is noticed that it outperformed the Shewhart- γ chart for all cases in terms of the out-of-control average time to signal (ATS_1) and out-of-control standard deviation of the time to signal ($SDTS_1$). Castagliola et al. (2015) modified the Shewhart- γ chart by implementing the strategy of variable sample size (VSS) and compared the proposed chart with the fixed sampling rate and VSI Shewhart- γ charts, and also the synthetic- γ charts. In terms of ARL_1 , $SDRL_1$ and out-of-control average sample size (ASS_1) values, the proposed chart outperformed the fixed sampling rate Shewhart- γ chart for all cases. It also showed better performance than the VSI Shewhart- γ chart and synthetic- γ chart for small and moderate shift sizes. Khaw et al. (2017) implemented the strategy of variable sample size and variable sampling interval (VSSI) on the Shewhart- γ chart and compared its performance with the fixed sampling rate and VSS Shewhart- γ , synthetic- γ , EWMA- γ^2 and 2-out-of-3 run rules charts. It can be observed that the proposed chart outperformed all other charts for moderate and large shift sizes in terms of ATS_1 and $SDTS_1$ values. Furthermore, it showed the best performance in terms of the out-of-control expected average time to signal ($EATS_1$) values for all cases. Thus, for small shift sizes, EWMA- γ^2 chart outperformed all the charts based on the performance of ATS_1 . Yeong et al. (2018a) introduced the variable parameters (VP) chart for monitoring the coefficient of variation and compared it with the control charts mentioned

by Khaw et al. (2017) except for 2-out-of-3 run rules chart. The results showed that the VP- γ chart outperformed all five control charts for all shift sizes. However, for small shift sizes, EWMA- γ^2 chart showed the best performance. Chew et al. (2022) introduced the economic and economic-statistical designs of the VSSI chart monitoring the coefficient of variation. It is found that the proposed chart was able to reduce the time in detecting the out-of-control condition, compared to the Shewhart- γ chart.

Apart from the Shewhart- γ chart with variable chart parameters described in the preceding paragraph, variable chart parameters were also adopted on other more complicated coefficient of variation charts. Yeong et al. (2017b) proposed a VSI EWMA chart to monitor the coefficient of variation and compared it with the Shewhart- γ , synthetic- γ , EWMA- γ^2 and VSI- γ charts. Based on the ATS_1 , $SDTS_1$ and $EATS_1$ obtained, the results showed that the proposed chart outperformed the other four charts. Muhammad et al. (2018) developed a VSS EWMA chart monitoring the coefficient of variation. It can be noticed that the proposed chart outperformed the Shewhart- γ , synthetic- γ , EWMA- γ^2 , VSS- γ and run rules- γ charts in detecting small and moderate shift sizes. Tran and Heuchenne (2021) proposed a VSI CUSUM chart to monitor the coefficient of variation in order to overcome the issue of handling downward shifts in the coefficient of variation. It is found that the proposed chart outperformed the fixed sampling interval (FSI) CUSUM- γ^2 chart. Furthermore, it was also able to identify both increasing and decreasing shift sizes efficiently.

Incorporating variable chart parameters into the existing coefficient of variation charts has attracted more attention from researchers lately. Hu et al. (2021) modified the three DEWMA- γ^2 charts which were proposed by Hu et al. (2022b) with the feature of VSI

and named them as VSI DEWMA1- γ^2 , VSI DEWMA2- γ^2 and VSI DEWMA3- γ^2 charts. The performance of the proposed charts was evaluated using the method of Monte Carlo simulations and comparison within these three proposed charts was conducted. Besides, they were compared with other coefficient of variation charts based on FSI and VSI features like FSI DEWMA- γ^2 , FSI EWMA- γ^2 , VSI EWMA- γ^2 and AEWMA- γ^2 charts. It is noticed that the three proposed charts outperformed all the coefficient of variation charts for small and moderate shift sizes. However, for larger shift sizes, VSI DEWMA2- γ^2 chart was inferior to the VSI EWMA- γ^2 chart. Hence, VSI DEWMA1- γ^2 and VSI DEWMA3- γ^2 showed better performance than the VSI DEWMA2- γ^2 chart and they were suggested as the recommendations for large γ_0 or smoothing parameter.

Yeong et al. (2022a) introduced a run sum- γ chart with the feature of VSI (VSI run sum- γ) in order to reduce the required average time of identifying the shifts in the process and control the sampling cost as well. The performance of the proposed chart was assessed in terms of the *ATS* and *EATS* and it was compared with the Shewhart- γ , VSI- γ , synthetic- γ , EWMA- γ^2 , VSI EWMA- γ^2 and run sum- γ charts. It is found that the proposed chart outperformed the Shewhart- γ , VSI- γ , synthetic- γ and run sum- γ charts for all cases as well as the EWMA- γ^2 chart for moderate and large shift sizes. Unfortunately, it did not outperform the VSI EWMA- γ^2 chart for all cases.

In the same year, Yeong et al. (2022b) incorporated the feature of VSS into the run sum- γ (VSS run sum- γ) chart and evaluated the proposed chart in terms of the performance of *ARL* and *EARL*. The corresponding *ARL* and *EARL* of the proposed chart were also compared with the Shewhart- γ , VSS- γ , synthetic- γ , EWMA- γ^2 , VSS

EWMA- γ^2 and run sum- γ charts. It is found that the proposed VSS run sum- γ chart outperformed the run sum- γ chart particularly for small sample and shift sizes. Generally, it also showed better results compared to the Shewhart- γ , VSS- γ and synthetic- γ charts for some cases. Nevertheless, the VSS EWMA- γ^2 chart outperformed the proposed chart for all cases whereas EWMA- γ^2 chart outperformed it for most cases.

Yeong et al. (2023) implemented the features of VSSI and VP into the existing run sum chart for improving its sensitivity for the shifts in the coefficient of variation and the performance of the two proposed charts were evaluated in terms of the *ATS*, *SDTS* and *EATS*. The corresponding *ATS*, *SDTS* and *EATS* of the proposed charts were also compared with other existing coefficient of variation charts such as the VSI run sum- γ , VSS run sum- γ , VSSI- γ , VSS- γ , VSI- γ , VSS EWMA- γ^2 , and VSI EWMA- γ^2 charts. Based on the results obtained, it can be observed that the proposed VP run sum- γ chart outperformed the proposed VSSI run sum- γ chart. Besides, for moderate and large shift sizes, both proposed charts showed better performance compared to VSI run sum- γ , VSS run sum- γ , VSSI- γ , VSS- γ , VSI- γ , VSS EWMA- γ^2 , and VSI EWMA- γ^2 charts.

Hu et al. (2023) proposed two one-sided Triple EWMA (TEWMA) charts with and without the feature of VSI for monitoring the coefficient of variation squared, namely FSI TEWMA- γ^2 and VSI TEWMA- γ^2 charts. The performance of the proposed charts for both zero-state and steady-state were evaluated using Monte Carlo simulations. Comparisons between the proposed TEWMA- γ^2 charts and other EWMA charts such as the EWMA- γ^2 , DEWMA1- γ^2 and DEWMA2- γ^2 charts were conducted for both FSI and VSI features. It is found that the proposed VSI TEWMA- γ^2 chart showed quicker

detection in shifts compared to the proposed FSI TEWMA- γ^2 chart. For small shift sizes, the VSI TEWMA- γ^2 chart also showed superior zero-state and steady-state performance compared to the EWMA- γ^2 and DEWMA- γ^2 charts. However, the VSI DEWMA2- γ^2 chart outperformed all other charts for large shift sizes under zero-state whereas for steady-state, the VSI DEWMA1- γ^2 was the best chart for moderate shift sizes and the VSI EWMA- γ^2 showed the best performance for large shift sizes.

In this subsection, several existing charts monitoring the coefficient of variation are reviewed, such as the Shewhart- γ , EWMA- γ , run rules- γ , run sum- γ , side-sensitive group runs- γ , CUSUM- γ , VP- γ , VSI- γ , VSS- γ and VSSI- γ charts. The summary of the literature described in this subsection is presented in Table 2.2. In the next subsection, a review of synthetic charts will be given.

Table 2.2 Meta-analysis of control chart monitoring coefficient of variation

Author(s) and Year	Proposed Control Chart	Competing Control chart	Shift Size	Best Method
Kang et al. (2007)	Shewhart	-	Small and large	Shewhart
Castagliola et al. (2013b)	VSI Shewhart	Shewhart	Small and large	VSI Shewhart
Castagliola et al. (2015)	VSS Shewhart	Shewhart, VSI Shewhart, Synthetic	Small	VSS Shewhart
			Large	Synthetic
Khaw et al. (2017)	VSSI Shewhart	VSI Shewhart, VSS Shewhart, Shewhart	Small and large	VSSI Shewhart
Yeong et al. (2018a)	VP Shewhart	VSSI Shewhart, VSI Shewhart, VSS Shewhart, EWMA, Synthetic Shewhart, Shewhart	Small and large	VP Shewhart
Chew et al. (2022)	VSSI Shewhart	Shewhart	Small and large	VSSI Shewhart
Hong et al. (2008)	EWMA	Shewhart	Small and moderate	EWMA

Table 2.2, continued

Author(s) and Year	Control Chart	Competing Control Chart	Shift Size	Best Method
Castagliola et al. (2011)	EWMA- γ^2	Shewhart, EWMA	Small and large	EWMA- γ^2
Zhang et al. (2014)	EWMA- γ^2	Run Rules Shewhart, Synthetic, EWMA	Small Large	EWMA- γ^2 Synthetic
Zhang et al. (2018)	EWMA- γ^2	EWMA, Run Rules Shewhart Synthetic, Side-sensitive Group Runs	Small and large	EWMA- γ^2
Yeong et al. (2017b)	VSI EWMA	Shewhart, Synthetic, EWMA, VSI	Small and large	VSI EWMA
Muhammad et al. (2018)	VSS EWMA	Shewhart, EWMA, Synthetic Shewhart, Run Rules Shewhart and VSS Shewhart	Small and large	VSS EWMA
Aslam et al. (2019)	HEWMA	EWMA- γ^2	Small and large	HEWMA
Haq and Khoo (2019)	AEWMA	Shewhart	Small Large	AEWMA Shewhart
Hu et al. (2022a)	DEWMA	EWMA- γ^2	Small Large	DEWMA EWMA
Hu et al. (2022b)	DEWMA	EWMA- γ^2	Small Large	DEWMA EWMA
Hu et al. (2021)	VSI DEWMA	DEWMA, EWMA, VSI EWMA, AEWMA	Small Large	VSI DEWMA VSI EWMA
Hu et al. (2023)	FSI TEWMA- γ^2 , VSI TEWMA- γ^2	FSI EWMA- γ^2 , VSI EWMA- γ^2 , FSI DEWMA1- γ^2 , VSI DEWMA1- γ^2 , FSI DEWMA2- γ^2 , VSI DEWMA2- γ^2	Small	VSI TEWMA- γ^2

Table 2.2, continued

Author(s) and Year	Control Chart	Competing Control Chart	Shift Size	Best Method
Castagliola et al. (2013a)	Run Rules	Shewhart	Small	Run Rules
			Large	Shewhart
Teoh et al. (2017)	Run Sum	Shewhart, EWMA	Small and large	EWMA
Yeong et al. (2022a)	VSI Run Sum	Shewhart, VSI, Synthetic, EWMA, VSI EWMA, Run Sum	Small	VSI EWMA
			Large	VSI Run Sum
Yeong et al. (2022b)	VSS Run Sum	Shewhart, VSS, Synthetic, EWMA, VSS EWMA, Run Sum	Small and large	VSS EWMA
Yeong et al. (2023)	VSSI Run Sum, VP Run Sum	VSI Run Sum, VSS Run Sum, VSSI- γ , VSS- γ , VSI- γ , VSS EWMA- γ^2 , VSI EWMA- γ^2	Moderate and large	VSSI and VP Run Sum
You et al. (2016)	Side-sensitive Group Runs	Shewhart, Run Rules, Synthetic, EWMA	Small	EWMA
			Large	Side-sensitive Group Runs
Saha et al. (2021)	Side-sensitive Modified Group Runs	EWMA, Run Sum, Side-sensitive Group Runs	Small	EWMA
			Large	Side-sensitive Modified Group Runs
Tran and Tran (2016)	CUSUM- γ^2	EWMA	Small	EWMA
			Large	CUSUM- γ^2
Tran and Heuchenne (2021)	VSI CUSUM	CUSUM- γ^2	Small and large	VSI CUSUM

From Table 2.2, it can be observed that most of the studies are focused on the Shewhart and EWMA charts. For Shewhart charts, studies in the literature focused on improving its performance by varying its chart parameters, for example through the VSI Shewhart, VSS Shewhart, VSSI Shewhart and VP Shewhart charts. As for the EWMA chart, practitioners had proposed numerous charts such as the EWMA- γ^2 , VSI EWMA, VSS

EWMA, HEWMA, AEWMA, DEWMA, VSI DEWMA and VSI TEWMA charts. According to the best method shown in the last column in Table 2.2, Shewhart chart has the best performance for large shift sizes whereas the EWMA chart outperforms all control charts for small and moderate shifts size. Hence, in this thesis, the performance of the proposed side-sensitive synthetic- γ chart is compared with the Shewhart- γ and EWMA- γ^2 charts. Since the purpose of this thesis is to improve the existing synthetic- γ chart, therefore the existing synthetic- γ chart is also being selected as one of the coefficient of variation charts for comparison.

2.3 Development of Synthetic Charts

Wu and Spedding (2000) were the pioneers for the synthetic chart, where a synthetic chart was proposed to monitor the process mean by combining the Shewhart \bar{X} and conforming run length (*CRL*) charts together. The authors found that the proposed synthetic chart produced a much smaller ARL_1 compared to the existing Shewhart \bar{X} for all shift sizes. Furthermore, it also outperformed the standard EWMA and the joint \bar{X} EWMA charts for large shift sizes. Subsequently, Wu et al. (2001) developed a new synthetic control chart for detecting the increase in the fraction non-conforming. The outcomes showed that the synthetic control chart had a greater power to detect the process shifts and produced a 50% or higher decrease in the out-of-control mean time to signal.

Ever since then, the study on synthetic control chart began to attract a lot of attention from researchers. Calzada and Scariano (2001) studied the robustness of the synthetic chart when the normal assumptions are violated. Davis and Woodall (2002) used Markov chains to evaluate the *ARL* performance under both zero-state and steady-state. Scariano and Calzada (2003) focused on the lower-sided synthetic chart for exponential data. Song and Park (2005) developed a new VSI synthetic chart for the purpose of the convenience

of using the control chart in the field. Lee and Lim (2005) proposed a VSSI-CRL synthetic chart for improving the statistical characteristics of both *CRL* and the VSSI synthetic charts. Chen and Huang (2006) modified the existing VSI synthetic chart by combining the features of the max chart and *CRL* chart for jointly monitoring the shift in the process mean and/or standard deviation for normal distribution. Costa and Rahim (2006) proposed a synthetic chart that is focused on the non-central chi-square statistic for identifying the change in the process mean or variance due to assignable cause(s). Khoo et al. (2008) developed a synthetic chart based on the weighted variance method for monitoring the mean of the process from skewed populations.

Due to the good reviews of synthetic control chart by the researchers mentioned above, the study of synthetic control chart became more aggressive. Aparisi and De Luna (2009) optimized the zero-state and steady-state performance of synthetic \bar{X} chart, while Castagliola and Khoo (2009) modified the existing synthetic chart that was developed by Khoo et al. (2008) with scaled weighted variance \bar{X} for monitoring the mean of the process of skewed population. Costa et al. (2009) proposed a synthetic control chart with two-stage testing for monitoring the process mean and standard deviation, and, Scariano and Calzada (2009) presented a generalized synthetic control chart by applying it to the EWMA and CUSUM charts. Subsequently, Khoo et al. (2010) proposed a synthetic double sampling chart for monitoring the process mean whereas Wu et al. (2010) combined the synthetic and \bar{X} charts (Syn- \bar{X} chart) to monitor the process mean. Next, Zhang et al. (2011) evaluated the performance of the existing synthetic \bar{X} chart using estimated process parameters from an in-control Phase I data set. Lastly, Khoo et al. (2012) developed an optimal design of the synthetic chart based on median run length for monitoring the process mean under the zero-state and steady-state modes.

The synthetic coefficient of variation chart, synthetic- γ chart used in this thesis was developed by Calzada and Scariano (2013). The proposed synthetic- γ chart's performance was compared with the Shewhart- γ and upward EWMA- γ^2 charts in terms of the $n \in \{5, 10, 15\}$, $\gamma_0 \in \{0.05, 0.10, 0.15\}$ and $\tau \in \{1, 1.25, 1.5, 1.75, 2, 2.25, 2.5, 2.75, 3\}$. The synthetic- γ chart performed better than the Shewhart- γ chart as it produced more stringent control limits, for instance, greater LCL and smaller UCL . Besides, in terms of ARL and $EARL$, the synthetic- γ chart showed better performance than the Shewhart- γ chart for all cases and EWMA- γ^2 chart for large shift sizes. Nevertheless, for small shift sizes, EWMA- γ^2 chart outperformed the proposed synthetic- γ chart.

Since there is no research regarding side-sensitive synthetic- γ chart, therefore this thesis will refer to the past studies of the synthetic \bar{X} chart with the feature of side sensitivity in order to investigate the performances between the non-side-sensitive and side-sensitive synthetic \bar{X} charts in terms of detecting the out-of-control signal. Machado and Costa (2014b) proposed a side-sensitive synthetic \bar{X} chart by dividing the chart into five regions compared to the original synthetic \bar{X} chart which consists of conforming and non-conforming regions only. Those regions are the upper action (above the UCL), upper warning (above the upper warning limit, UWL), lower warning (below the lower warning limit, LWL), lower action (below the LCL) and central region (between the LWL and UWL). An illustration of this feature of side sensitivity is shown in Figure 2.1.

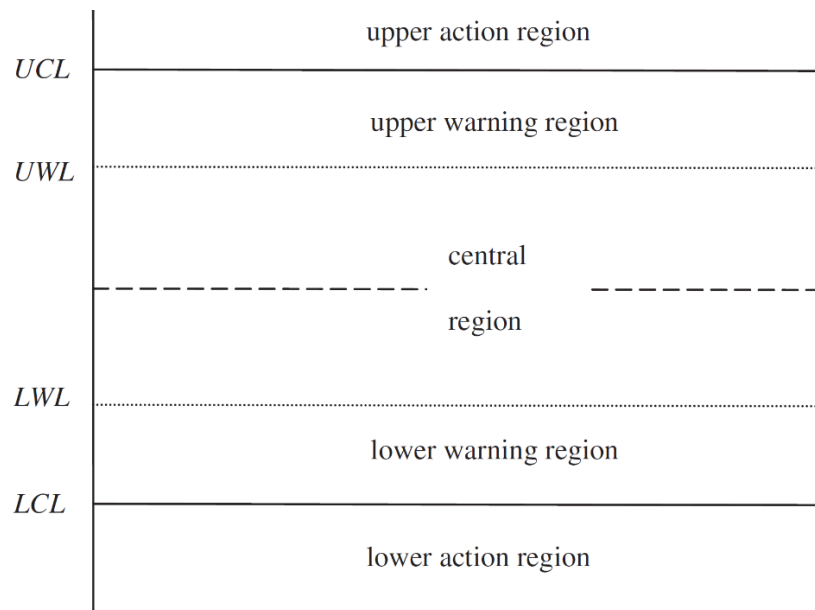


Figure 2.1 Feature of side-sensitivity with five regions

The side-sensitive synthetic \bar{X} chart provides the out-of-control signal when a second point falls beyond the warning limits which is not far from the first point and at the same time falls on the same side of the centre line, CL . However, it does not provide the signal when the points fall beyond the warning limits but are not on the same side of the CL . Based on the results obtained, it can be concluded that the side-sensitive synthetic \bar{X} chart outperformed the non-side-sensitive synthetic \bar{X} chart for both increasing and decreasing shift sizes. In fact, it was also able to give the out-of-control signal with 30% faster detection speed than the existing synthetic \bar{X} chart.

Shongwe and Graham (2018) extended the work of Machado and Costa (2014b) by modifying a side-sensitive synthetic \bar{X} chart into four regions instead of five regions. The modified side-sensitive charting regions are upper non-conforming (above the UCL), upper conforming (between the CL and UCL), lower conforming (between the CL and LCL) and lower non-conforming (below the LCL). An illustration of the feature of side sensitivity with four regions is shown in Figure 2.2.

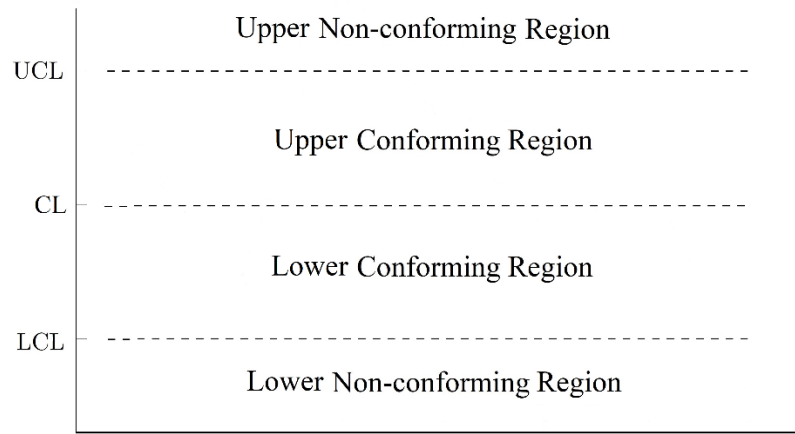


Figure 2.2 Feature of side-sensitivity with four regions

It generates an out-of-control signal when all the consecutive points fall on the same side of the CL . The objective of the study was to compare the performance of the proposed chart with the existing synthetic \bar{X} chart for non-side-sensitive, standard side-sensitive (upper non-conforming, conforming and lower non-conforming) by Davis and Woodall (2002) and revised side-sensitive by Machado and Costa (2014b). Based on the results obtained, it can be observed that the modified side-sensitive synthetic \bar{X} chart outperformed the other three synthetic \bar{X} charts for zero-state and steady-state. Besides, it was also being recognized as a strong contender to real life applications where the existing synthetic \bar{X} charts are currently being applied.

Yeong et al. (2018b) introduced the economic and economic-statistical designs of the synthetic- γ chart for practitioners in order to minimize the implementation cost of using a control chart. The proposed synthetic- γ chart of the zero-state was first compared with the synthetic- γ chart using cyclical and condition steady-states followed by the comparison with another three control charts, the Shewhart- γ , EWMA- γ and CUSUM- γ charts in terms of ARL and $EARL$ based on the values of $L \in \{1, 2, \dots, 30\}$ and $n \in \{2, 3, \dots, 30\}$ for the purpose of saving costs. For the first comparison, the proposed

synthetic- γ chart of the zero-state provided lower cost than the synthetic- γ chart for cyclical and conditional steady-states. For the second comparison, both economic and economic statistical designs of the synthetic- γ chart outperformed all three control charts in terms of the *ARL* performance. For the performance based on the *EARL*, the economic design of synthetic- γ chart performed the best among the four control charts. However, the economic-statistical design of synthetic- γ chart outperformed the Shewhart- γ chart only.

Guo and Wang (2018) proposed an *ARL*-unbiased Shewhart- γ chart for monitoring the two-sided shifts in the coefficient of variation. Furthermore, the researchers also introduced another control chart, the *ARL*-unbiased synthetic- γ chart where only a *LCL* was required in the *CRL* sub-chart for the purpose of improving the first proposed chart. A comparison between these two proposed charts was made in terms of *ARL* performance for $n \in \{5, 10, 15\}$, $\gamma_0 \in \{0.05, 0.10, 0.15\}$ and $\tau \in \{0.50, 0.65, 0.80, 0.90, 1.00, 1.25, 1.50, 2.00, 2.50, 4.00\}$. Based on the values of the *ARL* obtained, the results showed that the proposed *ARL*-unbiased synthetic- γ chart outperformed the proposed *ARL*-unbiased Shewhart- γ chart.

Tran et al. (2018) developed a one-sided synthetic control chart for monitoring the squared coefficient of variation with measurement errors for the purpose of improving the existing synthetic- γ chart which was introduced by Calzada and Scariano (2013). The authors created two one-sided synthetic- γ^2 charts for detecting both increasing and decreasing shifts using $\gamma_0 \in \{0.05, 0.10, 0.15\}$ and $\tau \in \{0.50, 0.75, 0.90, 1.10, 1.25, 1.50\}$. In order to meet the requirements of practical application, the steady-state case was

also taken into consideration. It is observed that the precision error, η and the accuracy error, θ had a negative effect on the charts in general. Furthermore, the increase in the quantity of repeated measurements on every item did not show a clear increase in the performance of the chart even though the standard error was associated with the ARL_1 . This explains that there was no significant reduction in the impact of measurement errors by the increase in the quantity of measurements of each item.

The development of synthetic chart for monitoring the coefficient of variation does not just focus on univariate processes, it is also extended to multivariate processes when there are two or more than two quality variables to be monitored by the control chart. Khaw et al. (2019) introduced the synthetic chart by monitoring the multivariate coefficient of variation (MCV) and assessed the proposed chart in terms of ARL , $SDRL$ and $EARL$ criteria based on number of quality variables, $p \in \{2, 3\}$, $n \in \{5, 10, 15\}$, $\tau \in \{1.10, 1.25, 1.50, 1.75, 2.00, 2.25, 2.50, 3.00\}$ and $\gamma_0 \in \{0.10, 0.30, 0.50\}$. A comparison was conducted between the proposed synthetic MCV chart with the Shewhart MCV and run sum MCV charts. The outcomes demonstrated that the synthetic MCV chart outperformed the other two MCV charts for most cases in terms of the performance of ARL and $EARL$. However, according to the $SDRL$ performance, Shewhart MCV chart had the least value compared to the proposed chart particularly for large shift sizes. For the implementation of a control chart using an actual industrial example, a comparison was made between the proposed synthetic MCV and Shewhart MCV charts. The outcomes showed that the synthetic MCV chart was able to provide earlier detection of out-of-control conditions compared to the Shewhart MCV chart which was unable to detect any out-of-control condition.

Rakitzis et al. (2019) studied several kinds of synthetic charts that are available in the literature for both zero-state and steady-state. For example, synthetic charts monitoring the process mean, synthetic charts monitoring the variation, synthetic charts for joint monitoring of mean and variance, synthetic charts monitoring the mean time between events, economic and economic-statistical designs for synthetic charts, synthetic charts for attribute data and multivariate synthetic charts. Generally, it can be observed that a synthetic chart is very useful to practitioners in real life applications when they decide to wait for the second point to fall in the non-conforming region in order to give the out-of-control signal. Besides, the synthetic charts with the feature of side sensitivity are found to perform better than those non-side-sensitive synthetic charts for normal processes even though there are not many studies regarding side sensitivity that has been done.

Yeong et al. (2021) evaluated the synthetic- γ chart based on different percentiles of the run length and proposed the *MRL*-based design for the synthetic- γ chart. The results showed that the evaluation of synthetic- γ chart's actual performance should not solely rely on *ARL* as the variation of run length was large particularly for in-control and out-of-control percentiles of small shift sizes. In addition, the synthetic- γ chart outperformed the *VSS- γ* and *Shewhart- γ* charts for *MRL*-based designs for all shift sizes. Furthermore, for small shift sizes, it also outperformed the *MRL*-based design for the *EWMA- γ* chart, although the *ARL*-based design for *EWMA- γ* chart showed better performance than the *ARL*-based design for the synthetic- γ chart.

Yahaya et al. (2022) introduced the scheme of *VSS* for non-side-sensitive synthetic chart to monitor the coefficient of variation. The proposed chart was assessed in terms of the performance of *ARL* and *EARL* and compared with synthetic- γ , *VSS- γ* , *VSS- γ^2* , *EWMA- γ^2* , *EWMA- γ* and *Shewhart- γ* charts. It is observed that the proposed chart

had shown significant improvement by outperforming synthetic- γ , VSS- γ and Shewhart- γ charts for all cases. It also showed better performance than VSS EWMA- γ^2 and EWMA- γ^2 charts for moderate and large shift sizes but not for very small shift sizes.

A summary of the development of synthetic chart which have been described in this subsection is presented in Table 2.3 below.

Table 2.3 Classification of synthetic charts according to their use

Synthetic Chart	Quality Characteristic/Process Parameter/Design Type	Author(s) and Year
For variables (parametric setup)	Mean	Wu and Spedding (2000), Calzada and Scariano (2001), Davis and Woodall (2002), Khoo et al. (2008) Aparisi and De Luna (2009), Castagliola and Khoo (2009), Scariano and Calzada (2009), Wu et al. (2010), Zhang et al. (2011), Khoo et al. (2012), Rakitzis et al. (2019)
	Mean and variance (joint monitoring)	Costa and Rahim (2006), Costa et al. (2009)
	Mean time between events	Scariano and Calzada (2003)
	Variable charting parameters	Song and Park (2005), Lee and Lim (2005), Chen and Huang (2006)
	Double sampling	Khoo et al. (2010), Calzada and Scariano (2013), Guo and Wang (2018), Tran et al. (2018), Khaw et al. (2019), Yeong et al. (2021)
	Coefficient of variation	Machado and Costa (2014b), Shongwe and Graham (2018)
	Side-sensitive	Yeong et al. (2018b), Yahaya et al. (2022)
	Economic and economic-statistical designs	
For attributes	Fraction/number of nonconforming	Wu et al. (2001)

By referring to the outcomes of different control charts monitoring the coefficient of variation mentioned in Section 2.2 and the synthetic charts in the current subsection, it is proven that the synthetic chart outperforms most of the control charts for small, moderate

and large shift sizes except for EWMA chart which demonstrates better performance than the synthetic chart for small and moderate shift sizes. Conversely, a synthetic chart with the feature of side sensitivity performs better than the existing synthetic chart without the feature of side sensitivity for all shift sizes. However, there are no studies regarding the synthetic- γ chart with the feature of side sensitivity that can be found in the literature. Therefore, the study of the side-sensitive synthetic chart for monitoring the coefficient of variation is proposed in this thesis.

2.4 Performance Measures of Control Charts

In order to evaluate the actual performance of a control chart, performance measures such as the *ARL*, *SDRL*, *MRL*, *EARL* and *EMRL* are commonly adopted in the literature. These performance measures are not only adopted by control charts monitoring the coefficient of variation, but are also commonly used by control charts monitoring other parameters. Adegoke et al. (2019) proposed a multivariate homogeneously weighted moving average control chart (MHWMA) to monitor the mean vector and *ARL* was selected as the performance measure to evaluate the proposed chart. It was then compared with other multivariate control charts in terms of *ARL* performance. Li et al. (2019) chose *ARL* and *SDRL* to investigate the two one-sided CUSUM charts to monitor a process with dependent count data with inflation or deflation of zeros. Aly et al. (2022) introduced an AEWMA to monitor a process of zero-inflated Poisson distribution and the proposed chart was evaluated in terms of *ARL* and *SDRL*.

Similar to the coefficient of variation charts, *EARL* is chosen as the alternative performance measure of the control chart for unknown shift size. Mim et al. (2019) selected the *ARL* and *EARL* as the performance measures for evaluating the proposed side-sensitive group runs control chart for detecting the shift in the process mean using

auxiliary information. You et al. (2020) studied the EWMA median chart with known and estimated process parameters based on the *ARL* and *EARL*. Abubakar et al. (2022) used a bivariate normal distribution to design a run sum control chart to monitor the ratio of population means and the performance of the proposed chart was assessed in terms of the *ARL* and *EARL*. Li et al. (2022) proposed a generally weighted moving average (GWMA) control chart with measurement errors by using two strategies which were the adjusted control limits and additive measurement error model to liaise with measurement errors. The performance of the proposed chart was evaluated in terms of the *ARL* and *EARL* through Monte Carlo simulations. Talordphop et al. (2022) introduced mixed Tukey modified EWMA – moving average control chart (MMEM-TCC) for monitoring the process mean under symmetric and non-symmetric distributions. *ARL*, *SDRL*, *MRL* and *EARL* were selected as the performance measures for assessing the performance of the proposed chart through Monte Carlo simulations. Malela-Majika et al. (2022a) chose *ARL*, *SDRL*, *MRL* and *EARL* as the performance measures to evaluate the performance of the proposed multivariate TEWMA (MTEWMA) chart using extensive simulations. Saha et al. (2023) assessed the proposed side-sensitive group runs *t* chart based on the performance of *ARL* and *EARL* and compared with other existing *t* charts.

If the run length distribution of a control chart is skewed, evaluation in terms of *ARL* alone may generate a misleading interpretation of the chart's real performance. Therefore, *MRL* is the appropriate performance measure for skewed run length distribution. Gao et al. (2019) studied a run sum *S* chart and selected the *ARL* and *MRL* as the performance measures to evaluate the chart. The performance measures *ARL*, *SDRL* and *MRL* were chosen by Taboran et al. (2020) for evaluating the proposed nonparametric MME-TCC chart for detecting the shifts in mean. De Araujo Lima-Filho & Mariano Bayer (2021) developed a Kumaraswamy control chart to monitor double bounded data for example

rates and proportions and its performance was evaluated based on the *ARL*, *SDRL* and *MRL* using Monte Carlo simulations. Taboran and Sukparungsee (2023) introduced the EWMA-double moving average control chart (EWMA-DMA) for detecting the shifts in mean with normal, laplace, exponential and gamma distributions. The proposed chart was evaluated based on the *ARL* and *MRL* by using Monte Carlo simulations.

If the run length distribution of a control chart is skewed and the shift size is unknown, *EMRL* can be selected as an alternative performance measure. Tang et al. (2019) studied the performance of AEWMA median chart with measurement errors based on *ARL*, *EARL* and *EMRL*. Chong et al. (2022) evaluated an optimal EWMA median chart with known and estimated parameters in terms of *MRL* and *EMRL* performances. Qiao et al. (2022) studied two one-sided exponential EWMA charts and evaluated the proposed chart based on *MRL* and *EMRL*. Tuh et al. (2022) have chosen *EMRL* as the performance measure to evaluate the performance of the optimal statistical design of the double sampling *np* chart. Malela-Majika et al. (2022b) proposed the TEWMA with fixed and random explanatory variables to monitor the univariate and multivariate profiles. The performance of the proposed chart was evaluated based on the *ARL*, *SDRL*, *MRL*, *EARL*, *EMRL* and expected standard deviation of the run length (*ESDRL*). Lee et al. (2023) chose *MRL* and *EMRL* as the performance measures to evaluate the synthetic *c* charts with known and estimated process parameters.

A summary of the selected performance measures for evaluating the performance of control charts which have been described in this subsection is presented in Table 2.4 below.

Table 2.4 Usage of performance measures for control chart

Year	Arthor(s)	Control Chart	Performance Measure
2019	Adegoke et al.	MHWMA	<i>ARL</i>
	Li et al.	CUSUM	<i>ARL, SDRL</i>
	Mim et al.	Side-sensitive Group Runs	<i>ARL, EARL</i>
	Gao et al.	Run Sum	<i>ARL, MRL</i>
	Tang et al.	AEWMA	<i>ARL, EARL, EMRL</i>
2020	You et al.	EWMA	<i>ARL, EARL</i>
	Taboran et al.	MME-TCC	<i>ARL, SDRL, MRL</i>
2021	Lima-Filho & Bayer	Kumuraswamy	<i>ARL, SDRL, MRL</i>
2022	Aly et al.	AEWMA	<i>ARL, SDRL</i>
	Abubakar et al.	Run Sum	<i>ARL, EARL</i>
	Li et al.	GWMA	<i>ARL, EARL</i>
	Talordphop et al.	MMEM-TCC	<i>ARL, SDRL, MRL, EARL</i>
	Malela-Majika et al.	TEWMA	<i>ARL, SDRL, MRL, EARL</i>
	Chong et al.	EWMA	<i>MRL, EMRL</i>
	Qiao et al.	EWMA	<i>MRL, EMRL</i>
	Tuh et al.	Double Sampling	<i>EMRL</i>
2023	Malela-Majika et al.	TEWMA	<i>ARL, SDRL, MRL, EARL, EMRL, ESDRL</i>
	Saha et al.	Side-sensitive Group Runs	<i>ARL, EARL</i>
	Taboran & Sukparungsee	EWMA-DMA	<i>ARL, MRL</i>
	Lee et al.	Synthetic	<i>MRL, EMRL</i>

Since *ARL*, *SDRL*, *MRL*, *EARL* and *EMRL* are the commonly used performance measures in evaluating control charts in general, therefore, these five performance measures are selected for assessing the performance of the side-sensitive synthetic- γ chart which is the proposed control chart in this thesis.

CHAPTER 3: METHODOLOGY

3.0 Introduction

This chapter commences with a thorough explanation of the sample coefficient of variation's distributional characteristics followed by a detailed explanation of the characteristics of the competing control charts, the Shewhart- γ and EWMA- γ^2 charts. It then delves into an exhaustive analysis of the side-sensitive synthetic- γ chart. This is followed by a discussion on how Markov chains are used to assess the *ARL*, *SDRL* and *EARL*. The chapter then details the process of creating the designs based on *ARL* and *EARL* for the side-sensitive synthetic- γ chart. Since the distribution of run length may be skewed, particularly for the in-control and out-of-control run lengths with small shift sizes, relying solely on *ARL* and *SDRL* to assess the chart performance may be insufficient. As a result, it is to investigate the run length distribution's percentiles. This chapter presents the methodology to determine the side-sensitive synthetic- γ chart's run length percentiles. Finally, the chapter concludes with the design of the side-sensitive synthetic- γ chart based on the *MRL* and *EMRL*. The procedure of simulation for validating the results obtained by the side-sensitive synthetic- γ chart is also included in this chapter, after the description on the algorithms for each design. As a summary, a flow chart of the methodology for the side-sensitive synthetic- γ chart is illustrated in Figure 3.1 for a better view as well as to link the methodologies with the achievement of each research objective stated in Section 1.5.

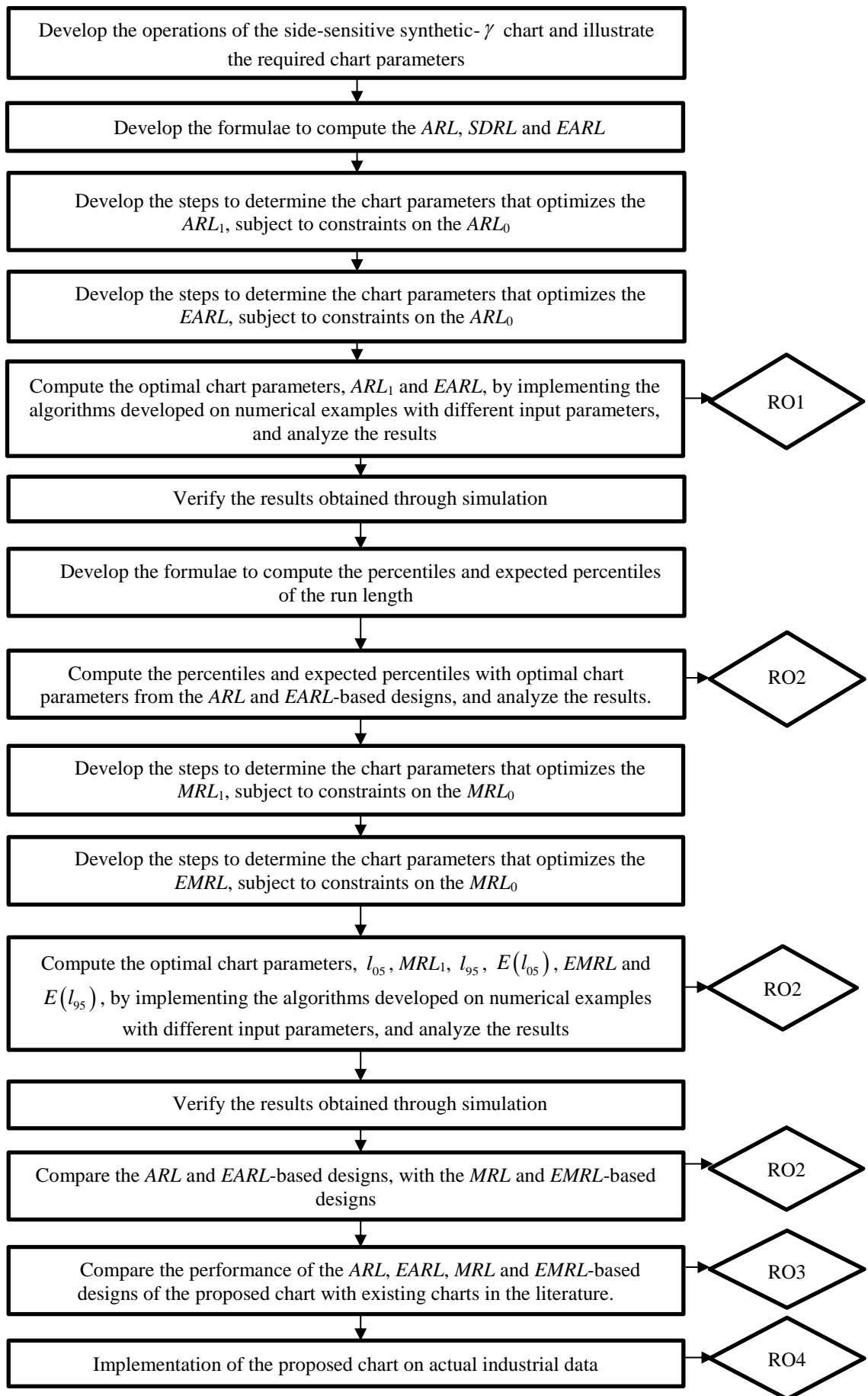


Figure 3.1 Flow chart of the methodology of the side-sensitive synthetic- γ chart

3.1 Sample Coefficient of Variation's Distribution Properties

Let X be a positive random variable that follows a normal distribution with mean, μ and variance, σ^2 . Suppose a sample of n identically distributed independent random variables are taken from X , and is defined as $\{X_1, X_2, \dots, X_n\}$. The computation of the $\hat{\gamma}$, is shown below:

$$\hat{\gamma} = \frac{S}{\bar{X}}, \quad (3.1)$$

where S represents the sample standard deviation and \bar{X} is the sample mean of n random variables taken from X , $\{X_1, X_2, \dots, X_n\}$. The sample mean, \bar{X} and the sample standard deviation, S can be computed as follows:

$$\bar{X} = \frac{\sum_{i=1}^n X_i}{n}, \quad (3.2)$$

and

$$S = \sqrt{\frac{\sum_{i=1}^n (X_i - \bar{X})^2}{n-1}}. \quad (3.3)$$

where $n \in \{1, 2, 3, \dots\}$ which is determined by the user.

According to Castagliola et al. (2011), the computation of the cumulative distribution function (c.d.f) for the sample coefficient of variation, can be obtained as below:

$$F_{\hat{\gamma}}(x|n, \gamma) = 1 - F_t\left(\frac{\sqrt{n}}{x} \middle| n-1, \frac{\sqrt{n}}{\gamma}\right), \quad (3.4)$$

where γ is the coefficient of variation and the c.d.f of the non-central t -distribution is represented by $F_t\left(\cdot \middle| n-1, \frac{\sqrt{n}}{\gamma}\right)$ with the degrees of freedom $n-1$ and non-centrality

parameter $\frac{\sqrt{n}}{\gamma}$. Regarding the inverse c.d.f of sample coefficient of variation, it is found

by inverting the existing $F_{\hat{\gamma}}(x|n, \gamma)$ as follows:

$$F_{\hat{\gamma}}^{-1}(\alpha|n, \gamma) = \frac{\sqrt{n}}{F_t^{-1}\left(1-\alpha|n-1, \frac{\sqrt{n}}{\gamma}\right)}, \quad (3.5)$$

where $F_t^{-1}\left(\cdot|n-1, \frac{\sqrt{n}}{\gamma}\right)$ is the inverse c.d.f of the non-central t -distribution with $n-1$

degrees of freedom and non-centrality parameter $\frac{\sqrt{n}}{\gamma}$. The information on how the

Equations (3.4) and (3.5) are being derived is demonstrated in the following paragraphs.

The distribution of $\frac{\sqrt{n}}{\hat{\gamma}}$ is required in order to obtain Equations (3.4) and (3.5).

Since $X \sim N(\mu, \sigma^2)$, then $\bar{X} \sim N\left(\mu, \frac{\sigma^2}{n}\right)$ and $\frac{(n-1)S^2}{\sigma^2} \sim \chi^2(n-1)$. With a few

mathematical operations,

$$\begin{aligned} \frac{\sqrt{n}}{\hat{\gamma}} &= \sqrt{n} \left(\frac{\bar{X}}{S} \right) = \frac{\sqrt{n} \left(\frac{\bar{X} - \mu}{\sigma} \right) + \sqrt{n} \left(\frac{\mu}{\sigma} \right)}{\frac{S}{\sigma}} \\ &= \frac{\left(\frac{\bar{X} - \mu}{\sigma/\sqrt{n}} \right) + \frac{\sqrt{n}}{\hat{\gamma}}}{\sqrt{\frac{(n-1)S^2}{\sigma^2} \div (n-1)}}. \end{aligned} \quad (3.6)$$

By making use of the fact when $T = \frac{Z + \mu}{\sqrt{\frac{V}{v}}}$, where $Z \sim N(0, 1)$ and $V \sim \chi^2(v)$, T will

follow a non-central t -distribution with degrees of freedom v and non-centrality parameter

μ , it can be observed from Equation (3.6) that $\frac{\sqrt{n}}{\hat{\gamma}}$ follows a non-central t -distribution with degrees of freedom $(n-1)$ and non-centrality parameter $\frac{\sqrt{n}}{\gamma}$.

$F_{\hat{\gamma}}(x|n, \gamma)$ in Equation (3.4) can be obtained as follows:

$$\begin{aligned} F_{\hat{\gamma}}(x|n, \gamma) &= P(\hat{\gamma} \leq x) \\ &= P\left(\frac{\sqrt{n}}{\hat{\gamma}} \geq \frac{\sqrt{n}}{x}\right) \\ &= 1 - F_t\left(\frac{\sqrt{n}}{x} \mid n-1, \frac{\sqrt{n}}{\gamma}\right), \end{aligned}$$

as displayed in Equation (3.4), since $\frac{\sqrt{n}}{\hat{\gamma}}$ will follow a non-central t -distribution with degrees of freedom $(n-1)$ and non-centrality parameter $\frac{\sqrt{n}}{\gamma}$. In order to obtain

$F_{\hat{\gamma}}^{-1}(\alpha|n, \gamma)$, define

$$F_{\hat{\gamma}}^{-1}(\alpha|n, \gamma) = y \tag{3.7}$$

where α is the quantile of $\hat{\gamma}$ obtained from the c.d.f of $\hat{\gamma}$.

By referring to Equation (3.7),

$$F_{\hat{\gamma}}(y|n, \gamma) = \alpha. \tag{3.8}$$

By replacing Equation (3.4) into Equation (3.8),

$$F_t\left(\frac{\sqrt{n}}{y} \mid n-1, \frac{\sqrt{n}}{\gamma}\right) = 1 - \alpha. \tag{3.9}$$

From Equation (3.9),

$$\frac{\sqrt{n}}{y} = F_t^{-1} \left(1 - \alpha \mid n-1, \frac{\sqrt{n}}{\gamma} \right)$$

$$y = \frac{\sqrt{n}}{F_t^{-1} \left(1 - \alpha \mid n-1, \frac{\sqrt{n}}{\gamma} \right)}. \quad (3.10)$$

It is proven that $F_{\hat{\gamma}}^{-1}(\alpha \mid n, \gamma) = \frac{\sqrt{n}}{F_t^{-1} \left(1 - \alpha \mid n-1, \frac{\sqrt{n}}{\gamma} \right)}$ as demonstrated in Equation (3.5)

since $y = F_{\hat{\gamma}}^{-1}(\alpha \mid n, \gamma)$.

3.2 Shewhart- γ and EWMA- γ^2 Charts

The Shewhart- γ chart is the first control chart to monitor the coefficient of variation which was proposed by Kang et al. (2007). The present sample coefficient of variation is used by the chart to determine whether the process is in-control or out-of-control. This chart consists of three lines, the *CL*, *UCL* and *LCL*. Kang et al. (2007) recommended to place the *CL* at the in-control target value of the coefficient of variation whereas the *UCL* and *LCL* are fixed using probability limits. The limits of the Shewhart- γ chart are calculated as

$$LCL = F_{\hat{\gamma}}^{-1} \left(\frac{\alpha_0}{2} \mid n, \gamma_0 \right) \quad (3.11)$$

and

$$UCL = F_{\hat{\gamma}}^{-1} \left(1 - \frac{\alpha_0}{2} \mid n, \gamma_0 \right) \quad (3.12)$$

where $F_{\hat{\gamma}}^{-1}(\cdot)$ is defined in Equation (3.5), α_0 denotes the type I error rate set by the user and γ_0 is the in-control coefficient of variation.

Castagliola et al. (2011) introduced the EWMA- γ^2 charts which is one of the commonly used control charts to monitor the coefficient of variation. The EWMA- γ^2 chart monitors the chart statistics Z_k , defined as

$$Z_k = (1 - \lambda)Z_{k-1} + \lambda\hat{\gamma}_k^2 \quad (3.13)$$

with k representing time that is defined as $k \in \{1, 2, 3, \dots\}$ and λ denotes the smoothing constant which is determined by the user. The control limits are calculated as

$$LCL = \mu_0(\hat{\gamma}^2) - K\sqrt{\frac{\lambda}{2-\lambda}}\sigma_0(\hat{\gamma}^2) \quad (3.14)$$

$$UCL = \mu_0(\hat{\gamma}^2) + K\sqrt{\frac{\lambda}{2-\lambda}}\sigma_0(\hat{\gamma}^2) \quad (3.15)$$

where K denotes the control limit coefficient which is determined by the user. Since there is no closed form for $\mu_0(\hat{\gamma}^2)$ and $\sigma_0(\hat{\gamma}^2)$, the following approximations proposed by Breunig (2001) will be used, i.e.

$$\mu_0(\hat{\gamma}^2) = \gamma_0^2 \left(1 - \frac{3\gamma_0^2}{n}\right) \quad (3.16)$$

and

$$\sigma_0(\hat{\gamma}^2) = \sqrt{\gamma_0^4 \left(\frac{2}{n-1} + \gamma_0^2 \left(\frac{4}{n} + \frac{20}{n(n-1)} + \frac{75\gamma_0^2}{n^2} \right) \right) - (\mu_0(\hat{\gamma}^2) - \gamma_0^2)^2}. \quad (3.17)$$

3.3 Side-sensitive Synthetic- γ Chart

The synthetic- γ chart without side sensitivity currently in use is designed to monitor a process by counting the quantity of conforming samples between two consecutive non-conforming samples. The quantity of conforming samples which includes the ending non-conforming sample, is referred to as the *CRL*. The synthetic- γ chart will generate an out-

of-control signal when the CRL is less than and equal to the threshold, L which is predetermined by the practitioner.

The LCL and UCL of the synthetic- γ chart are calculated as

$$LCL = \mu_0(\hat{\gamma}) - K\sigma_0(\hat{\gamma}), \quad (3.18)$$

and

$$UCL = \mu_0(\hat{\gamma}) + K\sigma_0(\hat{\gamma}), \quad (3.19)$$

where K denotes the control limit coefficient and $K \in \mathbb{R}$, while $\mu_0(\hat{\gamma})$ and $\sigma_0(\hat{\gamma})$ are the in-control mean and standard deviation of the sample coefficient of variation, respectively. Although $\mu_0(\hat{\gamma})$ and $\sigma_0(\hat{\gamma})$ have no closed forms, the following approximations by Reh and Scheffler (1996) will be used, i.e.

$$\mu_0(\hat{\gamma}) \approx \gamma_0 \left[1 + \frac{1}{n} \left(\gamma_0^2 - \frac{1}{4} \right) + \frac{1}{n^2} \left(3\gamma_0^4 - \frac{\gamma_0^2}{4} - \frac{7}{32} \right) + \frac{1}{n^3} \left(15\gamma_0^6 - \frac{3\gamma_0^4}{4} - \frac{7\gamma_0^2}{32} - \frac{19}{128} \right) \right], \quad (3.20)$$

and

$$\sigma_0(\hat{\gamma}) \approx \gamma_0 \sqrt{\frac{1}{n} \left(\gamma_0^2 + \frac{1}{2} \right) + \frac{1}{n^2} \left(8\gamma_0^4 + \gamma_0^2 + \frac{3}{8} \right) + \frac{1}{n^3} \left(69\gamma_0^6 + \frac{7\gamma_0^4}{2} + \frac{3\gamma_0^2}{4} + \frac{3}{16} \right)}. \quad (3.21)$$

For the existing synthetic- γ chart without the feature of side sensitivity, a sample is classified as non-conforming when the sample coefficient of variation falls either below the LCL or above the UCL . The synthetic- γ chart is comprised of two sub-charts: the coefficient of variation sub-chart and the CRL sub-chart. The coefficient of variation sub-chart is constructed in a similar manner to the Shewhart- γ chart, where the sample coefficient of variations are plotted against the LCL and UCL . Conversely, the CRL sub-chart calculates the quantity of conforming samples between consecutive non-conforming samples.

An illustration of the *CRL* sub-chart of the existing synthetic- γ chart is shown in Figure 3.2. The figure reveals that the 3rd and 7th samples are non-conforming samples because the sample coefficient of variation of these samples appear in the non-conforming region, where the 3rd sample appears in the region above the *UCL* and the 7th sample appears in the region below the *LCL*. The remaining samples are classified as conforming samples. *CRL*₁, the quantity of conforming samples until the existence of the first non-conforming sample occurs, is three, in order to give the chart a headstart. *CRL*₂, on the other hand, captures the quantity of conforming samples between the 4th and 7th samples since the first non-conforming sample appears in the region above the *UCL*, whereas the second non-conforming sample is found in the region below the *LCL*. It is worth nothing that a synthetic- γ chart without the feature of side sensitivity considers both aforementioned samples as non-conforming.

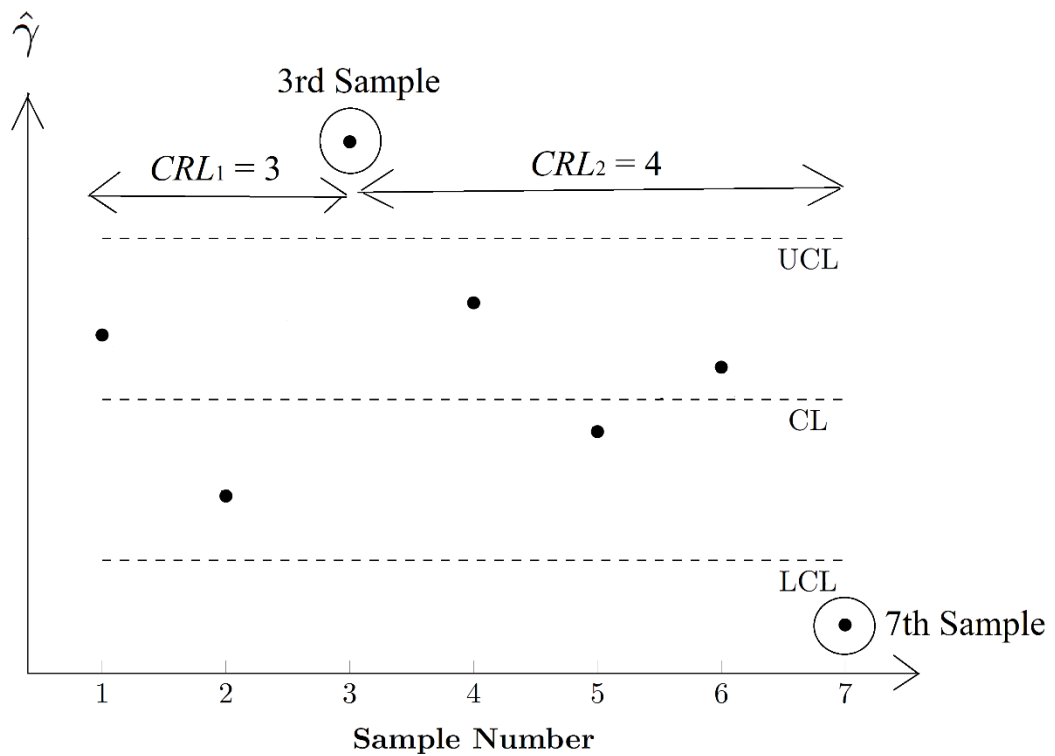


Figure 3.2 *CRL* sub-chart of the existing synthetic- γ chart

The side-sensitive synthetic- γ chart which is proposed in this thesis has a different approach compared to the non-side-sensitive version. In the side-sensitive synthetic- γ chart, the second sample is classified as non-conforming only if it appears in the region below the LCL (above the UCL), just like the first non-conforming sample which appears in the region below the LCL (above the UCL). Otherwise, the second sample is treated as a conforming sample if it falls within the control limits (between the UCL and LCL) or above the UCL (below the LCL). The importance of defining non-conforming samples as samples that fall on the same side of the non-conforming region is it allows for more stringent control limits to be adopted without increasing the number of false alarms, compared to the existing synthetic- γ chart where less stringent control limits needs to be adopted to control the number of false alarms, as false alarms from both sides of the non-conforming region needs to be controlled. As a result of adopting more stringent control limits, the side-sensitive synthetic- γ chart will require less samples to detect a shift. Furthermore, since processes usually experience either positive or negative shifts in γ_0 , and not both, successive non-conforming samples will either fall above the UCL or below the LCL , hence setting this requirement will not make process monitoring more restrictive.

Figure 3.3 illustrates the CRL sub-chart of the side-sensitive synthetic- γ chart. Like the existing synthetic- γ chart, CRL_1 calculates the quantity of conforming samples until the occurrence of the first non-conforming sample, which means CRL_1 is two in Figure 3.3. For the calculation of CRL_2 , only samples that appear in the region above the UCL are classified as non-conforming because the 2nd sample occurs in the region which is above the UCL . Therefore, the 5th sample is classified as a conforming sample despite appearing in the region below the LCL , whereas the 7th sample is classified as a non-

conforming sample as it occurs in the same region as the 2nd sample, which is the region above the *UCL*. Thus, CRL_2 is five, as demonstrated in Figure 3.3.

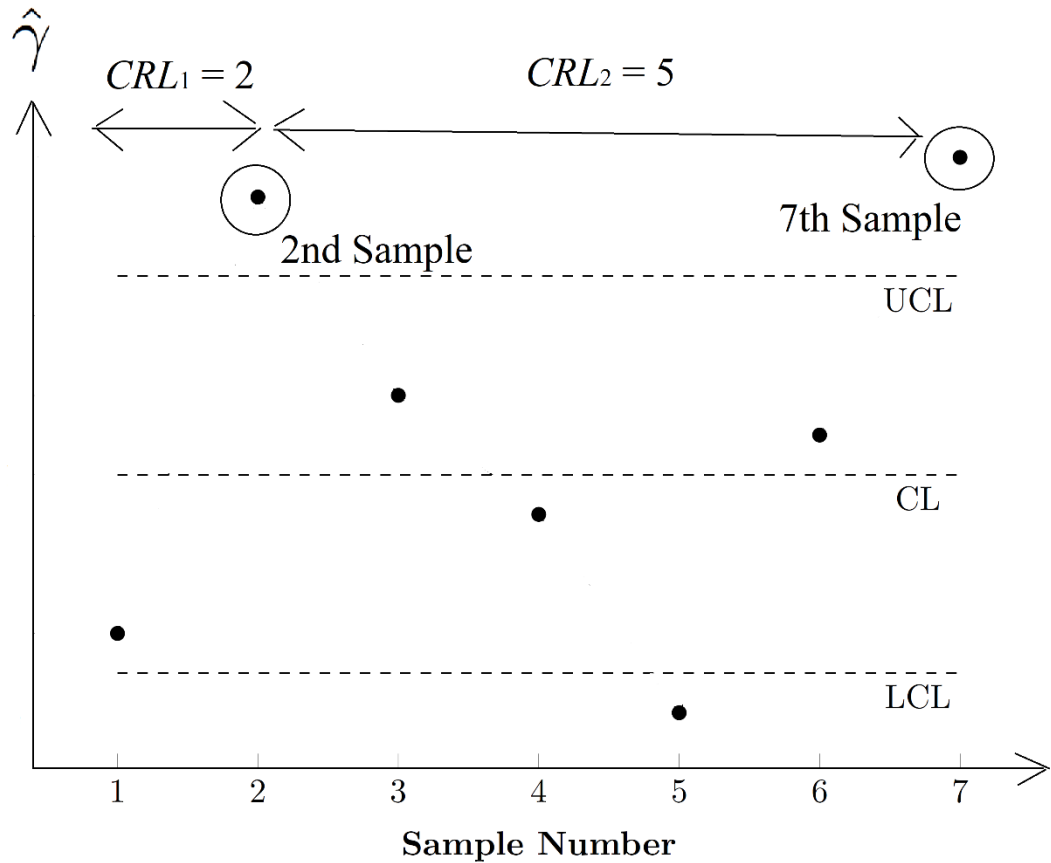


Figure 3.3 *CRL* sub-chart of the side-sensitive synthetic- γ chart

Similarly, when the first non-conforming sample appears in the region which is below the *LCL*, the second sample must occur in the region below the *LCL* as well in order to be classified as non-conforming, otherwise this sample is deemed as a conforming sample. Therefore, following the same approach as illustrated in Figure 3.3, *CRL* calculates the quantity of samples between consecutive samples that appear in the region which is below the *LCL*.

3.4 Performance Measures

A number of performance measures are chosen for evaluating the performance of the proposed side-sensitive synthetic- γ chart. The in-control *ARL* (ARL_0) measures the average quantity of samples required by the chart to produce a false alarm whereas the out-of-control *ARL* (ARL_1) measures the average quantity of samples required by the chart to produce an actual out-of-control signal. For out-of-control *SDRL* ($SDRL_1$), it measures the variability of the quantity of samples required to signal an out-of-control condition. If the proposed chart's run length distribution is skewed, the *MRL* performance of the chart will be studied as the *ARL* performance alone does not show the true performance of the proposed chart (Gan, 1993). The in-control *MRL* (MRL_0) measures the 50th percentile of the quantity of samples required to produce a false alarm while the out-of-control *MRL* (MRL_1) measures the 50th percentile of the quantity of samples required to give an actual out-of-control signal.

Shift size is required to be specified as an exact value for *ARL*, *SDRL* and *MRL*. However, it is not possible to specify the shift size in most practical scenarios due to a lack of data particularly for the out-of-control data since the assignable cause(s) are removed immediately once they are detected. Therefore, this thesis is considering another two performance criteria which are the *EARL* and *EMRL*. $EARL_1$ measures the expected average quantity of samples required to produce the out-of-control signal whereas $EMRL_1$ measures the 50th expected percentile of the quantity of samples required to spot the out-of-control condition. Hence, in this thesis, the proposed side-sensitive synthetic- γ chart's performance will be assessed based on the *ARL*, *SDRL*, *MRL*, *EARL* and *EMRL* as well as the run length distribution's percentiles.

3.5 Markov Chain Approach

For evaluating the performance of the proposed side-sensitive synthetic- γ chart, Markov chains are adopted. In this approach, 0 denotes a sample that appears in the conforming region which is the region between the LCL and UCL , $\underline{1}$ denotes a sample that appears in the region below the LCL and 1 denotes a sample that appears in the region above the UCL . The Markov chain's states are defined using a string of L samples as below:

State 1	: $\underline{1}00..0$
State 2	: $0\underline{1}0..0$
State 3	: $00\underline{1}..0$
	\vdots
State L	: $000..\underline{1}$
State $L + 1$: $00..00$
State $L + 2$: $0..001$
State $L + 3$: $0..010$
	\vdots
State $2L$: $010..0$
State $2L + 1$: $100..0$
State $2L + 2$: Signalling state (for instance, the states where the chart generates an out-of-control condition)

Based on the defined states described in the previous paragraph, the formation of a transition probability matrix with dimension $(2L + 2) \times (2L + 2)$ is shown below:

It is worth noting that the $F_{\hat{\gamma}}(\cdot)$ in Equations (3.23) to (3.25) is well-defined in Equation (3.4).

In general, the transition probability matrix, \mathbf{P} is defined as shown below:

1. Every entry of column $L + 2$ contains B^+ for rows 1 to $L + 1$.
2. Every entry of column L contains B^- for rows $L + 1$ to $2L + 1$.
3. Every entry of column $2L + 2$ contains B^- for rows 1 to L .
4. Every entry of column $2L + 2$ contains B^+ for rows $L + 2$ to $2L + 1$.
5. Every entry below the diagonal contains A for rows 1 to $L - 1$.
6. Every entry of rows 1, $L + 1$ and $2L + 1$ contains A for column $L + 1$.
7. Every entry above the diagonal contains A for rows $L + 3$ to $2L + 1$.
8. The entry of column $2L + 2$ and row $2L + 2$ is 1.
9. The remaining entries are zero.

The absorbing state of $2L + 2$ in \mathbf{P} is considered an out-of-control state. In order to obtain a matrix \mathbf{Q} of transient probabilities, the last row and column in \mathbf{P} can be removed. The computation of the ARL and $SDRL$ involves the application of factorial moments for the quantity of steps needed for the process to reach the absorbing state. The factorial moments can be obtained from the works of Neuts (1984) or Latouche and Ramaswami (1999) to compute the ARL and $SDRL$ as follows:

$$ARL = \mathbf{q}^T (\mathbf{I} - \mathbf{Q})^{-1} \mathbf{1}, \quad (3.26)$$

and

$$SDRL = \sqrt{2\mathbf{q}^T (\mathbf{I} - \mathbf{Q})^{-2} \mathbf{Q} \mathbf{1} - ARL^2 + ARL}, \quad (3.27)$$

where \mathbf{q} represents the $(2L + 1) \times 1$ vector of initial probabilities associated with the transient states while \mathbf{I} is an identity matrix, and $\mathbf{1}$ is a vector of ones. For this thesis, the

condition of zero-state is assumed, with \mathbf{q} having a value of one for the $(L+2)^{\text{th}}$ element and zeros for the remaining elements. The ARL_1 and $SDRL_1$ can be obtained by substituting $\gamma = \tau\gamma_0$ into Equations (3.26) and (3.27) to yield the out-of-control \mathbf{Q} . Similarly, the ARL_0 and $SDRL_0$ can be computed by substituting $\gamma = \gamma_0$ into Equations (3.26) and (3.27) to yield the in-control \mathbf{Q} . The derivation of Equations (3.26) and (3.27) is provided in the following paragraphs.

The probability mass function (p.m.f) for the quantity of transitions until the transition probability matrix \mathbf{P} arrives at the absorbing state needs to be derived in order to obtain the ARL and $SDRL$. The reason is each transition denotes a sample being taken, hence the quantity of transitions until arriving at the absorbing state shows the quantity of samples taken until it arrives at the out-of-control state. The time to absorption for \mathbf{P} follows a distribution of discrete phase-type with the parameters (\mathbf{Q}, \mathbf{q}) .

By denoting $p_i^{(n)} = \text{Prob}(X_n = i)$ as the probability that the Markov chain will be in State i after n transitions, with i being transient, these probabilities are then being collected in a vector $\mathbf{p}^{(n)} = (p_0^{(n)} \quad p_1^{(n)} \quad \dots \quad p_{2L+1}^{(n)})$. For a discrete time Markov chain, it is known that

$$\mathbf{p}^{(n)} = \mathbf{p}^{(n-1)}\mathbf{Q} = \mathbf{q}^T\mathbf{Q}^n. \quad (3.28)$$

The event that absorption appears at time x can be partitioned using the union of the events that the chain is in state i ($i = 0, 1, \dots, 2L+1$) at time $(x-1)$, and that absorption occurs at i at time x . The probability of the earlier event is denoted as $p_i^{(x-1)}$ whereby the

probability of the second event is denoted as r_i . Therefore, the p.m.f can be defined as follows:

$$f(x) = \sum_{i=0}^{2L+1} p_i^{(x-1)} r_i = \mathbf{p}^{(x-1)} \mathbf{r} = \mathbf{q}^T \mathbf{Q}^{(x-1)} \mathbf{r}, \text{ for } x > 0. \quad (3.29)$$

By referring to the p.m.f in Equation (3.29), the generating function of X can be found as follows:

$$\begin{aligned} H(z) &= \sum_{x=0}^{\infty} z^x f(x) \\ &= q_{2L+2} + \sum_{x=1}^{\infty} z^x \mathbf{q}^T \mathbf{Q}^{(x-1)} \mathbf{r}, \end{aligned} \quad (3.30)$$

where q_{2L+2} denotes the initial probability for the Markov chain to begin in the absorbing state, i.e. the out-of-control state. From the geometric series $\sum_{i=0}^{\infty} x^i = \frac{1}{1-x}$, Equation (3.30)

can be deduced from the following equation:

$$q_{2L+2} + \sum_{x=1}^{\infty} z^x \mathbf{q}^T \mathbf{Q}^{(x-1)} \mathbf{r} = q_{2L+2} + z \mathbf{q}^T (\mathbf{I} - z \mathbf{Q})^{-1} \mathbf{r}. \quad (3.31)$$

Next, the factorial moments can be found by the generating function's consecutive differentiation as follow:

$$\begin{aligned} E[X(X-1)\dots(X-(k-1))] &= \left. \frac{d^{H(z)} k}{dz^k} \right|_{z=1} \\ &= k! \mathbf{q}^T (\mathbf{I} - \mathbf{Q})^{-k} \mathbf{Q}^{(k-1)} \mathbf{1}. \end{aligned} \quad (3.32)$$

From Equation (3.32),

$$E[X] = \mathbf{q}^T (\mathbf{I} - \mathbf{Q})^{-1} \mathbf{1}. \quad (3.33)$$

$$E[X(X-1)] = 2\mathbf{q}^T (\mathbf{I} - \mathbf{Q})^{-2} \mathbf{Q}\mathbf{1}. \quad (3.34)$$

Since *ARL* and *SDRL* are equal to $E[X]$ and $\sqrt{\text{Var}[X]}$, respectively,

$$\begin{aligned} ARL &= E[X] \\ &= \mathbf{q}^T (\mathbf{I} - \mathbf{Q})^{-1} \mathbf{1}, \end{aligned} \quad (3.35)$$

whereas

$$\begin{aligned} SDRL &= \sqrt{E[X(X-1)] - (E[X])^2 + E[X]} \\ &= \sqrt{2\mathbf{q}^T (\mathbf{I} - \mathbf{Q})^{-2} \mathbf{Q}\mathbf{1} - ARL^2 + ARL}, \end{aligned} \quad (3.36)$$

as described in Equations (3.26) and (3.27).

To compute the *ARL*, knowing the exact value of shift size is necessary. However, estimating the exact value for shift size can be challenging in practical situations, according to Castagliola et al. (2011). To address this issue, this thesis proposes using the *EARL* criterion as an alternative performance measure when the exact value of shift size is unknown. When computing the *EARL*, the shift size can be estimated as a possible range of values $(\tau_{\min}, \tau_{\max})$, rather than an exact value.

The *EARL* can be calculated as shown below:

$$EARL = \int_{\tau_{\min}}^{\tau_{\max}} f_{\tau}(\tau) ARL(\tau, \gamma_0, n_s, n_L, W_1, W_2, K_1, K_2) d\tau \quad (3.37)$$

where $f_{\tau}(\tau)$ represents the probability density function (p.d.f) of shift size. Ideally, the exact distribution of $f_{\tau}(\tau)$ is known to quality practitioners, but in reality, it is often problematic to obtain because of the lack of historical data. Besides, the distribution of

shift size is case-dependent and can change over time. In this thesis, a uniform distribution of $f_{\tau}(\tau)$ over $(\tau_{\min}, \tau_{\max})$ is assumed, which is suggested by Sparks (2003). This is because it is generally assumed explicitly (Domangue and Patch, 1991; Sparks, 2003) or implicitly (Reynolds Jr and Stoumbos, 2004) that all process shifts appear with equal probability. Siddall (1983) has also recommended using a uniform distribution if there is complete uncertainty about a random variable except for its bounds. The integral in Equation (3.37) cannot be solved analytically, so this thesis employs the Gauss-Legendre quadrature to solve it. Kovvali (2011) provides a detailed explanation of the Gauss-Legendre quadrature.

3.6 *ARL* and *EARL*-based Designs

Moving forward, let's examine how the proposed side-sensitive synthetic- γ chart's optimal chart parameters, including the optimal L , LCL and UCL , can be determined. This thesis considers two criteria for this purpose. Initially, the chart parameters are selected to minimize the ARL_1 . Nevertheless, this criterion needs the exact value of shift size to be identified, which may not always be available. Therefore, the chart parameters are selected to minimize the $EARL$ in the second approach. In both approaches, the ARL_0 constraint must be met.

For the first approach, the procedure to obtain the optimal chart parameters is defined as follows:

1. Specify the values of n , γ_0 , ARL_0 and τ .
2. Set $L = 1$.
3. By using mathematical approaches, find K which provides $ARL_0 = \xi$, where ξ is decided by the practitioner, followed by the computation of the LCL and UCL from Equations (3.18) and (3.19), respectively.

4. Compute the ARL_1 from Equation (3.26) based on the obtained LCL and UCL in Step 3.
5. Increase L by 1.
6. Repeat Steps 3 to 5 until the ARL_1 for $L + 1$ is greater than the ARL_1 for L . This combination of (L, LCL, UCL) will represent the optimal chart parameters for the side-sensitive synthetic- γ chart.

The procedure to obtain the optimal chart parameters (L, LCL, UCL) as described above can be summarized as

$$(L^*, LCL^*, UCL^*) = \arg \min_{(L, LCL, UCL)} ARL_1(\tau, L, LCL, UCL | n, \gamma_0). \quad (3.38)$$

subject to $ARL_0(L, LCL, UCL | n, \gamma_0) = \xi$.

In order to validate the performance of the side-sensitive synthetic- γ chart with the optimal chart parameters (L^*, LCL^*, UCL^*) , 10,000 simulation trials will be performed, where each trial consists of the following procedures:

1. Initialize $m = 1$.
2. Initialize $i = 1$
3. Generate n values of X from a normal distribution with mean μ and standard deviation σ , such that $\gamma_0 = \frac{\sigma}{\mu}$ if the ARL_0 is being validated, and $\gamma_1 = \frac{\sigma}{\mu}$ if the ARL_1 is being validated.
4. Compute the \bar{X} and S , and compute the $\hat{\gamma}$ as $\frac{S}{\bar{X}}$.
5. If $LCL < \hat{\gamma} < UCL$, add one to m and i , and return to Step 3. Else, proceed to Step 6.

6. If the current $\hat{\gamma}$ is the first sample that falls above the UCL or below the LCL , then:

- i. if $i \leq L$, the run length is equals to m and the loop for this trial ends,
- ii. if $i > L$, add one to m and return to Step 2.

Else, if the current $\hat{\gamma}$ is not the first sample that falls above the UCL or below the LCL , then proceed to Step 7.

7. If the most recent non-conforming sample falls above the UCL , then:

- i. if $\hat{\gamma} > UCL$ and $i \leq L$, the run length is equals to m and the loop for this trial ends,
- ii. if $\hat{\gamma} > UCL$ and $i > L$, add one to m and return to Step 2,
- iii. if $\hat{\gamma} < LCL$, add one to m and i , and return to Step 3.

Conversely, if the most recent non-conforming sample falls below the LCL ,

- i. if $\hat{\gamma} > UCL$, add one to m and i , and return to Step 3,
- ii. if $\hat{\gamma} < LCL$ and $i \leq L$, the run length is equals to m and the loop for this trial ends,
- iii. if $\hat{\gamma} < LCL$ and $i > L$, add one to m and return to Step 2.

The ARL is calculated by averaging the run lengths obtained for each trial whereas the $SDRL$ is obtained by computing the standard deviation of the run lengths obtained from all trials.

The optimal chart parameters based on the $EARL$ criterion are found according to the procedure below:

1. Specify the values of n and γ_0 . Instead of specifying the exact value of τ , a possible range of values, the τ_{\min} and τ_{\max} are required to be specified.

2. Set $L = 1$.
3. By using mathematical approaches, find K which provides $ARL_0 = \xi$, where ξ is decided by the practitioner, followed by the computation of the LCL and UCL from Equations (3.18) and (3.19), respectively.
4. Compute the $EARL_1$ from Equation (3.37) based on the obtained LCL and UCL in Step 3.
5. Increase L by 1.
6. Instead of finding the combination that minimizes the ARL_1 value, the optimal (L, LCL, UCL) is the one that minimizes the value of $EARL_1$.

It is worth noting that all the steps described above are similar to the design based on ARL , except for the first, fourth and sixth steps.

The procedure to obtain the optimal chart parameters (L, LCL, UCL) as described above can be summarized as

$$(L^{**}, LCL^{**}, UCL^{**}) = \arg \min_{(L, LCL, UCL)} EARL_1(\tau_{\min}, \tau_{\max}, L, LCL, UCL | n, \gamma_0). \quad (3.39)$$

subject to $ARL_0(L, LCL, UCL | n, \gamma_0) = \xi$.

In order to validate the performance of the side-sensitive synthetic- γ chart with the optimal chart parameters $(L^{**}, LCL^{**}, UCL^{**})$, 10,000 simulation trials will be performed, where each trial consists of the following procedures:

1. Initialize $m = 1$.
2. Initialize $i = 1$

3. Generate n values of X from a normal distribution with mean μ and standard deviation σ , such that $\gamma_0 = \frac{\sigma}{\mu}$ if the $EARL_0$ is being validated, and $\gamma_1 = \frac{\sigma}{\mu}$ if the $EARL_1$ is being validated. Shift size needs to be generated randomly from a uniform distribution between δ_{\min} and δ_{\max} , in order to obtain the γ_1 .
4. Compute the \bar{X} and S , and compute the $\hat{\gamma}$ as $\frac{S}{\bar{X}}$.
5. If $LCL < \hat{\gamma} < UCL$, add one to m and i , and return to Step 3. Else, proceed to Step 6.
6. If the current $\hat{\gamma}$ is the first sample that falls above the UCL or below the LCL , then:
 - i. if $i \leq L$, the run length is equals to m and the loop for this trial ends,
 - ii. if $i > L$, add one to m and return to Step 2.
 Else, if the current $\hat{\gamma}$ is not the first sample that falls above the UCL or below the LCL , then proceed to Step 7.
7. If the most recent non-conforming sample falls above the UCL , then:
 - i. if $\hat{\gamma} > UCL$ and $i \leq L$, the run length is equals to m and the loop for this trial ends,
 - ii. if $\hat{\gamma} > UCL$ and $i > L$, add one to m and return to Step 2,
 - iii. if $\hat{\gamma} < LCL$, add one to m and i , and return to Step 3.
 Conversely, if the most recent non-conforming sample falls below the LCL ,
 - i. if $\hat{\gamma} > UCL$, add one to m and i , and return to Step 3,
 - ii. if $\hat{\gamma} < LCL$ and $i \leq L$, the run length is equals to m and the loop for this trial ends,
 - iii. if $\hat{\gamma} < LCL$ and $i > L$, add one to m and return to Step 2.

The *EARL* is calculated by averaging the run lengths obtained for each trial.

However, there is another concern that should be taken into consideration. If the proposed side-sensitive synthetic- γ chart's distribution of run length in this thesis is found to be skewed, which may most likely show a skewness to the right especially for small shift size, then the *ARL* is not an appropriate performance measure for evaluation purposes. In such cases, the *MRL* will be a better performance measure as the skewness of the distribution of run length has minimal effects on *MRL*. Therefore, it is important to analyze the distribution of run length for the side-sensitive synthetic- γ chart and implement both *ARL* and *MRL* as the performance measures. The next subsection describes how the distribution of the run length can be obtained.

3.7 Run Length Distribution's Percentiles

To analyze the run length distribution's percentiles for the side-sensitive synthetic- γ chart, it is necessary to determine the probability mass function (p.m.f) and c.d.f of the run length. These functions can be calculated as follows (Latouche and Ramaswami, 1999):

$$f_{RL}(l) = P(RL = l) = \mathbf{q}^T (\mathbf{Q}^{l-1}) \mathbf{r}, \quad (3.40)$$

and

$$F_{RL}(l) = P(RL \leq l) = 1 - \mathbf{q}^T (\mathbf{Q}^{l-1}) \mathbf{1}, \quad (3.41)$$

where $l \in (1, 2, 3, \dots)$, \mathbf{q} and $\mathbf{1}$ are well-defined in Equations (3.27) and (3.28), whereas \mathbf{Q} and \mathbf{r} are well-described in Section 3.3.

One way to determine the $(100\theta)^{\text{th}}$ percentile of the distribution of run length for the side-sensitive synthetic- γ chart is to find the values of l_θ in Equation (3.18) such that (Gan, 1993)

$$P(RL \leq l_\theta - 1) \leq \theta \text{ and } P(RL \leq l_\theta) > \theta, \quad (3.42)$$

where $0 < \theta < 1$. For instance, the *MRL* can be derived from Equation (3.42) by setting $\theta = 0.5$. When calculating the transition probabilities of \mathbf{Q} through Equations (3.23) to (3.25), the in-control percentiles can be attained by fixing $\gamma = \gamma_0$ while the out-of-control percentiles are attained by fixing $\gamma = \tau\gamma_0$, where τ represents the shift size.

To compute the run length's percentiles when the value of shift size is uncertain, the run length distribution's expected percentiles, $E(l_\theta)$ are assessed. This is because the exact value of shift size may be unknown, and possibly will vary based on several stochastic models (Castagliola et al., 2011). The computation of $E(l_\theta)$ requires shift size to be stated as a range of possible values, $(\tau_{\min}, \tau_{\max})$, rather than a specific value. $E(l_\theta)$ can be calculated as shown below:

$$E(l_\theta) = \int_{\tau_{\min}}^{\tau_{\max}} f_\tau(\tau) l_\theta(\tau) d\tau, \quad (3.43)$$

where $f_\tau(\tau)$ is the p.d.f of shift size. One assumption made is that $f_\tau(\tau)$ follows a uniform distribution that is continuous over the interval $(\tau_{\min}, \tau_{\max})$, as suggested by Castagliola et al. (2011). This thesis applies the Gauss-Legendre quadrature method for solving the integral in Equation (3.43). This method is explained in detail in Kovvali (2011).

3.8 *MRL* and *EMRL*-based Designs

Since the implementation of the side-sensitive synthetic- γ chart using the *ARL* and *EARL* may provide misleading results due to skewed run length distributions, thus, this subsection suggests an alternative approach that involves finding the optimal chart parameters that minimize the MRL_1 and $EMRL_1$, while meeting the constraints of the MRL_0 .

In order to obtain the optimal chart parameters using the design based on *MRL*, the following algorithms are employed.

1. Determine the values for γ_0 , n and τ .
2. Initialize $L = 1$.
3. Solve Equation (3.41) for K by setting $l_{0.5} = \xi$ and $\tau = 1$, followed by the computation of the *LCL* and *UCL* from Equations (3.18) and (3.19), respectively. This (*LCL*, *UCL*) combination will result in $MRL_0 = \xi$.
4. $l_{0.5}$ that fulfills Equation (3.42) for the γ_0 , n and τ determined in Step 1 is searched numerically based on the obtained (*LCL*, *UCL*) in Step 3. The $MRL_1 = l_{0.5}$.
5. Increase L by 1.
6. Repeat Steps 3 to 5 until the MRL_1 for $L + 1$ is greater than the MRL_1 for L . The optimal chart parameters for the side-sensitive synthetic- γ chart that is designed based on *MRL* will be determined by this (L , *LCL*, *UCL*) combination. In case multiple (L , *LCL*, *UCL*) combinations result in the lowest MRL_1 , the combination with the minimum difference between the 5th and 95th percentiles of the out-of-control run length distribution, denoted by $l_{0.05}$ and $l_{0.95}$, respectively, will be selected as the optimal chart parameters.

The procedure to obtain the optimal chart parameters (L, LCL, UCL) as described above can be summarized as

$$\left(L^{***}, LCL^{***}, UCL^{***} \right) = \arg \min_{(L, LCL, UCL)} MRL_1(\tau, L, LCL, UCL | n, \gamma_0). \quad (3.44)$$

subject to $MRL_0(L, LCL, UCL | n, \gamma_0) = \xi$.

In order to validate the performance of the side-sensitive synthetic- γ chart with the optimal chart parameters $(L^{***}, LCL^{***}, UCL^{***})$, 10,000 simulation trials will be performed, where each trial consists of the following procedures:

1. Initialize $m = 1$.
2. Initialize $i = 1$
3. Generate n values of X from a normal distribution with mean μ and standard deviation σ , such that $\gamma_0 = \frac{\sigma}{\mu}$ if the ARL_0 is being validated, and $\gamma_1 = \frac{\sigma}{\mu}$ if the ARL_1 is being validated.
4. Compute the \bar{X} and S , and compute the $\hat{\gamma}$ as $\frac{S}{\bar{X}}$.
5. If $LCL < \hat{\gamma} < UCL$, add one to m and i , and return to Step 3. Else, proceed to Step 6.
6. If the current $\hat{\gamma}$ is the first sample that falls above the UCL or below the LCL , then:
 - i. if $i \leq L$, the run length is equals to m and the loop for this trial ends,
 - ii. if $i > L$, add one to m and return to Step 2.

Else, if the current $\hat{\gamma}$ is not the first sample that falls above the UCL or below the LCL , then proceed to Step 7.
7. If the most recent non-conforming sample falls above the UCL , then:

- i. if $\hat{\gamma} > UCL$ and $i \leq L$, the run length is equals to m and the loop for this trial ends,
- ii. if $\hat{\gamma} > UCL$ and $i > L$, add one to m and return to Step 2,
- iii. if $\hat{\gamma} < LCL$, add one to m and i , and return to Step 3.

Conversely, if the most recent non-conforming sample falls below the LCL ,

- i. if $\hat{\gamma} > UCL$, add one to m and i , and return to Step 3,
- ii. if $\hat{\gamma} < LCL$ and $i \leq L$, the run length is equals to m and the loop for this trial ends,
- iii. if $\hat{\gamma} < LCL$ and $i > L$, add one to m and return to Step 2.

The MRL is obtained from the median of the run lengths obtained from all trials.

The design based on MRL is only feasible when the value of shift size is known beforehand. To address situations where shift size cannot be specified, this thesis also investigates the design based on $EMRL$. In order to get the optimal chart parameters using the design based on $EMRL$, the following algorithms are employed.

1. Determine the values for γ_0 , n , τ_{\min} and τ_{\max} .
2. Initialize $L = 1$.
3. Solve Equation (3.42) for K by setting $l_{0.5} = \xi$ and $\tau = 1$, followed by the computation of the LCL and UCL from Equations (3.18) and (3.19), respectively. This (LCL, UCL) combination will result in $MRL_0 = \xi$.
4. Evaluate $E(l_{0.5})$ from Equation (3.43) based on the obtained (LCL, UCL) in Step 3. The $EMRL = E(l_{0.5})$.
5. Increase L by 1.

6. Repeat Steps 3 to 5 until the $EMRL$ for $L + 1$ is greater than the $EMRL$ for L .

This particular (L, LCL, UCL) combination is being selected as the best optimal chart parameters for the side-sensitive synthetic- γ chart that is designed based on $EMRL$.

It is worth noting that although many of the steps outlined in the previous paragraph for the design based on MRL remain the same, the first, fourth and sixth steps, are substituted with the steps described above.

The procedure to obtain the optimal chart parameters (L, LCL, UCL) as described above can be summarized as

$$\left(L^{****}, LCL^{****}, UCL^{****} \right) = \arg \min_{(L, LCL, UCL)} EMRL_1(\tau_{\min}, \tau_{\max}, L, LCL, UCL | n, \gamma_0). \quad (3.45)$$

subject to $MRL_0(L, LCL, UCL | n, \gamma_0) = \xi$.

In order to validate the performance of the side-sensitive synthetic- γ chart with the optimal chart parameters $(L^{****}, LCL^{****}, UCL^{****})$, 10,000 simulation trials will be performed, where each trial consists of the following procedures:

1. Initialize $m = 1$.
2. Initialize $i = 1$
3. Generate n values of X from a normal distribution with mean μ and standard

deviation σ , such that $\gamma_0 = \frac{\sigma}{\mu}$ if the $EARL_0$ is being validated, and $\gamma_1 = \frac{\sigma}{\mu}$ if

the $EARL_1$ is being validated. Shift size needs to be generated randomly from

a uniform distribution between δ_{\min} and δ_{\max} , in order to obtain the γ_1 .

4. Compute the \bar{X} and S , and compute the $\hat{\gamma}$ as $\frac{S}{\bar{X}}$.
5. If $LCL < \hat{\gamma} < UCL$, add one to m and i , and return to Step 3. Else, proceed to Step 6.
6. If the current $\hat{\gamma}$ is the first sample that falls above the UCL or below the LCL , then:
 - i. if $i \leq L$, the run length is equals to m and the loop for this trial ends,
 - ii. if $i > L$, add one to m and return to Step 2.
 Else, if the current $\hat{\gamma}$ is not the first sample that falls above the UCL or below the LCL , then proceed to Step 7.
7. If the most recent non-conforming sample falls above the UCL , then:
 - i. if $\hat{\gamma} > UCL$ and $i \leq L$, the run length is equals to m and the loop for this trial ends,
 - ii. if $\hat{\gamma} > UCL$ and $i > L$, add one to m and return to Step 2,
 - iii. if $\hat{\gamma} < LCL$, add one to m and i , and return to Step 3.
 Conversely, if the most recent non-conforming sample falls below the LCL ,
 - i. if $\hat{\gamma} > UCL$, add one to m and i , and return to Step 3,
 - ii. if $\hat{\gamma} < LCL$ and $i \leq L$, the run length is equals to m and the loop for this trial ends,
 - iii. if $\hat{\gamma} < LCL$ and $i > L$, add one to m and return to Step 2.

The *EMRL* is obtained from the median of the run lengths obtained from all trials.

CHAPTER 4: ANALYSIS AND INTERPRETATION OF RESULT

4.0 Introduction

As described in the previous chapter, this chapter begins with the side-sensitive synthetic- γ chart that is designed based on the ARL and $EARL$, where the optimal chart parameters (L , LCL , UCL) are obtained to minimize the ARL_1 and $EARL_1$. Next, the analysis of the run length distribution's percentiles for the ARL and $EARL$ -based designs is clearly shown in the second subsection. For a side-sensitive synthetic- γ chart that is designed based on the MRL and $EMRL$, the optimal chart parameters (L , LCL , UCL) that minimizes the MRL_1 and $EMRL_1$ are obtained and elaborated in the following subsection after the analysis of the run length's percentiles. The performance of the proposed side-sensitive synthetic- γ chart is then compared with other coefficient of variation charts in terms of the ARL , $SDRL$, $EARL$, MRL and $EMRL$. Lastly, the implementation of the proposed charts using a real industry example will be explained in the final subsection.

4.1 ARL and $EARL$ -based Designs

This subsection presents the optimal values of L , LCL and UCL values for a given sample size, $n \in \{5, 7, 10, 15, 20\}$, shift size, $\tau \in \{1.1, 1.2, 1.3, 1.4, 1.5, 1.6, 1.7, 1.8, 1.9, 2.0\}$ and in-control coefficient of variation, $\gamma_0 \in \{0.05, 0.10, 0.15, 0.20\}$, as well as the corresponding ARL_1 , $SDRL_1$ and $EARL_1$. The ARL_0 is set as 370.4 as it is commonly used in many studies (see, for example, Calzada and Scariano, 2013). Practitioners are welcomed to use the optimal chart parameters presented in this subsection for these values of sample size, shift size and in-control coefficient of variation, while for other values, the methodology described in Chapter 3 can be used.

It is worth noting that these specific values of sample size, shift size and in-control coefficient of variation are being considered in this thesis since they are the frequently chosen values in numerous existing coefficient of variation charts, such as in Castagliola et al. (2013(b)), Zhang et al. (2014) and Muhammad et al. (2018), thereby facilitating comparison with other coefficient of variation charts. Furthermore, detecting a downward shift, $\tau < 1$, is not so important as it shows a decrease in variability. Hence, this thesis focuses solely on detecting an upward shift, $\tau > 1$, as it leads to a higher ratio of standard deviation to mean, i.e. a higher $\frac{\sigma}{\mu}$, indicating an increase in process variability caused by the presence of assignable cause(s).

The optimal chart parameters, L , LCL , UCL , and the corresponding ARL_1 and $SDRL_1$ values for $n \in \{5, 7, 10, 15, 20\}$ and $\tau \in \{1.1, 1.2, 1.3, 1.4, 1.5, 1.6, 1.7, 1.8, 1.9, 2.0\}$ are presented in Tables 4.1 and 4.2 for $\gamma_0 \in \{0.05, 0.10\}$ and $\gamma_0 \in \{0.15, 0.20\}$, respectively. The results obtained were validated by simulation with 10,000 trials as described in Section 3.6.

Table 4.1 The optimal chart parameters (L, LCL, UCL) of the side-sensitive synthetic- γ chart and the corresponding ARL_1 and $SDRL_1$ for $n \in \{5, 7, 10, 15, 20\}$, $\tau \in \{1.1, 1.2, 1.3, 1.4, 1.5, 1.6, 1.7, 1.8, 1.9, 2.0\}$ and $\gamma_0 \in \{0.05, 0.10\}$

τ	$\gamma_0 = 0.05$					$\gamma_0 = 0.10$				
	L	LCL	UCL	ARL_1	$SDRL_1$	L	LCL	UCL	ARL_1	$SDRL_1$
	$n = 5$									
1.1	42	0.0017	0.0924	64.74	84.69	42	0.0021	0.1863	65.20	85.30
1.2	23	0.0039	0.0902	21.35	27.11	23	0.0067	0.1817	21.58	27.43
1.3	15	0.0055	0.0885	10.18	12.25	15	0.0100	0.1784	10.31	12.42
1.4	11	0.0067	0.0873	6.07	6.83	11	0.0126	0.1758	6.15	6.94
1.5	8	0.0080	0.0860	4.18	4.44	8	0.0152	0.1732	4.23	4.52
1.6	7	0.0086	0.0855	3.16	3.09	7	0.0163	0.1721	3.20	3.15
1.7	6	0.0092	0.0849	2.56	2.32	6	0.0176	0.1708	2.59	2.36
1.8	5	0.0099	0.0841	2.17	1.85	5	0.0191	0.1692	2.20	1.89
1.9	5	0.0099	0.0841	1.91	1.47	5	0.0191	0.1692	1.93	1.50
2.0	4	0.0109	0.0832	1.72	1.27	4	0.0210	0.1674	1.74	1.30
	$n = 7$									
1.1	37	0.0116	0.0843	52.13	67.97	36	0.0225	0.1696	52.56	68.58
1.2	19	0.0136	0.0824	15.75	19.66	19	0.0264	0.1658	15.93	19.92
1.3	12	0.0150	0.0810	7.30	8.47	12	0.0292	0.1629	7.39	8.60
1.4	9	0.0158	0.0801	4.34	4.58	9	0.0310	0.1611	4.40	4.66
1.5	7	0.0166	0.0794	3.02	2.89	7	0.0326	0.1595	3.06	2.95
1.6	5	0.0176	0.0783	2.33	2.08	5	0.0347	0.1574	2.36	2.12
1.7	5	0.0176	0.0783	1.93	1.49	5	0.0347	0.1574	1.95	1.53
1.8	4	0.0183	0.0776	1.67	1.19	4	0.0362	0.1560	1.69	1.22
1.9	4	0.0183	0.0776	1.50	0.94	4	0.0362	0.1560	1.52	0.97
2.0	3	0.0192	0.0767	1.38	0.82	3	0.0380	0.1542	1.29	0.85
	$n = 10$									
1.1	35	0.0193	0.0780	41.27	53.44	35	0.0379	0.1568	51.55	53.83
1.2	16	0.0210	0.0762	11.43	13.91	16	0.0415	0.1532	11.56	14.08
1.3	10	0.0221	0.0752	5.19	5.68	10	0.0438	0.1509	5.26	5.77
1.4	7	0.0230	0.0743	3.12	3.02	7	0.0455	0.1492	3.16	3.08
1.5	5	0.0238	0.0735	2.22	1.91	5	0.0472	0.1476	2.25	1.96
1.6	4	0.0243	0.0730	1.76	1.33	4	0.0483	0.1464	1.78	1.36
1.7	4	0.0243	0.0730	1.50	0.94	4	0.0483	0.1464	1.52	0.97
1.8	3	0.0250	0.0723	1.34	0.75	3	0.0497	0.1450	1.35	0.77
1.9	3	0.0250	0.0723	1.24	0.58	3	0.0497	0.1450	1.25	0.60
2.0	3	0.0250	0.0723	1.17	0.47	3	0.0497	0.1450	1.18	0.48
	$n = 15$									
1.1	31	0.0259	0.0724	31.15	39.93	31	0.0513	0.1453	31.33	40.17
1.2	13	0.0274	0.0709	7.84	9.14	13	0.0544	0.1422	7.93	9.27
1.3	7	0.0285	0.0697	3.53	3.61	7	0.0567	0.1399	1.65	1.16
1.4	5	0.0286	0.0696	2.19	1.87	5	0.0580	0.1386	2.21	1.91
1.5	4	0.0296	0.0687	1.63	1.13	4	0.0588	0.1378	1.65	1.16
1.6	3	0.0301	0.0681	1.35	0.78	3	0.0600	0.1366	1.37	0.80
1.7	3	0.0301	0.0681	1.21	0.54	3	0.0600	0.1366	1.22	0.56
1.8	2	0.0309	0.0673	1.13	0.44	2	0.0616	0.1350	1.14	0.46
1.9	2	0.0309	0.0673	1.08	0.32	2	0.0616	0.1350	1.08	0.34
2.0	2	0.0309	0.0673	1.05	0.24	2	0.0616	0.1350	1.05	0.25
	$n = 20$									
1.1	27	0.0296	0.0691	24.98	31.76	27	0.0589	0.1386	25.14	31.98
1.2	10	0.0311	0.0676	5.92	6.72	10	0.0619	0.1356	6.00	6.82
1.3	6	0.0319	0.0668	2.70	2.52	6	0.0635	0.1340	2.74	2.58
1.4	4	0.0325	0.0662	1.74	1.30	4	0.0648	0.1327	1.76	1.33
1.5	3	0.0330	0.0657	1.36	0.79	3	0.0658	0.1317	1.37	0.81
1.6	3	0.0330	0.0657	1.19	0.50	3	0.0658	0.1317	1.19	0.51
1.7	2	0.0337	0.0650	1.10	0.37	2	0.0672	0.1303	1.10	0.38
1.8	2	0.0337	0.0650	1.05	0.25	2	0.0672	0.1303	1.05	0.26
1.9	2	0.0337	0.0650	1.03	0.17	2	0.0672	0.1303	1.03	0.18
2.0	2	0.0337	0.0650	1.01	0.12	2	0.0672	0.1303	1.02	0.13

Table 4.2 The optimal chart parameters (L, LCL, UCL) of the side-sensitive synthetic- γ chart and the corresponding ARL_1 and $SDRL_1$ for $n \in \{5, 7, 10, 15, 20\}$, $\tau \in \{1.1, 1.2, 1.3, 1.4, 1.5, 1.6, 1.7, 1.8, 1.9, 2.0\}$ and $\gamma_0 \in \{0.15, 0.20\}$

τ	$\gamma_0 = 0.15$					$\gamma_0 = 0.20$				
	L	LCL	UCL	ARL_1	$SDRL_1$	L	LCL	UCL	ARL_1	$SDRL_1$
	$n = 5$									
1.1	42	0.0042	0.2832	65.99	86.34	42	0.0059	0.3850	67.12	87.83
1.2	23	0.0072	0.2761	21.97	37.96	24	0.0035	0.3756	22.54	28.67
1.3	15	0.0125	0.2708	10.52	12.73	15	0.0118	0.3674	10.84	13.17
1.4	11	0.0165	0.2669	6.29	7.14	11	0.0173	0.3618	6.48	7.42
1.5	8	0.0206	0.2627	4.33	4.65	9	0.0210	0.3581	4.47	4.75
1.6	7	0.0224	0.2610	3.28	3.25	7	0.0257	0.3534	3.38	3.40
1.7	6	0.0244	0.2589	2.65	2.45	6	0.0286	0.3505	2.73	2.56
1.8	5	0.0268	0.2565	2.25	1.96	5	0.0320	0.3471	2.32	2.06
1.9	5	0.0268	0.2565	1.97	1.56	5	0.0320	0.3471	2.03	1.64
2.0	4	0.0298	0.2535	1.78	1.36	4	0.0363	0.3428	1.83	1.43
	$n = 7$									
1.1	36	0.0316	0.2572	53.33	69.62	36	0.0377	0.3483	54.48	71.15
1.2	19	0.0376	0.2512	16.26	20.37	19	0.0463	0.3397	16.74	21.05
1.3	12	0.0421	0.2467	7.56	8.83	12	0.0526	0.3334	7.80	9.18
1.4	9	0.0449	0.2439	4.50	4.80	9	0.0567	0.3293	4.65	5.02
1.5	7	0.0474	0.2414	3.13	3.05	7	0.0602	0.3258	3.24	3.19
1.6	5	0.0507	0.2380	2.41	2.20	6	0.0624	0.3236	2.49	2.22
1.7	5	0.0507	0.2380	1.99	1.59	5	0.0650	0.3210	2.05	1.67
1.8	4	0.0530	0.2358	1.72	1.27	4	0.0682	0.3178	1.77	1.35
1.9	4	0.0530	0.2358	1.54	1.01	4	0.0682	0.3178	1.59	1.07
2.0	3	0.0559	0.2329	1.42	0.89	3	0.0722	0.3137	1.46	0.95
	$n = 10$									
1.1	34	0.0555	0.2370	42.08	54.60	33	0.0711	0.3195	42.94	55.81
1.2	16	0.0609	0.2315	11.78	14.40	16	0.0786	0.3120	12.13	14.88
1.3	10	0.0645	0.2280	5.37	5.94	10	0.0835	0.3071	5.54	6.18
1.4	7	0.0672	0.2253	3.23	3.18	7	0.0874	0.3032	3.33	3.33
1.5	5	0.0697	0.2227	2.30	2.03	5	0.0910	0.2996	2.37	2.13
1.6	4	0.0715	0.2210	1.82	1.41	4	0.0935	0.2972	1.87	1.49
1.7	4	0.0715	0.2210	1.54	1.01	4	0.0935	0.2972	1.59	1.07
1.8	3	0.0737	0.2188	1.37	0.81	3	0.0966	0.2941	1.41	0.87
1.9	3	0.0737	0.2188	1.27	0.63	3	0.0966	0.2941	1.29	0.68
2.0	3	0.0737	0.2188	1.19	0.51	3	0.0866	0.2941	1.22	0.55
	$n = 15$									
1.1	30	0.0760	0.2191	31.67	40.71	30	0.0992	0.2948	32.24	41.49
1.2	13	0.0806	0.2145	8.09	9.49	13	0.1057	0.2883	8.32	9.82
1.3	8	0.0842	0.2109	3.66	3.80	7	0.1107	0.2833	3.78	3.97
1.4	5	0.0862	0.2089	2.26	1.98	5	0.1135	0.2805	2.34	2.08
1.5	4	0.0875	0.2076	1.68	1.21	4	0.1153	0.2787	1.73	1.28
1.6	3	0.0893	0.2059	1.39	0.84	3	0.1177	0.2763	1.43	0.90
1.7	3	0.0893	0.2059	1.24	0.59	3	0.1177	0.2763	1.26	0.63
1.8	2	0.0918	0.2034	1.15	0.49	3	0.1177	0.2763	1.17	0.46
1.9	2	0.0918	0.2034	1.09	0.36	2	0.1212	0.2728	1.11	0.39
2.0	2	0.0918	0.2034	1.06	0.27	2	0.1212	0.2728	1.07	0.30
	$n = 20$									
1.1	27	0.0875	0.2090	25.43	32.38	27	0.1149	0.2806	25.89	33.02
1.2	10	0.0921	0.2043	6.13	7.01	11	0.1208	0.2748	6.31	7.18
1.3	6	0.0946	0.2018	2.80	2.67	6	0.1249	0.2707	2.89	2.80
1.4	4	0.0966	0.1998	1.80	1.39	4	0.1277	0.2679	1.85	1.47
1.5	3	0.0981	0.1983	1.40	0.85	3	0.1297	0.2659	1.43	0.90
1.6	3	0.0981	0.1983	1.21	0.54	3	0.1297	0.2659	1.23	0.58
1.7	2	0.1002	0.1962	1.11	0.41	2	0.1326	0.2629	1.13	0.44
1.8	2	0.1002	0.1962	1.06	0.28	2	0.1326	0.2629	1.07	0.31
1.9	2	0.1002	0.1962	1.03	0.20	2	0.1326	0.2629	1.04	0.22
2.0	2	0.1002	0.1962	1.02	0.15	2	0.1326	0.2629	1.02	0.16

Tables 4.1 and 4.2 highlight a significant reduction in both the ARL_1 and $SDRL_1$ values as the sample size increases. For instance, in Table 4.1, when $n = 5$, $\tau = 1.1$ and $\gamma_0 = 0.05$, the ARL_1 and $SDRL_1$ values are 64.74 and 84.69, whereas, for $n = 20$ with the same values of shift size and in-control coefficient of variation, the corresponding ARL_1 and $SDRL_1$ values are 24.98 and 31.76, respectively. Thus, similar to other control charts, when the sample size increases, it results in better ARL_1 and $SDRL_1$ performances. Also, a greater sample size leads to smaller L and UCL , but greater LCL , particularly for small shift sizes. For instance, in Table 4.1, the optimal chart parameters, L , LCL , UCL , obtained are 42, 0.0017, 0.0924, respectively, for $n = 5$, $\tau = 1.1$ and $\gamma_0 = 0.05$, while the optimal chart parameters, L , LCL , UCL are 27, 0.0296, 0.0691, respectively, for $n = 20$ with the same values of shift size and in-control coefficient of variation. This indicates that a greater sample size results in a tighter region between LCL and UCL and has a smaller maximum quantity of conforming samples between two consecutive non-conforming samples for the control chart to provide an out-of-control signal.

The data in Tables 4.1 and 4.2 reveals that both the ARL_1 and $SDRL_1$ values decrease when the shift size increases. For instance, in Table 4.1, when $n = 5$, $\tau = 1.1$ and $\gamma_0 = 0.05$, the corresponding ARL_1 and $SDRL_1$ values are 64.74 and 84.69, respectively, while for $n = 5$, $\tau = 2.0$ and $\gamma_0 = 0.05$, the corresponding ARL_1 and $SDRL_1$ values are 1.72 and 1.27, respectively. Furthermore, an increase in shift size results in smaller optimal chart parameters, L and UCL , but a greater LCL value. For instance, in Table 4.1, the optimal chart parameters, L , LCL , UCL , obtained are 42, 0.0017, 0.0924, respectively, for $n = 5$, $\tau = 1.1$ and $\gamma_0 = 0.05$ whereas for $n = 5$, $\tau = 2.0$ and $\gamma_0 = 0.05$, the obtained optimal chart parameters, L , LCL , UCL , are 4, 0.0109, 0.0832, respectively.

It is also worth noting that an increase in the in-control coefficient of variation leads to slightly greater LCL , UCL , ARL_1 and $SDRL_1$ values. For instance, in Table 4.1, when $n = 5$, $\tau = 1.1$ and $\gamma_0 = 0.05$, the optimal chart parameters, LCL and UCL and the corresponding ARL_1 and $SDRL_1$ are 0.0017, 0.0924, 64.74 and 84.69, respectively, while for $n = 5$, $\tau = 1.1$ and $\gamma_0 = 0.20$ in Table 4.2, the optimal chart parameters, LCL and UCL and the corresponding ARL_1 and $SDRL_1$ are 0.0059, 0.3850, 67.12 and 87.83, respectively.

The optimal chart parameters presented in Tables 4.1 and 4.2 require the specific value of shift size but often, its precise value is unknown. To address this issue, this subsection provides the optimal chart parameters (L , LCL , UCL) that minimize the $EARL_1$ value. As discussed in Chapter 3, $EARL_1$ only needs a range of possible values for the shift size, denoted by $(\tau_{\min}, \tau_{\max})$, instead of an exact value as required by the ARL_1 . Following Castagliola et al. (2011), this thesis considers the range $(\tau_{\min}, \tau_{\max}) = (1, 2]$ and the same values of sample size and in-control coefficient of variation as presented in Tables 4.1 and 4.2. A range which excludes one and includes two is chosen as $\tau = 1$ denotes the in-control condition, hence it is excluded as the $EARL$ measures the average number of samples to detect an out-of-control condition, whereas $\tau = 2$ is included to consider a large range of possible shifts, as $\tau = 2$ denotes a 100% shift in γ_0 . Note that this thesis focuses solely on detecting an upward shift.

Table 4.3 presents the optimal chart parameters, L , LCL , UCL , and the corresponding $EARL_1$ values for $n \in \{5, 7, 10, 15, 20\}$ and $\gamma_0 \in \{0.05, 0.10, 0.15, 0.20\}$, where the range of $(\tau_{\min}, \tau_{\max})$ was set as $(1, 2]$. The results obtained were verified through simulation as described in Section 3.6.

Table 4.3 Optimal chart parameters (L , LCL , UCL) of the side-sensitive synthetic- γ chart and the corresponding $EARL_1$ for $n \in \{5, 7, 10, 15, 20\}$, $\gamma_0 \in \{0.05, 0.10, 0.15, 0.20\}$ and $(\tau_{\min}, \tau_{\max}) = (1, 2]$

	L	LCL	UCL	$EARL_1$
n				$\gamma_0 = 0.05$
5	25	0.0036	0.0905	16.90
7	25	0.0128	0.0832	13.73
10	27	0.0199	0.0774	11.16
15	29	0.0260	0.0723	8.85
20	29	0.0295	0.0692	7.48
n				$\gamma_0 = 0.10$
5	25	0.0060	0.1824	17.03
7	24	0.0250	0.1672	13.83
10	27	0.0391	0.1556	11.22
15	28	0.0517	0.1449	8.89
20	28	0.0588	0.1387	7.50
n				$\gamma_0 = 0.15$
5	25	0.0062	0.2771	17.25
7	24	0.0353	0.2534	14.02
10	25	0.0577	0.2348	11.34
15	27	0.0766	0.2186	8.96
20	27	0.0875	0.2090	7.55
n				$\gamma_0 = 0.20$
5	25	0.0065	0.3763	17.56
7	23	0.0437	0.3423	14.31
10	24	0.0744	0.3163	11.54
15	26	0.1003	0.2937	9.08
20	26	0.1152	0.2804	7.64

As indicated in Table 4.3, an increase in sample size leads to a decrease in the $EARL_1$ value. For instance, when $n = 5$ and $\gamma_0 = 0.05$, the corresponding $EARL_1$ value is 16.90 whereas for $n = 20$ and $\gamma_0 = 0.05$, the corresponding $EARL_1$ is 7.48. Additionally, larger values of sample size result in slightly smaller optimal UCL but greater LCL . For instance, the optimal chart parameters, LCL and UCL , obtained are 0.0036 and 0.0905, respectively for $n = 5$ and $\gamma_0 = 0.05$ whereas for $n = 20$ and $\gamma_0 = 0.05$, the optimal chart parameters, LCL and UCL , obtained are 0.0295 and 0.0692, respectively.

Table 4.3 also demonstrates that larger values of the in-control coefficient of variation results in marginally larger LCL , UCL and $EARL_1$ values. For instance, when $n = 5$ and $\gamma_0 = 0.05$, the optimal chart parameters, LCL and UCL , and the corresponding $EARL_1$ obtained are 0.0036, 0.0905 and 16.90, respectively, whereas the optimal chart parameters, LCL and UCL , and the corresponding $EARL_1$ obtained are 0.0065, 0.3763 and 17.56, respectively for $n = 5$ and $\gamma_0 = 0.20$.

4.2 Analysis of Run Length Distribution's Percentiles

ARL is frequently chosen as the performance measure for evaluating the control chart and this can be found in most studies. Gan (1993) suggests that the distribution of run length is heavily skewed to the right, particularly for small shift sizes. As such, in order to obtain an accurate understanding of a control chart's performance, it is crucial to analyze all percentiles of the run length distribution.

In this subsection, the analysis of both in-control and out-of-control percentiles of the run length distribution has been carried out using the optimal chart parameters (L , LCL , UCL) presented in Tables 4.1, 4.2 and 4.3. The 5th until 95th in-control percentiles of the ARL -based side-sensitive synthetic- γ chart for $n \in \{5, 7, 10, 15, 20\}$ and $\tau \in \{1.1, 1.2, 1.3, 1.4, 1.5, 1.6, 1.7, 1.8, 1.9, 2.0\}$ are shown in Tables 4.4, 4.5, 4.6 and 4.7 for $\gamma_0 = 0.05$, $\gamma_0 = 0.10$, $\gamma_0 = 0.15$ and $\gamma_0 = 0.20$, respectively while the 5th until 95th out-of-control percentiles of the ARL -based side-sensitive synthetic- γ chart for $n \in \{5, 7, 10, 15, 20\}$ and $\tau \in \{1.1, 1.2, 1.3, 1.4, 1.5, 1.6, 1.7, 1.8, 1.9, 2.0\}$ are shown in Table 4.8 for $\gamma_0 = 0.05$, Table 4.9 for $\gamma_0 = 0.10$, Table 4.10 for $\gamma_0 = 0.15$ and Table 4.11 for $\gamma_0 = 0.20$.

The run length distribution's percentiles was calculated using Equation (3.42), which involves the optimal chart parameters obtained from the side-sensitive synthetic- γ chart which is designed based on the ARL in Tables 4.1 and 4.2. It is worth noting that the in-control percentiles are determined using $\tau = 1$ for all cases, while the out-of-control percentiles are based on $\tau = \tau_{opt}$. Besides, the results obtained were validated by simulation with 10,000 trials.

Table 4.4 In-control percentiles of the run length distribution for the ARL -based side-sensitive synthetic- γ chart for $n \in \{5, 7, 10, 15, 20\}$, $\tau \in \{1.1, 1.2, 1.3, 1.4, 1.5, 1.6, 1.7, 1.8, 1.9, 2.0\}$ and $\gamma_0 = 0.05$

$\gamma_0 = 0.05$											
	5 th	10 th	20 th	30 th	40 th	50 th	60 th	70 th	80 th	90 th	95 th
$n = 5$											
τ	6	13	26	41	125	211	316	451	641	967	1293
1.1	6	13	26	41	125	211	316	451	641	967	1293
1.2	5	10	20	74	143	225	325	454	636	947	1258
1.3	4	8	26	84	150	229	325	448	623	921	1220
1.4	4	7	34	91	157	234	329	451	623	918	1212
1.5	3	6	41	97	161	237	329	449	618	906	1194
1.6	3	6	45	100	164	240	333	453	622	911	1199
1.7	3	5	48	104	168	243	336	456	624	913	1201
1.8	3	5	50	105	168	242	333	451	616	899	1181
1.9	3	5	50	105	168	242	333	451	616	899	1181
2.0	2	4	54	108	171	244	335	451	615	895	1176
$n = 7$											
τ	6	12	24	55	128	211	313	445	631	948	1266
1.1	6	12	24	55	128	211	313	445	631	948	1266
1.2	5	9	18	80	148	225	326	453	631	936	1242
1.3	4	7	34	90	156	233	328	450	622	917	1211
1.4	3	6	40	95	160	235	328	448	616	904	1192
1.5	3	6	46	102	166	242	336	456	625	914	1203
1.6	3	5	51	106	168	242	332	448	612	893	1173
1.7	3	5	51	106	168	242	332	448	612	893	1173
1.8	2	8	55	108	170	243	332	447	609	886	1163
1.9	2	8	55	108	170	243	332	447	609	886	1163
2.0	2	12	59	111	172	244	332	446	606	880	1154

Table 4.4, continued

$\gamma_0 = 0.05$											
	5 th	10 th	20 th	30 th	40 th	50 th	60 th	70 th	80 th	90 th	95 th
τ	$n = 10$										
1.1	6	12	24	63	133	216	318	449	634	950	1266
1.2	4	8	27	84	150	228	323	446	619	915	1210
1.3	4	7	41	98	164	242	337	460	633	928	1224
1.4	3	6	47	102	165	240	331	449	616	900	1184
1.5	3	5	53	107	170	243	334	450	614	895	1175
1.6	3	10	58	112	175	249	340	457	622	904	1186
1.7	3	10	58	112	175	249	340	457	622	904	1186
1.8	2	14	62	116	178	251	341	457	621	900	1180
1.9	2	14	62	116	178	251	341	457	621	900	1180
2.0	2	14	62	116	178	251	341	457	621	900	1180
τ	$n = 15$										
1.1	6	12	24	72	141	224	325	455	638	951	1265
1.2	4	8	37	94	160	238	334	457	630	927	1223
1.3	3	6	48	102	165	239	329	445	609	890	1170
1.4	3	13	74	142	222	315	430	578	786	1142	1498
1.5	3	11	58	111	173	246	335	450	612	888	1165
1.6	2	15	61	113	174	246	333	446	606	878	1150
1.7	2	15	61	113	174	246	333	446	606	878	1150
1.8	2	20	65	117	177	247	334	446	603	872	1141
1.9	2	20	65	117	177	247	334	446	603	872	1141
2.0	2	20	65	117	177	247	334	446	603	872	1141
τ	$n = 20$										
1.1	6	11	23	78	146	227	326	454	634	942	1250
1.2	4	7	43	98	161	236	328	447	613	898	1183
1.3	3	6	52	106	167	240	330	445	607	885	1163
1.4	3	12	60	114	177	250	341	458	622	903	1184
1.5	2	16	62	115	176	248	336	450	610	884	1158
1.6	2	16	62	115	176	248	336	450	610	884	1158
1.7	2	20	66	117	177	247	334	445	602	870	1138
1.8	2	20	66	117	177	247	334	445	602	870	1138
1.9	2	20	66	117	177	247	334	445	602	870	1138
2.0	2	20	66	117	177	247	334	445	602	870	1138

Table 4.5 In-control percentiles of the run length distribution for the ARL-based side-sensitive synthetic- γ chart for $n \in \{5, 7, 10, 15, 20\}$, $\tau \in \{1.1, 1.2, 1.3, 1.4, 1.5, 1.6, 1.7, 1.8, 1.9, 2.0\}$ and $\gamma_0 = 0.10$

$\gamma_0 = 0.10$											
τ	5 th	10 th	20 th	30 th	40 th	50 th	60 th	70 th	80 th	90 th	95 th
$n = 5$											
1.1	6	13	26	41	125	211	316	452	642	968	1295
1.2	5	10	20	73	142	223	322	451	631	941	1250
1.3	4	8	27	85	152	232	329	455	632	934	1237
1.4	4	7	34	91	156	234	329	451	623	917	1211
1.5	3	6	42	98	162	238	332	452	622	912	1202
1.6	3	6	45	100	164	240	333	453	622	910	1199
1.7	3	5	47	103	166	242	334	453	620	906	1193
1.8	3	5	50	105	167	241	332	449	614	896	1179
1.9	3	5	50	105	167	241	332	449	614	896	1179
2.0	2	4	54	109	171	245	336	453	618	900	1181
$n = 7$											
1.1	6	12	24	59	130	214	317	450	637	957	1276
1.2	5	9	18	80	148	228	327	454	633	939	1246
1.3	4	7	33	90	156	233	328	451	623	918	1213
1.4	3	6	40	96	161	237	330	451	621	911	1201
1.5	3	6	45	100	164	239	331	450	617	903	1188
1.6	3	5	52	106	169	243	334	451	617	899	1182
1.7	3	5	52	106	169	243	334	451	617	899	1182
1.8	2	8	55	109	172	245	335	451	615	895	1175
1.9	2	8	55	109	172	245	335	451	615	895	1175
2.0	2	13	60	113	175	248	338	453	616	894	1172
$n = 10$											
1.1	6	12	24	63	133	216	319	451	636	954	1272
1.2	4	8	28	86	153	232	329	454	631	932	1233
1.3	4	7	40	95	160	236	329	450	619	909	1199
1.4	3	6	47	102	166	241	333	452	619	905	1191
1.5	3	5	54	108	171	245	336	454	619	902	1185
1.6	3	9	56	109	171	244	333	447	609	886	1162
1.7	3	9	56	109	171	244	333	447	609	886	1162
1.8	2	14	60	113	175	247	336	450	611	887	1163
1.9	2	14	60	113	175	247	336	450	611	887	1163
2.0	2	14	60	113	175	247	336	450	611	887	1163
$n = 15$											
1.1	6	11	24	70	140	222	322	452	635	947	1260
1.2	4	8	36	93	158	235	330	452	624	917	1211
1.3	3	6	49	104	167	241	333	451	617	901	1185
1.4	3	5	54	108	170	243	333	448	611	889	1168
1.5	3	11	58	112	175	248	338	455	618	898	1178
1.6	2	15	61	113	174	246	333	446	606	878	1150
1.7	2	15	61	113	174	246	333	446	606	878	1150
1.8	2	20	65	118	178	249	336	448	606	876	1146
1.9	2	20	65	118	178	249	336	448	606	876	1146
2.0	2	20	65	118	178	249	336	448	606	876	1146
$n = 20$											
1.1	6	11	23	76	144	225	324	451	630	937	1243
1.2	4	7	43	99	163	238	331	451	619	907	1195
1.3	3	6	53	107	170	244	335	452	617	900	1182
1.4	3	12	59	113	175	249	338	454	618	897	1176
1.5	2	15	62	114	175	247	335	449	608	882	1155
1.6	2	15	62	114	175	247	335	449	608	882	1155
1.7	2	20	66	117	177	248	334	445	603	871	1139
1.8	2	20	66	117	177	248	334	445	603	871	1139
1.9	2	20	66	117	177	248	334	445	603	871	1139
2.0	2	20	66	117	177	248	334	445	603	871	1139

Table 4.6 In-control percentiles of the run length distribution for the *ARL*-based side-sensitive synthetic- γ chart for $n \in \{5, 7, 10, 15, 20\}$, $\tau \in \{1.1, 1.2, 1.3, 1.4, 1.5, 1.6, 1.7, 1.8, 1.9, 2.0\}$ and $\gamma_0 = 0.15$

$\gamma_0 = 0.15$											
τ	5 th	10 th	20 th	30 th	40 th	50 th	60 th	70 th	80 th	90 th	95 th
$n = 5$											
1.1	6	12	26	41	125	210	315	449	639	964	1289
1.2	5	10	20	73	142	224	324	453	634	945	1255
1.3	4	8	27	85	152	231	328	453	629	930	1231
1.4	4	7	35	92	158	236	331	454	627	924	1220
1.5	3	6	42	97	162	238	332	452	621	911	1201
1.6	3	6	45	100	164	240	334	453	622	911	1200
1.7	3	5	47	102	166	241	333	451	618	904	1190
1.8	3	5	50	105	168	243	334	452	618	901	1185
1.9	3	5	50	105	168	243	334	452	618	901	1185
2.0	2	4	54	108	170	244	334	451	615	895	1175
$n = 7$											
1.1	6	12	24	59	130	214	318	451	638	958	1279
1.2	5	9	18	79	147	228	327	454	633	939	1245
1.3	4	7	33	90	156	234	330	453	626	922	1219
1.4	3	6	40	97	162	239	333	454	625	918	1210
1.5	3	6	46	101	165	241	334	454	622	911	1199
1.6	3	5	51	106	169	243	334	452	617	900	1183
1.7	3	5	51	106	169	243	334	452	617	900	1183
1.8	2	7	55	109	172	245	336	452	616	896	1177
1.9	2	7	55	109	172	245	336	452	616	896	1177
2.0	2	12	59	112	174	246	335	450	612	888	1165
$n = 10$											
1.1	6	11	24	64	133	217	319	451	637	954	1272
1.2	4	8	27	85	152	231	327	452	628	928	1228
1.3	4	7	39	96	160	237	331	452	623	915	1206
1.4	3	6	47	102	166	241	333	452	619	906	1192
1.5	3	5	53	107	170	244	334	451	616	897	1179
1.6	3	9	56	110	172	245	335	451	614	893	1171
1.7	3	9	56	110	172	245	335	451	614	893	1171
1.8	2	13	60	114	175	248	337	452	614	891	1168
1.9	2	13	60	114	175	248	337	452	614	891	1168
2.0	2	13	60	114	175	248	337	452	614	891	1168
$n = 15$											
1.1	6	11	23	70	139	221	321	450	632	943	1254
1.2	4	8	35	92	158	236	331	453	626	921	1217
1.3	3	6	39	88	144	211	293	399	548	802	1057
1.4	3	5	54	108	170	243	333	448	612	891	1169
1.5	3	10	57	111	173	246	335	450	613	891	1168
1.6	2	14	61	114	175	248	336	450	611	886	1161
1.7	2	14	61	114	175	248	336	450	611	886	1161
1.8	2	19	65	118	178	249	337	449	608	879	1150
1.9	2	19	65	118	178	249	337	449	608	879	1150
2.0	2	19	65	118	178	249	337	449	608	879	1150
$n = 20$											
1.1	6	11	23	76	145	226	325	454	635	944	1253
1.2	4	7	43	98	162	238	331	450	619	907	1195
1.3	3	6	52	106	168	242	333	449	614	894	1175
1.4	3	11	58	112	174	247	336	452	614	892	1170
1.5	2	15	62	114	175	247	335	449	609	882	1156
1.6	2	15	62	114	175	247	335	449	609	882	1156
1.7	2	20	66	118	178	250	337	449	608	879	1150
1.8	2	20	66	118	178	250	337	449	608	879	1150
1.9	2	20	66	118	178	250	337	449	608	879	1150
2.0	2	20	66	118	178	250	337	449	608	879	1150

Table 4.7 In-control percentiles of the run length distribution for the ARL-based side-sensitive synthetic- γ chart for $n \in \{5, 7, 10, 15, 20\}$, $\tau \in \{1.1, 1.2, 1.3, 1.4, 1.5, 1.6, 1.7, 1.8, 1.9, 2.0\}$ and $\gamma_0 = 0.20$

$\gamma_0 = 0.20$											
τ	5 th	10 th	20 th	30 th	40 th	50 th	60 th	70 th	80 th	90 th	95 th
$n = 5$											
1.1	6	12	26	41	125	210	315	450	640	964	1289
1.2	5	10	20	72	141	223	323	452	634	945	1257
1.3	4	8	27	85	152	231	328	454	630	932	1233
1.4	4	7	35	92	157	235	331	453	626	922	1218
1.5	3	6	39	95	160	237	331	453	624	916	1208
1.6	3	6	44	100	164	240	332	452	620	908	1196
1.7	3	5	47	102	166	241	333	452	619	904	1190
1.8	3	5	50	105	168	243	334	452	618	902	1186
1.9	3	5	50	105	168	243	334	452	618	902	1186
2.0	2	4	54	108	170	244	334	451	615	895	1176
$n = 7$											
1.1	6	12	24	58	130	215	318	451	639	960	1281
1.2	5	9	18	79	147	227	325	452	630	935	1240
1.3	4	7	33	90	156	235	330	454	627	924	1222
1.4	3	6	40	96	160	237	331	452	622	913	1204
1.5	3	6	45	101	165	241	333	453	622	910	1198
1.6	3	5	48	103	167	242	334	452	620	905	1191
1.7	3	5	51	106	169	243	334	452	617	900	1184
1.8	2	6	55	108	171	244	334	450	614	894	1174
1.9	2	6	55	108	171	244	334	450	614	894	1174
2.0	2	12	59	112	173	246	335	450	611	888	1164
$n = 10$											
1.1	6	11	23	64	133	217	319	450	636	952	1269
1.2	4	8	26	84	151	230	326	451	627	927	1227
1.3	4	7	39	95	161	238	332	454	626	919	1212
1.4	3	6	46	101	165	240	332	451	618	904	1190
1.5	3	5	52	107	169	244	334	451	616	898	1181
1.6	3	8	56	110	172	245	335	451	614	894	1173
1.7	3	8	56	110	172	245	335	451	614	894	1173
1.8	2	13	60	113	175	248	337	452	614	891	1167
1.9	2	13	60	113	175	248	337	452	614	891	1167
2.0	2	13	60	113	175	248	337	452	614	891	1167
$n = 15$											
1.1	6	11	23	69	139	221	322	453	636	950	1264
1.2	4	8	35	92	158	236	331	454	628	925	1221
1.3	3	6	48	103	167	242	334	453	620	907	1193
1.4	3	5	54	108	170	244	334	450	615	895	1176
1.5	3	10	57	111	173	247	337	453	616	895	1175
1.6	2	14	61	114	176	249	338	453	614	891	1168
1.7	2	14	61	114	176	249	338	453	614	891	1168
1.8	2	14	61	114	176	249	338	453	614	891	1168
1.9	2	19	65	117	178	249	336	449	608	879	1150
2.0	2	19	65	117	178	249	336	449	608	879	1150
$n = 20$											
1.1	5	11	22	74	142	223	323	451	631	939	1247
1.2	4	7	40	96	161	237	331	452	622	914	1205
1.3	3	6	52	106	169	243	334	451	616	898	1181
1.4	3	11	58	111	173	246	336	451	613	891	1169
1.5	2	15	62	115	176	249	338	452	614	890	1165
1.6	2	15	62	115	176	249	338	452	614	890	1165
1.7	2	19	65	118	178	249	336	448	607	877	1148
1.8	2	19	65	118	178	249	336	448	607	877	1148
1.9	2	19	65	118	178	249	336	448	607	877	1148
2.0	2	19	65	118	178	249	336	448	607	877	1148

Table 4.8 Out-of-control percentiles of the run length distribution for the *ARL*-based side-sensitive synthetic- γ chart for $n \in \{5, 7, 10, 15, 20\}$, $\tau \in \{1.1, 1.2, 1.3, 1.4, 1.5, 1.6, 1.7, 1.8, 1.9, 2.0\}$ and $\gamma_0 = 0.05$

$\gamma_0 = 0.05$											
	5 th	10 th	20 th	30 th	40 th	50 th	60 th	70 th	80 th	90 th	95 th
τ	$n = 5$										
1.1	3	5	10	15	21	29	38	73	109	175	240
1.2	1	2	4	6	9	12	15	20	35	56	78
1.3	1	1	2	3	5	6	8	10	13	26	35
1.4	1	1	2	2	3	4	5	6	8	14	21
1.5	1	1	1	2	2	3	4	4	6	8	14
1.6	1	1	1	1	2	2	3	3	4	6	10
1.7	1	1	1	1	1	2	2	3	4	5	6
1.8	1	1	1	1	1	2	2	2	3	4	5
1.9	1	1	1	1	1	1	2	2	3	4	4
2.0	1	1	1	1	1	1	2	2	2	3	4
τ	$n = 7$										
1.1	2	4	8	13	18	24	32	57	86	139	191
1.2	1	2	3	5	7	9	12	15	23	41	57
1.3	1	1	2	3	3	5	6	8	10	18	25
1.4	1	1	1	2	2	3	4	5	6	9	14
1.5	1	1	1	1	2	2	3	3	4	6	9
1.6	1	1	1	1	1	2	2	2	3	4	5
1.7	1	1	1	1	1	1	2	2	3	4	4
1.8	1	1	1	1	1	1	1	2	2	3	4
1.9	1	1	1	1	1	1	1	2	2	3	2
2.0	1	1	1	1	1	1	1	1	2	2	3
τ	$n = 10$										
1.1	2	3	7	11	15	20	27	35	69	110	152
1.2	1	1	2	4	5	7	9	11	15	29	40
1.3	1	1	1	2	3	3	4	6	7	10	18
1.4	1	1	1	1	2	2	3	3	4	6	9
1.5	1	1	1	1	1	2	2	2	3	4	5
1.6	1	1	1	1	1	1	2	2	2	3	4
1.7	1	1	1	1	1	1	1	2	2	3	3
1.8	1	1	1	1	1	1	1	1	2	2	3
1.9	1	1	1	1	1	1	1	1	1	2	2
2.0	1	1	1	1	1	1	1	1	1	2	2
τ	$n = 15$										
1.1	2	3	6	9	12	16	21	28	52	83	115
1.2	1	1	2	3	4	5	6	8	11	20	27
1.3	1	1	1	1	2	2	3	4	5	7	11
1.4	1	1	1	1	1	2	2	2	3	4	5
1.5	1	1	1	1	1	1	1	2	2	3	4
1.6	1	1	1	1	1	1	1	1	2	2	3
1.7	1	1	1	1	1	1	1	1	1	2	2
1.8	1	1	1	1	1	1	1	1	1	2	2
1.9	1	1	1	1	1	1	1	1	1	1	2
2.0	1	1	1	1	1	1	1	1	1	1	1
τ	$n = 20$										
1.1	1	2	5	7	10	13	18	23	41	65	91
1.2	1	1	2	2	3	4	5	6	8	14	20
1.3	1	1	1	1	2	2	2	3	4	5	8
1.4	1	1	1	1	1	1	2	2	2	3	4
1.5	1	1	1	1	1	1	1	1	2	2	3
1.6	1	1	1	1	1	1	1	1	1	2	2
1.7	1	1	1	1	1	1	1	1	1	1	2
1.8	1	1	1	1	1	1	1	1	1	1	1
1.9	1	1	1	1	1	1	1	1	1	1	1
2.0	1	1	1	1	1	1	1	1	1	1	1

Table 4.9 Out-of-control percentiles of the run length distribution for the *ARL*-based side-sensitive synthetic- γ chart for $n \in \{5, 7, 10, 15, 20\}$, $\tau \in \{1.1, 1.2, 1.3, 1.4, 1.5, 1.6, 1.7, 1.8, 1.9, 2.0\}$ and $\gamma_0 = 0.10$

$\gamma_0 = 0.10$											
	5 th	10 th	20 th	30 th	40 th	50 th	60 th	70 th	80 th	90 th	95 th
τ	<i>n</i> = 5										
1.1	3	5	10	15	22	29	38	74	110	176	242
1.2	1	2	4	6	9	12	15	20	35	56	79
1.3	1	1	2	3	5	6	8	10	14	27	36
1.4	1	1	2	2	3	4	5	6	8	14	21
1.5	1	1	1	2	2	3	4	5	6	8	14
1.6	1	1	1	1	2	2	3	3	4	6	10
1.7	1	1	1	1	1	2	2	3	4	5	6
1.8	1	1	1	1	1	2	2	2	3	4	5
1.9	1	1	1	1	1	1	2	2	3	4	4
2.0	1	1	1	1	1	1	2	2	2	3	4
τ	<i>n</i> = 7										
1.1	2	4	8	13	18	24	32	58	88	141	194
1.2	1	2	3	5	7	9	12	15	24	41	58
1.3	1	1	2	3	4	5	6	8	10	18	25
1.4	1	1	1	2	2	3	4	5	6	9	14
1.5	1	1	1	1	2	2	3	3	4	6	9
1.6	1	1	1	1	1	2	2	3	3	4	7
1.7	1	1	1	1	1	1	2	2	3	4	5
1.8	1	1	1	1	1	1	1	2	2	3	4
1.9	1	1	1	1	1	1	1	2	2	3	3
2.0	1	1	1	1	1	1	1	1	2	2	3
τ	<i>n</i> = 10										
1.1	2	4	7	11	15	20	27	35	69	111	153
1.2	1	1	3	4	5	7	9	11	15	30	41
1.3	1	1	1	2	3	3	4	6	7	10	18
1.4	1	1	1	1	2	2	3	3	4	6	10
1.5	1	1	1	1	1	2	2	2	3	4	5
1.6	1	1	1	1	1	1	2	2	2	3	4
1.7	1	1	1	1	1	1	1	2	2	3	3
1.8	1	1	1	1	1	1	1	1	2	2	3
1.9	1	1	1	1	1	1	1	1	1	2	2
2.0	1	1	1	1	1	1	1	1	1	2	2
τ	<i>n</i> = 15										
1.1	2	3	6	9	12	16	21	28	52	83	115
1.2	1	1	2	3	4	5	6	8	11	20	27
1.3	1	1	1	1	2	2	3	4	5	7	12
1.4	1	1	1	1	1	2	2	2	3	4	5
1.5	1	1	1	1	1	1	1	2	2	3	4
1.6	1	1	1	1	1	1	1	1	2	2	3
1.7	1	1	1	1	1	1	1	1	1	2	2
1.8	1	1	1	1	1	1	1	1	1	2	2
1.9	1	1	1	1	1	1	1	1	1	1	2
2.0	1	1	1	1	1	1	1	1	1	1	1
τ	<i>n</i> = 20										
1.1	1	2	5	7	10	13	18	23	41	66	92
1.2	1	1	2	2	3	4	5	6	8	15	20
1.3	1	1	1	1	2	2	2	3	4	5	8
1.4	1	1	1	1	1	1	2	2	2	3	4
1.5	1	1	1	1	1	1	1	1	2	2	3
1.6	1	1	1	1	1	1	1	1	1	2	2
1.7	1	1	1	1	1	1	1	1	1	1	2
1.8	1	1	1	1	1	1	1	1	1	1	1
1.9	1	1	1	1	1	1	1	1	1	1	1
2.0	1	1	1	1	1	1	1	1	1	1	1

Table 4.10 Out-of-control percentiles of the run length distribution for the ARL-based side-sensitive synthetic- γ chart for $n \in \{5, 7, 10, 15, 20\}$, $\tau \in \{1.1, 1.2, 1.3, 1.4, 1.5, 1.6, 1.7, 1.8, 1.9, 2.0\}$ and $\gamma_0 = 0.15$

$\gamma_0 = 0.15$											
	5 th	10 th	20 th	30 th	40 th	50 th	60 th	70 th	80 th	90 th	95 th
τ	$n = 5$										
1.1	3	5	10	15	22	29	39	74	111	178	244
1.2	1	2	4	6	9	12	15	20	36	58	80
1.3	1	1	2	3	5	6	8	10	14	27	37
1.4	1	1	2	2	3	4	5	7	9	15	22
1.5	1	1	1	2	2	3	4	5	6	8	14
1.6	1	1	1	1	2	2	3	4	5	6	10
1.7	1	1	1	1	2	2	2	3	4	5	6
1.8	1	1	1	1	1	2	2	2	3	4	5
1.9	1	1	1	1	1	1	2	2	3	4	5
2.0	1	1	1	1	1	1	2	2	2	3	4
τ	$n = 7$										
1.1	2	4	8	13	18	24	32	59	89	143	197
1.2	1	2	3	5	7	9	12	15	25	42	59
1.3	1	1	2	3	4	5	6	8	10	19	26
1.4	1	1	1	2	2	3	4	5	6	9	15
1.5	1	1	1	1	2	2	3	3	4	6	9
1.6	1	1	1	1	1	2	2	3	3	4	7
1.7	1	1	1	1	1	1	2	2	3	4	5
1.8	1	1	1	1	1	1	2	2	2	3	4
1.9	1	1	1	1	1	1	1	2	2	3	3
2.0	1	1	1	1	1	1	1	1	2	2	3
τ	$n = 10$										
1.1	2	4	7	11	15	20	27	42	70	113	155
1.2	1	1	3	4	5	7	9	12	15	30	42
1.3	1	1	1	2	3	3	4	6	7	10	18
1.4	1	1	1	1	2	2	3	4	5	6	10
1.5	1	1	1	1	1	2	2	2	3	4	5
1.6	1	1	1	1	1	1	2	2	2	3	4
1.7	1	1	1	1	1	1	1	2	2	3	3
1.8	1	1	1	1	1	1	1	1	2	2	3
1.9	1	1	1	1	1	1	1	1	2	2	2
2.0	1	1	1	1	1	1	1	1	1	2	2
τ	$n = 15$										
1.1	2	3	6	9	12	16	21	28	53	84	116
1.2	1	1	2	3	4	5	6	8	11	20	28
1.3	1	1	1	2	2	2	3	4	5	7	11
1.4	1	1	1	1	1	2	2	2	3	4	5
1.5	1	1	1	1	1	1	1	2	2	3	4
1.6	1	1	1	1	1	1	1	1	2	2	3
1.7	1	1	1	1	1	1	1	1	1	2	2
1.8	1	1	1	1	1	1	1	1	1	2	2
1.9	1	1	1	1	1	1	1	1	1	1	2
2.0	1	1	1	1	1	1	1	1	1	1	2
τ	$n = 20$										
1.1	1	2	5	7	10	14	18	23	42	67	93
1.2	1	1	2	2	3	4	5	6	8	15	21
1.3	1	1	1	1	2	2	2	3	4	5	8
1.4	1	1	1	1	1	1	2	2	2	3	4
1.5	1	1	1	1	1	1	1	1	2	2	3
1.6	1	1	1	1	1	1	1	1	1	2	2
1.7	1	1	1	1	1	1	1	1	1	1	2
1.8	1	1	1	1	1	1	1	1	1	1	2
1.9	1	1	1	1	1	1	1	1	1	1	1
2.0	1	1	1	1	1	1	1	1	1	1	1

Table 4.11 Out-of-control percentiles of the run length distribution for the ARL-based side-sensitive synthetic- γ chart for $n \in \{5, 7, 10, 15, 20\}$, $\tau \in \{1.1, 1.2, 1.3, 1.4, 1.5, 1.6, 1.7, 1.8, 1.9, 2.0\}$ and $\gamma_0 = 0.20$

$\gamma_0 = 0.20$											
	5 th	10 th	20 th	30 th	40 th	50 th	60 th	70 th	80 th	90 th	95 th
τ											
1.1	3	5	10	15	22	30	39	76	113	181	248
1.2	1	2	4	6	9	12	16	21	37	59	82
1.3	1	1	2	4	5	6	8	11	14	28	38
1.4	1	1	2	2	3	4	5	7	9	16	22
1.5	1	1	1	2	2	3	4	5	6	9	15
1.6	1	1	1	1	2	2	3	4	5	7	11
1.7	1	1	1	1	2	2	2	3	4	5	8
1.8	1	1	1	1	1	2	2	2	3	4	5
1.9	1	1	1	1	1	1	2	2	3	4	5
2.0	1	1	1	1	1	1	2	2	2	3	4
τ											
1.1	2	4	8	13	18	25	32	61	92	147	202
1.2	1	2	3	5	7	9	12	16	26	43	61
1.3	1	1	2	3	4	5	6	8	10	20	27
1.4	1	1	1	2	2	3	4	5	6	9	16
1.5	1	1	1	1	2	2	3	4	5	6	10
1.6	1	1	1	1	1	2	2	3	3	5	6
1.7	1	1	1	1	1	1	2	2	3	4	5
1.8	1	1	1	1	1	1	2	2	2	3	4
1.9	1	1	1	1	1	1	1	2	2	3	3
2.0	1	1	1	1	1	1	1	1	2	2	3
τ											
1.1	2	4	7	11	15	20	27	45	71	115	158
1.2	1	1	3	4	5	7	9	12	16	31	43
1.3	1	1	1	2	3	4	5	6	8	13	19
1.4	1	1	1	1	2	2	3	4	5	6	11
1.5	1	1	1	1	1	2	2	3	3	4	7
1.6	1	1	1	1	1	1	2	2	2	3	4
1.7	1	1	1	1	1	1	1	2	2	3	3
1.8	1	1	1	1	1	1	1	1	2	2	3
1.9	1	1	1	1	1	1	1	1	2	2	2
2.0	1	1	1	1	1	1	1	1	1	2	2
τ											
1.1	2	3	6	9	12	16	22	28	54	86	119
1.2	1	1	2	3	4	5	7	9	11	21	29
1.3	1	1	1	2	2	3	3	4	5	7	12
1.4	1	1	1	1	1	2	2	3	3	4	6
1.5	1	1	1	1	1	1	2	2	2	3	4
1.6	1	1	1	1	1	1	1	1	2	2	3
1.7	1	1	1	1	1	1	1	1	2	2	2
1.8	1	1	1	1	1	1	1	1	1	2	2
1.9	1	1	1	1	1	1	1	1	1	1	2
2.0	1	1	1	1	1	1	1	1	1	1	2
τ											
1.1	1	2	5	7	10	14	18	24	42	68	94
1.2	1	1	2	2	3	4	5	7	9	15	22
1.3	1	1	1	1	2	2	2	3	4	6	9
1.4	1	1	1	1	1	1	2	2	2	3	4
1.5	1	1	1	1	1	1	1	1	2	2	3
1.6	1	1	1	1	1	1	1	1	1	2	2
1.7	1	1	1	1	1	1	1	1	1	2	2
1.8	1	1	1	1	1	1	1	1	1	1	2
1.9	1	1	1	1	1	1	1	1	1	1	1
2.0	1	1	1	1	1	1	1	1	1	1	1

By referring to Tables 4.4 to 4.7, it is noticeable that the MRL_0 or in-control 50th percentiles fall between 210 to 251 for all cases when the optimal chart parameters from the designs based on ARL are applied. These values not only show a significant difference between the obtained MRL_0 and ARL_0 of 370.4, but they also indicate that the false alarm should occur much earlier. For example, in Table 4.4, the MRL_0 obtained is 211 for $n = 5$, $\tau = 1.1$ and $\gamma_0 = 0.05$. This indicates that around half of the time, one false alarm will occur by the 211th sample in reality, although there will be an average of 1 false alarm for every 370 samples. In addition, the value of 370 falls between the 60th and 70th percentiles for all cases, indicating that the distribution of the in-control run length is positively skewed. Therefore, it is not advisable to evaluate the side-sensitive synthetic- γ chart's actual performance solely based on the ARL , as it may result in a misrepresentation of the actual frequency of false alarms.

Tables 4.4, 4.5, 4.6 and 4.7 also show that as the sample size and shift size increase, the MRL_0 is increased as well. For instance, in Table 4.4, the MRL_0 obtained is 227 for $n = 20$, $\tau = 1.1$ and $\gamma_0 = 0.05$ which is greater than the value of MRL_0 of 211 for $n = 5$, $\tau = 1.1$ and $\gamma_0 = 0.05$. For the increase in shift size, it can be observed that larger shift sizes result in larger MRL_0 . For example, in Table 4.4, when $n = 5$, $\tau = 2.0$ and $\gamma_0 = 0.05$, MRL_0 is 244, which is larger than the MRL_0 of 211 for $n = 5$, $\tau = 1.1$ and $\gamma_0 = 0.05$. However, there is not much difference in the MRL_0 as the in-control coefficient of variation increases, for example, the MRL_0 obtained is 210 for $n = 5$, $\tau = 1.1$ and $\gamma_0 = 0.20$ in Table 4.7 which shows minimal difference compared to $MRL_0 = 211$ for $n = 5$, $\tau = 1.1$ and $\gamma_0 = 0.05$ in Table 4.4

Apart from studying the MRL_0 , the smaller percentiles like the 5th, 10th and 20th percentiles and larger percentiles such as the 80th, 90th and 95th percentiles can offer valuable insights about the side-sensitive synthetic- γ chart's run length characteristics to practitioners. For example, in Table 4.4, the 5th percentile is 6 for $n = 5$, $\tau = 1.1$ and $\gamma_0 = 0.05$. This means that for an in-control process, there is a 5% chance of an early false alarm occurring by the 6th sample. The 95th percentile for the same case is 1293, indicating that there is a 95% chance that a false alarm will occur by the 1293rd sample for an in-control process. This information allows practitioners to make accurate decisions for both short and long run lengths without experiencing any assignable cause(s).

Another important analysis for a control chart is the difference between the in-control 5th and 95th percentiles of the run length. This provides valuable information to practitioners about the spread, variation, and skewness of the run length distribution. According to Tables 4.4 to 4.7, it is found that the differences between two extreme percentiles are generally very large, which are between 1136 and 1495 for all cases. This indicates that the distribution of in-control run length has a huge spread and is very skewed. Furthermore, as sample size and shift size increase, the differences between the 5th and 95th percentiles display a decreasing pattern. For instance, in Table 4.4, the difference is 1287 for $n = 5$, $\tau = 1.1$ and $\gamma_0 = 0.05$ whereas the difference is 1136 for $n = 20$, $\tau = 2.0$ and $\gamma_0 = 0.05$. Similar to the analysis of MRL_0 , the differences between the extreme percentiles are similar for different in-control coefficient of variation. For instance, the difference is 1283 for $n = 5$, $\tau = 1.1$ and $\gamma_0 = 0.20$ in Table 4.7 compared to 1287 for $n = 5$, $\tau = 1.1$ and $\gamma_0 = 0.05$ in Table 4.4.

Next, from Tables 4.8 to 4.11, it can be observed that the out-of-control percentiles show similar patterns as the in-control percentiles in terms of MRL and the difference between the 5th and 95th percentiles. Generally, the MRL_1 is smaller than the ARL_1 for all cases. For example, the obtained MRL_1 is 29 for $n = 5$, $\tau = 1.1$ and $\gamma_0 = 0.05$ in Table 4.8 whereas the ARL_1 is 64.74 in Table 4.1 for the same case. This explains that there will be an out-of-control signal by the 29th sample for about 50% of the time, although there will be 1 signal in every 64th sample on average. In fact, the values of ARL_1 for most of the cases fall between the 60th and 70th percentiles. Therefore, the side-sensitive synthetic- γ chart's actual performance is not advisable to be assessed solely based on the ARL_1 as it will mislead practitioners to the wrong conclusion since the out-of-control condition is often spotted earlier than the ARL_1 for almost all cases.

Furthermore, the differences between MRL_1 and ARL_1 are smaller for larger shift sizes. For instance, the difference ($MRL_1 = 29$ in Table 4.8 and $ARL_1 = 64.74$ in Table 4.1) is 35.74 for $n = 5$, $\tau = 1.1$ and $\gamma_0 = 0.05$ whereas the difference ($MRL_1 = 1$ in Table 4.8 and $ARL_1 = 1.72$ in Table 4.1) is 0.72 for $n = 5$, $\tau = 2.0$ and $\gamma_0 = 0.05$. It is also observed that the differences between MRL_1 and ARL_1 in Tables 4.8, 4.9, 4.10 and 4.11 are smaller than the differences between MRL_0 and ARL_0 in Tables 4.4, 4.5, 4.6 and 4.7. For instance, the differences between MRL_1 and ARL_1 fall between 0.01 and 37.12 for all cases whereas the differences between MRL_0 and ARL_0 fall between 119 and 160 for all cases.

By referring to Tables 4.8 to 4.11, it is observed that when sample size and shift size increase, there is a decreasing trend for the difference between the 5th and 95th percentiles for all cases. For instance, in Table 4.8, the difference between the 5th and 95th percentiles is 237 for $n = 5$, $\tau = 1.1$ and $\gamma_0 = 0.05$ whereas the difference between the 5th and 95th

percentiles is 2 for $n = 20$, $\tau = 1.5$ and $\gamma_0 = 0.05$. Besides, the results also show similar differences between the extreme percentiles for a different in-control coefficient of variation. For instance, the difference is 245 for $n = 5$, $\tau = 1.1$ and $\gamma_0 = 0.20$ in Table 4.11 compared with the difference of 237 for $n = 5$, $\tau = 1.1$ and $\gamma_0 = 0.05$ in Table 4.8. This shows that the run length distribution's out-of-control percentiles is positively skewed for small shift size but the run length is approximately symmetrical when the shift size is large.

Note that the in-control and out-of-control percentiles in Tables 4.4 until 4.11 are obtained based on the specific values of shift size. However, it is always a challenge for practitioners to estimate shift size in practical scenarios. Hence, in this subsection, the run length distribution's expected percentiles for the proposed side-sensitive synthetic- γ chart was studied using a range of $(\tau_{\min}, \tau_{\max})$ which was fixed as $(1, 2]$.

Tables 4.12 and 4.13 display the expected percentiles of the side-sensitive synthetic- γ chart which is designed based on *EARL* for both in-control and out-of-control scenarios, from the 5th to the 95th percentiles, for the values of $n \in \{5, 7, 10, 15, 20\}$ and $\gamma_0 \in \{0.05, 0.10, 0.15, 0.20\}$, respectively. The optimal chart parameters in Table 4.3 were used to calculate the expected percentiles through Equation (3.43). All results were verified using simulation with 10,000 trials.

Table 4.12 In-control expected percentile of the run length distribution for the EARL-based side-sensitive synthetic- γ chart for $n \in \{5, 7, 10, 15, 20\}$,

$$\gamma_0 \in \{0.05, 0.10, 0.15, 0.20\} \text{ and } (\tau_{\min}, \tau_{\max}) = (1, 2]$$

	5 th	10 th	20 th	30 th	40 th	50 th	60 th	70 th	80 th	90 th	95 th
<i>n</i>	$\gamma_0 = 0.05$										
5	5	10	21	71	140	222	323	452	635	947	1259
7	5	10	21	71	140	222	322	451	633	943	1254
10	5	10	22	70	139	219	318	446	625	932	1239
15	6	11	24	74	144	226	327	458	641	955	1268
20	6	11	24	75	144	225	324	452	632	940	1248
<i>n</i>	$\gamma_0 = 0.10$										
5	5	10	21	71	141	223	324	453	636	949	1262
7	5	10	20	73	142	223	323	452	634	944	1255
10	5	10	22	71	140	221	321	450	632	942	1253
15	6	11	23	72	140	221	320	447	627	934	1240
20	6	11	23	75	144	225	324	452	632	940	1247
<i>n</i>	$\gamma_0 = 0.15$										
5	5	10	21	71	140	222	323	452	635	947	1259
7	5	10	20	72	141	223	323	452	633	944	1254
10	5	10	21	73	142	224	324	452	634	945	1255
15	5	11	22	74	143	225	325	454	636	947	1259
20	6	11	23	75	144	225	324	452	632	940	1248
<i>n</i>	$\gamma_0 = 0.20$										
5	5	10	21	71	140	222	323	452	635	947	1259
7	5	10	20	73	142	223	323	451	632	942	1251
10	5	10	20	74	143	224	324	453	635	945	1256
15	5	10	22	73	142	224	324	453	634	945	1255
20	5	11	22	75	144	225	324	452	632	940	1248

Table 4.13 Out-of-control expected percentile of the run length distribution for the EARL-based side-sensitive synthetic- γ chart for $n \in \{5, 7, 10, 15, 20\}$,

$$\gamma_0 \in \{0.05, 0.10, 0.15, 0.20\} \text{ and } (\tau_{\min}, \tau_{\max}) = (1, 2]$$

	5 th	10 th	20 th	30 th	40 th	50 th	60 th	70 th	80 th	90 th	95 th
<i>n</i>	$\gamma_0 = 0.05$										
5	1.24	1.65	2.56	3.82	5.84	9.02	13.58	18.85	27.82	43.04	57.82
7	1.15	1.49	2.29	3.32	4.96	7.33	10.90	15.56	22.63	34.49	47.04
10	1.15	1.39	2.15	2.87	4.07	6.06	8.71	12.61	18.02	27.81	37.37
15	1.12	1.36	1.90	2.59	3.24	4.76	7.14	9.83	14.63	22.05	29.92
20	1.07	1.24	1.70	2.31	3.03	4.12	5.94	8.28	11.77	18.27	24.33
<i>n</i>	$\gamma_0 = 0.10$										
5	1.24	1.65	2.56	3.92	5.84	9.10	13.63	19.33	28.08	43.42	58.70
7	1.15	1.48	2.29	3.43	4.99	7.38	11.06	15.68	22.82	34.72	47.49
10	1.15	1.39	2.15	2.94	4.27	6.25	8.76	12.79	18.18	28.06	37.69
15	1.12	1.36	1.90	2.59	3.23	4.73	7.01	9.74	14.48	21.68	29.54
20	1.07	1.24	1.65	2.31	3.02	4.17	5.97	8.28	11.93	18.25	24.59

Table 4.13, continued

	5 th	10 th	20 th	30 th	40 th	50 th	60 th	70 th	80 th	90 th	95 th
<i>n</i>	$\gamma_0 = 0.15$										
5	1.24	1.65	2.56	4.01	5.84	9.21	13.80	19.43	28.47	43.98	59.51
7	1.15	1.49	2.29	3.43	4.98	7.56	11.21	15.87	23.12	35.09	48.06
10	1.15	1.39	2.12	2.85	4.26	6.39	8.81	12.94	18.33	28.46	38.19
15	1.12	1.36	1.89	2.59	3.45	4.73	7.13	9.80	14.65	22.17	30.01
20	1.07	1.24	1.65	2.28	3.02	4.27	6.16	8.32	12.14	18.49	24.79
<i>n</i>	$\gamma_0 = 0.20$										
5	1.24	1.65	2.65	4.01	6.01	9.41	13.92	20.18	29.02	44.64	60.50
7	1.15	1.48	2.29	3.43	4.99	7.71	11.49	16.13	23.49	36.09	48.79
10	1.15	1.39	2.12	2.92	4.28	6.44	8.86	13.16	18.54	29.09	39.12
15	1.12	1.36	1.89	2.58	3.43	4.81	7.22	9.92	14.82	22.32	30.56
20	1.07	1.24	1.73	2.26	3.00	4.27	6.16	8.32	12.23	18.58	25.35

Tables 4.12 and 4.13 reveal that the trend of the expected percentiles for both in-control and out-of-control cases in the design based on *EARL* is comparable to that of the design based on *ARL* shown in Tables 4.4 to 4.11. In Table 4.12, the values of MRL_0 are smaller than $ARL_0 = 370.4$ for all cases and these values fall between 219 and 226. For instance, the MRL_0 is 222 for $n = 5$ and $\gamma_0 = 0.05$. Besides, the ARL_0 of 370.4 also falls between the 60th and 70th percentiles, similar to the *ARL*-based design. As the sample size increases, the MRL_0 increases for most cases. For instance, the MRL_0 is 222 for $n = 5$ and $\gamma_0 = 0.05$ whereas when $n = 20$, the MRL_0 is 225 for $\gamma_0 = 0.05$. As for the larger in-control coefficient of variation, it shows minimal effect on MRL_0 . For instance, when $n = 7$ and $\gamma_0 = 0.05$, the MRL_0 is 222 while the MRL_0 is 223 for $n = 7$ and $\gamma_0 = 0.20$.

In Table 4.13, it is found that the $EMRL_1$ is smaller compared to the $EARL_1$ in Table 4.3 for all cases. For example, the $EMRL_1$ is 9.02 for $n = 5$ and $\gamma_0 = 0.05$ in Table 4.13 whereas the $EARL_1$ is 16.90 in Table 4.3 for the same values of n and γ_0 . Similar to *ARL*-based design, $EMRL_1$ shows a decreasing trend as sample size increases. For instance, the $EMRL_1$ is 9.02 for $n = 5$ and $\gamma_0 = 0.05$ while for $n = 20$ and $\gamma_0 = 0.05$, the $EMRL_1$ is 4.12. Besides, minimal differences in the values of $EMRL_1$ are observed for different in-control

coefficient of variation. For instance, the $EMRL_1$ is 9.02 for $n = 5$ and $\gamma_0 = 0.05$ whereas when $n = 5$ and $\gamma_0 = 0.20$, the $EMRL_1$ is 9.41.

Apart from the MRL_0 and $EMRL_1$, the difference between two extreme expected in-control percentiles demonstrates a large variation while the difference between two extreme expected out-of-control extreme percentiles shows lesser variation. For instance, in Table 4.12, the differences between two extreme expected in-control percentiles fall between 1234 and 1262 while the differences between two extreme expected out-of-control percentiles fall between 20.21 and 51.09 in Table 4.13.

Furthermore, both differences are found to follow a decreasing trend as the sample size increases. For instance, in Table 4.12, when $\gamma_0 = 0.05$, the difference between two extreme expected in-control percentiles is 1254 for $n = 5$ whereas for $n = 20$, the difference between two extreme expected in-control percentiles is 1242. For the difference between two extreme expected out-of-control percentiles in Table 4.13, the value is 56.58 when $n = 5$ and $\gamma_0 = 0.05$ while for $n = 20$ and $\gamma_0 = 0.05$, the value is 23.26. When the in-control coefficient of variation increases, the differences between the 5th and 95th expected in-control and out-of-control percentiles for all cases have minimal differences.

4.3 MRL and EMRL-based Designs

In this subsection, the aim is to get the optimal chart parameters (L , LCL , UCL) for the side-sensitive synthetic- γ chart which is designed based on the MRL and $EMRL$. The objective is to minimize the MRL_1 and $EMRL_1$ while satisfying the constraints in the

MRL_0 . This approach is taken because the previous subsection demonstrated that the distribution of the run length is positively skewed.

In order to assess the side-sensitive synthetic- γ chart's performance between the designs based on ARL and MRL fairly, the in-control 50th percentile of the design based on ARL is chosen as the MRL_0 . For example, the in-control 50th percentile of the ARL -based design is 211 for $n = 5$, $\tau = 1.1$ and $\gamma_0 = 0.05$ in Table 4.4. This value of 211 is used as the MRL_0 for $n = 5$, $\tau = 1.1$ and $\gamma_0 = 0.05$ to get the optimal chart parameters of the design based on MRL which minimize the MRL_1 .

The optimal chart parameters (L , LCL , UCL) and the corresponding 5th percentile (l_{05}), MRL_1 , 95th percentile (l_{95}), ARL_1 and ARL_0 values for the side-sensitive synthetic- γ chart that is designed based on the MRL for $n \in \{5, 7, 10, 15, 20\}$ and $\tau \in \{1.1, 1.2, 1.3, 1.4, 1.5, 1.6, 1.7, 1.8, 1.9, 2.0\}$ are shown in Table 4.14 for $\gamma_0 = 0.05$, Table 4.15 for $\gamma_0 = 0.10$, Table 4.16 for $\gamma_0 = 0.15$ and Table 4.17 for $\gamma_0 = 0.20$. All results obtained were validated through simulation as described in Section 3.8.

Table 4.14 Optimal chart parameters and the corresponding l_{05} , MRL_1 , l_{95} , ARL_1 and ARL_0 for the MRL -based side-sensitive synthetic- γ chart for $n \in \{5, 7, 10, 15, 20\}$, $\tau \in \{1.1, 1.2, 1.3, 1.4, 1.5, 1.6, 1.7, 1.8, 1.9, 2.0\}$ and $\gamma_0 = 0.05$

$\gamma_0 = 0.05$								
	L	LCL	UCL	l_{05}	MRL_1	l_{95}	ARL_1	ARL_0
τ	$n = 5$							
1.1	22	0.0043	0.0898	2	22	231	63.38	350.42
1.2	8	0.0083	0.0858	1	8	81	22.58	350.87
1.3	4	0.0111	0.0829	1	4	42	11.78	348.18
1.4	6	0.0093	0.0847	1	3	22	6.77	449.52
1.5	4	0.0110	0.0831	1	2	15	4.44	360.02
1.6	10	0.0070	0.0870	1	2	8	3.23	376.95
1.7	1	0.0166	0.0775	1	1	13	3.91	358.78
1.8	3	0.0121	0.0820	1	1	7	2.25	364.63
1.9	5	0.0099	0.0841	1	1	4	1.91	369.90
2.0	4	0.0109	0.0832	1	1	4	1.89	392.54
τ	$n = 7$							
1.1	18	0.0140	0.0820	2	18	186	51.10	344.30
1.2	6	0.0173	0.0787	1	6	62	17.42	350.38
1.3	3	0.0194	0.0766	1	3	31	8.93	350.55
1.4	3	0.0194	0.0766	1	2	17	4.94	353.50
1.5	13	0.0146	0.0814	1	2	8	3.19	384.04
1.6	2	0.0206	0.0754	1	1	8	2.65	360.73
1.7	5	0.0177	0.0783	1	1	4	1.92	368.97
1.8	23	0.0128	0.0832	1	1	4	1.90	399.81
1.9	10	0.0154	0.0806	1	1	3	1.58	380.50
2.0	3	0.0193	0.0767	1	1	3	1.58	420.07
τ	$n = 10$							
1.1	16	0.0212	0.0761	2	15	151	41.38	347.30
1.2	7	0.0231	0.0742	1	5	43	12.04	351.20
1.3	11	0.0219	0.0754	1	3	17	5.23	379.19
1.4	11	0.0219	0.0754	1	2	8	3.21	376.18
1.5	3	0.0251	0.0722	1	1	7	2.29	364.56
1.6	12	0.0216	0.0757	1	1	4	1.90	391.36
1.7	9	0.0223	0.0750	1	1	3	1.57	386.27
1.8	58	0.0177	0.0796	1	1	3	1.58	447.40
1.9	9	0.0223	0.0750	1	1	2	1.29	389.26
2.0	2	0.0260	0.0713	1	1	2	1.29	434.75
τ	$n = 15$							
1.1	13	0.0275	0.0708	1	12	117	32.12	353.27
1.2	3	0.0302	0.0681	1	3	34	9.64	356.54
1.3	9	0.0280	0.0702	1	2	9	3.55	369.80
1.4	2	0.0304	0.6781	1	1	8	2.53	466.56
1.5	3	0.0301	0.0681	1	1	3	1.63	368.30
1.6	40	0.0252	0.0730	1	1	3	1.58	417.73
1.7	13	0.0273	0.0710	1	1	2	1.28	386.47
1.8	100	0.2350	0.0748	1	1	2	1.27	469.89
1.9	100	0.0235	0.0748	1	1	2	1.18	469.89
2.0	1	0.0324	0.0659	1	1	1	1.05	369.78
τ	$n = 20$							
1.1	9	0.0313	0.0674	1	9	96	26.68	350.95
1.2	7	0.0317	0.0670	1	3	21	5.97	361.14
1.3	1	0.0350	0.0637	1	1	13	3.92	353.25
1.4	12	0.0307	0.0680	1	1	4	1.90	389.86
1.5	34	0.0291	0.0696	1	1	3	1.58	412.22
1.6	22	0.0298	0.0689	1	1	2	1.29	399.54
1.7	100	0.0275	0.0712	1	1	2	1.22	463.76
1.8	2	0.0337	0.0650	1	1	1	1.05	366.74
1.9	26	0.0295	0.0692	1	1	1	1.05	402.45
2.0	100	0.0275	0.0712	1	1	1	1.04	463.76

Table 4.15 Optimal chart parameters and the corresponding l_{05} , MRL_1 , l_{95} , ARL_1 and ARL_0 for the MRL -based side-sensitive synthetic- γ chart for $n \in \{5, 7, 10, 15, 20\}$, $\tau \in \{1.1, 1.2, 1.3, 1.4, 1.5, 1.6, 1.7, 1.8, 1.9, 2.0\}$ and $\gamma_0 = 0.10$

$\gamma_0 = 0.10$								
	L	LCL	UCL	l_{05}	MRL_1	l_{95}	ARL_1	ARL_0
τ	$n = 5$							
1.1	22	0.0075	0.1809	2	22	232	63.83	350.44
1.2	8	0.0158	0.1726	1	8	82	22.70	347.93
1.3	4	0.0215	0.1669	1	4	43	11.98	352.69
1.4	3	0.0179	0.1705	1	3	22	6.34	360.33
1.5	4	0.0212	0.1671	1	2	15	4.50	361.57
1.6	10	0.0132	0.1752	1	2	8	3.27	376.98
1.7	1	0.0328	0.1555	1	1	13	3.96	357.37
1.8	3	0.0236	0.1648	1	1	7	2.27	363.24
1.9	5	0.0192	0.1692	1	1	4	1.93	368.48
2.0	14	0.0101	0.1783	1	1	4	1.89	391.05
τ	$n = 7$							
1.1	18	0.0271	0.1650	2	18	189	66.88	349.08
1.2	6	0.0340	0.1582	1	6	63	17.65	282.95
1.3	3	0.0384	0.1538	1	3	32	9.03	350.68
1.4	3	0.0383	0.1539	1	2	17	5.02	356.58
1.5	12	0.0291	0.1631	1	2	8	3.19	378.08
1.6	1	0.0453	0.1469	1	1	11	3.47	358.42
1.7	4	0.0362	0.1559	1	1	4	1.95	368.15
1.8	19	0.0259	0.1663	1	1	4	1.89	397.68
1.9	8	0.0316	0.1606	1	1	3	1.57	379.96
2.0	31	0.0226	0.1696	1	1	3	1.58	417.48
τ	$n = 10$							
1.1	16	0.0419	0.1528	2	15	151	41.57	347.66
1.2	7	0.0457	0.1490	1	5	44	12.26	357.39
1.3	11	0.0433	0.1514	1	3	18	5.27	370.45
1.4	10	0.0437	0.1510	1	2	8	3.23	376.30
1.5	2	0.0519	0.1429	1	1	8	2.52	364.67
1.6	10	0.0436	0.1511	1	1	4	1.88	380.80
1.7	8	0.0448	0.1500	1	1	3	1.58	377.21
1.8	48	0.0357	0.1591	1	1	3	1.58	432.04
1.9	7	0.0454	0.1493	1	1	2	1.28	379.76
2.0	34	0.0374	0.1573	1	1	2	1.29	417.35
τ	$n = 15$							
1.1	13	0.0546	0.1420	1	12	117	32.11	350.62
1.2	8	0.0563	0.1403	1	4	29	8.06	362.41
1.3	8	0.0562	0.1404	1	2	11	3.59	371.37
1.4	3	0.0600	0.1366	1	1	7	2.27	364.01
1.5	3	0.0599	0.1366	1	1	3	1.66	371.37
1.6	33	0.0507	0.1459	1	1	3	1.58	411.33
1.7	11	0.0549	0.1417	1	1	2	1.29	383.81
1.8	97	0.0465	0.1501	1	1	2	1.29	472.52
1.9	100	0.0464	0.1502	1	1	2	1.19	474.78
2.0	2	0.0616	0.1350	1	1	1	1.05	370.04
τ	$n = 20$							
1.1	9	0.0624	0.1351	1	9	96	26.71	348.23
1.2	6	0.0636	0.1339	1	3	22	6.16	362.56
1.3	11	0.0615	0.1360	1	2	7	2.87	379.74
1.4	10	0.0617	0.1357	1	1	4	1.88	385.70
1.5	29	0.0584	0.1391	1	1	3	1.58	406.31
1.6	17	0.0601	0.1374	1	1	2	1.28	392.49
1.7	100	0.0545	0.1430	1	1	2	1.23	467.28
1.8	2	0.0672	0.1303	1	1	1	1.05	368.29
1.9	18	0.0599	0.1376	1	1	1	1.05	395.28
2.0	100	0.0545	0.1430	1	1	1	1.05	467.28

Table 4.16 Optimal chart parameters and the corresponding l_{05} , MRL_1 , l_{95} , ARL_1 and ARL_0 for the MRL -based side-sensitive synthetic- γ chart for $n \in \{5, 7, 10, 15, 20\}$, $\tau \in \{1.1, 1.2, 1.3, 1.4, 1.5, 1.6, 1.7, 1.8, 1.9, 2.0\}$ and $\gamma_0 = 0.15$

$\gamma_0 = 0.15$								
	L	LCL	UCL	l_{05}	MRL_1	l_{95}	ARL_1	ARL_0
τ	$n = 5$							
1.1	22	0.0086	0.2747	2	22	234	64.41	348.92
1.2	8	0.0214	0.2619	1	8	84	23.16	349.48
1.3	4	0.0305	0.2528	1	4	43	12.19	351.31
1.4	5	0.0272	0.2561	1	3	24	6.68	361.14
1.5	3	0.0341	0.2493	1	2	17	4.91	358.92
1.6	9	0.0189	0.2644	1	2	8	3.31	375.23
1.7	6	0.0244	0.2589	1	2	6	2.65	370.80
1.8	2	0.0392	0.2441	1	1	8	2.54	363.05
1.9	4	0.0298	0.2535	1	1	4	1.98	369.06
2.0	11	0.0159	0.2674	1	1	4	1.89	384.73
τ	$n = 7$							
1.1	18	0.0387	0.2500	2	18	181	52.57	349.34
1.2	6	0.0495	0.2392	1	6	64	17.85	350.77
1.3	3	0.0564	0.2324	1	3	32	9.22	352.33
1.4	3	0.0562	0.2326	1	2	18	5.15	359.71
1.5	11	0.0426	0.2461	1	2	8	3.24	379.66
1.6	1	0.0672	0.2216	1	1	12	3.56	358.51
1.7	4	0.0530	0.2357	1	1	4	1.99	368.35
1.8	15	0.0392	0.2495	1	1	4	1.89	392.10
1.9	6	0.0488	0.2400	1	1	3	1.57	376.07
2.0	22	0.0352	0.2535	1	1	3	1.58	403.49
τ	$n = 10$							
1.1	15	0.0619	0.2305	2	15	153	42.25	348.29
1.2	6	0.0687	0.2237	1	5	46	12.78	354.23
1.3	10	0.0645	0.2280	1	3	18	5.37	370.70
1.4	9	0.0652	0.2273	1	2	8	3.27	374.94
1.5	2	0.0770	0.2154	1	1	8	2.58	363.36
1.6	8	0.6596	0.2265	1	1	4	1.88	379.07
1.7	6	0.0682	0.2242	1	1	3	1.57	375.06
1.8	34	0.0544	0.2381	1	1	3	1.58	419.58
1.9	5	0.0696	0.2229	1	1	2	1.29	377.31
2.0	22	0.0578	0.2346	1	1	2	1.29	405.10
τ	$n = 15$							
1.1	13	0.0810	0.2141	1	12	118	32.32	349.67
1.2	8	0.0835	0.2116	1	4	29	8.24	364.31
1.3	8	0.0842	0.2109	1	2	11	3.56	326.92
1.4	2	0.0919	0.2032	1	1	8	2.52	361.40
1.5	18	0.0784	0.2167	1	1	4	1.90	394.51
1.6	24	0.0766	0.2185	1	1	3	1.58	405.19
1.7	8	0.0832	0.2119	1	1	2	1.29	382.23
1.8	62	0.0710	0.2242	1	1	2	1.29	445.28
1.9	100	0.0681	0.2270	1	1	2	1.21	477.04
2.0	1	0.0962	0.1989	1	1	1	1.10	366.66
τ	$n = 20$							
1.1	12	0.0914	0.2050	1	10	95	26.16	354.67
1.2	6	0.0947	0.2017	1	3	22	6.30	362.90
1.3	10	0.0920	0.2044	1	2	7	2.90	375.74
1.4	8	0.0930	0.2034	1	1	4	1.88	379.89
1.5	22	0.0880	0.2084	1	1	3	1.58	399.44
1.6	12	0.0910	0.2054	1	1	2	1.28	386.27
1.7	100	0.0805	0.2159	1	1	2	1.26	473.42
1.8	1	0.1040	0.1924	1	1	1	1.10	367.95
1.9	10	0.0918	0.2046	1	1	1	1.05	387.69
2.0	87	0.0812	0.2152	1	1	1	1.05	463.42

Table 4.17 Optimal chart parameters and the corresponding l_{05} , MRL_1 , l_{95} , ARL_1 and ARL_0 for the MRL -based side-sensitive synthetic- γ chart for $n \in \{5, 7, 10, 15, 20\}$, $\tau \in \{1.1, 1.2, 1.3, 1.4, 1.5, 1.6, 1.7, 1.8, 1.9, 2.0\}$ and $\gamma_0 = 0.20$

$\gamma_0 = 0.20$								
	L	LCL	UCL	l_{05}	MRL_1	l_{95}	ARL_1	ARL_0
τ	$n = 5$							
1.1	23	0.0054	0.3737	2	23	239	65.53	350.16
1.2	8	0.0245	0.3546	1	8	85	23.70	348.03
1.3	4	0.0373	0.3418	1	4	44	12.53	351.41
1.4	5	0.0326	0.3465	1	3	24	6.89	359.74
1.5	3	0.0425	0.3367	1	2	18	5.07	357.56
1.6	11	0.0169	0.3622	1	2	9	3.47	378.75
1.7	12	0.0152	0.3640	1	2	7	2.88	381.90
1.8	2	0.0498	0.3293	1	1	8	2.62	363.18
1.9	5	0.0320	0.3471	1	1	5	2.03	371.59
2.0	8	0.0227	0.3564	1	1	4	1.89	379.37
τ	$n = 7$							
1.1	20	0.0463	0.3397	2	19	196	53.69	353.75
1.2	6	0.0633	0.3227	1	6	65	18.25	349.54
1.3	3	0.0729	0.3131	1	3	33	9.50	354.03
1.4	2	0.0786	0.3074	1	2	21	6.00	353.82
1.5	9	0.0564	0.3296	1	2	8	3.28	376.36
1.6	1	0.0882	0.2978	1	1	12	3.69	357.18
1.7	5	0.0650	0.3210	1	1	5	2.05	371.07
1.8	11	0.0533	0.3327	1	1	4	1.89	384.40
1.9	4	0.0682	0.3178	1	1	3	1.59	370.07
2.0	14	0.0496	0.3364	1	1	3	1.58	392.30
τ	$n = 10$							
1.1	15	0.0800	0.3106	2	15	156	42.92	348.86
1.2	6	0.0896	0.3010	1	5	47	13.08	353.13
1.3	8	0.0860	0.3046	1	3	19	5.56	369.05
1.4	8	0.0859	0.3047	1	2	8	3.35	372.04
1.5	1	0.1090	0.2816	1	1	11	3.42	359.77
1.6	6	0.0889	0.3017	1	1	4	1.89	375.45
1.7	4	0.0934	0.2972	1	1	3	1.59	370.79
1.8	22	0.0742	0.3165	1	1	3	1.58	405.72
1.9	3	0.0965	0.2941	1	1	2	1.29	372.53
2.0	13	0.0801	0.3105	1	1	2	1.29	392.74
τ	$n = 15$							
1.1	13	0.1062	0.2878	1	12	119	32.80	350.37
1.2	7	0.1109	0.2831	1	4	31	8.60	362.98
1.3	6	0.1120	0.2820	1	2	13	3.80	369.94
1.4	2	0.1214	0.2726	1	1	8	2.61	363.06
1.5	13	0.1053	0.2887	1	1	4	1.89	389.66
1.6	17	0.1029	0.2910	1	1	3	1.58	398.55
1.7	5	0.1133	0.2807	1	1	2	1.28	378.20
1.8	35	0.0969	0.2971	1	1	2	1.29	420.50
1.9	100	0.0880	0.3060	1	1	2	1.24	479.46
2.0	100	0.0880	0.3060	1	1	2	1.17	479.46
τ	$n = 20$							
1.1	11	0.1212	0.2744	1	10	97	26.64	349.34
1.2	5	0.1263	0.2692	1	3	24	6.67	359.81
1.3	8	0.1228	0.2727	1	2	7	2.93	374.45
1.4	7	0.1237	0.2719	1	1	4	1.91	377.11
1.5	15	0.1183	0.2773	1	1	3	1.58	394.40
1.6	8	0.1227	0.2729	1	1	2	1.28	383.41
1.7	94	0.1056	0.2900	1	1	2	1.29	470.39
1.8	100	0.1051	0.2904	1	1	2	1.18	475.02
1.9	5	0.1260	0.2696	1	1	1	1.05	377.59
2.0	36	0.1122	0.2834	1	1	1	1.05	419.33

Tables 4.14 until 4.17 demonstrate that the optimal chart parameters (L , LCL , UCL) for the side-sensitive synthetic- γ chart which is designed based on MRL are relatively smaller than those for the ARL -based design, especially for small shift sizes such as $\tau \in \{1.1, 1.2\}$ for all sample sizes and in-control coefficients of variations. In the design based on MRL , the optimal L is smaller than the optimal L in the design based on ARL . For instance, in Table 4.14, when $n = 5$, $\tau = 1.1$ and $\gamma_0 = 0.05$, the design based on MRL suggests an optimal L , of 22 while the design based on ARL in Table 4.1 suggests an optimal L , of 42. This smaller L also results in a tighter conforming region, i.e. the region between the LCL and UCL . For instance, in Table 4.14, when $n = 5$, $\tau = 1.1$ and $\gamma_0 = 0.05$, the design based on MRL suggests optimal LCL and UCL of 0.0043 and 0.0898, respectively, while the design based on ARL in Table 4.1 suggests an optimal LCL and UCL of 0.0017 and 0.0924, respectively. Consequently, it is evident that the side-sensitive synthetic- γ chart that is designed based on MRL generates a tighter conforming region than the design based on ARL for small shift sizes.

Upon comparing Tables 4.8 until 4.11 for the side-sensitive synthetic- γ chart that is designed based on ARL with Tables 4.14 until 4.17 for the design based on MRL of the same chart, it is noticeable that the design based on MRL yields smaller MRL_1 than the design based on ARL , particularly for smaller shift sizes. For instance, in Table 4.14, when $n = 5$, $\tau = 1.1$ and $\gamma_0 = 0.05$, the MRL_1 for the design based on MRL is 22 while in Table 4.8, the MRL_1 is 29 for the design based on ARL . This indicates that the design based on MRL performs better than the ARL -based design in terms of MRL_1 , while both have the same MRL_0 . Additionally, the design based on MRL provides a smaller difference between the 5th and 95th percentiles for smaller shift sizes, suggesting that it has less spread and variation than the design based on ARL . For instance, the difference

for $n = 5$, $\tau = 1.1$ and $\gamma_0 = 0.05$ is 229 in Table 4.14 for the design based on *MRL* and 237 in Table 4.8 for the design based on *ARL*.

In terms of the performance of ARL_1 obtained in Tables 4.1 and 4.2, and 4.14 to 4.17, it can be observed that both *MRL* and *ARL*-based designs provide similar results in general. In fact, the design based on *MRL* is found to have a smaller ARL_1 compared to the design based on *ARL* for small shift sizes. For instance, when $n = 5$, $\tau = 1.1$ and $\gamma_0 = 0.05$ for both designs, the *MRL*-based design produces an ARL_1 of 63.38 in Table 4.14 while the *ARL*-based design produces an ARL_1 of 64.74 in Table 4.1. This result suggests that the design based on *MRL* is superior in detecting shifts compared to the *ARL*-based design because it generates a similar average quantity of samples to spot the shift, but with a smaller MRL_1 .

The side-sensitive synthetic- γ chart that is designed based on *MRL* does not have a fixed value of ARL_0 , unlike the design based on *ARL* for the same chart which is fixed at 370.4 for all cases. The values of ARL_0 for the design based on *MRL* are calculated by inputting the optimal chart parameters (L , LCL , UCL) into Equation (3.42). Note that the shift size is set as 1 for all cases. By referring to the columns of ARL_0 in Tables 4.14 to 4.17, it is observed that the obtained ARL_0 for *MRL*-based design generally lies between 282.95 and 479.46. The ARL_0 values for the design based on *MRL* are generally observed to be slightly lower than those for the design based on *ARL* in most cases, although the difference is not significant.

Both designs based on *MRL* and *ARL* need to specify the values of shift size to obtain the optimal chart parameters. However, in practical scenarios, it can be difficult to do so. To address this issue, the side-sensitive synthetic- γ chart which is designed based on

EMRL is introduced in this thesis, with a range of shift sizes fixed as $(\tau_{\min}, \tau_{\max}) = (1, 2]$ since this thesis focuses solely on detecting an upward shift as explained in Section 4.1 for *EARL*. For the design based on *EMRL*, the in-control 50th expected percentile of the side-sensitive synthetic- γ chart from Table 4.12, which is obtained by adopting the optimal chart parameters that minimize the *EARL*, is selected as the *MRL*₀. Table 4.18 presents the optimal chart parameters (*L*, *LCL*, *UCL*), and the corresponding 5th expected percentile ($E(l_{05})$), *EMRL*₁, 95th expected percentile ($E(l_{95})$), *EARL*₁ and *ARL*₀ values for $n \in \{5, 7, 10, 15, 20\}$ and $\gamma_0 \in \{0.05, 0.10, 0.15, 0.20\}$.

Table 4.18 Optimal chart parameters and the corresponding $E(l_{05})$, *EMRL*₁, $E(l_{95})$, *EARL* and *ARL*₀ for the *EMRL*-based side-sensitive synthetic- γ chart for $n \in \{5, 7, 10, 15, 20\}$, $\gamma_0 \in \{0.05, 0.10, 0.15, 0.20\}$ and $(\tau_{\min}, \tau_{\max}) = (1, 2]$

	<i>L</i>	<i>LCL</i>	<i>UCL</i>	$E(l_{05})$	<i>EMRL</i> ₁	$E(l_{95})$	<i>EARL</i> ₁	<i>ARL</i> ₀
<i>n</i>	$\gamma_0 = 0.05$							
5	7	0.0089	0.0852	1.10	9.90	57.99	17.20	344.46
7	15	0.0144	0.0816	1.12	7.49	46.17	13.58	356.84
10	14	0.0215	0.0758	1.12	5.90	37.05	11.02	349.06
15	12	0.0276	0.0706	1.05	5.03	29.72	8.97	354.87
20	14	0.0306	0.0681	1.05	4.25	24.54	7.48	354.92
<i>n</i>	$\gamma_0 = 0.10$							
5	6	0.0183	0.1701	1.05	10.09	59.04	17.59	343.97
7	14	0.0285	0.1636	1.12	7.65	46.57	13.71	357.06
10	14	0.0424	0.1523	1.12	5.95	37.42	11.12	352.43
15	12	0.0549	0.1417	1.05	4.96	29.43	8.88	347.68
20	10	0.0621	0.1354	1.05	4.37	25.05	7.65	349.74
<i>n</i>	$\gamma_0 = 0.15$							
5	6	0.0255	0.2578	1.05	10.16	59.60	17.73	342.56
7	13	0.0417	0.2470	1.12	7.70	47.08	13.89	355.78
10	14	0.0622	0.2302	1.12	6.02	38.15	11.30	357.46
15	11	0.0819	0.2132	1.05	5.03	30.26	9.07	352.74
20	13	0.0911	0.2053	1.05	4.29	24.79	7.58	354.54
<i>n</i>	$\gamma_0 = 0.20$							
5	12	0.0167	0.3624	1.12	9.58	59.36	17.37	353.33
7	12	0.0533	0.3327	1.12	7.86	47.96	14.16	354.46
10	8	0.0867	0.3039	1.05	6.71	39.46	11.79	348.10
15	7	0.1113	0.2826	1.05	5.54	31.25	9.47	345.07
20	12	0.1205	0.2750	1.05	4.34	25.07	7.68	353.83

Table 4.18 displays that the optimal L for the design based on $EMRL$ is consistently smaller than the design based on $EARL$ in Table 4.3. For instance, when $n = 5$ and $\gamma_0 = 0.05$, the optimal L is 7 for $EMRL$ -based design in Table 4.18 whereas it is 25 for $EARL$ -based design in Table 4.3. In addition, $EMRL$ -based design generates a smaller conforming region with a larger LCL and a smaller UCL than $EARL$ -based design for all cases. For example, in Table 4.18, the optimal chart parameters, LCL , UCL for $EMRL$ -based design are 0.0089 and 0.0852, respectively, while in Table 4.3, the optimal chart parameters, LCL , UCL is 0.0036 and 0.0905, respectively, for $EARL$ -based design. However, Tables 4.13 and 4.18 do not show any obvious difference between $EMRL_1$, $E(l_{05})$, and $E(l_{95})$ for both designs. Also, the ARL_0 of the $EMRL$ -based design in the last column of Table 4.18 is a little smaller than that of the design based on $EARL$, which is 370.4, but the difference is not significant. Thus, both designs of the side-sensitive synthetic- γ chart based on $EMRL$ and $EARL$ shows similar performance.

4.4 Comparison with Other Coefficient of Variation Charts

The effectiveness of the proposed side-sensitive synthetic- γ chart was evaluated against three frequently used control charts based on the coefficient of variation, namely the Shewhart- γ , EWMA- γ^2 and non-side-sensitive synthetic- γ charts. To compare these charts, five criteria were employed in this subsection. Initially, the optimal chart parameters of the side-sensitive synthetic- γ chart which is designed based on ARL were compared with those of the non-side-sensitive synthetic- γ chart. Then, the performance of all four control charts was evaluated based on their ARL_1 and $SDRL_1$. The $EARL_1$ performance of the charts was compared in the third comparison, followed by a fourth comparison based on the performance of the 5th percentile, 95th percentile and MRL_1 . Lastly, the performance of the charts was assessed in terms of the $EMRL_1$.

Evaluation between the design based on ARL of the side-sensitive synthetic- γ and the non-side-sensitive synthetic- γ charts in terms of the optimal chart parameters (L , LCL , UCL) obtained for $n \in \{5, 7, 10, 15, 20\}$ and $\tau \in \{1.1, 1.2, 1.3, 1.4, 1.5, 1.6, 1.7, 1.8, 1.9, 2.0\}$ are shown in Table 4.19 for $\gamma_0 = 0.05$, Table 4.20 for $\gamma_0 = 0.10$, Table 4.21 for $\gamma_0 = 0.15$ and Table 4.22 for $\gamma_0 = 0.20$. All results obtained were validated using simulation with 10,000 trials.

Table 4.19 Comparison of the optimal chart parameters (L , LCL , UCL) of the ARL -based design of the side-sensitive synthetic- γ (SS Syn) and non-side-sensitive synthetic- γ charts (NSS Syn) for $n \in \{5, 7, 10, 15, 20\}$, $\tau \in \{1.1, 1.2, 1.3, 1.4, 1.5, 1.6, 1.7, 1.8, 1.9, 2.0\}$ and $\gamma_0 = 0.05$

τ	$\gamma_0 = 0.05$					
	SS Syn			NSS Syn		
	L	LCL	UCL	L	LCL	UCL
	$n = 5$					
1.1	42	0.0017	0.0924	74	0.0103	0.0995
1.2	23	0.0039	0.0902	39	0.0111	0.0974
1.3	15	0.0055	0.0885	24	0.0117	0.0957
1.4	11	0.0067	0.0873	16	0.0123	0.0943
1.5	8	0.0080	0.0860	12	0.0128	0.0933
1.6	7	0.0086	0.0855	9	0.0132	0.0922
1.7	6	0.0092	0.0849	7	0.0137	0.0912
1.8	5	0.0099	0.0841	6	0.0139	0.0906
1.9	5	0.0099	0.0841	6	0.0139	0.0906
2.0	4	0.0109	0.0832	5	0.0143	0.0899
	$n = 7$					
1.1	37	0.0116	0.0843	67	0.0158	0.0901
1.2	19	0.0136	0.0824	32	0.0167	0.0882
1.3	12	0.0150	0.0810	18	0.0176	0.0866
1.4	9	0.0158	0.0801	12	0.0182	0.0854
1.5	7	0.0166	0.0794	8	0.0189	0.0842
1.6	5	0.0176	0.0783	7	0.0191	0.0838
1.7	5	0.0176	0.0783	5	0.0197	0.0828
1.8	4	0.0183	0.0776	5	0.0197	0.0828
1.9	4	0.0183	0.0776	4	0.0201	0.0821
2.0	3	0.0192	0.0767	4	0.0201	0.0821

Table 4.19, continued

τ	$\gamma_0 = 0.05$					
	SS Syn			NSS Syn		
	L	LCL	UCL	L	LCL	UCL
$n = 10$						
1.1	35	0.0193	0.0780	56	0.0212	0.0823
1.2	16	0.0210	0.0762	24	0.0223	0.0805
1.3	10	0.0221	0.0752	13	0.0232	0.0791
1.4	7	0.0230	0.0743	8	0.0239	0.0780
1.5	5	0.0238	0.0735	6	0.0244	0.0773
1.6	4	0.0243	0.0730	5	0.0246	0.0768
1.7	4	0.0243	0.0730	4	0.0250	0.0763
1.8	3	0.0250	0.0723	3	0.0255	0.0755
1.9	3	0.0250	0.0723	3	0.0255	0.0755
2.0	3	0.0250	0.0723	3	0.0255	0.0755
$n = 15$						
1.1	31	0.0259	0.0724	47	0.0265	0.0756
1.2	13	0.0274	0.0709	17	0.0277	0.0738
1.3	7	0.0285	0.0697	9	0.0285	0.0727
1.4	5	0.0286	0.0696	6	0.0291	0.0719
1.5	4	0.0296	0.0687	4	0.0297	0.0711
1.6	3	0.0301	0.0681	3	0.0301	0.0705
1.7	3	0.0301	0.0681	3	0.0301	0.0705
1.8	2	0.0309	0.0673	3	0.0301	0.0705
1.9	2	0.0309	0.0673	2	0.0307	0.0697
2.0	2	0.0309	0.0673	2	0.0307	0.0697
$n = 20$						
1.1	27	0.0296	0.0691	39	0.0298	0.0717
1.2	10	0.0311	0.0676	13	0.0310	0.0700
1.3	6	0.0319	0.0668	7	0.0317	0.0690
1.4	4	0.0325	0.0662	4	0.0324	0.0681
1.5	3	0.0330	0.0657	3	0.0328	0.0676
1.6	2	0.0330	0.0657	3	0.0328	0.0676
1.7	2	0.0337	0.0650	2	0.0333	0.0669
1.8	2	0.0337	0.0650	2	0.0333	0.0669
1.9	2	0.0337	0.0650	2	0.0333	0.0669
2.0	2	0.0337	0.0650	2	0.0333	0.0669

Table 4.20 Comparison of the optimal chart parameters (L, LCL, UCL) of the ARL -based design of the side-sensitive synthetic- γ (SS Syn) and non-side-sensitive synthetic- γ charts (NSS Syn) for $n \in \{5, 7, 10, 15, 20\}$, $\tau \in \{1.1, 1.2, 1.3, 1.4, 1.5, 1.6, 1.7, 1.8, 1.9, 2.0\}$ and $\gamma_0 = 0.10$

τ	$\gamma_0 = 0.10$					
	SS Syn			NSS Syn		
	L	LCL	UCL	L	LCL	UCL
$n = 5$						
1.1	42	0.0021	0.1863	74	0.0205	0.2009
1.2	23	0.0067	0.1817	41	0.0220	0.1969
1.3	15	0.0100	0.1784	24	0.0234	0.1932
1.4	11	0.0126	0.1758	16	0.0246	0.1902
1.5	8	0.0152	0.1732	12	0.0255	0.1880
1.6	7	0.0163	0.1721	9	0.0264	0.1858
1.7	6	0.0176	0.1708	8	0.0268	0.1849
1.8	5	0.0191	0.1692	6	0.0278	0.1827
1.9	5	0.0191	0.1692	6	0.0278	0.1827
2.0	4	0.0210	0.1674	5	0.0285	0.1812
$n = 7$						
1.1	36	0.0225	0.1696	67	0.0315	0.1816
1.2	19	0.0264	0.1658	32	0.0334	0.1777
1.3	12	0.0292	0.1629	18	0.0351	0.1744
1.4	9	0.0310	0.1611	12	0.0363	0.1720
1.5	7	0.0326	0.1595	8	0.0377	0.1695
1.6	5	0.0347	0.1574	7	0.0381	0.1687
1.7	5	0.0347	0.1574	5	0.0393	0.1665
1.8	4	0.0362	0.1560	5	0.0393	0.1665
1.9	4	0.0362	0.1560	4	0.0401	0.1651
2.0	3	0.0380	0.1542	4	0.0401	0.1651
$n = 10$						
1.1	35	0.0379	0.1568	56	0.0423	0.1657
1.2	16	0.0415	0.1532	25	0.0444	0.1622
1.3	10	0.0438	0.1509	13	0.0462	0.1591
1.4	7	0.0455	0.1492	8	0.0477	0.1568
1.5	5	0.0472	0.1476	6	0.0486	0.1553
1.6	4	0.0483	0.1464	5	0.0492	0.1544
1.7	4	0.0483	0.1464	4	0.0499	0.1532
1.8	3	0.0497	0.1450	3	0.0509	0.1517
1.9	3	0.0497	0.1450	3	0.0509	0.1517
2.0	3	0.0497	0.1450	3	0.0509	0.1517
$n = 15$						
1.1	31	0.0513	0.1453	47	0.0529	0.1519
1.2	13	0.0544	0.1422	17	0.0553	0.1483
1.3	7	0.0567	0.1399	9	0.0569	0.1459
1.4	5	0.0580	0.1386	6	0.0580	0.1443
1.5	4	0.0588	0.1378	4	0.0592	0.1427
1.6	3	0.0600	0.1366	3	0.0600	0.1415
1.7	3	0.0600	0.1366	3	0.0600	0.1415
1.8	2	0.0616	0.1350	3	0.0600	0.1415
1.9	2	0.0616	0.1350	2	0.0613	0.1398
2.0	2	0.0616	0.1350	2	0.0613	0.1398
$n = 20$						
1.1	27	0.0589	0.1386	39	0.0594	0.1439
1.2	10	0.0619	0.1356	14	0.0616	0.1408
1.3	6	0.0635	0.1340	7	0.0633	0.1386
1.4	4	0.0648	0.1327	4	0.0647	0.1367
1.5	3	0.0658	0.1317	3	0.0655	0.1357
1.6	3	0.0658	0.1317	3	0.0655	0.1357
1.7	2	0.0672	0.1303	2	0.0666	0.1342
1.8	2	0.0672	0.1303	2	0.0666	0.1342
1.9	2	0.0672	0.1303	2	0.0666	0.1342
2.0	2	0.0672	0.1303	2	0.0666	0.1342

Table 4.21 Comparison of the optimal chart parameters (L, LCL, UCL) of the ARL -based design of the side-sensitive synthetic- γ (SS Syn) and non-side-sensitive synthetic- γ charts (NSS Syn) for $n \in \{5, 7, 10, 15, 20\}$, $\tau \in \{1.1, 1.2, 1.3, 1.4, 1.5, 1.6, 1.7, 1.8, 1.9, 2.0\}$ and $\gamma_0 = 0.15$

τ	$\gamma_0 = 0.15$					
	SS Syn			NSS Syn		
	L	LCL	UCL	L	LCL	UCL
$n = 5$						
1.1	42	0.0001	0.2832	74	0.0307	0.3063
1.2	23	0.0072	0.2761	41	0.0329	0.3000
1.3	15	0.0125	0.2708	24	0.0350	0.2941
1.4	11	0.0165	0.2669	16	0.0368	0.2894
1.5	8	0.0206	0.2627	12	0.0381	0.2860
1.6	7	0.0224	0.2610	9	0.0395	0.2825
1.7	6	0.0244	0.2589	8	0.0401	0.2811
1.8	5	0.0268	0.2565	7	0.0408	0.2795
1.9	5	0.0268	0.2565	6	0.0416	0.2775
2.0	4	0.0298	0.2535	5	0.0425	0.2752
$n = 7$						
1.1	36	0.0316	0.2572	67	0.0470	0.2760
1.2	19	0.0376	0.2512	32	0.0499	0.2698
1.3	12	0.0421	0.2467	18	0.0524	0.2646
1.4	9	0.0449	0.2439	12	0.0543	0.2609
1.5	7	0.0474	0.2414	9	0.0557	0.2581
1.6	5	0.0507	0.2380	7	0.0569	0.2557
1.7	5	0.0507	0.2380	6	0.0577	0.2542
1.8	4	0.0530	0.2358	5	0.0587	0.2524
1.9	4	0.0530	0.2358	4	0.0599	0.2501
2.0	3	0.0559	0.2329	4	0.0599	0.2501
$n = 10$						
1.1	34	0.0555	0.2370	56	0.0632	0.2511
1.2	16	0.0609	0.2315	25	0.0663	0.2456
1.3	10	0.0645	0.2280	13	0.0691	0.2409
1.4	7	0.0672	0.2253	9	0.0707	0.2381
1.5	5	0.0697	0.2227	6	0.0726	0.2350
1.6	4	0.0715	0.2210	5	0.0735	0.2335
1.7	4	0.0715	0.2210	4	0.0746	0.2317
1.8	3	0.0737	0.2188	4	0.0746	0.2317
1.9	3	0.0737	0.2188	3	0.0761	0.2294
2.0	3	0.0737	0.2188	3	0.0761	0.2294
$n = 15$						
1.1	30	0.0760	0.2191	48	0.0789	0.2297
1.2	13	0.0806	0.2145	18	0.0824	0.2244
1.3	8	0.0842	0.2109	9	0.0851	0.2204
1.4	5	0.0862	0.2089	6	0.0868	0.2180
1.5	4	0.0875	0.2076	4	0.0885	0.2155
1.6	3	0.0893	0.2059	4	0.0885	0.2155
1.7	3	0.0893	0.2059	3	0.0898	0.2136
1.8	2	0.0918	0.2034	3	0.0898	0.2136
1.9	2	0.0918	0.2034	2	0.0916	0.2110
2.0	2	0.0918	0.2034	2	0.0916	0.2110
$n = 20$						
1.1	27	0.0875	0.2090	39	0.0888	0.2172
1.2	10	0.0921	0.2043	14	0.0921	0.2125
1.3	6	0.0946	0.2018	7	0.0946	0.2090
1.4	4	0.0966	0.1998	5	0.0959	0.2073
1.5	3	0.0981	0.1983	3	0.0979	0.2046
1.6	3	0.0981	0.1983	3	0.0979	0.2046
1.7	2	0.1002	0.1962	2	0.0995	0.2024
1.8	2	0.1002	0.1962	2	0.0995	0.2024
1.9	2	0.1002	0.1962	2	0.0995	0.2024
2.0	2	0.1002	0.1962	2	0.0995	0.2024

Table 4.22 Comparison of the optimal chart parameters (L, LCL, UCL) of the ARL -based design of the side-sensitive synthetic- γ (SS Syn) and non-side-sensitive synthetic- γ charts (NSS Syn) for $n \in \{5, 7, 10, 15, 20\}$, $\tau \in \{1.1, 1.2, 1.3, 1.4, 1.5, 1.6, 1.7, 1.8, 1.9, 2.0\}$ and $\gamma_0 = 0.20$

τ	$\gamma_0 = 0.20$					
	SS Syn			NSS Syn		
	L	LCL	UCL	L	LCL	UCL
$n = 5$						
1.1	42	0.0059	0.3850	76	0.0406	0.4186
1.2	24	0.0035	0.3756	42	0.0435	0.4053
1.3	15	0.0118	0.3674	25	0.0462	0.4012
1.4	11	0.0173	0.3618	17	0.0485	0.3949
1.5	9	0.0210	0.3581	12	0.0506	0.3890
1.6	7	0.0257	0.3534	10	0.0517	0.3859
1.7	6	0.0286	0.3505	8	0.0532	0.3820
1.8	5	0.0320	0.3471	7	0.0541	0.3796
1.9	5	0.0320	0.3471	6	0.0552	0.3769
2.0	4	0.0363	0.3428	5	0.0565	0.3737
$n = 7$						
1.1	36	0.0377	0.3483	67	0.0623	0.3750
1.2	19	0.0463	0.3397	33	0.0660	0.3665
1.3	12	0.0526	0.3334	19	0.0692	0.3595
1.4	9	0.0567	0.3293	12	0.0720	0.3534
1.5	7	0.0602	0.3258	9	0.0739	0.3496
1.6	6	0.0624	0.3236	7	0.0756	0.3461
1.7	5	0.0650	0.3210	6	0.0766	0.3440
1.8	4	0.0682	0.3178	5	0.0779	0.3414
1.9	4	0.0682	0.3178	4	0.0795	0.3383
2.0	3	0.0722	0.3137	4	0.0795	0.3383
$n = 10$						
1.1	33	0.0711	0.3195	60	0.0835	0.3404
1.2	16	0.0789	0.3120	26	0.0877	0.3324
1.3	10	0.0835	0.3071	14	0.0912	0.3261
1.4	7	0.0874	0.3032	9	0.0938	0.3214
1.5	5	0.0910	0.2996	6	0.0964	0.3170
1.6	4	0.0935	0.2972	5	0.0975	0.3150
1.7	4	0.0935	0.2972	4	0.0990	0.3125
1.8	3	0.0966	0.2941	4	0.0990	0.3125
1.9	3	0.0966	0.2941	3	0.1010	0.3093
2.0	3	0.0966	0.2941	3	0.1010	0.3093
$n = 15$						
1.1	30	0.0992	0.2948	48	0.1047	0.3097
1.2	13	0.1057	0.2883	18	0.1093	0.3023
1.3	7	0.1107	0.2833	10	0.1124	0.2976
1.4	5	0.1135	0.2805	6	0.1151	0.2933
1.5	4	0.1153	0.2787	5	0.1162	0.2918
1.6	3	0.1177	0.2763	4	0.1175	0.2898
1.7	3	0.1177	0.2763	3	0.1192	0.2873
1.8	3	0.1177	0.2763	3	0.1192	0.2873
1.9	2	0.1212	0.2728	2	0.1216	0.2837
2.0	2	0.1212	0.2728	2	0.1216	0.2837
$n = 20$						
1.1	27	0.1149	0.2806	42	0.1175	0.2928
1.2	11	0.1208	0.2748	14	0.1223	0.2857
1.3	6	0.1249	0.2707	7	0.1256	0.2809
1.4	4	0.1277	0.2679	5	0.1273	0.2785
1.5	3	0.1297	0.2659	4	0.1285	0.2769
1.6	3	0.1297	0.2659	3	0.1300	0.2748
1.7	2	0.1326	0.2629	3	0.1300	0.2748
1.8	2	0.1326	0.2629	2	0.1322	0.2717
1.9	2	0.1326	0.2629	2	0.1322	0.2717
2.0	2	0.1326	0.2629	2	0.1322	0.2717

Tables 4.19 to 4.22 indicate the side-sensitive synthetic- γ chart that is designed based on ARL has smaller optimal chart parameters, namely L , LCL and UCL , compared to those optimal chart parameters of the non-side-sensitive synthetic- γ chart, particularly for small shift sizes. For the side-sensitive synthetic- γ chart, the values of optimal L , LCL and UCL are 42, 0.0017 and 0.0924, respectively, when $n = 5$, $\tau = 1.1$ and $\gamma_0 = 0.05$, while for the non-side-sensitive synthetic- γ chart, those optimal values are 74, 0.0103 and 0.0995, respectively (see Table 4.19). In addition, the conforming region which is the region between the LCL and UCL of the side-sensitive synthetic- γ chart, is also tighter compared to that of the non-side-sensitive synthetic- γ chart. These observations indicate that the side-sensitive synthetic- γ chart which is designed based on the ARL has a tighter conforming region compared to the non-side-sensitive synthetic- γ chart.

Next, a comparison of the ARL_1 and $SDRL_1$ of the Shewhart- γ , EWMA- γ^2 , non-side-sensitive synthetic- γ , and side-sensitive synthetic- γ charts with the same values of $n \in \{5, 7, 10, 15, 20\}$ and $\tau \in \{1.1, 1.2, 1.3, 1.4, 1.5, 1.6, 1.7, 1.8, 1.9, 2.0\}$ is presented in Table 4.23 for $\gamma_0 = 0.05$, Table 4.24 for $\gamma_0 = 0.10$, Table 4.25 for $\gamma_0 = 0.15$ and Table 4.26 for $\gamma_0 = 0.20$. All results obtained were verified through simulation with 10,000 trials.

Table 4.23 The ARL_1 and $SDRL_1$ of the ARL -based design of the Shewhart- γ , EWMA- γ^2 , non-side-sensitive synthetic- γ (NSS Syn) and side-sensitive synthetic- γ (SS Syn) charts for $n \in \{5, 7, 10, 15, 20\}$, $\tau \in \{1.1, 1.2, 1.3, 1.4, 1.5, 1.6, 1.7, 1.8, 1.9, 2.0\}$ and $\gamma_0 = 0.05$

τ	$\gamma_0 = 0.05$								Best Chart
	Shewhart		EWMA		NSS Syn		SS Syn		
	ARL_1	$SDRL_1$	ARL_1	$SDRL_1$	ARL_1	$SDRL_1$	ARL_1	$SDRL_1$	
$n = 5$									
1.1	159.86	159.36	51.03	37.11	115.42	151.33	64.74	84.69	EWMA
1.2	64.69	64.19	20.38	14.63	37.67	48.39	21.35	27.11	EWMA
1.3	30.61	30.10	11.80	8.10	16.38	20.11	10.18	12.25	SS Syn
1.4	16.92	16.41	7.86	5.38	8.97	10.44	6.07	6.83	SS Syn
1.5	10.57	10.06	5.76	3.93	5.76	6.29	4.18	4.44	SS Syn
1.6	7.26	6.74	4.49	3.05	4.12	4.27	3.16	3.09	SS Syn
1.7	5.36	4.84	3.66	2.48	3.13	3.13	2.56	2.32	SS Syn
1.8	4.19	3.65	3.09	2.07	2.62	2.40	2.17	1.85	SS Syn
1.9	3.42	2.88	2.67	1.77	2.24	1.86	1.91	1.47	SS Syn
2.0	2.89	2.34	2.36	1.54	1.97	1.56	1.72	1.27	SS Syn
$n = 7$									
1.1	141.22	140.71	39.32	28.67	97.69	127.96	52.13	67.97	EWMA
1.2	50.26	40.76	15.44	10.58	27.65	35.11	15.75	19.66	EWMA
1.3	22.09	21.58	8.81	5.83	11.35	13.60	7.30	8.47	SS Syn
1.4	11.74	11.23	5.84	3.84	6.12	6.80	4.34	4.58	SS Syn
1.5	7.21	6.69	4.26	2.80	3.95	4.11	3.02	2.89	SS Syn
1.6	4.93	4.40	3.34	2.17	2.88	2.68	2.33	2.08	SS Syn
1.7	3.66	3.12	2.73	1.76	2.28	2.00	1.93	1.49	SS Syn
1.8	2.89	2.34	2.32	1.46	1.91	1.47	1.67	1.19	SS Syn
1.9	2.39	1.83	2.02	1.25	1.67	1.19	1.50	0.94	SS Syn
2.0	2.05	1.48	1.80	1.08	1.51	0.95	1.38	0.82	SS Syn
$n = 10$									
1.1	102.27	119.77	30.09	21.37	78.87	103.16	41.27	53.44	EWMA
1.2	37.09	36.59	11.60	7.65	19.24	24.10	11.43	13.91	SS Syn
1.3	15.17	14.67	6.54	4.17	7.57	8.76	5.19	5.68	SS Syn
1.4	7.82	7.31	4.33	2.74	4.10	4.33	3.12	3.02	SS Syn
1.5	4.77	4.25	3.16	1.99	2.71	2.53	2.22	1.91	SS Syn
1.6	3.30	2.76	2.49	1.54	2.04	1.66	1.76	1.33	SS Syn
1.7	2.50	1.93	2.06	1.24	1.67	1.20	1.50	0.94	SS Syn
1.8	2.02	1.44	1.76	1.02	1.46	0.95	1.34	0.75	SS Syn
1.9	1.72	1.12	1.56	0.86	1.32	0.72	1.24	0.58	SS Syn
2.0	1.52	0.89	1.41	0.73	1.22	0.56	1.17	0.47	SS Syn
$n = 15$									
1.1	95.85	95.35	22.46	15.32	58.48	76.18	31.15	39.93	EWMA
1.2	25.03	24.53	8.43	5.33	12.24	14.95	7.84	9.14	SS Syn
1.3	9.57	9.05	4.71	2.89	4.74	5.14	3.53	3.61	SS Syn
1.4	4.86	4.33	3.13	1.90	2.66	2.46	2.19	1.87	SS Syn
1.5	3.02	2.47	2.30	1.38	1.86	1.47	1.63	1.13	SS Syn
1.6	2.16	1.58	1.83	1.05	1.48	0.99	1.35	0.78	SS Syn
1.7	1.71	1.10	1.53	0.83	1.28	0.66	1.21	0.54	SS Syn
1.8	1.45	0.80	1.35	0.66	1.17	0.47	1.13	0.44	SS Syn
1.9	1.29	0.61	1.23	0.52	1.11	0.39	1.08	0.32	SS Syn
2.0	1.19	0.48	1.15	0.42	1.07	0.29	1.05	0.24	SS Syn
$n = 20$									
1.1	78.98	78.48	18.62	12.10	45.46	59.03	24.98	31.76	EWMA
1.2	18.37	17.86	6.79	4.14	8.71	10.37	5.92	6.72	SS Syn
1.3	6.78	6.26	3.75	2.24	3.43	3.46	2.70	2.52	SS Syn
1.4	3.47	2.93	2.50	1.47	2.02	1.71	1.74	1.30	SS Syn
1.5	2.22	1.65	1.85	1.06	1.49	0.99	1.36	0.79	SS Syn
1.6	1.66	1.05	1.50	0.79	1.25	0.60	1.19	0.50	SS Syn
1.7	1.37	0.71	1.29	0.59	1.13	0.45	1.10	0.37	SS Syn
1.8	1.22	0.51	1.17	0.44	1.07	0.30	1.05	0.25	SS Syn
1.9	1.13	0.38	1.10	0.33	1.04	0.21	1.03	0.17	SS Syn
2.0	1.07	0.28	1.06	0.25	1.02	0.15	1.01	0.12	SS Syn

Table 4.24 The ARL_1 and $SDRL_1$ of the ARL -based design of the Shewhart- γ , EWMA- γ^2 , non-side-sensitive synthetic- γ (NSS Syn) and side-sensitive synthetic- γ (SS Syn) charts for $n \in \{5, 7, 10, 15, 20\}$, $\tau \in \{1.1, 1.2, 1.3, 1.4, 1.5, 1.6, 1.7, 1.8, 1.9, 2.0\}$ and $\gamma_0 = 0.10$

τ	$\gamma_0 = 0.10$								Best Chart
	Shewhart		EWMA		NSS Syn		SS Syn		
	ARL_1	$SDRL_1$	ARL_1	$SDRL_1$	ARL_1	$SDRL_1$	ARL_1	$SDRL_1$	
$n = 5$									
1.1	160.64	160.14	51.34	37.41	116.07	152.31	65.20	85.30	EWMA
1.2	65.33	64.82	20.99	14.80	38.09	48.86	21.58	27.43	EWMA
1.3	31.02	30.52	11.92	8.19	16.62	20.44	10.31	12.42	SS Syn
1.4	17.19	16.68	7.95	5.45	9.11	10.64	6.15	6.94	SS Syn
1.5	10.76	10.25	5.83	3.98	5.85	6.42	4.23	4.52	SS Syn
1.6	7.40	6.88	4.54	3.09	4.19	4.36	3.20	3.15	SS Syn
1.7	5.47	4.94	3.71	2.51	3.25	3.12	2.59	2.36	SS Syn
1.8	4.27	3.74	3.13	2.10	2.66	2.46	2.20	1.89	SS Syn
1.9	3.49	2.95	2.71	1.80	2.27	1.91	1.93	1.50	SS Syn
2.0	2.95	2.40	2.40	1.57	2.00	1.60	1.74	1.30	SS Syn
$n = 7$									
1.1	142.15	141.65	40.39	28.92	98.47	129.11	52.56	68.58	EWMA
1.2	50.91	50.41	15.87	10.70	28.06	35.69	15.93	19.92	EWMA
1.3	22.47	21.96	8.91	5.91	11.55	13.89	7.39	8.60	SS Syn
1.4	11.97	11.46	5.92	3.89	6.23	6.96	4.40	4.66	SS Syn
1.5	7.36	6.85	4.34	2.84	4.03	4.22	3.06	2.95	SS Syn
1.6	5.04	4.52	3.39	2.20	2.93	2.76	2.36	2.12	SS Syn
1.7	3.74	3.21	2.78	1.79	2.32	2.06	1.95	1.53	SS Syn
1.8	2.96	2.41	2.36	1.49	1.94	1.52	1.69	1.22	SS Syn
1.9	2.45	1.88	2.06	1.27	1.70	1.23	1.52	0.97	SS Syn
2.0	2.10	1.52	1.84	1.10	1.53	0.99	1.29	0.85	SS Syn
$n = 10$									
1.1	121.32	120.82	31.19	21.59	79.71	104.36	51.55	53.83	EWMA
1.2	37.69	37.19	11.89	7.74	19.58	24.50	11.56	14.08	SS Syn
1.3	15.49	14.98	6.63	4.22	7.72	8.97	5.26	5.77	SS Syn
1.4	8.00	7.49	4.39	2.78	4.18	4.45	3.16	3.08	SS Syn
1.5	4.89	4.36	3.22	2.02	2.76	2.61	2.25	1.96	SS Syn
1.6	3.38	2.84	2.53	1.57	2.08	1.71	1.78	1.36	SS Syn
1.7	2.56	2.00	2.09	1.26	1.70	1.24	1.52	0.97	SS Syn
1.8	2.07	1.49	1.79	1.04	1.48	0.98	1.35	0.77	SS Syn
1.9	1.76	1.15	1.58	0.88	1.33	0.74	1.25	0.60	SS Syn
2.0	1.55	0.93	1.44	0.75	1.24	0.59	1.18	0.48	SS Syn
$n = 15$									
1.1	96.92	96.40	23.22	15.44	59.28	77.31	31.33	40.17	EWMA
1.2	25.51	25.01	8.62	5.39	12.49	15.31	7.93	9.27	SS Syn
1.3	9.79	9.28	4.78	2.92	4.84	5.29	3.58	3.68	SS Syn
1.4	4.98	4.45	3.17	1.92	2.71	2.54	2.21	1.91	SS Syn
1.5	3.09	2.54	2.34	1.40	1.89	1.52	1.65	1.16	SS Syn
1.6	2.21	1.63	1.86	1.07	1.50	1.02	1.37	0.80	SS Syn
1.7	1.74	1.14	1.56	0.85	1.30	0.69	1.22	0.56	SS Syn
1.8	1.47	0.83	1.37	0.68	1.18	0.49	1.14	0.46	SS Syn
1.9	1.31	0.64	1.24	0.54	1.11	0.41	1.08	0.34	SS Syn
2.0	1.21	0.50	1.16	0.43	1.07	0.31	1.05	0.25	SS Syn
$n = 20$									
1.1	79.99	79.49	18.80	12.18	46.21	60.04	25.14	31.98	EWMA
1.2	18.76	18.25	6.88	4.18	8.90	10.54	6.00	6.82	SS Syn
1.3	6.94	6.42	3.80	2.27	3.50	3.57	2.74	2.58	SS Syn
1.4	3.56	3.01	2.53	1.50	2.05	1.77	1.76	1.33	SS Syn
1.5	2.27	1.70	1.88	1.08	1.51	1.03	1.37	0.81	SS Syn
1.6	1.69	1.08	1.52	0.81	1.26	0.63	1.19	0.51	SS Syn
1.7	1.39	0.74	1.30	0.61	1.14	0.47	1.10	0.38	SS Syn
1.8	1.23	0.53	1.18	0.46	1.08	0.32	1.05	0.26	SS Syn
1.9	1.14	0.40	1.11	0.34	1.04	0.22	1.03	0.18	SS Syn
2.0	1.08	0.30	1.06	0.26	1.02	0.16	1.02	0.13	SS Syn

Table 4.25 The ARL_1 and $SDRL_1$ of the ARL -based design of the Shewhart- γ , EWMA- γ^2 , non-side-sensitive synthetic- γ (NSS Syn) and side-sensitive synthetic- γ (SS Syn) charts for $n \in \{5, 7, 10, 15, 20\}$, $\tau \in \{1.1, 1.2, 1.3, 1.4, 1.5, 1.6, 1.7, 1.8, 1.9, 2.0\}$ and $\gamma_0 = 0.15$

τ	$\gamma_0 = 0.15$								Best Chart
	Shewhart		EWMA		NSS Syn		SS Syn		
	ARL_1	$SDRL_1$	ARL_1	$SDRL_1$	ARL_1	$SDRL_1$	ARL_1	$SDRL_1$	
$n = 5$									
1.1	161.99	161.49	52.01	38.04	117.35	154.00	65.99	86.34	EWMA
1.2	66.44	65.93	21.37	15.09	38.85	49.89	21.97	37.96	EWMA
1.3	31.74	31.23	12.15	8.36	17.02	21.01	10.52	12.73	SS Syn
1.4	17.66	17.15	8.12	5.56	9.35	10.98	6.29	7.14	SS Syn
1.5	11.09	10.58	5.95	4.07	6.01	6.65	4.33	4.65	SS Syn
1.6	7.64	7.12	4.65	3.17	4.31	4.53	3.28	3.25	SS Syn
1.7	5.66	5.13	3.80	2.58	3.34	3.25	2.65	2.45	SS Syn
1.8	4.42	3.89	3.21	2.16	2.73	2.48	2.25	1.96	SS Syn
1.9	3.61	3.07	2.78	1.85	2.33	2.00	1.97	1.56	SS Syn
2.0	3.05	2.51	2.47	1.62	2.05	1.68	1.78	1.36	SS Syn
$n = 7$									
1.1	143.78	143.28	41.05	29.40	99.95	131.06	53.33	69.62	EWMA
1.2	52.05	51.55	16.18	10.92	28.77	36.67	16.26	20.37	EWMA
1.3	23.13	22.62	9.11	6.04	11.89	14.37	7.56	8.83	SS Syn
1.4	12.38	11.87	6.06	3.99	6.43	7.24	4.50	4.80	SS Syn
1.5	7.63	7.12	4.44	2.91	4.15	4.30	3.13	3.05	SS Syn
1.6	5.24	4.71	3.48	2.26	3.02	2.88	2.41	2.20	SS Syn
1.7	3.89	3.35	2.85	1.84	2.39	2.07	1.99	1.59	SS Syn
1.8	3.07	2.52	2.42	1.54	2.00	1.59	1.72	1.27	SS Syn
1.9	2.54	1.98	2.11	1.31	1.74	1.30	1.54	1.01	SS Syn
2.0	2.18	1.61	1.89	1.14	1.57	1.04	1.42	0.89	SS Syn
$n = 10$									
1.1	123.13	122.63	31.73	21.97	81.25	106.40	42.08	54.60	EWMA
1.2	38.72	38.22	12.14	7.91	20.18	25.33	11.78	14.40	SS Syn
1.3	16.02	15.51	6.78	4.33	7.98	9.34	5.37	5.94	SS Syn
1.4	8.31	7.80	4.50	2.85	4.32	4.55	3.23	3.18	SS Syn
1.5	5.09	4.56	3.31	2.08	2.85	2.74	2.30	2.03	SS Syn
1.6	3.52	2.98	2.60	1.61	2.14	1.80	1.82	1.41	SS Syn
1.7	2.66	2.10	2.15	1.31	1.75	1.31	1.54	1.01	SS Syn
1.8	2.15	1.57	1.84	1.08	1.51	0.96	1.37	0.81	SS Syn
1.9	1.82	1.22	1.63	0.91	1.36	0.79	1.27	0.63	SS Syn
2.0	1.60	0.98	1.47	0.78	1.26	0.62	1.19	0.51	SS Syn
$n = 15$									
1.1	98.75	98.25	23.65	15.74	60.71	79.19	31.67	40.71	EWMA
1.2	26.34	25.84	8.81	5.51	12.92	15.82	8.09	9.49	SS Syn
1.3	10.17	9.66	4.89	2.99	5.02	5.53	3.66	3.80	SS Syn
1.4	5.19	4.66	3.25	1.97	2.80	2.66	2.26	1.98	SS Syn
1.5	3.22	2.67	2.40	1.44	1.94	1.60	1.68	1.21	SS Syn
1.6	2.29	1.72	1.91	1.11	1.54	1.00	1.39	0.84	SS Syn
1.7	1.80	1.20	1.60	0.88	1.32	0.73	1.24	0.59	SS Syn
1.8	1.52	0.89	1.40	0.71	1.20	0.53	1.15	0.49	SS Syn
1.9	1.34	0.68	1.27	0.57	1.13	0.44	1.09	0.36	SS Syn
2.0	1.23	0.54	1.18	0.46	1.08	0.33	1.06	0.27	SS Syn
$n = 20$									
1.1	81.74	81.24	19.16	12.41	47.48	61.75	25.43	32.38	EWMA
1.2	19.42	18.92	7.03	4.28	9.23	11.00	6.13	7.01	SS Syn
1.3	7.23	6.71	3.90	2.32	3.62	3.74	2.80	2.67	SS Syn
1.4	3.70	3.16	2.60	1.54	2.11	1.76	2.32	2.06	SS Syn
1.5	2.36	1.79	1.93	1.11	1.55	1.09	1.40	0.85	SS Syn
1.6	1.75	1.14	1.56	0.84	1.29	0.67	1.21	0.54	SS Syn
1.7	1.43	0.79	1.33	0.64	1.16	0.50	1.11	0.41	SS Syn
1.8	1.26	0.57	1.20	0.49	1.09	0.34	1.06	0.28	SS Syn
1.9	1.16	0.43	1.12	0.37	1.05	0.24	1.03	0.20	SS Syn
2.0	1.10	0.33	1.07	0.28	1.03	0.18	1.02	0.15	SS Syn

Table 4.26 The ARL_1 and $SDRL_1$ of the ARL -based design of the Shewhart- γ , EWMA- γ^2 , non-side-sensitive synthetic- γ (NSS Syn) and side-sensitive synthetic- γ (SS Syn) charts for $n \in \{5, 7, 10, 15, 20\}$, $\tau \in \{1.1, 1.2, 1.3, 1.4, 1.5, 1.6, 1.7, 1.8, 1.9, 2.0\}$ and $\gamma_0 = 0.20$

τ	$\gamma_0 = 0.20$								Best Chart
	Shewhart		EWMA		NSS Syn		SS Syn		
	ARL_1	$SDRL_1$	ARL_1	$SDRL_1$	ARL_1	$SDRL_1$	ARL_1	$SDRL_1$	
$n = 5$									
1.1	163.95	163.45	53.01	38.97	119.19	156.43	67.12	87.83	EWMA
1.2	68.06	67.56	21.94	15.52	39.94	51.33	22.54	28.67	EWMA
1.3	32.79	32.29	12.49	8.62	17.61	21.75	10.84	13.17	SS Syn
1.4	18.35	17.85	8.35	5.73	9.70	11.38	6.48	7.42	SS Syn
1.5	11.57	11.06	6.14	4.21	6.25	6.68	4.47	4.75	SS Syn
1.6	8.00	7.48	4.80	3.28	4.48	4.68	3.38	3.40	SS Syn
1.7	5.93	5.08	3.92	2.67	3.47	3.43	2.73	2.56	SS Syn
1.8	4.65	4.11	3.32	2.24	2.84	2.63	2.32	2.06	SS Syn
1.9	3.80	3.26	2.88	1.93	2.42	2.12	2.03	1.64	SS Syn
2.0	3.21	2.66	2.56	1.69	2.13	1.79	1.83	1.43	SS Syn
$n = 7$									
1.1	146.12	145.62	42.00	30.05	102.05	133.84	54.48	71.15	EWMA
1.2	53.69	53.18	16.63	11.25	29.81	38.02	16.74	21.05	EWMA
1.3	24.08	23.58	9.38	6.24	12.39	14.98	7.80	9.18	SS Syn
1.4	12.97	12.46	6.25	4.13	6.71	7.64	4.65	5.02	SS Syn
1.5	8.03	7.51	4.59	3.02	4.33	4.56	3.24	3.19	SS Syn
1.6	5.52	4.99	3.60	2.35	3.15	3.07	2.49	2.22	SS Syn
1.7	4.10	3.57	2.95	1.91	2.48	2.21	2.05	1.67	SS Syn
1.8	3.24	2.69	2.51	1.60	2.07	1.70	1.77	1.35	SS Syn
1.9	2.68	2.12	2.19	1.37	1.81	1.40	1.59	1.07	SS Syn
2.0	2.30	1.72	1.96	1.20	1.62	1.12	1.46	0.95	SS Syn
$n = 10$									
1.1	125.69	125.19	32.54	22.58	83.42	109.22	42.94	55.81	EWMA
1.2	40.21	39.70	12.50	8.16	21.03	26.44	12.13	14.88	SS Syn
1.3	16.80	16.29	7.00	4.47	8.36	9.78	5.54	6.18	SS Syn
1.4	8.76	8.25	4.66	2.95	4.53	4.84	3.33	3.33	SS Syn
1.5	5.38	4.85	3.43	2.16	2.98	2.92	2.37	2.13	SS Syn
1.6	3.72	3.18	2.70	1.68	2.23	1.93	1.87	1.49	SS Syn
1.7	2.80	2.25	2.23	1.36	1.81	1.41	1.59	1.07	SS Syn
1.8	2.26	1.69	1.91	1.14	1.56	1.03	1.41	0.87	SS Syn
1.9	1.91	1.32	1.69	0.96	1.40	0.86	1.29	0.68	SS Syn
2.0	1.68	1.07	1.53	0.83	1.29	0.68	1.22	0.55	SS Syn
$n = 15$									
1.1	101.34	100.83	24.28	16.18	62.73	81.90	32.24	41.49	EWMA
1.2	27.53	27.02	9.08	5.69	13.54	16.69	8.32	9.82	SS Syn
1.3	10.72	10.21	5.05	3.10	5.27	5.79	3.78	3.97	SS Syn
1.4	5.48	4.96	3.37	2.05	2.93	2.85	2.34	2.08	SS Syn
1.5	3.40	2.86	2.49	1.50	2.02	1.63	1.73	1.28	SS Syn
1.6	2.41	1.85	1.98	1.16	1.59	1.08	1.43	0.90	SS Syn
1.7	1.89	1.29	1.66	0.92	1.36	0.79	1.26	0.63	SS Syn
1.8	1.58	0.96	1.45	0.75	1.23	0.57	1.17	0.46	SS Syn
1.9	1.39	0.74	1.31	0.61	1.15	0.49	1.11	0.39	SS Syn
2.0	1.27	0.59	1.21	0.51	1.10	0.37	1.07	0.30	SS Syn
$n = 20$									
1.1	84.21	83.71	19.67	12.77	49.27	64.04	25.89	33.02	EWMA
1.2	20.38	19.87	7.25	4.42	9.69	11.65	6.31	7.18	SS Syn
1.3	7.64	7.12	4.03	2.40	3.80	3.99	2.89	2.80	SS Syn
1.4	3.91	3.38	2.69	1.59	2.20	1.89	1.85	1.47	SS Syn
1.5	2.49	1.92	2.00	1.16	1.60	1.09	1.43	0.90	SS Syn
1.6	1.83	1.23	1.61	0.88	1.32	0.72	1.23	0.58	SS Syn
1.7	1.49	0.85	1.37	0.68	1.18	0.49	1.13	0.44	SS Syn
1.8	1.30	0.62	1.23	0.53	1.10	0.38	1.07	0.31	SS Syn
1.9	1.30	0.62	1.14	0.40	1.06	0.27	1.04	0.22	SS Syn
2.0	1.12	0.36	1.09	0.31	1.03	0.20	1.02	0.16	SS Syn

Tables 4.23 to 4.26 demonstrate that the *ARL*-based design of the side-sensitive synthetic- γ chart outperforms the non-side-sensitive synthetic- γ chart significantly, particularly for small shift sizes. For instance, in Table 4.23, when $n = 5$, $\tau = 1.1$ and $\gamma_0 = 0.05$, the non-side-sensitive synthetic- γ chart has ARL_1 and $SDRL_1$ values of 115.42 and 151.33, respectively. However, when the feature of side sensitivity is incorporated, the ARL_1 and $SDRL_1$ values decrease to 64.74 and 84.69, respectively. This represents a 43.91% improvement in the ARL_1 . Therefore, it is evident that including the feature of side sensitivity results in a noteworthy enhancement of the synthetic- γ chart's performance.

Tables 4.23 to 4.26 reveal that the EWMA- γ^2 chart demonstrates better performance compared to the non-side-sensitive synthetic- γ chart for $\tau \in \{1.1, 1.2, 1.3\}$, but exhibits similar or weaker performance for $\tau \in \{1.5, 1.6, 1.7, 1.8, 1.9, 2.0\}$. For instance, in Table 4.23, when $n = 5$, $\tau = 1.1$ and $\gamma_0 = 0.05$, the EWMA- γ^2 chart has ARL_1 and $SDRL_1$ values of 51.03 and 37.11, respectively, whereas the non-side-sensitive synthetic- γ chart has ARL_1 and $SDRL_1$ values of 115.42 and 151.33, respectively. As for $n = 5$, $\tau = 2.0$ and $\gamma_0 = 0.05$ in Table 4.23, the EWMA- γ^2 chart has ARL_1 and $SDRL_1$ values of 2.36 and 1.54, respectively, while the non-side-sensitive synthetic- γ chart has ARL_1 and $SDRL_1$ values of 1.97 and 1.56, respectively.

However, for $\tau = 1.2$, the side-sensitive synthetic- γ chart exhibits comparable performance to the EWMA- γ^2 chart and outperforms it for $\tau \in \{1.3, 1.4, 1.5, 1.6, 1.7, 1.8, 1.9, 2.0\}$. For instance, in Table 4.23, when $n = 5$, $\tau = 1.3$ and $\gamma_0 = 0.05$, the EWMA- γ^2 chart has ARL_1 and $SDRL_1$ values of 11.80 and 8.10,

respectively, whereas the side-sensitive synthetic- γ chart has ARL_1 and $SDRL_1$ values of 10.18 and 12.25, respectively. As for $n = 5$, $\tau = 2.0$ and $\gamma_0 = 0.05$, the EWMA- γ^2 chart has ARL_1 and $SDRL_1$ values of 2.36 and 1.54, respectively, while the side-sensitive synthetic- γ chart has ARL_1 and $SDRL_1$ values of 1.72 and 1.27, respectively (see Table 4.23). It is noteworthy that the EWMA- γ^2 chart is famous for its sensitivity to small shifts, hence the comparison suggests that the proposed side-sensitive synthetic- γ chart can be considered a competitive chart. Moreover, the side-sensitive synthetic- γ chart performs better than the Shewhart- γ chart for all values of sample size and shift size.

According to the last column in Tables 4.23 to 4.26, it can be observed that for $\tau = 1.1$, the EWMA- γ^2 chart is the best chart among all four charts for all values of n and γ_0 as it is famous on its sensitivity toward small shift sizes. However, for $\tau = 1.2$, the EWMA- γ^2 chart performed the best only when $n \in \{5, 7\}$ for all values of γ_0 . For $n \in \{10, 15, 20\}$, the proposed side-sensitive synthetic- γ chart is the best chart when $\tau = 1.2$ for all values of γ_0 . Furthermore, the proposed chart is also the best chart among all four charts for $\tau \in \{1.3, 1.4, 1.5, 1.6, 1.7, 1.8, 1.9, 2.0\}$ for all values of n and γ_0 .

Table 4.27 presents a comparison between the Shewhart- γ , EWMA- γ^2 , non-side-sensitive synthetic- γ , and side-sensitive synthetic- γ charts which are designed based on the $EARL$, in terms of $EARL_1$ performance for $n \in \{5, 7, 10, 15, 20\}$ and $\gamma_0 \in \{0.05, 0.10, 0.15, 0.20\}$. The range for $(\tau_{\min}, \tau_{\max})$ is set as $(1, 2]$. All results obtained were validated using simulation.

Table 4.27 The $EARL_1$ values of the $EARL$ -based design of the Shewhart- γ , EWMA- γ^2 , non-side-sensitive synthetic- γ (NSS Syn) and side-sensitive synthetic- γ (SS Syn) charts for $n \in \{5, 7, 10, 15, 20\}$, $\gamma_0 \in \{0.05, 0.10, 0.15, 0.20\}$ and $(\tau_{\min}, \tau_{\max}) = (1, 2]$

n	Shewhart		EWMA		NSS Syn		SS Syn	Best Chart
	$EARL_1$	$REARL_1$	$EARL_1$	$REARL_1$	$EARL_1$	$REARL_1$	$EARL_1$	
$\gamma_0 = 0.05$								
5	38.06	2.25	15.72	0.93	27.18	1.61	16.90	EWMA
7	32.12	2.34	12.52	0.91	22.76	1.66	13.73	EWMA
10	26.66	2.39	9.89	0.89	18.70	1.68	11.16	EWMA
15	21.30	2.41	7.60	0.86	14.73	1.66	8.85	EWMA
20	17.99	2.41	6.40	0.86	12.29	1.64	7.48	EWMA
$\gamma_0 = 0.10$								
5	38.34	2.25	15.84	0.93	27.39	1.61	17.03	EWMA
7	32.41	2.34	12.62	0.91	22.96	1.66	13.83	EWMA
10	26.93	2.40	9.98	0.89	18.89	1.68	11.22	EWMA
15	21.53	2.42	7.66	0.86	14.90	1.68	8.89	EWMA
20	18.19	2.43	6.46	0.86	12.43	1.66	7.50	EWMA
$\gamma_0 = 0.15$								
5	38.34	2.22	16.04	0.93	27.74	1.61	17.25	EWMA
7	32.90	2.35	12.81	0.91	23.31	1.66	14.02	EWMA
10	27.39	2.41	10.14	0.89	19.22	1.69	11.34	EWMA
15	21.93	2.45	7.79	0.87	15.19	1.70	8.96	EWMA
20	18.54	2.46	6.57	0.87	12.68	1.68	7.55	EWMA
$\gamma_0 = 0.20$								
5	39.57	2.25	16.36	0.93	28.25	1.61	17.56	EWMA
7	33.62	2.35	13.08	0.91	23.82	1.67	14.31	EWMA
10	21.93	2.45	7.79	0.87	15.17	1.70	8.96	EWMA
15	22.50	2.48	7.98	0.88	15.59	1.72	9.08	EWMA
20	19.04	2.49	6.73	0.88	13.04	1.71	7.64	EWMA

Table 4.27 includes the relative $EARL_1$ ($REARL_1$) values to facilitate comparisons. $REARL_1$ is calculated by dividing the $EARL_1$ value of the chart being compared by the $EARL_1$ value of the side-sensitive synthetic- γ chart. For example, when $n = 5$ and $\gamma_0 = 0.05$ for the Shewhart- γ chart, the $REARL_1$ is calculated as $\frac{38.06}{16.90} = 2.25$. A $REARL_1$ value greater than 1 indicates better performance for the side-sensitive synthetic- γ chart compared to the chart being compared. Results in Table 4.27 show that the side-sensitive synthetic- γ chart performs better than the Shewhart- γ and non-side-sensitive synthetic- γ charts for all sample sizes and in-control coefficient of variation values. Nevertheless, the EWMA- γ^2 chart exhibits better performance compared to the side-

sensitive synthetic- γ chart, with $REARL_1$ ranging from 0.86 and 0.93. Hence, the EWMA- γ^2 chart is the best chart according to the $EARL$ performance measure.

According to the results obtained in Tables 4.23 to 4.27, it is proven that the proposed side-sensitive synthetic- γ chart outperforms the Shewhart- γ and non-side-sensitive synthetic- γ charts for all cases in terms of both ARL and $EARL$ -based designs. Furthermore, it also shows better and comparative performance than EWMA- γ^2 chart for moderate and large shift sizes. In order to evaluate the actual performance of the proposed chart accurately, a comparison among all four control charts which are designed based on MRL and $EMRL$ is also being conducted in this subsection. The design based on MRL is evaluated using the l_{05} , MRL_1 , and l_{95} , whereas the $EMRL$ -based design is evaluated using the $E(l_{05})$, $EMRL_1$, and $E(l_{05})$.

Specifically, with the same value of $n \in \{5, 7, 10, 15, 20\}$ and $\tau \in \{1.1, 1.2, 1.3, 1.4, 1.5, 1.6, 1.7, 1.8, 1.9, 2.0\}$, Table 4.28 compares the Shewhart- γ , EWMA- γ^2 , non-side-sensitive synthetic- γ and side-sensitive synthetic- γ charts for $\gamma_0 = 0.05$, while Tables 4.29 to 4.31 compare all four control charts for $\gamma_0 = 0.10$, $\gamma_0 = 0.15$ and $\gamma_0 = 0.20$, respectively. The performance of control charts in both tables is compared in terms of $Q05$, MRL_1 and $Q95$. All results obtained were validated using simulation with 10,000 trials.

Table 4.28 The l_{05} , MRL_1 and l_{95} values of the MRL -based Shewhart- γ , EWMA- γ^2 , non-side-sensitive synthetic- γ (NSS Syn) and side-sensitive synthetic- γ (SS Syn) charts for $n \in \{5, 7, 10, 15, 20\}$, $\tau \in \{1.1, 1.2, 1.3, 1.4, 1.5, 1.6, 1.7, 1.8, 1.9, 2.0\}$ and $\gamma_0 = 0.05$

τ	$\gamma_0 = 0.05$												Best Chart
	Shewhart			EWMA			NSS Syn			SS Syn			
	l_{05}	MRL_1	l_{95}	l_{05}	MRL_1	l_{95}	l_{05}	MRL_1	l_{95}	l_{05}	MRL_1	l_{95}	
$n = 5$													
1.1	5	64	273	9	35	120	3	32	343	2	22	231	SS Syn
1.2	2	27	116	5	16	45	1	10	106	1	8	81	SS Syn
1.3	1	14	59	2	9	29	1	5	52	1	4	42	SS Syn
1.4	1	8	34	2	6	21	1	3	28	1	3	22	SS Syn
1.5	1	6	22	1	5	17	1	2	23	1	2	15	SS Syn
1.6	1	4	16	1	4	12	1	2	14	1	2	8	SS Syn
1.7	1	3	12	1	3	10	1	2	11	1	1	13	SS Syn
1.8	1	3	9	1	2	8	1	1	11	1	1	7	NSS & SS Syn
1.9	1	2	8	1	2	6	1	1	9	1	1	4	NSS & SS Syn
2.0	1	2	6	1	2	5	1	1	4	1	1	4	NSS & SS Syn
$n = 7$													
1.1	5	55	234	8	28	89	2	27	279	2	18	186	SS Syn
1.2	2	21	90	3	12	41	1	8	85	1	6	62	SS Syn
1.3	1	10	43	2	7	24	1	4	40	1	3	31	SS Syn
1.4	1	6	24	1	5	18	1	2	22	1	2	17	NSS & SS Syn
1.5	1	4	16	1	3	11	1	2	15	1	2	8	NSS & SS Syn
1.6	1	3	11	1	3	8	1	1	13	1	1	8	NSS & SS Syn
1.7	1	2	8	1	2	6	1	1	9	1	1	4	NSS & SS Syn
1.8	1	2	6	1	2	5	1	1	7	1	1	4	NSS & SS Syn
1.9	1	2	5	1	2	4	1	1	6	1	1	3	NSS & SS Syn
2.0	1	1	4	1	1	4	1	1	3	1	1	3	ALL
$n = 10$													
1.1	4	47	204	7	23	66	2	23	236	2	15	151	SS Syn
1.2	2	16	69	3	9	28	1	7	64	1	5	43	SS Syn
1.3	1	8	31	2	5	16	1	3	27	1	3	17	NSS & SS Syn
1.4	1	4	17	1	4	12	1	2	15	1	2	8	NSS & SS Syn
1.5	1	3	10	1	3	8	1	1	13	1	1	7	NSS & SS Syn
1.6	1	2	7	1	2	6	1	1	8	1	1	4	NSS & SS Syn
1.7	1	2	5	1	2	4	1	1	6	1	1	3	NSS & SS Syn
1.8	1	1	4	1	1	4	1	1	5	1	1	3	ALL
1.9	1	1	3	1	1	3	1	1	4	1	1	2	ALL
2.0	1	1	3	1	1	3	1	1	2	1	1	2	ALL
$n = 15$													
1.1	3	40	173	7	18	47	2	18	189	1	12	117	SS Syn
1.2	1	12	51	2	7	22	1	5	45	1	3	34	SS Syn
1.3	1	5	21	1	4	13	1	2	18	1	2	9	NSS & SS Syn
1.4	1	3	12	1	3	8	1	1	12	1	1	8	NSS & SS Syn
1.5	1	2	7	1	2	5	1	1	5	1	1	3	NSS & SS Syn
1.6	1	1	5	1	1	4	1	1	5	1	1	3	ALL
1.7	1	1	3	1	1	3	1	1	3	1	1	2	ALL
1.8	1	1	3	1	1	3	1	1	3	1	1	2	ALL
1.9	1	1	2	1	1	2	1	1	3	1	1	2	ALL
2.0	1	1	2	1	1	2	1	1	1	1	1	1	ALL
$n = 20$													
1.1	3	35	150	5	14	43	1	12	123	1	9	96	SS Syn
1.2	1	9	39	1	6	22	1	3	31	1	3	21	NSS & SS Syn
1.3	1	4	15	1	3	9	1	2	12	1	1	13	SS Syn
1.4	1	2	8	1	2	5	1	1	8	1	1	4	NSS & SS Syn
1.5	1	2	5	1	2	4	1	1	5	1	1	3	NSS & SS Syn
1.6	1	1	3	1	1	3	1	1	3	1	1	2	ALL
1.7	1	1	3	1	1	2	1	1	3	1	1	2	ALL
1.8	1	1	2	1	1	2	1	1	1	1	1	1	ALL
1.9	1	1	2	1	1	2	1	1	1	1	1	1	ALL
2.0	1	1	2	1	1	2	1	1	1	1	1	1	ALL

Table 4.29 The l_{05} , MRL_1 and l_{95} values of the MRL -based Shewhart- γ , EWMA- γ^2 , non-side-sensitive synthetic- γ (NSS Syn) and side-sensitive synthetic- γ (SS Syn) charts for $n \in \{5, 7, 10, 15, 20\}$, $\tau \in \{1.1, 1.2, 1.3, 1.4, 1.5, 1.6, 1.7, 1.8, 1.9, 2.0\}$ and $\gamma_0 = 0.10$

τ	$\gamma_0 = 0.10$												Best Chart
	Shewhart			EWMA			NSS Syn			SS Syn			
	l_{05}	MRL_1	l_{95}	l_{05}	MRL_1	l_{95}	l_{05}	MRL_1	l_{95}	l_{05}	MRL_1	l_{95}	
$n = 5$													
1.1	5	64	275	9	36	120	3	32	340	2	22	232	SS Syn
1.2	2	27	117	3	16	59	1	10	107	1	8	82	SS Syn
1.3	2	14	60	2	9	30	1	5	52	1	4	43	SS Syn
1.4	1	8	35	2	6	21	1	3	28	1	3	22	NSS & SS Syn
1.5	1	6	23	1	5	18	1	2	23	1	2	15	NSS & SS Syn
1.6	1	4	16	1	4	13	1	2	14	1	2	8	NSS & SS Syn
1.7	1	3	12	1	3	10	1	2	11	1	1	13	SS Syn
1.8	1	3	9	1	2	8	1	1	11	1	1	7	NSS & SS Syn
1.9	1	2	8	1	2	7	1	1	9	1	1	4	NSS & SS Syn
2.0	1	2	7	1	2	6	1	1	4	1	1	4	NSS & SS Syn
$n = 7$													
1.1	5	56	238	8	29	90	2	27	279	2	18	189	SS Syn
1.2	2	22	92	3	12	41	1	8	85	1	6	63	SS Syn
1.3	1	11	44	2	7	24	1	4	40	1	3	32	SS Syn
1.4	1	6	25	1	5	18	1	2	23	1	2	17	NSS & SS Syn
1.5	1	4	16	1	4	12	1	2	16	1	2	8	NSS & SS Syn
1.6	1	3	11	1	3	9	1	1	13	1	1	11	NSS & SS Syn
1.7	1	2	8	1	2	7	1	1	9	1	1	4	NSS & SS Syn
1.8	1	2	6	1	2	5	1	1	7	1	1	4	NSS & SS Syn
1.9	1	2	5	1	2	5	1	1	6	1	1	3	NSS & SS Syn
2.0	1	1	4	1	1	4	1	1	5	1	1	3	ALL
$n = 10$													
1.1	4	48	204	8	23	67	2	23	235	2	15	151	SS Syn
1.2	2	17	70	3	9	28	1	7	64	1	5	44	SS Syn
1.3	1	8	31	2	5	16	1	3	30	1	3	18	NSS & SS Syn
1.4	1	4	17	1	4	12	1	2	15	1	2	8	NSS & SS Syn
1.5	1	3	11	1	3	18	1	1	3	1	1	8	NSS & SS Syn
1.6	1	2	7	1	2	6	1	1	8	1	1	4	NSS & SS Syn
1.7	1	2	5	1	2	5	1	1	6	1	1	3	NSS & SS Syn
1.8	1	1	4	1	1	4	1	1	5	1	1	3	ALL
1.9	1	1	4	1	1	3	1	1	4	1	1	2	ALL
2.0	1	1	3	1	1	3	1	1	2	1	1	2	ALL
$n = 15$													
1.1	3	40	172	7	18	48	2	18	189	1	2	117	SS Syn
1.2	1	12	51	2	7	22	1	5	46	1	4	29	SS Syn
1.3	1	5	21	1	4	13	1	2	20	1	2	11	NSS & SS Syn
1.4	1	3	11	1	3	8	1	1	12	1	1	7	NSS & SS Syn
1.5	1	2	7	1	2	5	1	1	4	1	1	3	NSS & SS Syn
1.6	1	1	5	1	1	4	1	1	5	1	1	3	ALL
1.7	1	1	4	1	1	3	1	1	3	1	1	2	ALL
1.8	1	1	3	1	1	3	1	1	3	1	1	2	ALL
1.9	1	1	2	1	1	2	1	1	3	1	1	2	ALL
2.0	1	1	2	1	1	2	1	1	2	1	1	1	ALL
$n = 20$													
1.1	3	35	149	4	15	50	1	12	123	1	9	96	SS Syn
1.2	1	9	39	1	6	23	1	3	31	1	3	22	NSS & SS Syn
1.3	1	4	15	1	3	10	1	2	12	1	2	7	NSS & SS Syn
1.4	1	2	8	1	2	6	1	1	8	1	1	4	NSS & SS Syn
1.5	1	2	5	1	2	4	1	1	5	1	1	3	NSS & SS Syn
1.6	1	1	3	1	1	3	1	1	3	1	1	2	ALL
1.7	1	1	3	1	1	2	1	1	3	1	1	2	ALL
1.8	1	1	2	1	1	2	1	1	1	1	1	1	ALL
1.9	1	1	2	1	1	2	1	1	1	1	1	1	ALL
2.0	1	1	2	1	1	2	1	1	1	1	1	1	ALL

Table.4.30 The l_{05} , MRL_1 and l_{95} values of the MRL -based Shewhart- γ , EWMA- γ^2 , non-side-sensitive synthetic- γ (NSS Syn) and side-sensitive synthetic- γ (SS Syn) charts for $n \in \{5, 7, 10, 15, 20\}$, $\tau \in \{1.1, 1.2, 1.3, 1.4, 1.5, 1.6, 1.7, 1.8, 1.9, 2.0\}$ and $\gamma_0 = 0.15$

τ	$\gamma_0 = 0.15$												Best Chart
	Shewhart			EWMA			NSS Syn			SS Syn			
	l_{05}	MRL_1	l_{95}	l_{05}	MRL_1	l_{95}	l_{05}	MRL_1	l_{95}	l_{05}	MRL_1	l_{95}	
$n = 5$													
1.1	5	64	276	9	36	120	3	33	345	2	22	234	SS Syn
1.2	3	28	119	4	16	52	1	11	107	1	8	84	SS Syn
1.3	2	14	61	2	9	30	1	5	53	1	4	43	SS Syn
1.4	1	9	36	2	6	22	1	3	28	1	3	24	NSS & SS Syn
1.5	1	6	23	1	5	18	1	2	24	1	2	17	NSS & SS Syn
1.6	1	4	17	1	4	13	1	2	15	1	2	8	NSS & SS Syn
1.7	1	3	12	1	3	10	1	2	11	1	2	6	NSS & SS Syn
1.8	1	3	10	1	3	8	1	1	12	1	1	8	NSS & SS Syn
1.9	1	2	8	1	2	7	1	1	9	1	1	4	NSS & SS Syn
2.0	1	2	7	1	2	6	1	1	8	1	1	4	NSS & SS Syn
$n = 7$													
1.1	5	56	241	9	29	91	2	27	280	2	18	181	SS Syn
1.2	2	22	94	3	13	42	1	8	86	1	6	64	SS Syn
1.3	1	11	45	2	7	25	1	4	41	1	3	32	SS Syn
1.4	1	6	26	1	5	19	1	2	23	1	2	18	NSS & SS Syn
1.5	1	4	16	1	4	12	1	2	16	1	2	8	NSS & SS Syn
1.6	1	3	11	1	3	9	1	1	13	1	1	12	NSS & SS Syn
1.7	1	2	9	1	2	7	1	1	10	1	1	4	NSS & SS Syn
1.8	1	2	7	1	2	6	1	1	8	1	1	4	NSS & SS Syn
1.9	1	2	5	1	2	5	1	1	6	1	1	3	NSS & SS Syn
2.0	1	1	5	1	1	4	1	1	5	1	1	3	ALL
$n = 10$													
1.1	4	48	206	6	23	75	2	23	234	2	15	153	SS Syn
1.2	2	17	72	2	10	36	1	7	65	1	5	46	SS Syn
1.3	1	8	32	1	6	22	1	3	30	1	3	18	NSS & SS Syn
1.4	1	4	18	1	4	12	1	2	15	1	2	8	NSS & SS Syn
1.5	1	3	11	1	3	8	1	2	10	1	1	8	SS Syn
1.6	1	2	8	1	2	6	1	1	8	1	1	4	NSS & SS Syn
1.7	1	2	6	1	2	5	1	1	6	1	1	3	NSS & SS Syn
1.8	1	1	5	1	1	4	1	1	5	1	1	3	ALL
1.9	1	1	4	1	1	3	1	1	4	1	1	2	ALL
2.0	1	1	3	1	1	3	1	1	3	1	1	2	ALL
$n = 15$													
1.1	3	40	172	5	18	57	2	18	188	1	12	118	SS Syn
1.2	1	12	52	2	7	23	1	5	46	1	4	29	SS Syn
1.3	1	5	20	1	4	13	1	2	21	1	2	11	NSS & SS Syn
1.4	1	3	11	1	3	8	1	1	12	1	1	8	NSS & SS Syn
1.5	1	2	7	1	2	5	1	1	8	1	1	4	NSS & SS Syn
1.6	1	2	5	1	2	4	1	1	5	1	1	3	NSS & SS Syn
1.7	1	1	4	1	1	3	1	1	4	1	1	2	ALL
1.8	1	1	3	1	1	3	1	1	3	1	1	2	ALL
1.9	1	1	2	1	1	2	1	1	3	1	1	2	ALL
2.0	1	1	2	1	1	2	1	1	3	1	1	1	ALL
$n = 20$													
1.1	3	35	150	4	15	51	1	12	123	1	10	95	SS Syn
1.2	1	10	40	2	6	17	1	3	32	1	3	22	NSS & SS Syn
1.3	1	4	16	1	3	10	1	2	13	1	2	7	NSS & SS Syn
1.4	1	2	8	1	2	6	1	1	8	1	1	4	NSS & SS Syn
1.5	1	2	5	1	2	4	1	1	5	1	1	3	NSS & SS Syn
1.6	1	1	4	1	1	3	1	1	3	1	1	2	ALL
1.7	1	1	3	1	1	2	1	1	3	1	1	2	ALL
1.8	1	1	2	1	1	2	1	1	3	1	1	1	ALL
1.9	1	1	2	1	1	2	1	1	1	1	1	1	ALL
2.0	1	1	2	1	1	2	1	1	1	1	1	1	ALL

Table 4.31 The l_{05} , MRL_1 and l_{95} values of the MRL -based Shewhart- γ , EWMA- γ^2 , non-side-sensitive synthetic- γ (NSS Syn) and side-sensitive synthetic- γ (SS Syn) charts for $n \in \{5, 7, 10, 15, 20\}$, $\tau \in \{1.1, 1.2, 1.3, 1.4, 1.5, 1.6, 1.7, 1.8, 1.9, 2.0\}$ and $\gamma_0 = 0.20$

τ	$\gamma_0 = 0.20$												Best Chart
	Shewhart			EWMA			NSS Syn			SS Syn			
	l_{05}	MRL_1	l_{95}	l_{05}	MRL_1	l_{95}	l_{05}	MRL_1	l_{95}	l_{05}	MRL_1	l_{95}	
$n = 5$													
1.1	5	65	280	10	37	121	3	34	352	2	23	239	SS Syn
1.2	3	28	121	4	16	53	1	11	110	1	8	85	SS Syn
1.3	2	15	63	2	10	38	1	5	54	1	4	44	SS Syn
1.4	1	9	37	1	7	29	1	3	29	1	3	24	NSS & SS Syn
1.5	1	6	24	1	5	19	1	3	13	1	2	18	SS Syn
1.6	1	4	17	1	4	14	1	2	15	1	2	9	NSS & SS Syn
1.7	1	3	13	1	3	11	1	2	11	1	2	7	NSS & SS Syn
1.8	1	3	10	1	3	9	1	1	12	1	1	8	NSS & SS Syn
1.9	1	2	8	1	2	7	1	1	10	1	1	5	NSS & SS Syn
2.0	1	2	7	1	2	6	1	1	4	1	1	4	NSS & SS Syn
$n = 7$													
1.1	5	57	246	9	30	92	2	27	284	2	19	196	SS Syn
1.2	2	23	96	3	13	43	1	8	87	1	6	65	SS Syn
1.3	1	11	47	2	8	26	1	4	41	1	3	33	SS Syn
1.4	1	7	27	1	5	20	1	3	21	1	2	21	SS Syn
1.5	1	4	17	1	4	13	1	2	16	1	2	8	NSS & SS Syn
1.6	1	3	12	1	3	9	1	2	10	1	1	12	SS Syn
1.7	1	2	9	1	2	7	1	1	10	1	1	5	NSS & SS Syn
1.8	1	2	7	1	2	6	1	1	8	1	1	4	NSS & SS Syn
1.9	1	2	6	1	2	5	1	1	7	1	1	3	NSS & SS Syn
2.0	1	2	5	1	2	4	1	1	6	1	1	3	NSS & SS Syn
$n = 10$													
1.1	4	49	209	8	24	69	2	23	234	2	15	156	SS Syn
1.2	2	17	74	3	10	30	1	7	66	1	5	47	SS Syn
1.3	1	8	34	1	6	23	1	3	31	1	3	19	NSS & SS Syn
1.4	1	5	18	1	4	13	1	2	16	1	2	8	NSS & SS Syn
1.5	1	3	12	1	3	9	1	2	6	1	1	11	SS Syn
1.6	1	2	8	1	2	6	1	1	9	1	1	4	NSS & SS Syn
1.7	1	2	6	1	2	5	1	1	7	1	1	3	NSS & SS Syn
1.8	1	2	5	1	2	4	1	1	5	1	1	3	NSS & SS Syn
1.9	1	1	4	1	1	3	1	1	4	1	1	2	ALL
2.0	1	1	3	1	1	3	1	1	2	1	1	2	ALL
$n = 15$													
1.1	3	41	174	5	18	58	2	18	187	1	12	119	SS Syn
1.2	1	13	53	2	7	24	1	5	47	1	4	31	SS Syn
1.3	1	6	22	1	4	15	1	2	22	1	2	13	NSS & SS Syn
1.4	1	3	12	1	3	8	1	1	13	1	1	8	NSS & SS Syn
1.5	1	2	7	1	2	6	1	1	4	1	1	4	NSS & SS Syn
1.6	1	2	5	1	2	4	1	1	5	1	1	3	NSS & SS Syn
1.7	1	1	4	1	1	3	1	1	4	1	1	2	ALL
1.8	1	1	3	1	1	3	1	1	3	1	1	2	ALL
1.9	1	1	3	1	1	2	1	1	3	1	1	2	ALL
2.0	1	1	2	1	1	2	1	1	2	1	1	2	ALL
$n = 20$													
1.1	3	35	150	5	15	45	1	12	122	1	10	97	SS Syn
1.2	1	10	41	2	6	18	1	3	33	1	3	24	NSS & SS Syn
1.3	1	4	16	1	3	11	1	2	13	1	2	7	NSS & SS Syn
1.4	1	2	9	1	2	6	1	1	9	1	1	4	NSS & SS Syn
1.5	1	2	5	1	2	4	1	1	5	1	1	3	NSS & SS Syn
1.6	1	1	4	1	1	3	1	1	4	1	1	2	ALL
1.7	1	1	3	1	1	3	1	1	3	1	1	2	ALL
1.8	1	1	2	1	1	2	1	1	3	1	1	2	ALL
1.9	1	1	2	1	1	2	1	1	1	1	1	1	ALL
2.0	1	1	2	1	1	2	1	1	1	1	1	1	ALL

From Tables 4.28 to 4.31, it can be observed that the MRL -based design of the side-sensitive synthetic- γ chart produces smaller MRL_1 compared to the non-side-sensitive synthetic- γ chart, particularly for small shift sizes. For instance, the MRL_1 (SS Syn) is 22 and the MRL_1 (NSS Syn) is 32 for $n = 5$, $\tau = 1.1$ and $\gamma_0 = 0.05$ in Table 4.28. This suggests that the proposed chart requires fewer samples to detect out-of-control signals compared to the non-side-sensitive synthetic- γ chart, as evidenced by the lower MRL_1 . Furthermore, the side-sensitive synthetic- γ chart demonstrates lower variability than the non-side-sensitive synthetic- γ chart, as shown by the smaller difference between the l_{05} and l_{95} in most cases. An instance of improvement in the side-sensitive synthetic- γ chart over the non-side-sensitive synthetic- γ chart for MRL -based design can be observed at $n = 5$, $\tau = 1.1$ and $\gamma_0 = 0.05$ in Table 4.28. In this case, the l_{05} and l_{95} values of the side-sensitive synthetic- γ chart is 2 and 231, respectively, while that of the non-side-sensitive synthetic- γ chart is 3 and 343, respectively. This indicates that the side-sensitive synthetic- γ chart performs better than the existing non-side-sensitive synthetic- γ chart.

Tables 4.28 to 4.31 reveal that the proposed side-sensitive synthetic- γ chart performs better than the Shewhart- γ chart in terms of smaller MRL_1 values and smaller differences between two extreme percentiles for all values of sample size, shift size and in-control coefficient of variation except for $n = 15$, $\tau = 2.0$ and $\gamma_0 = 0.20$ in Table 4.31, where the two charts provide the same results for l_{05} , MRL_1 and l_{95} . The side-sensitive synthetic- γ chart also exhibits better MRL_1 performance compared to the EWMA- γ^2 chart, particularly for $\tau \in \{1.1, 1.2, 1.3, 1.4, 1.5, 1.6, 1.7\}$. However, for $\tau = 2.0$, both charts yield the same MRL_1 values in most cases. In terms of the difference between the l_{05} and l_{95} , the side-sensitive synthetic- γ chart exhibits less variation than the EWMA- γ^2 chart

for $\tau \in \{1.5, 1.6, 1.7, 1.8, 1.9, 2.0\}$. Nevertheless, the EWMA- γ^2 chart shows a smaller difference between l_{05} and l_{95} compared to the proposed chart for small shift sizes.

From Tables 4.28 to 4.31, it can be observed that there are many results with the digit “1”, especially for l_{05} which denotes the 5th percentile. Since $P(RL \leq l_{05}) = 0.05$, the chart will detect the out-of-control condition by l_{05} for only 5% of the time, and for 95% of the time the chart will detect the out-of-control condition after l_{05} . Thus, the values of l_{05} will be small and quite frequently appears as 1, since it denotes the early percentiles of the run length. In addition, for larger sample sizes and shift sizes, a quick detection of out-of-control condition is expected. Hence, the l_{05} , MRL_1 and l_{95} are frequently small values for such cases.

By referring to the last column in Tables 4.28 to 4.31, it can be observed that the proposed side-sensitive synthetic- γ chart is the best chart among all four charts for most cases particularly for small shift sizes. Besides, when the sample size and shift size increase, the non-side-sensitive and side-sensitive synthetic- γ charts are the best charts for all values of γ_0 due to the same values of MRL_1 obtained. Nevertheless, for large shift sizes, all four charts are the best charts for all values of n and γ_0 as generally a quick detection of the out-of-control condition is shown for larger sample sizes and shift sizes. Therefore, the proposed side-sensitive synthetic- γ chart is the best chart in terms of the MRL performance.

Table 4.32 presents a comparison of the $E(l_{05})$, $EMRL_1$, and $E(l_{95})$ for the Shewhart- γ , EWMA- γ^2 , non-side-sensitive synthetic- γ (NSS Syn) and side-sensitive synthetic- γ (SS Syn) charts that are designed based on $EMRL$. The comparison is conducted for different values of $n \in \{5, 7, 10, 15, 20\}$, $\gamma_0 \in \{0.05, 0.10, 0.15, 0.20\}$ and $(\tau_{\min}, \tau_{\max}) = (1, 2]$ and all results obtained were verified using simulation.

Table 4.32 The $E(l_{05})$, $EMRL_1$ and $E(l_{95})$ values of the $EMRL$ -based of the Shewhart- γ , EWMA- γ^2 , non-side-sensitive synthetic- γ (NSS Syn) and side-sensitive synthetic- γ (SS Syn) charts for $n \in \{5, 7, 10, 15, 20\}$, $\gamma_0 \in \{0.05, 0.10, 0.15, 0.20\}$ and $(\tau_{\min}, \tau_{\max}) = (1, 2]$

n	Shewhart			EWMA			NSS Syn			SS Syn			Best Chart
	$E(l_{05})$	$EMRL_1$	$E(l_{95})$	$E(l_{05})$	$EMRL_1$	$E(l_{95})$	$E(l_{05})$	$EMRL_1$	$E(l_{95})$	$E(l_{05})$	$EMRL_1$	$E(l_{95})$	
$\gamma_0 = 0.05$													
5	1.84	17.03	74.92	2.65	11.58	39.71	1.24	12.98	79.49	1.10	9.90	57.99	SS Syn
7	1.73	14.14	62.56	2.75	9.33	28.66	1.17	11.05	67.49	1.12	7.49	46.17	SS Syn
10	1.56	11.66	52.12	2.29	7.50	22.42	1.15	10.07	58.92	1.12	5.90	37.05	SS Syn
15	1.48	9.96	44.18	1.81	5.88	19.12	1.17	7.71	47.52	1.05	5.03	29.72	SS Syn
20	1.41	8.76	38.57	1.67	4.88	15.69	1.07	5.08	30.51	1.05	4.25	24.54	SS Syn
$\gamma_0 = 0.10$													
5	1.84	17.10	75.62	3.03	11.77	37.54	1.24	13.01	80.18	1.05	10.09	59.04	SS Syn
7	1.79	14.28	63.27	2.79	9.43	28.56	1.15	11.35	68.38	1.12	7.65	46.57	SS Syn
10	1.56	11.84	52.63	2.29	7.56	23.05	1.17	9.61	57.27	1.12	5.95	37.42	SS Syn
15	1.48	9.84	43.54	1.88	5.87	17.78	1.17	7.60	47.11	1.05	4.96	29.43	SS Syn
20	1.48	8.83	38.57	1.68	4.85	15.09	1.07	5.03	30.38	1.05	4.37	25.05	SS Syn
$\gamma_0 = 0.15$													
5	1.84	17.33	76.19	3.06	11.84	37.57	1.24	13.23	81.06	1.05	10.16	59.60	SS Syn
7	1.79	14.37	64.08	2.65	9.50	30.01	1.15	11.37	68.81	1.12	7.70	47.08	SS Syn
10	1.58	11.97	53.67	2.30	7.76	22.80	1.17	8.94	56.72	1.12	6.02	38.15	SS Syn
15	1.48	9.89	44.28	1.88	5.98	18.47	1.17	7.53	46.95	1.05	5.03	30.26	SS Syn
20	1.48	8.87	38.58	1.68	5.02	15.56	1.05	5.18	31.03	1.29	4.79	27.58	SS Syn
$\gamma_0 = 0.20$													
5	1.84	17.62	77.61	2.91	12.00	39.54	1.22	13.92	82.84	1.12	9.58	59.36	SS Syn
7	1.79	14.81	65.45	2.56	9.72	31.41	1.15	11.46	68.58	1.05	4.96	29.43	SS Syn
10	1.58	12.36	54.60	2.89	7.84	23.84	1.17	8.87	56.87	1.05	6.71	39.46	SS Syn
15	1.48	9.95	44.54	1.88	6.17	19.26	1.17	7.57	46.85	1.05	5.54	31.25	SS Syn
20	1.48	8.82	38.75	1.83	5.19	14.80	1.07	5.11	30.99	1.05	4.34	25.07	SS Syn

From Table 4.32, it is noticeable that the side-sensitive synthetic- γ chart which is designed based on $EMRL$ performs better than the Shewhart- γ and non-side-sensitive synthetic- γ charts for all values of sample size and in-control coefficient of variation, as well as the EWMA- γ^2 chart for all cases in terms of the performance of $EMRL_1$. However, the EWMA chart exhibits a smaller difference between the $E(l_{05})$ and $E(l_{95})$ for all cases compared to the side-sensitive synthetic- γ chart that is introduced in this

thesis. Therefore, the proposed side-sensitive synthetic- γ chart is the best chart among all four charts in terms of the *EMRL* performance.

4.5 Implementation Based on Real Industrial Example

This subsection demonstrates the application of the side-sensitive synthetic- γ chart for both *ARL* and *MRL*-based designs using an actual industrial example which was used by Castagliola et al. (2011). This industrial example was collected from an Italian company which produces sintered mechanical parts using power metallurgy, whereby compressed metal powder is heated to bond the individual particles. Sintering is utilized in the manufacture of complex-shaped mechanical components such as gears, resulting in cost savings compared to old machining operations.

Pore shrinkage is a crucial factor that impacts the strength of the bond between particles (Kalpakjian, 1992). The pressure test drop time, T_{pd} , from 2 bar to 1.5 bar is a quality characteristic related to pore shrinkage, and it should be greater than 30 seconds. If a bigger amount of molten copper is used to fill the pores in the process of sintering, the pressure test drop time will be longer. The company led a regression analysis and found that there is a constant proportionality between the standard deviation and mean of the pressure drop time, such that $\sigma_{pd} = \gamma_{pd} \times \mu_{pd}$, where σ_{pd} , γ_{pd} and μ_{pd} are the pressure drop time's standard deviation, coefficient of variation and mean, respectively. Consequently, the company decided to monitor the coefficient of variation, i.e.

$\gamma_{pd} = \frac{\sigma_{pd}}{\mu_{pd}}$, to identify any fluctuations in the process variability.

After obtaining a nominal quantity of copper, a set of Phase I data consisting of 20 samples ($m = 20$) with a sample size of 5 ($n = 5$) each was gathered. The data collected

during the Phase I study is presented in Table 4.33, which was sourced from Castagliola et al. (2011).

Table 4.33 Phase I dataset from a sintering process

k	\bar{X}_k	S_k	$\hat{\gamma}_k$
1	664.2	268.9	0.405
2	705.6	308.6	0.437
3	1051.5	539.9	0.513
4	1047.3	359.0	0.343
5	618.2	136.3	0.220
6	781.4	446.4	0.571
7	797.8	342.5	0.429
8	678.9	275.4	0.406
9	848.3	320.5	0.378
10	1015.3	453.7	0.447
11	777.4	276.4	0.356
12	813.9	170.7	0.210
13	716.9	397.4	0.554
14	937.6	421.2	0.449
15	915.1	331.9	0.363
16	873.2	285.0	0.326
17	984.3	573.7	0.583
18	819.3	156.2	0.191
19	839.0	244.0	0.291
20	585.8	322.3	0.550

By using the computation of root-mean-square, Castagliola et al. (2011) demonstrated that the Phase I data is under control with an estimated in-control sample coefficient of variation of 0.417. The process engineers explained that the heterogeneous microstructure of sintering steel with uneven grain size will result in an anomalous increase in pressure drop time's standard deviation. This happens because it impacts the way copper is absorbed in every sintered part and its pore filling, leading to an effect on pressure drop time. An alteration in the correlation structure between pressure drop time's mean and standard deviation will result in shifts in the in-control coefficient of variation. Consequently, assignable cause(s) can be identified by monitoring the coefficient of variation.

Process engineers have suggested that a 25% shift in the in-control coefficient of variation indicates a production problem. Therefore, this thesis proposed the side-sensitive synthetic- γ chart that is designed based on ARL and MRL to improve the detection of a shift of $\tau = 1.25$. It should be noted that Castagliola et al. (2011) also developed the EWMA- γ^2 chart based on $\tau = 1.25$. The methodology presented in Section 3.5 is used for ARL -based design to obtain the optimal chart parameters of $L = 21$, $LCL = 0$, $UCL = 0.9065$. The results show that the side-sensitive synthetic- γ chart has a minimum ARL_1 of 18.8 compared to the EWMA- γ^2 , non-side-sensitive synthetic- γ and Shewhart- γ charts, with ARL_1 of 20.2, 33.1 and 58.8, respectively.

The data for Phase II is presented in Table 4.34. It should be noted that the data comprises 20 new samples that were collected from the process after the existence of an assignable cause that led to an increase in process variability.

Table 4.34 Phase II dataset from a sintering process

k	\bar{X}_k	S_k	$\hat{\gamma}_k$
1	906.4	476.0	0.525
2	805.1	493.9	0.613
3	1187.2	1105.9	0.932
4	663.4	304.8	0.459
5	1012.1	367.4	0.363
6	863.2	350.4	0.406
7	1561.0	1652.2	1.058
8	697.1	253.2	0.363
9	1024.6	120.9	0.118
10	355.3	235.2	0.662
11	485.6	106.5	0.219
12	1224.3	915.4	0.748
13	1365.0	1051.6	0.770
14	704.0	449.7	0.639
15	1584.7	1050.8	0.663
16	1130.0	680.6	0.602
17	824.7	393.5	0.477
18	921.2	391.0	0.424
19	870.3	730.0	0.839
20	1068.3	150.8	0.141

The Phase II data was monitored using the side-sensitive synthetic- γ chart, as presented in Figure 4.1.

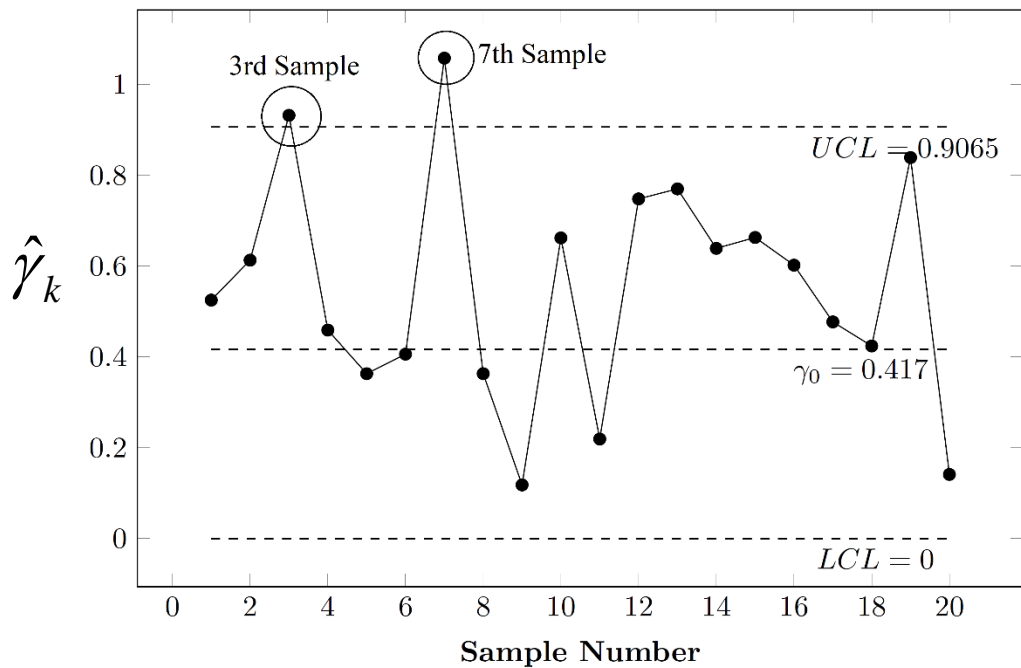


Figure 4.1 The γ sub-chart of the ARL-based design of the side-sensitive synthetic- γ chart

Figure 4.1 displays the side-sensitive synthetic- γ chart utilized for monitoring the Phase II data, revealing two non-conforming samples, the 3rd and 7th samples, which appear in the region above the UCL . Since the values of CRL_1 and CRL_2 are less than $L = 21$, specifically 3 and 4, respectively, the side-sensitive synthetic- γ chart will generate out-of-control signals at the 3rd and 7th samples. Thus, the special cause was promptly detected by the side-sensitive synthetic- γ chart. To facilitate comparison, Figures 4.2 to 4.4 show the Phase II data being monitored using the EWMA- γ^2 , non-side-sensitive synthetic- γ and Shewhart- γ charts.

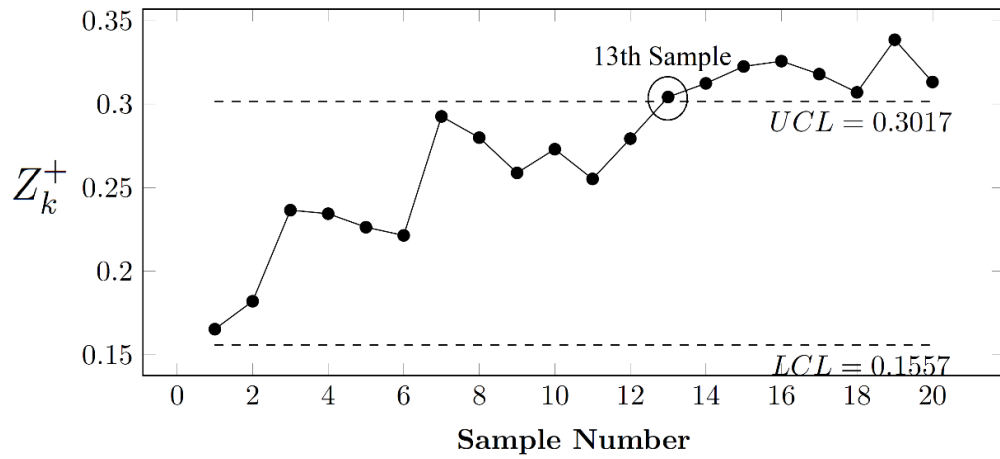


Figure 4.2 The ARL-based design of the EWMA- γ^2 chart

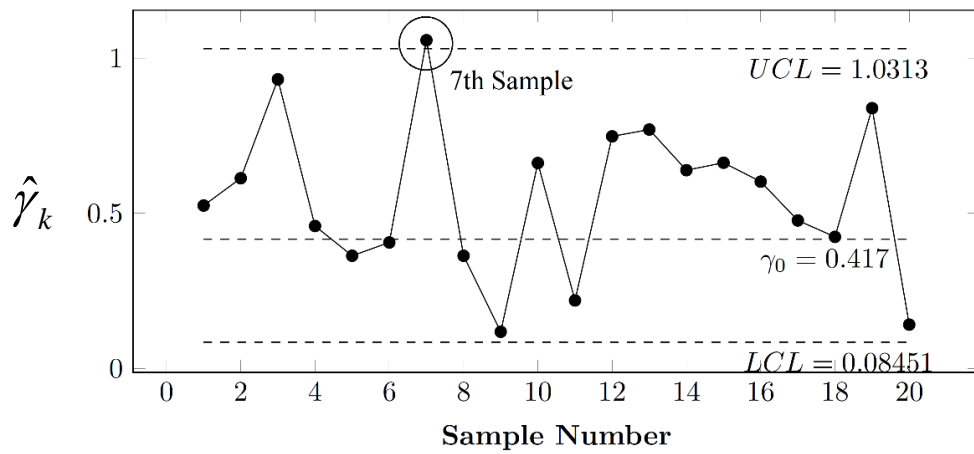


Figure 4.3 The γ sub-chart of the ARL-based design of the non-side-sensitive synthetic- γ chart

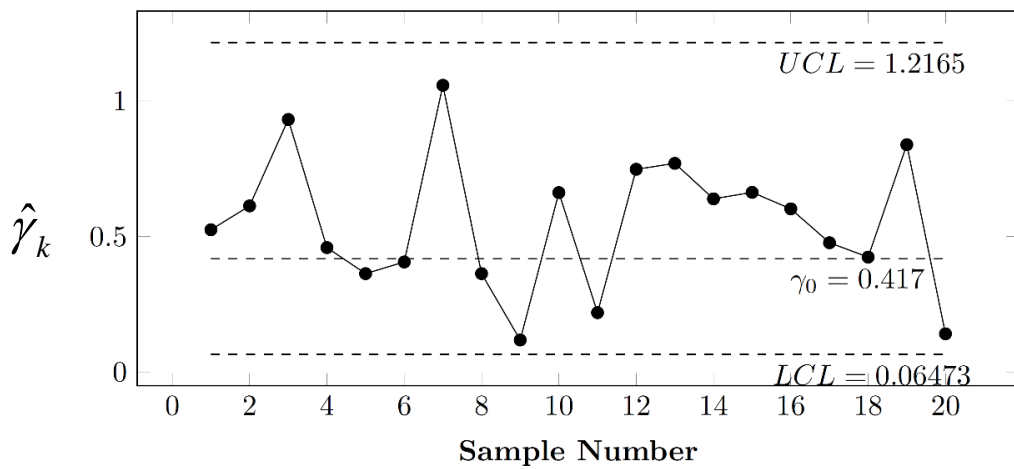


Figure 4.4 The ARL-based design of the Shewhart- γ chart

Figure 4.2 indicates that the EWMA- γ^2 chart produces an out-of-control signal at the 13th sample. Nevertheless, the side-sensitive synthetic- γ chart detected the out-of-control condition at the third sample which is earlier than the EWMA- γ^2 chart. Figure 4.3 illustrates that the 7th sample is classified as a non-conforming sample for the non-side-sensitive synthetic- γ chart, resulting in $CRL_1 = 7$. With the optimal L being 35, the non-side-sensitive synthetic- γ chart generates an out-of-control signal at the 7th sample. From Figure 4.4, the Shewhart- γ chart did not identify any samples that are outside the control limits. However, there are seven successive samples, i.e. samples 12 to 18, that falls above the CL , which indicates the possible presence of assignable cause(s). By comparing Figure 4.1 with Figures 4.2 to 4.4, the side-sensitive synthetic- γ chart which is designed based on the ARL resulted in the fastest discovery of out-of-control conditions among all the four charts. Hence, quicker corrective action can be engaged to identify and remove the unusual causes.

To accurately assess the side-sensitive synthetic- γ chart's performance, the design based on MRL was also used with the same Phase II dataset, following the methodology presented in Section 3.7 with $MRL_0 = 250$. The optimal chart parameters, L , LCL , and UCL , obtained were 7, 0, and 0.8418, respectively, and the corresponding values of $Q05$, MRL_1 and $Q95$ were 1, 7 and 76 respectively. Figure 4.5 illustrates the side-sensitive synthetic- γ chart's γ sub-chart which is designed based on the MRL , when implemented on the Phase II dataset.

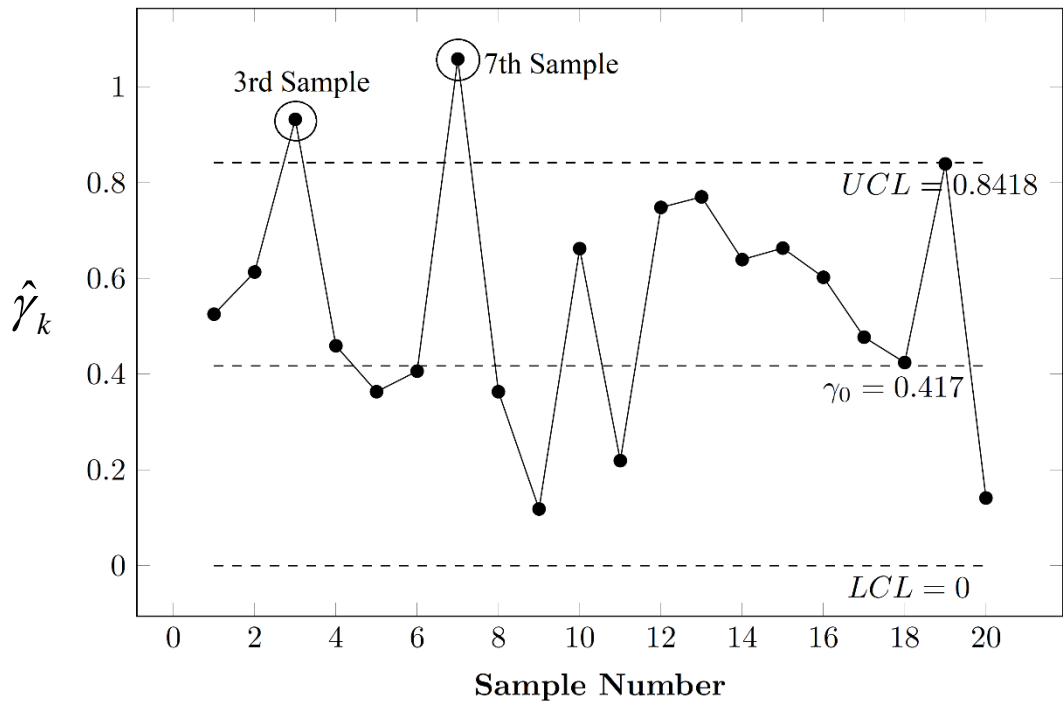


Figure 4.5 The γ sub-chart of the *MRL*-based design of the side-sensitive synthetic- γ chart

Figure 4.5 indicates that the 3rd and 7th samples exceed the *UCL*, and thus, they are identified as two consecutive non-conforming samples. Additionally, the *CRL*₁, which considers the quantity of conforming samples until the occurrence of the first non-conforming sample, is three, while the *CRL*₂ is four, obtained from the quantity of conforming samples between the 4th and 7th samples. Since the optimal *L* is 7, and both *CRL* values are smaller than 7, the out-of-control signal is triggered at the 3rd and 7th samples. This result is consistent with the *ARL*-based design shown in Figure 4.1. Nonetheless, the design based on *MRL* yields a slightly smaller conforming region with a lower *UCL* value than the design based on *ARL*. Consequently, both designs of side-sensitive synthetic- γ chart based on *ARL* and *MRL* exhibit comparable performance in this example.

CHAPTER 5: CONCLUSION

5.0 Introduction

The opening of this chapter provides an overview of the performance of the side-sensitive synthetic- γ chart proposed in this thesis, based on the obtained optimal chart parameters and performance measures obtained. Additionally, a comparison is made between the proposed chart and three other coefficient of variation charts used in this thesis, namely the Shewhart- γ , EWMA- γ^2 and non-side-sensitive synthetic- γ charts. Subsequently, the limitation of the research and recommendation for future study are explained in the last subsection of this thesis.

5.1 Discussion and Summary

In this thesis, a synthetic chart that incorporates side sensitivity with *ARL*, *EARL*, *MRL* and *EMRL*-based designs is proposed to improve the existing non-side-sensitive synthetic- γ chart's performance in monitoring the coefficient of variation and this study is not available in the existing literature. The performance of the proposed chart is evaluated for sample sizes, $n \in \{5, 7, 10, 15, 20\}$, shift sizes, $\tau \in \{1.1, 1.2, 1.3, 1.4, 1.5, 1.6, 1.7, 1.8, 1.9, 2.0\}$ and in-control coefficient of variations, $\gamma_0 \in \{0.05, 0.10, 0.15, 0.20\}$. Besides, the side-sensitive synthetic- γ chart's entire distribution of run length is also being studied in order to precisely assess the actual performance of the proposed chart.

The *ARL* and *SDRL* are derived as shown in Equations (3.18) and (3.19), respectively. Since it is hard to specify the value of shift size in most real-world situations, which is required to calculate the *ARL* and *SDRL*, the *EARL* is selected as one of the performance measures when shift size could not be specified. The formula for *EARL* is derived as

shown in Equation (3.29) with a range of possible values $(\tau_{\min}, \tau_{\max})$ which is set as $(1, 2]$. Subsequently, algorithms to optimize the ARL and $EARL$ are formulated in Sections 3.4 and 3.5, respectively. These are related to the achievement of the first research objective in this thesis.

By referring to the results of the ARL -based design with the constraint of ARL_0 being set as 370.4, it can be observed that as sample size increases, the values of ARL_1 and $SDRL_1$ decrease significantly. Besides, the conforming region and maximum quantity of conforming samples between two consecutive non-conforming samples (L) are getting smaller for large sample sizes. Similarly, as shift size increases, the ARL_1 , $SDRL_1$, conforming region and L shows a similar trend as that shown by an increase in sample size. For the in-control coefficient of variation (γ_0) , the values of ARL_1 , $SDRL_1$, LCL and UCL are slightly larger when the in-control coefficient of variation increases. In terms of the $EARL$ performance, the value of $EARL_1$ decreases significantly as the sample size increases. Furthermore, the increase in sample size also results in tighter conforming region. However, a different trend is observed as the in-control coefficient of variation increases, where the values of $EARL_1$, LCL and UCL increase.

Existing works of literature have explained the risks of evaluating a control chart solely based on the ARL and $EARL$ performance especially for skewed distributions. Numerical analysis in this thesis shows that the distribution of run length of the side-sensitive synthetic- γ chart that is designed based on ARL and $EARL$ is positively skewed. Besides, false alarms often occur earlier than what is designated by the ARL . These are related to the second research objective of studying the side-sensitive synthetic- γ chart's distribution of run length. Hence, the proposed chart should also be assessed based on

another two performance measures, the *MRL* and *EMRL*. The formula to evaluate the *MRL* is derived in Equation (3.32) by setting $\theta = 0.5$ with specific values of shift size whereas the formula for *EMRL* for unknown shift size is derived as shown in Equation (3.33) with a range of possible values $(\tau_{\min}, \tau_{\max})$ which is set as $(1, 2]$. Algorithms to optimize these performance measures are shown in Sections 3.6 and 3.7, respectively. These are related to the achievement of the first research objective. The numerical analysis indicates that the design based on *MRL* performs better than the design based on *ARL* as it has a smaller conforming region for small shift sizes. Besides, it has a smaller spread and variation in the run lengths. Furthermore, it needs a smaller median quantity of samples in detecting the shifts. As for the design based on *EMRL*, it has a similar performance as the design based on *EARL*.

Comparing it to other monitoring coefficient of variation charts based on *ARL*, *EARL*, *MRL*, and *EMRL*-based designs, the proposed chart displays better performance than the Shewhart- γ and non-side-sensitive synthetic- γ charts in all cases considered. In most cases, it also exhibits comparable or better performance than the EWMA chart, excluding small shift sizes where the EWMA- γ^2 chart performs better than the proposed chart. Hence, the side-sensitive synthetic- γ chart can be considered a competitive chart for monitoring shifts in the coefficient of variation, and it marks a noteworthy enhancement over the existing synthetic chart, accomplishing the third research objective of this thesis.

The actual performance of the proposed chart is assessed on an actual industry example taken from Castagliola et al. (2011) by implementing the design based on *ARL*. The performance is compared with the Shewhart- γ , EWMA- γ^2 , and non-side-sensitive synthetic- γ charts. The numerical analysis demonstrates that the proposed side-sensitive

synthetic- γ chart which is designed based on *ARL* has the smallest ARL_1 among all four charts and detects the out-of-control condition quicker than the other coefficient of variation charts which are designed based on *ARL*, enabling prompt action to be engaged to eliminate the assignable cause(s) and bring the process back to a state of in-control, thereby enhancing the quality of products or services delivered. To ensure the accuracy of the evaluation, the proposed side-sensitive synthetic- γ chart that is designed based on *MRL* is also implemented on the same real industry example, which yields similar results to the *ARL*-based design. Hence, the last research objective of this thesis is successfully accomplished.

As a conclusion, incorporating the feature of side sensitivity into the existing synthetic- γ chart has brought a significant improvement to the existing synthetic- γ chart and this outcome has accomplished the purpose of this thesis.

5.2 Limitation of Research and Future Recommendation

This thesis has identified four research limitations. The first limitation pertains to the proposed side-sensitive synthetic- γ chart, which solely considers three regions, namely the conforming, upper non-conforming and lower non-conforming regions, which may reduce the sensitivity of the chart. Although considering three regions results in better performance than the existing synthetic- γ chart which considers only two regions, i.e. the conforming and non-conforming regions, future research which considers more regions as explained in the next paragraph might result in further improvement of the proposed side-sensitive synthetic- γ chart. The second limitation is that the proposed side-sensitive synthetic- γ chart has only been examined in the context of a univariate process. Hence, the proposed chart could not be applied to monitor multivariate processes with several correlated quality characteristics. The third limitation of this thesis is that

fixed chart parameters are adopted, irrespective of the present sample information. Since the operations and formulae to evaluate the proposed chart's performance are based on fixed chart parameters, hence modifications need to be made on the operations and performance measures if variable chart parameters are going to be adopted. Finally, the last limitation is the data being monitored is assumed to be independent and normally distributed, which affects the distributional properties of $\hat{\gamma}$ and the formulae to evaluate the performance of the chart. For non-normal data, the distributional properties of $\hat{\gamma}$ needs to be derived according to the new distribution, and the formulae for the performance measures also needs to be modified for dependent data by taking the dependency into consideration.

Since the proposed side-sensitive synthetic- γ chart has four limitations as mentioned in the previous paragraph, therefore several future research can be recommended. First, the study of the side-sensitive synthetic- γ chart can be continued with more than three regions such as implementing the modified side-sensitive regions introduced by Shongwe and Graham (2018). The control chart can be separated into four regions which are the upper conforming, lower conforming, upper non-conforming and lower non-conforming regions. Another recommendation for future research includes exploring the application of the side-sensitive synthetic- γ chart to multivariate processes. Another potential research area involves investigating the use of variable chart parameters for the side-sensitive synthetic- γ chart. Additionally, studies can be conducted to create a side-sensitive synthetic- γ chart suitable for non-normal and autocorrelated data.

REFERENCES

- Abubakar, S. S., Khoo, M. B., Saha, S., & Teoh, W. L. (2022). Run sum control chart for monitoring the ratio of population means of a bivariate normal distribution. *Communications in Statistics-Theory and Methods*, 51(13), 4559-4588.
- Adegoke, N. A., Abbasi, S. A., Smith, A. N., Anderson, M. J., & Pawley, M. D. (2019). A multivariate homogeneously weighted moving average control chart. *IEEE Access*, 7, 9586-9597.
- Aly, A. A., Saleh, N. A., & Mahmoud, M. A. (2022). An adaptive EWMA control chart for monitoring zero-inflated poisson processes. *Communications in Statistics-Simulation and Computation*, 51(4), 1564-1677.
- Aparisi, F., & De Luna, M. A. (2009). Synthetic-X control charts optimized for in-control and out-of-control regions. *Computers & Operations Research*, 36(12), 3204-3214.
- Aslam, M., Gadde, S. R., Aldosari, M. S., & Jun, C. H. (2019). A hybrid EWMA chart using coefficient of variation. *International Journal of Quality & Reliability Management*, 36(4), 587-600.
- Babu, J. J. J., & Sudha, G. F. (2016). Adaptive speckle reduction in ultrasound images using fuzzy logic on coefficient of variation. *Biomedical Signal Processing and Control*, 23, 93-103.
- Banik, S., & Kibria, B. G. (2011). Estimating the population coefficient of variation by confidence intervals. *Communications in Statistics-Simulation and Computation*, 40(8), 1236-1261.
- Breunig, R. (2001). An almost unbiased estimator of the coefficient of variation. *Economics Letters*, 70(1), 15-19.
- Calzada, M. E., & Scariano, S. M. (2001). The robustness of the synthetic control chart to non-normality. *Communications in Statistics-Simulation and Computation*, 30(2), 311-326.
- Calzada, M. E., & Scariano, S. M. (2013). A synthetic control chart for the coefficient of variation. *Journal of Statistical Computation and Simulation*, 83(5), 853-867.
- Castagliola, P., Achouri, A., Taleb, H., Celano, G., & Psarakis, S. (2013a). Monitoring the coefficient of variation using control charts with run rules. *Quality Technology & Quantitative Management*, 10(1), 75-94.

- Castagliola, P., Achouri, A., Taleb, H., Celano, G., & Psarakis, S. (2013b). Monitoring the coefficient of variation using a variable sampling interval control chart. *Quality and Reliability Engineering International*, 29(8), 1135-1149.
- Castagliola, P., Achouri, A., Taleb, H., Celano, G., & Psarakis, S. (2015). Monitoring the coefficient of variation using a variable sample size control chart. *The International Journal of Advanced Manufacturing Technology*, 80, 1561-1576.
- Castagliola, P., Celano, G., & Psarakis, S. (2011). Monitoring the coefficient of variation using EWMA charts. *Journal of Quality Technology*, 43(3), 249-265.
- Castagliola, P., & Khoo, M. B. (2009). A synthetic scaled weighted variance control chart for monitoring the process mean of skewed populations. *Communications in Statistics-Simulation and Computation*, 38(8), 1659-1674.
- Chaudhari, K., & Thakkar, A. (2023). Neural network systems with an integrated coefficient of variation-based feature selection for stock price and trend prediction. *Expert Systems with Applications*, 219, 119527.
- Chen, F. L., & Huang, H. J. (2006). Variable sampling interval synthetic control charts for jointly monitoring process mean and standard deviation. *International Journal of Industrial Engineering: Theory, Applications, and Practice*, 13(2), 136-146.
- Chew, X., Khoo, M. B. C., Khaw, K. W., Yeong, W. C., & Chong, Z. L. (2019). A proposed variable parameter control chart for monitoring the multivariate coefficient of variation. *Quality and Reliability Engineering International*, 35(7), 2442-2461.
- Chew, Y., Khoo, M. B., Khaw, K. W., & Yeong, W. C. (2022). Economic and economic-statistical designs of variable sample size and sampling interval coefficient of variation chart. *Communications in Statistics-Theory and Methods*, 51(6), 1811-1835.
- Chong, Z. L., Tan, K. L., Khoo, M. B., Teoh, W. L., & Castagliola, P. (2022). Optimal designs of the exponentially weighted moving average (EWMA) median chart for known and estimated parameters based on median run length. *Communications in Statistics-Simulation and Computation*, 51(7), 3660-3684.
- Costa, A. F., De Magalhaes, M. S., & Epprecht, E. K. (2009). Monitoring the process mean and variance using a synthetic control chart with two-stage testing. *International Journal of Production Research*, 47(18), 5067-5086.

- Costa, A. F. B., & Rahim, M. A. (2006). A synthetic control chart for monitoring the process mean and variance. *Journal of Quality in Maintenance Engineering*, 12(1), 81-88.
- Davis, R. B., & Woodall, W. H. (2002). Evaluating and improving the synthetic control chart. *Journal of Quality Technology*, 34(2), 200-208.
- Dawod, A. B., Abbasi, S. A., & Al-Momani, M. (2018). On the performance of coefficient of variation control charts in Phase I. *Quality and Reliability Engineering International*, 34(6), 1029-1040.
- De Araujo Lima-Filho, L. M., & Mariano Bayer, F. (2021). Kumaraswamy control chart for monitoring double bounded environmental data. *Communications in Statistics-Simulation and Computation*, 50(9), 2513-2528.
- Domangue, R., & Patch, S. C. (1991). Some omnibus exponentially weighted moving average statistical process monitoring schemes. *Technometrics*, 33(3), 299-313.
- Doring, T. F., & Reckling, M. (2018). Detecting global trends of cereal yield stability by adjusting the coefficient of variation. *European Journal of Agronomy*, 99, 30-36.
- El-Din, M. M., Ameen, M. M., Abd El-Raheem, A. M., El-Attar, H. E., & Hafez, E. H. (2019). Estimation of the coefficient of variation for lindley distribution based on progressive first failure censored data. *J Stat Appl Prob*, 8, 83-90.
- England, A. D., Gharib-Naseri, K., Kheravii, S. K., & Wu, S. B. (2022). Rearing broilers as mixed or single-sex: relevance to performance, coefficient of variation, and flock uniformity. *Poultry Science*, 101(12), 102176.
- Gan, F. F. (1993). An optimal design of EWMA control charts based on median run length. *Journal of Statistical Computation and Simulation*, 45(3-4), 169-184.
- Gao, H., Khoo, M. B. C., Teh, S. Y., & Teoh, W. L. (2019). A study on the median run length performance of the run sum s control chart. *International Journal of Mechanical Engineering and Robotics Research*, 8(6), 885-890.
- Giner-Bosch, V., Tran, K. P., Castagliola, P., & Khoo, M. B. C. (2019). An EWMA control chart for the multivariate coefficient of variation. *Quality and Reliability Engineering International*, 35(6), 1515-1541.

- Gulhar, M., Kibria, B. G., Albatineh, A. N., & Ahmed, N. U. (2012). A comparison of some confidence intervals for estimating the population coefficient of variation: a simulation study. *SORT-Statistics and Operations Research Transactions*, 36(1), 45-68.
- Guo, B., & Wang, B. X. (2018). Control charts for the coefficient of variation. *Statistical Papers*, 59, 933-955.
- Haq, A., & Khoo, M. B. (2019). New adaptive EWMA control charts for monitoring univariate and multivariate coefficient of variation. *Computers & Industrial Engineering*, 131, 28-40.
- Hong, E. P., Kang, C. W., Baek, J. W., & Kang, H. W. (2008). Development of CV control chart using EWMA technique. *Journal of the Society of Korea Industrial and Systems Engineering*, 31(4), 114-120.
- Hu, X., Zhang, S., & Sun, G. (2022a). One-sided double EWMA charts for monitoring the coefficient of variation. In *2022 41st Chinese Control Conference (CCC)*(pp. 5905-5910). IEEE.
- Hu, X., Zhang, S., Xie, F., & Song, Z. (2023). Triple exponentially weighted moving average control charts without or with variable sampling interval for monitoring the coefficient of variation. *Journal of Statistical Computation and Simulation*, 1-35.
- Hu, X., Zhang, S., Zhang, Y., Zhang, J., & Zhou, P. (2021). Monitoring coefficient of variation using variable sampling interval double exponentially weighted moving average charts. *Scientia Iranica*.
- Hu, X., Zhang, S., Zhou, X., Tang, A., & Xie, F. (2022b). The performance of double exponentially weighted moving average control charts for monitoring the coefficient of variation. *Communications in Statistics-Simulation and Computation*, 1-20.
- Jiang, M., Hooper, A., Tian, X., Xu, J., Chen, S. N., Ma, Z. F., & Cheng, X. (2020). Delineation of built-up land change from SAR stack by analysing the coefficient of variation. *ISPRS Journal of Photogrammetry and Remote Sensing*, 169, 93-108.
- Kalpakjian, S. (1992). *Manufacturing engineering and technology (2nd ed)*. New York: Addison Wesley.
- Kang, C. W., Lee, M. S., Seong, Y. J., & Hawkins, D. M. (2007). A control chart for the coefficient of variation. *Journal of quality technology*, 39(2), 151-158.

- Khaw, K. W., Khoo, M. B., Yeong, W. C., & Wu, Z. (2017). Monitoring the coefficient of variation using a variable sample size and sampling interval control chart. *Communications in Statistics-Simulation and Computation*, 46(7), 5772-5794.
- Khaw, K. W., Chew, X., Yeong, W. C., & Lim, S. L. (2019). Optimal design of the synthetic control chart for monitoring the multivariate coefficient of variation. *Chemometrics and Intelligent Laboratory Systems*, 186, 33-40.
- Khoo, M. B., Lee, H. C., Wu, Z., Chen, C. H., & Castagliola, P. (2010). A synthetic double sampling control chart for the process mean. *IIE Transactions*, 43(1), 23-38.
- Khoo, M. B., Wong, V. H., Wu, Z., & Castagliola, P. (2012). Optimal design of the synthetic chart for the process mean based on median run length. *IIE Transactions*, 44(9), 765-779.
- Khoo, M. B., Wu, Z., & Atta, A. M. (2008). A synthetic control chart for monitoring the process mean of skewed populations based on the weighted variance method. *International Journal of Reliability, Quality and Safety Engineering*, 15(3), 217-245.
- Kong, Q. Y., Zhao, C. F., Wang, M. M., & Zhao, H. Z. (2022). Coefficient of variation of heart rate and blood pressure in rapid identification of children with suspected orthostatis intolerance. *Zhonghua er ke za zhi = Chinese Journal of Pediatrics*, 60(1), 25-29.
- Kovvali, N. (2011). Theory and applications of gaussian quadrature methods. *Synthesis Lectures on Algorithms and Software in Engineering*, 3(2), 1-65.
- Latouche, G., & Ramaswami, V. (1999). *Introduction to matrix analytic methods in stochastic modeling*. Society for Industrial and Applied Mathematics.
- Lee, J. W., & Lim, T. J. (2005). A VSSI-CRL synthetic control chart. *Journal of the Korean Operations Research and Management Science Society*, 30(4), 1-14.
- Lee, M. H., Khoo, M. B., Haq, A., Wong, D. M., & Chew, X. (2023). Synthetic c charts with known and estimated process parameters based on median run length and expected median run length. *Quality Technology & Quantitative Management*, 20(2), 168-183.
- Li, C., Wang, D., & Sun, J. (2019). Control charts based on dependent count data with deflation or inflation of zeros. *Journal of Statistical Computation and Simulation*, 89(17), 3273-3289.

- Li, Q., Yang, J., Huang, S., & Zhao, Y. (2022). Generally weighted moving average control chart for monitoring two-parameter exponential distribution with measurement errors. *Computers & Industrial Engineering*, 165, 107902.
- Lopes, B. G., Faria, G. A., Maltoni, K. L., Rocha, P. S., Peixoto, A. P. B., Oliveira, T. A. D., Fonseca, A. D. D., & Felizardo, L. M. (2021). Classification of the coefficient of variation for experiments with eucalyptus seedlings in greenhouse. *Revista Ciencia Agronomica*, 52.
- Lynn, F., Reed, G. F., & Meade, B. D. (1996). Collaborative study for the evaluation of enzyme-linked immunosorbent assays used to measure human antibodies to Bordetella pertussis antigens. *Clinical Diagnostic Laboratory Immunology*, 3(6), 689-700.
- Ma, S., Xing, W., Liu, X., & Wang, L. (2021). Advance booking discount for risk-averse firm in the presence of spot market. *Emerging Markets Finance and Trade*, 57(8), 2246-2258.
- Machado, M. A., & Costa, A. F. (2014a). Some comments regarding the synthetic chart. *Communications in Statistics-Theory and Methods*, 43(14), 2897-2906.
- Machado, M. A., & Costa, A. F. (2014b). A side-sensitive synthetic chart combined with an X chart. *International Journal of Production Research*, 52(11), 3404-3416.
- Malela-Majika, J. C., Chatterjee, K., & Koukouvinos, C. (2022a). A multivariate triple exponentially weighted moving average control chart. *Quality and Reliability Engineering International*, 38(4), 1558-1589.
- Malela-Majika, J. C., Shongwe, S. C., Chatterjee, K., & Koukouvinos, C. (2022b). Monitoring univariate and multivariate profiles using the triple exponentially weighted moving average scheme with fixed and random explanatory variables. *Computers & Industrial Engineering*, 163, 107846.
- Mim, F. N., Saha, S., Khoo, M. B. C., & Khatun, M. (2019). A side-sensitive modified group runs control chart with auxiliary information to detect process mean shifts. *Pertanika Journal of Science & Technology*, 27(2), 847-866.
- Montgomery, D. C., Runger, G. C., & Hubele, N. F. (2009). *Engineering statistics*. John Wiley & Sons.
- Muhammad, A. N. B., Yeong, W. C., Chong, Z. L., Lim, S. L., & Khoo, M. B. C. (2018). Monitoring the coefficient of variation using a variable sample size EWMA chart. *Computers & Industrial Engineering*, 126, 378-398.

- Neuts, M. F. (1984). Matrix-geometric solutions to stochastic models. In: Steckhan, H., Buhler, W., Jager, K. E., Schneeweib, C., Schwarze, J. (eds) DGOR. *Operations Research Proceedings, 1983*. Springer, Berlin, Heidelberg.
- Noor-ul-Amin, M., Arif, F., & Hanif, M. (2019). Joint monitoring of mean and variance using likelihood ratio test statistic under pair ranked set sampling scheme. *Iranian Journal of Science and Technology, Transactions A: Science*, 43, 2449-2460.
- P Obite, C., C Bartholomew, D., U Ugwuanyim, G., & P Olewuezi, N. (2020). Assessment of the disparities in the applications to higher education in Nigeria: a coefficient of variation approach. *Asian Journal of Advanced Research and Reports*, 8(3), 23-29.
- Pearson, K. (1896). VII. Mathematical contributions to the theory of evolution. – III. Regression, heredity, and panmixia. *Philosophical Transactions of the Royal Society of London. Series A*, 187, 253-318.
- Qiao, Y., Sun, J., Castagliola, P., & Hu, X. (2022). Optimal design of one-sided exponential EWMA charts based on median run length and expected median run length. *Communications in Statistics-Theory and Methods*, 51(9), 2887-2907.
- Rakitzis, A. C., Chakraborti, S., Shongwe, S. C., Graham, M. A., & Khoo, M. B. C. (2019). An overview of synthetic-type control charts: Techniques and methodology. *Quality and Reliability Engineering International*, 35(7), 2081-2096.
- Rangasamy, V., Xu, X., Susheela, A. T., & Subramaniam, B. (2020). Comparison of glycemic variability indices: blood glucose, risk index, and coefficient of variation in predicting adverse outcomes for patients undergoing cardiac surgery. *Journal of Cardiothoracic and Vascular Anesthesia*, 34(7), 1794-1802.
- Reh, W., & Scheffler, B. (1996). Significance tests and confidence intervals for coefficients of variation. *Computational Statistics & Data Analysis*, 22(4), 449-452.
- Reynolds Jr, M. R., & Stoumbos, Z. G. (2004). Should observations be grouped for effective process monitoring?. *Journal of Quality Technology*, 36(4), 343-366.
- Saha, S., Khoo, M. B., Castagliola, P., & Haq, A. (2021). Side-sensitive modified group runs charts with and without measurement errors for monitoring the coefficient of variation. *Quality and Reliability Engineering International*, 37(2), 598-617.

- Saha, S., Khoo, M. B., Mim, F. N., Ng, T. F., & Khaw, K. W. (2023). Side sensitive group runs t chart and its application in manufacturing. *Communications in Statistics-Simulation and Computation*, 52(9), 4036-4051.
- Scariano, S. M., & Calzada, M. E. (2003). A note on the lower-sided synthetic chart for exponentials. *Quality Engineering*, 15(4), 677-680.
- Scariano, S. M., & Calzada, M. E. (2009). The generalized synthetic chart. *Sequential Analysis*, 28(1), 54-68.
- Shechtman, O. (2013). The coefficient of variation as an index of measurement reliability. In *Methods of Clinical Epidemiology* (pp. 39-49). Berlin, Heidelberg: Springer Berlin Heidelberg.
- Singh, G., & Singh, K. (2019). Video frame and region duplication forgery detection based on correlation coefficient and coefficient of variation. *Multimedia Tools and Applications*, 78, 11527-11562.
- Shongwe, S. C., & Graham, M. A. (2018). A modified side-sensitive synthetic chart to monitor the process mean. *Quality Technology & Quantitative Management*, 15(3), 328-353.
- Song, S. I., & Park, H. K. (2005). Development of VSI synthetic control chart. *Journal of the Korean Society for Quality Management*, 33(1), 1-10.
- Sparks, R. S. (2003). A group of moving averages control plan for signaling varying location shifts. *Quality Engineering*, 15(4), 519-532.
- Siddall, J. N. (1983). *Probabilistic engineering design*. CRC press.
- Sun, Y., Liang, X., & Xiao, C. (2019). Assessing the influence of land use on groundwater pollution based on coefficient of variation weight method: A case study of shuangliao city. *Environmental Science and Pollution Research*, 26, 34964-34976.
- Taboran, R., & Sukparungsee, S. (2023). On designing of a new EWMA-DMA control chart for detecting mean shifts and its application. *Thailand Statistician*, 21(1), 148-164.
- Taboran, R., Sukparungsee, S., & Areepong, Y. (2020). A new nonparametric Tukey MA-EWMA control charts for detecting mean shifts. *IEEE Access*, 8, 207249-207259.

- Talordphop, K., Sukparungsee, S., & Areepong, Y. (2022). Performance of new nonparametric Tukey modified exponentially weighted moving average-moving average control chart. *Plos one*, *17*(9), e0275260.
- Tang, A., Castagliola, P., Hu, X., & Sun, J. (2019). The performance of the adaptive EWMA median chart in the presence of measurement error. *Quality and Reliability Engineering International*, *35*(1), 423-438.
- Teoh, W. L., Khoo, M. B., Castagliola, P., Yeong, W. C., & Teh, S. Y. (2017). Run-sum control charts for monitoring the coefficient of variation. *European Journal of Operational Research*, *257*(1), 144-158.
- Tran, P. H., Heuchenne, C. (2021). Monitoring the coefficient of variation using variable sampling interval CUSUM control charts. *Journal of Statistical Computation and Simulation*, *91*(3), 501-521.
- Tran, K. P., Heuchenne, C., & Balakrishnan, N. (2019). On the performance of coefficient of variation charts in the presence of measurement errors. *Quality and Reliability Engineering International*, *35*(1), 329-350.
- Tran, K. P., Nguyen, H. D., Nguyen, Q. T., & Chattinnawat, W. (2018). One-sided synthetic control charts for monitoring the coefficient of variation with measurement errors. In *2018 IEEE International Conference on Industrial Engineering and Engineering Management (IEEM)* (pp. 1667-1671). IEEE.
- Tran, P. H., & Tran, K. P. (2016). The efficiency of CUSUM schemes for monitoring the coefficient of variation. *Applied Stochastic Models in Business and Industry*, *32*(6), 870-881.
- Tuh, M. H., Kon, C. M. L., Chua, H. S., & Lau, M. F. (2022). Optimal statistical design of the double sampling np chart based on expected median run length. *Frontiers in Applied Mathematics and Statistics*, *8*, 993152.
- Tuovinen, T., Rytty, R., Moilanen, V., Abou Elseoud, A., Veijola, J., Remes, A. M., & Kiviniemi, V. J. (2017). The effect of gray matter ICA and coefficient of variation mapping of BOLD data on the detection of functional connectivity changes in Alzheimer's disease and bvFTD. *Frontiers in Human Neuroscience*, *10*, 680.
- Wu, Z., Ou, Y., Castagliola, P., & Khoo, M. B. (2010). A combined synthetic & X chart for monitoring the process mean. *International Journal of Production Research*, *48*(24), 7423-7436.
- Wu, Z., & Spedding, T. A. (2000). A synthetic control chart for detecting small shifts in the process mean. *Journal of Quality Technology*, *32*(1), 32-38.

- Wu, Z., Yeo, S. H., & Spedding, T. A. (2001). A synthetic control chart for detecting fraction nonconforming increases. *Journal of Quality Technology*, 33(1), 104-111.
- Xu, H., Zhang, Y., Liu, J., & Lv, D. (2021). Feature selection using maximum feature tree embedded with mutual information and coefficient of variation for bird sound classification. *Mathematical Problems in Engineering*, 2021, 1-14.
- Yahaya, M., Lim, S. L., Ibrahim, A. I. N., Yeong, W. C., & Khoo, M. B. C. (2022). A variable sample size synthetic chart for the coefficient of variation. *South African Journal of Industrial Engineering*, 33(1), 1-15.
- Yeong, W. C., Khoo, M. B. C., Lim, S. L., & Teoh, W. L. (2017a). The coefficient of variation chart with measurement error. *Quality Technology & Quantitative Management*, 14(4), 353-377.
- Yeong, W. C., Khoo, M. B., Tham, L. K., Teoh, W. L., & Rahim, M. A. (2017b). Monitoring the coefficient of variation using a variable sampling interval EWMA chart. *Journal of Quality Technology*, 49(4), 380-401.
- Yeong, W. C., Lim, S. L., Khoo, M. B. C., & Castagliola, P. (2018a). Monitoring the coefficient of variation using a variable parameters chart. *Quality Engineering*, 30(2), 212-235.
- Yeong, W. C., Lim, S. L., Khoo, M. B. C., Chuah, M. H., & Lim, A. X. J. (2018b). The economic and economic-statistical designs of the synthetic chart for the coefficient of variation. *Journal of Testing and Evaluation*, 46(3), 1175-1195.
- Yeong, W. C., Lim, S. L., Khoo, M. B. C., Khaw, K. W., & Ng, P. S. (2021). An optimal design of the synthetic coefficient of variation chart based on the median run length. *International Journal of Reliability, Quality and Safety Engineering*, 28(3), 2150018.
- Yeong, W. C., Lim, S. L., Khoo, M. B., Ng, P. S., & Chong, Z. L. (2022a). A variable sampling interval run sum chart for the coefficient of variation. *Journal of Statistical Computation and Simulation*, 92(15), 3150-3166.
- Yeong, W. C., Tan, Y. Y., Lim, S. L., Khaw, K. W., & Khoo, M. B. C. (2022b). A variable sample size run sum coefficient of variation chart. *Quality and Reliability Engineering International*, 38(4), 1869-1885.

- Yeong, W. C., Tan, Y. Y., Lim, S. L., Khaw, K. W., & Khoo, M. B. C. (2023). Variable sample size and sampling interval (VSSI) and variable parameters (VP) run sum charts for the coefficient of variation. *Quality Technology & Quantitative Management*, 1-23.
- You, H. W., Khoo, M. B., Castagliola, P., & Haq, A. (2016). Monitoring the coefficient of variation using the side sensitive group runs chart. *Quality and Reliability Engineering International*, 32(5), 1913-1927.
- You, H. W., Chong, M. K. B., Lin, C. Z., & Lin, T. W. (2020). The expected average run length of the EWMA median chart with estimated process parameters. *Austrian Journal of Statistics*, 49(3), 19-24.
- Zhang, J., Li, Z., Chen, B., & Wang, Z. (2014). A new exponentially weighted moving average control chart for monitoring the coefficient of variation. *Computers & Industrial Engineering*, 78, 205-212.
- Zhang, J., Li, Z., & Wang, Z. (2018). Control chart for monitoring the coefficient of variation with an exponentially weighted moving average procedure. *Quality and Reliability Engineering International*, 34(2), 188-202.
- Zhang, Y., Castagliola, P., Wu, Z., & Khoo, M. B. (2011). The synthetic [Xbar] chart with estimated parameters. *IIE Transactions*, 43(9), 676-687.
- Zhao, H., Wang, X., & Li, X. (2017). Quantifying grain-size variability of metal pollutants in road-deposited sediments using the coefficient of variation. *International Journal of Environmental Research and Public Health*, 14(8), 850.

LIST OF PUBLICATIONS

Yeong, W. C., Lee, P. Y., Lim, S. L., Khaw, K. W., & Khoo, M. B. C. (2021). A side-sensitive synthetic coefficient of variation chart. *Quality and Reliability Engineering International*, 37(5), 2014-2033.

Yeong, W. C., Lee, P. Y., Lim, S. L., Ng, P. S., & Khaw, K. W. (2021). Optimal designs of the side sensitive synthetic chart for the coefficient of variation based on the median run length and expected median run length. *Plos one*, 16(7), e0255366.

APPENDIX

APPENDIX A: COMPUTER PROGRAMMING FOR ARL AND EARL-BASED DESIGNS OF SIDE-SENSITIVE SYNTHETIC- γ CHART

```
//-----  
function Y=cdfcv(X,n,cv)//to obtain the cdf of CV  
//-----  
[argout,argin]=argn()  
if nargin~=3  
    error("incorrect number of arguments")  
end  
if (n<=0)|(n~=floor(n))  
    error("argument "n" must be an integer >= 1")  
end  
if cv<=0  
    error("argument "cv" must be > 0")  
end  
Y=zeros(X)  
i=(X>0)  
if or(i)  
    Y(i)=1-cdfstudent(sqrt(n)./X(i),n-1,sqrt(n)/cv)  
end  
endfunction  
  
//-----  
function [mu,sigma]=musigmaCV(n,cv)//to compute the mean and standard deviation of  
the in-control CV  
//-----  
[argout,argin]=argn()  
if nargin~=2  
    error("incorrect number of arguments")  
end  
if cv<=0  
    error("argument "cv" must be > 0")  
end  
cv2=cv^2  
mu=cv*(1+((cv2-0.25)+((3*cv2^2-cv2/4-7/32)+(15*cv2^3-3*cv2^2/4-7*cv2/32-  
19/128)/n)/n)/n)  
  
sigma=cv*sqrt(((cv2+0.5)+((8*cv2^2+cv2+3/8)+(69*cv2^3+7*cv2^2/2+3*cv2/4+3/16)  
/n)/n)/n)  
endfunction  
  
//-----  
function [A,B1,B2]=prob(LCL,UCL,n,cv)//to calculate the probability for a sample to  
fall between UCL and LCL, above UCL, and below LCL, respectively
```

```

//-----
A=cdfcv(UCL,n,cv)-cdfcv(LCL,n,cv)//Prob conforming
B1=1-cdfcv(UCL,n,cv)//B1=B+
B2=cdfcv(LCL,n,cv)//B2=B-
endfunction

//-----
function [Q,q]=qsyncvI(n,L,LCL,UCL,cv0,delta)//to calculate the transition probability
matrix and initial probability vector
//-----

cv1=delta*cv0
[A,B1,B2]=prob(LCL,UCL,n,cv1)

Q=zeros(2*L+1,2*L+1)

Q(1,L+1)=A
Q(L+1,L+1)=A
Q(2*L+1,L+1)=A

for i=2:L
    Q(i,i-1)=A
end
for j=L+1:2*L+1
    Q(j,L)=B2
end

for k=1:L+1
    Q(k,L+2)=B1
end

for m=L+2:2*L
    Q(m,m+1)=A
end

q=zeros(2*L+1,1)
q(L+2)=1
endfunction

//-----
function [mu,sd,sk,ku]=momdphase(Q,q)
//-----
[argout,argin]=argn()
if argin~=2
    error("incorrect number of arguments")
end
q=q(:)'
W=inv(eye(Q)-Q)
z=q*W
nu1=sum(z)

```

```

mu=nu1
if argout>=2
    WQ=W*Q
    z=z*WQ
    nu2=2*sum(z)
    sd=sqrt(nu2-nu1^2+nu1)
end
if argout>=3
    z=z*WQ
    nu3=6*sum(z)
    mu3=nu3+3*(1-nu1)*nu2+2*nu1^3-3*nu1^2+nu1
    sk=mu3/sd^3
end
if argout>=4
    z=z*WQ
    nu4=24*sum(z)
    mu4=nu4+6*nu3+nu1*(1-4*nu3)+(6*nu1^2-12*nu1+7)*nu2-3*nu1^4+6*nu1^3-
4*nu1^2
    ku=mu4/sd^4-3
end
endfunction

```

```

//-----
function [ARL,SDRL]=rlsyncvI(n,L,K,cv0,delta)//to calculate the ARL and SDRL with
K
//-----
[mu,sigma]=musigmaCV(n,cv0)
LCL=mu-K*sigma
UCL=mu+K*sigma
[Q,q]=qsyncvI(n,L,LCL,UCL,cv0,delta)
[ARL,SDRL]=momdphase(Q,q)
endfunction

```

```

//-----
function [ARL,SDRL]=rlsyncvI2(n,L,LCL,UCL,cv0,delta)//to calculate the ARL and
SDRL with LCL and UCL
//-----
[mu,sigma]=musigmaCV(n,cv0)
[Q,q]=qsyncvI(n,L,LCL,UCL,cv0,delta)
[ARL,SDRL]=momdphase(Q,q)
endfunction

```

```

//-----
function dif=optKI(K,L,n,cv0)//to find the optimal K that satisfies the ARL0 constraint
//-----
if K<=0
    dif=%inf
else
    [ARL0,SDRL0]=rlsyncvI(n,L,K,cv0,1)

```

```

    dif=(370.4-ARL0)/370.4
end
endfunction

//-----
function xsol=simplexolve(x0,fun,extra,tol)
//-----
[argout,argin]=argn()
if (argin<2)|(argin>4)
    error("incorrect number of arguments")
end
[j,p]=size(x0)
if j~=1
    error("argument "x0" must be a row vector")
end
if ~exists("extra","local")
    extra=list()
end
if ~exists("tol","local")
    tol=1e-12
end
if typeof(fun)~="function"
    error("argument "fun" must be a function")
end
if typeof(extra)~="list"
    error("argument "extra" must be a list")
end
if tol<=0
    error("argument "tol" must be > 0")
end
r=1
while %t
    X=simplex(x0,r)
    for i=1:p+1
        f(i)=norm(fun(X(i,:),extra(:)))
    end
    if and(isinf(f))
        r=r/2
    else
        break
    end
end
onesp1=ones(p+1,1)
while %t
    [f,j]=sort(f)
    X=X(j,:)
    fsol=f(p+1)
    xsol=X(p+1,:)
    fw=f(1)
    xw=X(1,:)
    xm=mean(X(2:p+1,:),"r")

```

```

if sqrt(sum((xw-xm).^2))<=tol
    break
end
d=xm-xw
xr=xw+2*d
fr=norm(fun(xr,extra(:)))
if fr<fsol
    xe=xr+d
    fe=norm(fun(xe,extra(:)))
    if fe<fr
        f(1)=fe
        X(1,:)=xe
    else
        f(1)=fr
        X(1,:)=xr
    end
end
else
    xc=xw+0.5*d
    fc=norm(fun(xc,extra(:)))
    if fc<fsol
        f(1)=fc
        X(1,:)=xc
    else
        X=0.5*(X+onesp1*xsol)
        for i=1:p
            f(i)=norm(fun(X(i,:),extra(:)))
        end
    end
end
end
endfunction

```

```

//-----
function [L,K,ARL1,SDRL1,ARL0]=optsyncvI(n,cv0,delta)//to find the optimal chart
parameters, ARL1 and SDRL1
//-----

```

```

ARL1=%inf
for iL=1:100//change
    iK0=3
    iK=simplexolve(iK0,optKI,list(iL,n,cv0))
    [iARL1,iSDRL1]=rlsyncvI(n,iL,iK,cv0,delta)
    [iARL0,iSDRL0]=rlsyncvI(n,iL,iK,cv0,1)
    mprintf("L=%6.4f      K=%6.4f      ARL1=%6.4f      SDRL1=%6.4f\n",iL,iK,iARL1,iSDRL1,iARL0)
    if (iARL1<ARL1)
        ARL1=iARL1
        SDRL1=iSDRL1
        ARL0=iARL0
        L=iL
        K=iK
    end
end

```

```

    else ARL1=ARL1
    end
end
endfunction

//-----
function [x,w]=quadlegendre(n,a,b)//to obtain Gauss-Legendre Quadrature
//-----
[argout,argin]=argn()
if (argin<1)|(argin>3)
    error("incorrect number of arguments")
end
if argout~=2
    error("incorrect number of output arguments")
end
if ~exists("a","local")
    a=-1
end
if ~exists("b","local")
    b=+1
end
if a>=b
    error("argument "a" must be < argument "b"")
end
x=[2.01194093997434522301e-1;
    3.94151347077563369897e-1;
    5.70972172608538847537e-1;
    7.24417731360170047416e-1;
    8.48206583410427216201e-1;
    9.37273392400705904308e-1;
    9.87992518020485428490e-1]
w=[2.02578241925561272881e-1;
    1.98431485327111576456e-1;
    1.86161000015562211027e-1;
    1.66269205816993933553e-1;
    1.39570677926154314447e-1;
    1.07159220467171935012e-1;
    7.03660474881081247100e-2;
    3.07532419961172683551e-2]
x=(-x((n-1)/2:-1:1);0;x)*(b-a)+a+b)/2
w=[w((n+1)/2:-1:2);w]*(b-a)/2
endfunction

//-----
function EARL=earlsyncvI(n,L,K,cv0)//to compute the EARL with K
//-----
[xi,wi]=quadlegendre(15,1.03,2)
EARL=0
for il=1:15
    xil=xi(il)
    wil=wi(il)
end

```

```

[ARL,SDRL]=rlsyncvI(n,L,K,cv0,xil)
EARL=EARL+ARL.*wil
end

```

```

EARL=EARL/(2-1.03)
endfunction

```

```

//-----
function EARL=earlsyncvI2(n,L,LCL,UCL,cv0)//to compute the EARL with LCL and
UCL

```

```

//-----
[xi,wi]=quadlegendre(15,1.03,2)
EARL=0
for il=1:15
    xil=xi(il)
    wil=wi(il)
    [ARL,SDRL]=rlsyncvI2(n,L,LCL,UCL,cv0,xil)
    EARL=EARL+ARL.*wil
end

```

```

EARL=EARL/(2-1.03)
endfunction

```

```

//-----
function [L,K,EARL]=optsyncvE(n,cv0)//to find the optimal chart parameters and EARL
//-----

```

```

EARL=%inf
for iL=1:100
    iK0=3
    iK=simplexolve(iK0,optKI,list(iL,n,cv0))
    iEARL=earlsyncvI(n,iL,iK,cv0)
    mprintf("L=%6.4f K=%6.4f EARL=%6.4f\n",iL,iK,iEARL)
    if (iEARL<EARL)
        EARL=iEARL
        L=iL
        K=iK
    else EARL=EARL
    end
end
endfunction

```

APPENDIX B: COMPUTER PROGRAMMING FOR *MRL* AND *EMRL*-BASED

DESIGNS OF SIDE-SENSITIVE SYNTHETIC- γ CHART

```
//-----  
function Y=cdfcv(X,n,cv)//to obtain the cdf of CV  
//-----  
[argout,argin]=argn()  
if argin~=3  
    error("incorrect number of arguments")  
end  
if (n<=0)|(n~=floor(n))  
    error("argument "n" must be an integer >= 1")  
end  
if cv<=0  
    error("argument "cv" must be > 0")  
end  
Y=zeros(X)  
i=(X>0)  
if or(i)  
    Y(i)=1-cdfstudent(sqrt(n)./X(i),n-1,sqrt(n)/cv)  
end  
endfunction  
  
//-----  
function [mu,sigma]=musigmaCV(n,cv)//to compute the mean and standard deviation of  
the in-control sample CV  
//-----  
[argout,argin]=argn()  
if argin~=2  
    error("incorrect number of arguments")  
end  
if cv<=0  
    error("argument "cv" must be > 0")  
end  
cv2=cv^2  
mu=cv*(1+((cv2-0.25)+((3*cv2^2-cv2/4-7/32)+(15*cv2^3-3*cv2^2/4-7*cv2/32-  
19/128)/n)/n)/n)  
  
sigma=cv*sqrt(((cv2+0.5)+((8*cv2^2+cv2+3/8)+(69*cv2^3+7*cv2^2/2+3*cv2/4+3/16)  
/n)/n)/n)  
endfunction  
  
//-----  
function [A,B1,B2]=prob(LCL,UCL,n,cv)//to compute the probability a sample will fall  
within the UCL and LCL, above the UCL, and below the LCL, respectively  
//-----  
A=cdfcv(UCL,n,cv)-cdfcv(LCL,n,cv)//Prob conforming  
B1=1-cdfcv(UCL,n,cv)//B1=B+
```

```
B2=cdfcv(LCL,n,cv)//B2=B-
endfunction
```

```
//-----
function [Q,q]=qsyncvI(n,L,LCL,UCL,cv0,delta)//to compute the transition probability
matrix and initial probability vector
//-----
```

```
cv1=delta*cv0
[A,B1,B2]=prob(LCL,UCL,n,cv1)
```

```
Q=zeros(2*L+1,2*L+1)
```

```
Q(1,L+1)=A
Q(L+1,L+1)=A
Q(2*L+1,L+1)=A
```

```
for i=2:L
    Q(i,i-1)=A
end
for j=L+1:2*L+1
    Q(j,L)=B2
end
```

```
for k=1:L+1
    Q(k,L+2)=B1
end
```

```
for m=L+2:2*L
    Q(m,m+1)=A
end
```

```
q=zeros(2*L+1,1)
q(L+2)=1
endfunction
```

```
//-----
function F=cdfsyncv(Q,q,pct)//to compute the probability that the run length will be
larger than the percentile
//-----
```

```
[argout,argin]=argn()
if argin~=3
    error("incorrect number of arguments")
end
q=q(:)'
Ft1=q*Q^pct
Ft2=sum(Ft1)
F=Ft2
endfunction
```

```

//-----
function X=pcrlsyncv(pcrl,mrlini,n,L,LCL,UCL,cv0,delta)//to obtain the percentile
//-----
[argout,argin]=argn()
if (argin<7)|(argin>8)
    error("incorrect number of arguments")
end
if (n<=1)|(n~=floor(n))
    error("argument "n" must be an integer >= 2")
end
if (L<=0)|(L~=floor(L))
    error("argument "L" must be an integer >= 1")
end
if argin==7
    delta=1
end
if delta<=0
    error("argument "delta" must be >0")
end

[Q,q]=qsyncvI(n,L,LCL,UCL,cv0,delta)

for X=mrlini:500000
    F=1-cdfsyncv(Q,q,X)
    if F>=pcrl
        break
    end
end
endfunction

//-----
function z=optKsyncv(K,n,L,mrl0,cv0)//to obtain the value of K that satisfies the mrl0
constraint
//-----

if (K<=0)
    z=%inf
else
    [mu,sigma]=musigmaCV(n,cv0)
    LCL=mu-K*sigma
    UCL=mu+K*sigma
    [Q,q]=qsyncvI(n,L,LCL,UCL,cv0,1)
    probMRL=1-cdfsyncv(Q,q,mrl0)
    z=(probMRL-0.5001)*10
end
endfunction

```

```

//-----
function xsol=simplexolve(x0,fun,extra,tol)
//-----
[argout,argin]=argn()
if (argin<2)|(argin>4)
    error("incorrect number of arguments")
end
[j,p]=size(x0)
if j~=1
    error("argument "x0" must be a row vector")
end
if ~exists("extra","local")
    extra=list()
end
if ~exists("tol","local")
    tol=1e-12
end
if typeof(fun)~="function"
    error("argument "fun" must be a function")
end
if typeof(extra)~="list"
    error("argument "extra" must be a list")
end
if tol<=0
    error("argument "tol" must be > 0")
end
r=1
while %t
    X=simplex(x0,r)
    for i=1:p+1
        f(i)=norm(fun(X(i,:),extra(:)))
    end
    if and(isinf(f))
        r=r/2
    else
        break
    end
end
onesp1=ones(p+1,1)
while %t
    [f,j]=sort(f)
    X=X(j,:)
    fsol=f(p+1)
    xsol=X(p+1,:)
    fw=f(1)
    xw=X(1,:)
    xm=mean(X(2:p+1,:),"r")
    if sqrt(sum((xw-xm).^2))<=tol
        break
    end
    d=xm-xw
    xr=xw+2*d
end

```

```

fr=norm(fun(xr,extra(:)))
if fr<fsol
    xe=xr+d
    fe=norm(fun(xe,extra(:)))
    if fe<fr
        f(1)=fe
        X(1,:)=xe
    else
        f(1)=fr
        X(1,:)=xr
    end
end
else
    xc=xw+0.5*d
    fc=norm(fun(xc,extra(:)))
    if fc<fsol
        f(1)=fc
        X(1,:)=xc
    else
        X=0.5*(X+onesp1*xsol)
        for i=1:p
            f(i)=norm(fun(X(i,:),extra(:)))
        end
    end
end
end
endfunction

```

```

//-----
function [L,LCL,UCL,Q05,MRL1,Q95]=optsyncv(n,mrl0,cv0,delta)//to obtain the
optimal chart parameters, and the 5th, 50th and 95th percentiles of the run length
//-----
[argout,argin]=argn()
if argin~=4
    error("incorrect number of arguments")
end
if (n<=1)|(n~=floor(n))
    error("argument "n" must be an integer >= 2")
end
mprintf("delta=%3.2f\n\n",delta)
sol=[]
ii=1
MRL1=%inf
diffPCRmin=%inf

for iL=1:100
    K0=3
    iK=simplexolve(K0,optKsyncv,list(n,iL,mrl0,cv0),tol=1e-6)
    [mu,sigma]=musigmaCV(n,cv0)
    iLCL=mu-iK*sigma
    iUCL=mu+iK*sigma
    iPCR5=pcr5syncv(0.05,1,n,iL,iLCL,iUCL,cv0,delta)
end

```

```

iMRL1=pcrlsyncv(0.5,iPCR5,n,iL,iLCL,iUCL,cv0,delta)
iPCR95=pcrlsyncv(0.95,iMRL1,n,iL,iLCL,iUCL,cv0,delta)
MRL00=pcrlsyncv(0.5,mrl0-5,n,iL,iLCL,iUCL,cv0,1)
diffPCR=iPCR95-iPCR5
mprintf("%2d          %8.6f          %8.6f          %5d          %5d          %5d\n",iL,iLCL,iUCL,iPCR5,iMRL1,iPCR95,MRL00)

if (iMRL1<MRL1)
L=iL
LCL=iLCL
UCL=iUCL
Q05=iPCR5
MRL1=iMRL1
Q95=iPCR95
diffPCRmin=diffPCR
elseif (iMRL1==MRL1)&(diffPCR<=diffPCRmin)
L=iL
LCL=iLCL
UCL=iUCL
Q05=iPCR5
MRL1=iMRL1
Q95=iPCR95
diffPCRmin=diffPCR
elseif (iMRL1>MRL1)
MRL1=MRL1
diffPCRmin=diffPCRmin
end

if (iMRL1>MRL1)
break
end

end
endfunction

//-----
function [x,w]=quadlegendre(n,a,b)//to obtain the Gauss-Legendre Quadrature
//-----
[argout,argin]=argn()
if (argin<1)|(argin>3)
error("incorrect number of arguments")
end
if argout~=2
error("incorrect number of output arguments")
end
if ~exists("a","local")
a=-1
end
if ~exists("b","local")
b=+1
end
end

```

```

if a>=b
    error("argument "a" must be < argument "b'")
end
x=[2.01194093997434522301e-1;
    3.94151347077563369897e-1;
    5.70972172608538847537e-1;
    7.24417731360170047416e-1;
    8.48206583410427216201e-1;
    9.37273392400705904308e-1;
    9.87992518020485428490e-1]
w=[2.02578241925561272881e-1;
    1.98431485327111576456e-1;
    1.86161000015562211027e-1;
    1.66269205816993933553e-1;
    1.39570677926154314447e-1;
    1.07159220467171935012e-1;
    7.03660474881081247100e-2;
    3.07532419961172683551e-2]
x=(-x((n-1)/2:-1:1);0;x)*(b-a)+a+b)/2
w=[w((n+1)/2:-1:2);w]*(b-a)/2
endfunction

```

```

//-----
function Xe=pcrlsyncve(pcrle,emrlini,n,L,LCL,UCL,cv0,deltamin,deltamax)//to obtain
the percentile
//-----
[xi,wi]=quadlegendre(15,deltamin,deltamax)
Xe=0
for il=1:15
    xil=xi(il)
    wil=wi(il)
    XXe=pcrlsyncv(pcrle,emrlini,n,L,LCL,UCL,cv0,xil)
    Xe=Xe+XXe.*wil
end
Xe=Xe/(deltamax-deltamin)
endfunction

```

```

//-----
function
[L,LCL,UCL,EQ05,EMRL1,EQ95]=optsyncve(n,mrl0,cv0,deltamin,deltamax)//to
obtain the optimal chart parameters, and the 5th, 50th and 95th percentiles of the run length
//-----
[argout,argin]=argn()
if argin~=5
    error("incorrect number of arguments")
end
if (n<=1)|(n~=floor(n))
    error("argument "n" must be an integer >= 2")
end
sol=[]

```

```

ii=1
EMRL1=%inf
diffEPCRmin=%inf

for iL=1:100
    K0=3
    iK=simplexolve(K0,optKsyncv,list(n,iL,mrl0,cv0),tol=1e-6)
    [mu,sigma]=musigmaCV(n,cv0)
    iLCL=mu-iK*sigma
    iUCL=mu+iK*sigma
    iEPCR5=pcrlsyncve(0.05,1,n,iL,iLCL,iUCL,cv0,deltamin,deltamax)
    iEMRL1=pcrlsyncve(0.5,1,n,iL,iLCL,iUCL,cv0,deltamin,deltamax)
    iEPCR95=pcrlsyncve(0.95,1,n,iL,iLCL,iUCL,cv0,deltamin,deltamax)
    MRL00=pcrlsyncv(0.5,mrl0-5,n,iL,iLCL,iUCL,cv0,1)
    diffEPCR=iEPCR95-iEPCR5
    mprintf("%2d      %8.6f      %8.6f      %8.6f      %8.6f      %8.6f
%5d\n",[iL,iLCL,iUCL,iEPCR5,iEMRL1,iEPCR95,MRL00])

    if (iEMRL1<EMRL1)
        L=iL
        LCL=iLCL
        UCL=iUCL
        EQ05=iEPCR5
        EMRL1=iEMRL1
        EQ95=iEPCR95
        diffEPCRmin=diffEPCR
    elseif (iEMRL1==EMRL1)&(diffEPCR<=diffEPCRmin)
        L=iL
        LCL=iLCL
        UCL=iUCL
        EQ05=iEPCR5
        EMRL1=iEMRL1
        EQ95=iEPCR95
        diffEPCRmin=diffEPCR
    elseif (iEMRL1>EMRL1)
        EMRL1=EMRL1
        diffEPCRmin=diffEPCRmin
    end

    if (iEMRL1>EMRL1)
        break
    end

end
endfunction

```

APPENDIX C: COMPUTER PROGRAMMING FOR *ARL* AND *EARL*-BASED

DESIGNS OF NON-SIDE-SENSITIVE SYNTHETIC- γ CHART

```
//-----  
function X=idfcv(Y,n,cv)//to obtain the idf of CV  
//-----  
[argout,argin]=argn()  
if argin~=3  
    error("incorrect number of arguments")  
end  
if or((Y<=0)|(Y>=1))  
    error("all elements of argument "Y" must be in (0,1)")  
end  
if (n<=0)|(n~=floor(n))  
    error("argument "n" must be an integer >= 1")  
end  
if cv<=0  
    error("argument "cv" must be > 0")  
end  
X=sqrt(n)./idfstudent(1-Y,n-1,sqrt(n)/cv)  
endfunction  
  
//-----  
function Y=cdfcv(X,n,cv)//to obtain the cdf of CV  
//-----  
[argout,argin]=argn()  
if argin~=3  
    error("incorrect number of arguments")  
end  
if (n<=0)|(n~=floor(n))  
    error("argument "n" must be an integer >= 1")  
end  
if cv<=0  
    error("argument "cv" must be > 0")  
end  
Y=zeros(X)  
i=(X>0)  
if or(i)  
    Y(i)=1-cdfstudent(sqrt(n)./X(i),n-1,sqrt(n)/cv)  
end  
endfunction  
  
//-----  
function [LCL,UCL,ARL,SDRL]=rlsyncv(n,cv0,delta,p,L)//to calculate the LCL, UCL,  
ARL and SDRL with p  
//-----  
cv1=delta*cv0  
LCL=idfcv(p/2,n,cv0)
```

```

UCL=idfcv(1-p/2,n,cv0)
P1=1+cdfcv(LCL,n,cv1)-cdfcv(UCL,n,cv1)
ARL=(1/(1-(1-P1)^L))*(1/P1)
total=0
for t=1:L
total=total+t*(1-P1)^(t-1)
end
SDRL2=((2-P1)/((1-(1-P1)^L)*P1^2))+1/(1-(1-P1)^L)^2*(1/(P1^2)-2*total)
SDRL=sqrt(SDRL2)

```

```

//-----
function dif=optp(p,L)//to find the optimal p
//-----
if p<=0
    dif=%inf
else
dif=370-(1/(1-(1-p)^L))*(1/p)
end

```

```

//-----
function xsol=simplexolve(x0,fun,extra,tol)
//-----
[argout,argin]=argn()
if (argin<2)|(argin>4)
    error("incorrect number of arguments")
end
[j,p]=size(x0)
if j~=1
    error("argument "x0" must be a row vector")
end
if ~exists("extra","local")
    extra=list()
end
if ~exists("tol","local")
    tol=1e-12
end
if typeof(fun)~="function"
    error("argument "fun" must be a function")
end
if typeof(extra)~="list"
    error("argument "extra" must be a list")
end
if tol<=0
    error("argument "tol" must be > 0")
end
r=1
while %t
    X=simplex(x0,r)
    for i=1:p+1
        f(i)=norm(fun(X(i,:),extra(:)))
    end
end

```

```

end
if and(isinf(f))
    r=r/2
else
    break
end
end
onesp1=ones(p+1,1)
while %t
    [f,j]=sort(f)
    X=X(j,:)
    fsol=f(p+1)
    xsol=X(p+1,:)
    fw=f(1)
    xw=X(1,:)
    xm=mean(X(2:p+1,:),"r")
    if sqrt(sum((xw-xm).^2))<=tol
        break
    end
    d=xm-xw
    xr=xw+2*d
    fr=norm(fun(xr,extra(:)))
    if fr<fsol
        xe=xr+d
        fe=norm(fun(xe,extra(:)))
        if fe<fr
            f(1)=fe
            X(1,:)=xe
        else
            f(1)=fr
            X(1,:)=xr
        end
    end
    else
        xc=xw+0.5*d
        fc=norm(fun(xc,extra(:)))
        if fc<fsol
            f(1)=fc
            X(1,:)=xc
        else
            X=0.5*(X+onesp1*xsol)
            for i=1:p
                f(i)=norm(fun(X(i,:),extra(:)))
            end
        end
    end
end
end
endfunction

```

```

//-----
function p=limit(L)
//-----

p0=0.5;
p=simplexolve(p0,optp,list(L),tol=1e-6)

//-----
function [L,LCL,UCL,ARL,SDRL]=optsyncv(n,cv0,delta)//to find the optimal chart
parameters, ARL1 and SDRL1
//-----
ARL=%inf
for iL=1:100//change
    p=limit(iL)
    [iLCL,iUCL,iARL,iSDRL]=rlsyncv(n,cv0,delta,p,iL)
    if (iARL<ARL)
        ARL=iARL
        SDRL=iSDRL
        L=iL
        LCL=iLCL
        UCL=iUCL
    else ARL=ARL
    end
end

//-----
function [x,w]=quadlegendre(n,a,b)//to obtain the Gauss-Legendre Quadrature
//-----
[argout,argin]=argn()
if (argin<1)|(argin>3)
    error("incorrect number of arguments")
end
if argout~=2
    error("incorrect number of output arguments")
end
if ~exists("a","local")
    a=-1
end
if ~exists("b","local")
    b=+1
end
if a>=b
    error("argument "a" must be < argument "b"")
end
x=[2.01194093997434522301e-1;
    3.94151347077563369897e-1;
    5.70972172608538847537e-1;
    7.24417731360170047416e-1;
    8.48206583410427216201e-1;
    9.37273392400705904308e-1;

```

```

9.87992518020485428490e-1]
w=[2.02578241925561272881e-1;
1.98431485327111576456e-1;
1.86161000015562211027e-1;
1.66269205816993933553e-1;
1.39570677926154314447e-1;
1.07159220467171935012e-1;
7.03660474881081247100e-2;
3.07532419961172683551e-2]
x=[-x((n-1)/2:-1:1);0;x]*(b-a)+a+b)/2
w=[w((n+1)/2:-1:2);w]*(b-a)/2
endfunction

```

```

//-----
function EARL=earlsyncv(n,cv0,p,L)//to compute the EARL with p
//-----
[xi,wi]=quadlegendre(15,1.03,2)
EARL=0
for il=1:15
    xil=xi(il)
    wil=wi(il)
    [LCL,UCL,ARL,SDRL]=rlsyncv(n,cv0,xil,p,L)
    EARL=EARL+ARL.*wil
end

EARL=EARL/(2-1.03)
endfunction

```

```

//-----
function [L,LCL,UCL,EARL]=optsyncvE(n,cv0)//to find the optimal chart parameters
and EARL
//-----
EARL=%inf
for iL=1:100
    ip=limit(iL)
    iEARL=earlsyncv(n,cv0,ip,iL)
    if (iEARL<EARL)
        EARL=iEARL
        L=iL
        p=ip
        LCL=idfcv(p/2,n,cv0)
        UCL=idfcv(1-p/2,n,cv0)
    else EARL=EARL
end
end
end

```

APPENDIX D: COMPUTER PROGRAMMING FOR *MRL* AND *EMRL*-BASED

DESIGNS OF NON-SIDE-SENSITIVE SYNTHETIC- γ CHART

```
//-----  
function [mu,sigma]=musigmaCV(n,cv)//to compute the mean and standard deviation of  
the in-control sample CV  
//-----  
[argout,argin]=argn()  
if nargin~=2  
    error("incorrect number of arguments")  
end  
if cv<=0  
    error("argument \"cv\" must be > 0")  
end  
cv2=cv^2  
mu=cv*(1+((cv2-0.25)+((3*cv2^2-cv2/4-7/32)+(15*cv2^3-3*cv2^2/4-7*cv2/32-  
19/128)/n)/n)/n)  
  
sigma=cv*sqrt(((cv2+0.5)+((8*cv2^2+cv2+3/8)+(69*cv2^3+7*cv2^2/2+3*cv2/4+3/16)  
/n)/n)/n)  
endfunction  
  
//-----  
function Y=cdfcv(X,n,cv)//to obtain the cdf of CV  
//-----  
[argout,argin]=argn()  
if nargin~=3  
    error("incorrect number of arguments")  
end  
if (n<=0)|(n~=floor(n))  
    error("argument \"n\" must be an integer >= 1")  
end  
if cv<=0  
    error("argument \"cv\" must be > 0")  
end  
Y=zeros(X)  
i=(X>0)  
if or(i)  
    Y(i)=1-cdfstudent(sqrt(n)./X(i),n-1,sqrt(n)/cv)  
end  
endfunction  
  
//-----  
function [Q,q]=qsyncv(n,L,LCL,UCL,cv0,delta)//to compute the transition probability  
matrix and initial probability vector  
//-----  
cv1=delta*cv0  
A=cdfcv(UCL,n,cv1)-cdfcv(LCL,n,cv1)//Prob conforming
```

```
B=1-A//Prob non-conforming
```

```
Q=zeros(L+1,L+1)
```

```
Q(1,1)=A
```

```
Q(1,2)=B
```

```
for i=2:L
```

```
    Q(i,i+1)=A
```

```
end
```

```
Q(L+1,1)=A
```

```
q=zeros(L+1,1)
```

```
q(2)=1
```

```
endfunction
```

```
//-----
```

```
function [mu,sd,sk,ku]=momdphase(Q,q)
```

```
//-----
```

```
[argout,argin]=argn()
```

```
if argin~=2
```

```
    error("incorrect number of arguments")
```

```
end
```

```
q=q(:)'
```

```
W=inv(eye(Q)-Q)
```

```
z=q*W
```

```
nu1=sum(z)
```

```
mu=nu1
```

```
if argout>=2
```

```
    WQ=W*Q
```

```
    z=z*WQ
```

```
    nu2=2*sum(z)
```

```
    sd=sqrt(nu2-nu1^2+nu1)
```

```
end
```

```
if argout>=3
```

```
    z=z*WQ
```

```
    nu3=6*sum(z)
```

```
    mu3=nu3+3*(1-nu1)*nu2+2*nu1^3-3*nu1^2+nu1
```

```
    sk=mu3/sd^3
```

```
end
```

```
if argout>=4
```

```
    z=z*WQ
```

```
    nu4=24*sum(z)
```

```
    mu4=nu4+6*nu3+nu1*(1-4*nu3)+(6*nu1^2-12*nu1+7)*nu2-3*nu1^4+6*nu1^3-4*nu1^2
```

```
    ku=mu4/sd^4-3
```

```
end
```

```
endfunction
```

```

//-----
function [ARL,SDRL]=rlsyncv(n,L,LCL,UCL,cv0,delta)//to calculate the ARL and
SDRL
//-----
[Q,q]=qsyncv(n,L,LCL,UCL,cv0,delta)
[ARL,SDRL]=momdphase(Q,q)
endfunction

//-----
function F=cdfsyncv(Q,q,pct)//to compute the probability that the run length will be
larger than the percentile
//-----
[argout,argin]=argn()
if argin~=3
    error("incorrect number of arguments")
end
q=q(:)'
Ft1=q*Q^pct
Ft2=sum(Ft1)
F=Ft2
endfunction

//-----
function X=prlsyncv(prcl,mrlini,n,L,LCL,UCL,cv0,delta)//to obtain the percentile with
optimal L, LCL and UCL
//-----
[argout,argin]=argn()
if (argin<7)|(argin>8)
    error("incorrect number of arguments")
end
if (n<=1)|(n~=floor(n))
    error("argument "n" must be an integer >= 2")
end
if (L<=0)|(L~=floor(L))
    error("argument "L" must be an integer >= 1")
end
if argin==7
    delta=1
end
if delta<=0
    error("argument "delta" must be >0")
end

[Q,q]=qsyncv(n,L,LCL,UCL,cv0,delta)

for X=mrlini:500000
    F=1-cdfsyncv(Q,q,X)
    if F>=prcl
        break
    end
end

```

```

end
endfunction

//-----
function X=pcrlsyncv2(pcrl,mrlini,n,L,K,cv0,delta)//to obtain the percentile with optimal
L and K
//-----
[mu,sigma]=musigmaCV(n,cv0)
LCL=mu-K*sigma
UCL=mu+K*sigma
[Q,q]=qsyncv(n,L,LCL,UCL,cv0,delta)

for X=mrlini:500000
    F=1-cdfsyncv(Q,q,X)
    if F>=pcrl
        break
    end
end
endfunction

//-----
function z=optKsyncv(K,n,L,mrl0,cv0)//to obtain the value of K that satisfies the mrl0
constraint
//-----

if (K<=0)
    z=%inf
else
    [mu,sigma]=musigmaCV(n,cv0)
    LCL=mu-K*sigma
    UCL=mu+K*sigma
    [Q,q]=qsyncv(n,L,LCL,UCL,cv0,1)
    probMRL=1-cdfsyncv(Q,q,mrl0)
    z=(probMRL-0.5001)*10
end
endfunction

//-----
function xsol=simplexolve(x0,fun,extra,tol)
//-----
[argout,argin]=argn()
if (argin<2)|(argin>4)
    error("incorrect number of arguments")
end
[j,p]=size(x0)
if j~=1
    error("argument "x0" must be a row vector")
end
if ~exists("extra","local")

```

```

    extra=list()
end
if ~exists("tol","local")
    tol=1e-12
end
if typeof(fun)~="function"
    error("argument "fun" must be a function")
end
if typeof(extra)~="list"
    error("argument "extra" must be a list")
end
if tol<=0
    error("argument "tol" must be > 0")
end
r=1
while %t
    X=simplex(x0,r)
    for i=1:p+1
        f(i)=norm(fun(X(i,:),extra(:)))
    end
    if and(isinf(f))
        r=r/2
    else
        break
    end
end
onesp1=ones(p+1,1)
while %t
    [f,j]=sort(f)
    X=X(j,:)
    fsol=f(p+1)
    xsol=X(p+1,:)
    fw=f(1)
    xw=X(1,:)
    xm=mean(X(2:p+1,:),"r")
    if sqrt(sum((xw-xm).^2))<=tol
        break
    end
    d=xm-xw
    xr=xw+2*d
    fr=norm(fun(xr,extra(:)))
    if fr<fsol
        xe=xr+d
        fe=norm(fun(xe,extra(:)))
        if fe<fr
            f(1)=fe
            X(1,:)=xe
        else
            f(1)=fr
            X(1,:)=xr
        end
    end
else

```

```

xc=xw+0.5*d
fc=norm(fun(xc,extra(:)))
if fc<fsol
    f(1)=fc
    X(1,:)=xc
else
    X=0.5*(X+onesp1*xsol)
    for i=1:p
        f(i)=norm(fun(X(i,:),extra(:)))
    end
end
end
end
endfunction

```

```

//-----
function [L,LCL,UCL,Q05,MRL1,Q95]=optsyncv(n,mrl0,cv0,delta)//to obtain the
optimal chart parameters, and the 5th, 50th and 95th percentiles of the run length
//-----
[argout,argin]=argn()
if argin~=4
    error("incorrect number of arguments")
end
if (n<=1)|(n~=floor(n))
    error("argument "n" must be an integer >= 2")
end
mprintf("delta=%3.2f\n\n",delta)
sol=[]
ii=1
MRL1=%inf
diffPCRmin=%inf

for iL=1:50
    K0=3
    iK=simplexolve(K0,optKsyncv,list(n,iL,mrl0,cv0),tol=1e-6)
    [mu,sigma]=musigmaCV(n,cv0)
    iLCL=mu-iK*sigma
    iUCL=mu+iK*sigma
    iPCR5=pcrlsyncv(0.05,1,n,iL,iLCL,iUCL,cv0,delta)
    iMRL1=pcrlsyncv(0.5,iPCR5,n,iL,iLCL,iUCL,cv0,delta)
    iPCR95=pcrlsyncv(0.95,iMRL1,n,iL,iLCL,iUCL,cv0,delta)
    MRL00=pcrlsyncv(0.5,mrl0-5,n,iL,iLCL,iUCL,cv0,1)
    diffPCR=iPCR95-iPCR5
    mprintf("%2d          %8.6f          %8.6f          %5d          %5d          %5d\n",iL,iLCL,iUCL,iPCR5,iMRL1,iPCR95,MRL00)

    if (iMRL1<MRL1)
        L=iL
        LCL=iLCL
        UCL=iUCL
        Q05=iPCR5
    end
end

```

```

MRL1=iMRL1
Q95=iPCR95
diffPCRmin=diffPCR
else
MRL1=MRL1
diffPCRmin=diffPCRmin
end

if (iMRL1>MRL1)
break
end

end
endfunction

```

```

//-----
function [x,w]=quadlegendre(n,a,b)//to obtain Gauss-Legendre Quadrature
//-----
[argout,argin]=argn()
if (argin<1)|(argin>3)
error("incorrect number of arguments")
end
if argout~=2
error("incorrect number of output arguments")
end
if ~exists("a","local")
a=-1
end
if ~exists("b","local")
b=+1
end
if a>=b
error("argument "a" must be < argument "b"")
end
x=[2.01194093997434522301e-1;
3.94151347077563369897e-1;
5.70972172608538847537e-1;
7.24417731360170047416e-1;
8.48206583410427216201e-1;
9.37273392400705904308e-1;
9.87992518020485428490e-1]
w=[2.02578241925561272881e-1;
1.98431485327111576456e-1;
1.86161000015562211027e-1;
1.66269205816993933553e-1;
1.39570677926154314447e-1;
1.07159220467171935012e-1;
7.03660474881081247100e-2;
3.07532419961172683551e-2]
x=(-x((n-1)/2:-1:1);0;x)*(b-a)+a+b)/2
w=[w((n+1)/2:-1:2);w]*(b-a)/2

```

```
endfunction
```

```
//-----  
function Xe=pcrlsyncve(pcrle,emrlini,n,L,LCL,UCL,cv0,deltamin,deltamax)  
//-----  
[xi,wi]=quadlegendre(15,deltamin,deltamax)  
Xe=0  
for il=1:15  
    xil=xi(il)  
    wil=wi(il)  
    XXe=pcrlsyncv(pcrle,emrlini,n,L,LCL,UCL,cv0,xil)  
    Xe=Xe+XXe.*wil  
end  
Xe=Xe/(deltamax-deltamin)  
endfunction
```

```
//-----  
function  
[L,LCL,UCL,EQ05,EMRL1,EQ95]=optsyncve(n,mrl0,cv0,deltamin,deltamax)//to  
obtain the percentile  
//-----  
[argout,argin]=argn()  
if argin~=5  
    error("incorrect number of arguments")  
end  
if (n<=1)|(n~=floor(n))  
    error("argument \"n\" must be an integer >= 2")  
end  
  
sol=[]  
ii=1  
EMRL1=%inf  
diffEPCRmin=%inf  
  
for iL=1:50  
    K0=3  
    iK=simplexolve(K0,optKsyncv,list(n,iL,mrl0,cv0),tol=1e-6)  
    [mu,sigma]=musigmaCV(n,cv0)  
    iLCL=mu-iK*sigma  
    iUCL=mu+iK*sigma  
    iEPCR5=pcrlsyncve(0.05,1,n,iL,iLCL,iUCL,cv0,deltamin,deltamax)  
    iEMRL1=pcrlsyncve(0.5,1,n,iL,iLCL,iUCL,cv0,deltamin,deltamax)  
    iEPCR95=pcrlsyncve(0.95,1,n,iL,iLCL,iUCL,cv0,deltamin,deltamax)  
    MRL00=pcrlsyncv(0.5,mrl0-5,n,iL,iLCL,iUCL,cv0,1)  
    diffEPCR=iEPCR95-iEPCR5  
    mprintf("%2d      %8.6f      %8.6f      %8.6f      %8.6f      %8.6f  
%5d\n",iL,iLCL,iUCL,iEPCR5,iEMRL1,iEPCR95,MRL00)  
  
    if (iEMRL1<EMRL1)  
        L=iL
```

```

LCL=iLCL
UCL=iUCL
EQ05=iEPCR5
EMRL1=iEMRL1
EQ95=iEPCR95
diffEPCRmin=diffEPCR
elseif (iEMRL1==EMRL1)&(diffEPCR<=diffEPCRmin)
L=iL
LCL=iLCL
UCL=iUCL
EQ05=iEPCR5
EMRL1=iEMRL1
EQ95=iEPCR95
diffEPCRmin=diffEPCR
elseif (iEMRL1>EMRL1)
EMRL1=EMRL1
diffEPCRmin=diffEPCRmin
end

if (iEMRL1>EMRL1)
break
end

end
endfunction

```

```

//-----
function K=optK(n,cv0,UCL)
//-----
[mu,sigma]=musigmaCV(n,cv0)
K=(UCL-mu)/sigma
endfunction

```

```

//-----
function [LCL,UCL]=optCL(K,n,cv0)//to obtain LCL and UCL
//-----
[mu,sigma]=musigmaCV(n,cv0)
LCL=mu-K*sigma
UCL=mu+K*sigma

```

APPENDIX E: COMPUTER PROGRAMMING FOR ARL AND EARL-BASED

DESIGNS OF SHEWHART- γ CHART

```
//-----  
function [mu,sigma]=musigmaCV(n,cv)//to compute the mean and standard deviation of  
the in-control CV  
//-----  
[argout,argin]=argn()  
if argin~=2  
    error("incorrect number of arguments")  
end  
if cv<=0  
    error("argument \"cv\" must be > 0")  
end  
cv2=cv^2  
mu=cv*(1+((cv2-0.25)+((3*cv2^2-cv2/4-7/32)+(15*cv2^3-3*cv2^2/4-7*cv2/32-  
19/128)/n)/n)/n)  
  
sigma=cv*sqrt(((cv2+0.5)+((8*cv2^2+cv2+3/8)+(69*cv2^3+7*cv2^2/2+3*cv2/4+3/16)  
/n)/n)/n)  
endfunction  
  
//-----  
function Y=cdfcv(X,n,cv)//to obtain the cdf of CV  
//-----  
[argout,argin]=argn()  
if argin~=3  
    error("incorrect number of arguments")  
end  
if (n<=0)|(n~=floor(n))  
    error("argument \"n\" must be an integer >= 1")  
end  
if cv<=0  
    error("argument \"cv\" must be > 0")  
end  
Y=zeros(X)  
i=(X>0)  
if or(i)  
    Y(i)=1-cdfstudent(sqrt(n)./X(i),n-1,sqrt(n)/cv)  
end  
endfunction  
  
//-----  
function [ARL,SDRL]=rlshcv(n,K,cv0,delta)//to obtain ARL and SDRL  
//-----  
cv1=delta*cv0  
[mu,sigma]=musigmaCV(n,cv0)  
LCL=mu-K*sigma
```

```

UCL=mu+K*sigma
P=1+cdfcv(LCL,n,cv1)-cdfcv(UCL,n,cv1)
ARL=1/P
SDRL=sqrt(1-P)/P
endfunction

```

```

//-----
function X=idfcv(Y,n,cv)//to obtain idf of CV
//-----
[argout,argin]=argn()
if argin~=3
    error("incorrect number of arguments")
end
if or((Y<=0)|(Y>=1))
    error("all elements of argument "Y" must be in (0,1)")
end
if (n<=0)|(n~=floor(n))
    error("argument "n" must be an integer >= 1")
end
if cv<=0
    error("argument "cv" must be > 0")
end
X=sqrt(n)./idfstudent(1-Y,n-1,sqrt(n)/cv)
endfunction

```

```

//-----
function [LCL,UCL,ARL,SDRL]=optrlshcv(n,cv0,delta)//to find the optimal chart
parameters, ARL and SDRL
//-----

```

```

cv1=delta*cv0
alpha=0.0027
LCL=idfcv(alpha/2,n,cv0)
UCL=idfcv(1-alpha/2,n,cv0)
P=1+cdfcv(LCL,n,cv1)-cdfcv(UCL,n,cv1)
ARL=1/P
SDRL=sqrt(1-P)/P
endfunction

```

```

//-----
function [x,w]=quadlegendre(n,a,b)//to obtain Gauss-Legendre Quadrature
//-----
[argout,argin]=argn()
if (argin<1)|(argin>3)
    error("incorrect number of arguments")
end
if argout~=2
    error("incorrect number of output arguments")
end

```

```

if ~exists("a","local")
    a=-1
end
if ~exists("b","local")
    b=+1
end
if a>=b
    error("argument "a" must be < argument "b'")
end
x=[2.01194093997434522301e-1;
    3.94151347077563369897e-1;
    5.70972172608538847537e-1;
    7.24417731360170047416e-1;
    8.48206583410427216201e-1;
    9.37273392400705904308e-1;
    9.87992518020485428490e-1]
w=[2.02578241925561272881e-1;
    1.98431485327111576456e-1;
    1.86161000015562211027e-1;
    1.66269205816993933553e-1;
    1.39570677926154314447e-1;
    1.07159220467171935012e-1;
    7.03660474881081247100e-2;
    3.07532419961172683551e-2]
x=(-x((n-1)/2:-1:1);0;x)*(b-a)+a+b)/2
w=[w((n+1)/2:-1:2);w]*(b-a)/2
endfunction

//-----
function EARL=earlshcv(n,cv0)//to compute the EARL
//-----
[xi,wi]=quadlegendre(15,1.03,2)
EARL=0
for il=1:15
    xil=xi(il)
    wil=wi(il)
    [LCL,UCL,ARL,SDRL]=rlshcv(n,cv0,xil)
    EARL=EARL+ARL.*wil
end

EARL=EARL/(2-1.03)
endfunction

```

APPENDIX F: COMPUTER PROGRAMMING FOR *MRL* AND *EMRL*-BASED

DESIGNS OF SHEWHART- γ CHART

```
//-----  
function [mu,sigma]=musigmaCV(n,cv)//to compute the mean and standard deviation of  
the in-control sample CV  
//-----  
[argout,argin]=argn()  
if argin~=2  
    error("incorrect number of arguments")  
end  
if (n<=0)|(n~=floor(n))  
    error("argument "n" must be an integer >= 1")  
end  
if cv<=0  
    error("argument "cv" must be > 0")  
end  
cv2=cv^2  
mu=cv*(1+((cv2-0.25)+((3*cv2^2-cv2/4-7/32)+(15*cv2^3-3*cv2^2/4-7*cv2/32-  
19/128)/n)/n)/n)  
sigma=cv*sqrt(((cv2+0.5)+((8*cv2^2+cv2+3/8)+(69*cv2^3+7*cv2^2/2+3*cv2/4+3/16)  
/n)/n)/n)  
endfunction  
  
//-----  
function [LCL,UCL]=ctrlmt(K,n,cv0)//to obtain LCL and UCL  
//-----  
  
    [mu,sigma]=musigmaCV(n,cv0)  
    LCL=mu-K*sigma  
    UCL=mu+K*sigma  
  
endfunction  
  
//-----  
function Y=cdfcv(X,n,cv)//to obtain the cdf of CV  
//-----  
[argout,argin]=argn()  
if argin~=3  
    error("incorrect number of arguments")  
end  
if (n<=0)|(n~=floor(n))  
    error("argument "n" must be an integer >= 1")  
end  
if cv<=0  
    error("argument "cv" must be > 0")  
end  
Y=zeros(X)
```

```

i=(X>0)
if or(i)
  Y(i)=1-cdfstudent(sqrt(n)./X(i),n-1,sqrt(n)/cv)
end
endfunction

//-----
function PRL=pctlXbar(n,K,delta,pctl,mrlini,cv0)//to obtain the percentile
//-----
[argout,argin]=argn()
if argin>6
  error("incorrect number of arguments")
end
if (n<=1)|(n~=floor(n))
  error("argument "n" must be an integer >= 2")
end
if K<=0
  error("argument "L" must be an integer > 0")
end
if delta<0
  error("argument "delta" must be an integer >= 0")
end
if (pctl<=0)|(pctl>=1)
  error("argument "percentile" must be an integer > 0 or < 1")
end
if mrlini<=0
  error("argument "mrlini" must be an integer > 0")
end

[mu,sigma]=musigmaCV(n,cv0)
LCL=mu-K*sigma
UCL=mu+K*sigma
cv1=delta*cv0
P=cdfcv(UCL,n,cv1)-cdfcv(LCL,n,cv1)

for PRL=mrlini:5000
  prob_percen=1-P.^PRL
  if prob_percen>=pctl
    break
  end
end

endfunction

//-----
function dif=minKcv(K,n,mrl0,cv0)
//-----
if K<=0
  dif=%inf
else

```

```

[mu,sigma]=musigmaCV(n,cv0)
LCL=mu-K*sigma
UCL=mu+K*sigma
P=cdfcv(UCL,n,cv0)-cdfcv(LCL,n,cv0)
dif=0.50001-(1-P.^mr10)
end

```

```
endfunction
```

```

//-----
function xsol=simplexolve(x0,fun,extra,tol)
//-----
[argout,argin]=argn()
if (argin<2)|(argin>4)
    error("incorrect number of arguments")
end
[j,p]=size(x0)
if j~=1
    error("argument "x0" must be a row vector")
end
if ~exists("extra","local")
    extra=list()
end
if ~exists("tol","local")
    tol=1e-12
end
if typeof(fun)~="function"
    error("argument "fun" must be a function")
end
if typeof(extra)~="list"
    error("argument "extra" must be a list")
end
if tol<=0
    error("argument "tol" must be > 0")
end
r=1
while %t
    X=simplex(x0,r)
    for i=1:p+1
        f(i)=norm(fun(X(i,:),extra(:)))
    end
    if and(isinf(f))
        r=r/2
    else
        break
    end
end
onesp1=ones(p+1,1)
while %t
    [f,j]=sort(f)
    X=X(j,:)
end

```

```

fsol=f(p+1)
xsol=X(p+1,:)
fw=f(1)
xw=X(1,:)
xm=mean(X(2:p+1,:),"r")
if sqrt(sum((xw-xm).^2))<=tol
    break
end
d=xm-xw
xr=xw+2*d
fr=norm(fun(xr,extra(:)))
if fr<fsol
    xe=xr+d
    fe=norm(fun(xe,extra(:)))
    if fe<fr
        f(1)=fe
        X(1,:)=xe
    else
        f(1)=fr
        X(1,:)=xr
    end
end
else
    xc=xw+0.5*d
    fc=norm(fun(xc,extra(:)))
    if fc<fsol
        f(1)=fc
        X(1,:)=xc
    else
        X=0.5*(X+onesp1*xsol)
        for i=1:p
            f(i)=norm(fun(X(i,:),extra(:)))
        end
    end
end
end
endfunction

```

```

//-----
function [K,Q05,MRL,Q95,MRL0]=opmrl(n,mrl0,delta,cv0)//to obtain the optimal chart
parameters, and the 5th, 50th and 95th percentiles of the run length
//-----
[argout,argin]=argn()

if (n<=1)|(n~=floor(n))
    error("argument "n" must be an integer >= 2")
end
if mrl0<0
    error("argument "mrl0" must be an integer > 0")
end
if delta<0
    error("argument "delta" must be >= 0")
end

```

```

end

K=simplexolve(3,minKcv,list(n,mrl0,cv0),tol=1e-6)
Q05=pctlXbar(n,K,delta,0.05,1,cv0)
MRL=pctlXbar(n,K,delta,0.50,Q05,cv0)
Q95=pctlXbar(n,K,delta,0.95,MRL,cv0)

MRL0=pctlXbar(n,K,1,0.50,1,cv0)

endfunction

//-----
function [x,w]=quadlegendre(n,a,b)//to obtain the Gauss-Legendre Quadrature
//-----
[argout,argin]=argn()
if (argin<1)|(argin>3)
    error("incorrect number of arguments")
end
if argout~=2
    error("incorrect number of output arguments")
end
if ~exists("a","local")
    a=-1
end
if ~exists("b","local")
    b=+1
end
if a>=b
    error("argument "a" must be < argument "b"")
end
x=[2.01194093997434522301e-1;
    3.94151347077563369897e-1;
    5.70972172608538847537e-1;
    7.24417731360170047416e-1;
    8.48206583410427216201e-1;
    9.37273392400705904308e-1;
    9.87992518020485428490e-1]
w=[2.02578241925561272881e-1;
    1.98431485327111576456e-1;
    1.86161000015562211027e-1;
    1.66269205816993933553e-1;
    1.39570677926154314447e-1;
    1.07159220467171935012e-1;
    7.03660474881081247100e-2;
    3.07532419961172683551e-2]
x=(-x((n-1)/2:-1:1);0;x)*(b-a)+a+b)/2
w=[w((n+1)/2:-1:2);w]*(b-a)/2
endfunction

```

```

//-----
function Xe=pctlXe(n,K,deltamin,deltamax,pctl,mrlini,cv0)//to obtain the percentile
//-----
[xi,wi]=quadlegendre(15,deltamin,deltamax)
Xe=0
for il=1:15
    xil=xi(il)
    wil=wi(il)
    XXe=pctlXbar(n,K,xil,pctl,mrlini,cv0)
    Xe=Xe+XXe.*wil
end
Xe=Xe/(deltamax-deltamin)
endfunction

//-----
function [K,QE05,EMRL,QE95]=opmrle(n,mrl0,cv0,deltamin,deltamax)//to obtain the
optimal chart parameters, and the 5th, 50th and 95th percentiles of the run length
//-----
[argout,argin]=argn()
if argin~=5
    error("incorrect number of arguments")
end
if (n<=1)|(n~=floor(n))
    error("argument "n" must be an integer >= 1")
end

K=simplexolve(3,minKcv,list(n,mrl0,cv0),tol=1e-6)
QE05=pctlXe(n,K,deltamin,deltamax,0.05,1,cv0)
EMRL=pctlXe(n,K,deltamin,deltamax,0.50,QE05,cv0)
QE95=pctlXe(n,K,deltamin,deltamax,0.95,EMRL,cv0)

endfunction

```

APPENDIX G: COMPUTER PROGRAMMING FOR ARL AND EARL-BASED

DESIGNS OF EWMA- γ^2 CHART

```
//-----  
function Y=cdffisher(X,m,n,nc)//to obtain the cdf  
//-----  
[argout,argin]=argn()  
if (argin<3)|(argin>4)  
    error("incorrect number of arguments")  
end  
if (m<=0)|(m~=floor(m))  
    error("argument "m" must be an integer >= 1")  
end  
if (n<=0)|(n~=floor(n))  
    error("argument "n" must be an integer >= 1")  
end  
if nargin==3  
    nc=0  
end  
if nc<0  
    error("argument "nc" must be >= 0")  
end  
Y=zeros(X)  
i=(X>0)  
if or(i)  
    Xi=X(i)  
    if nc==0  
        Y(i)=cdf("PQ",Xi,m*ones(Xi),n*ones(Xi))  
    else  
        Y(i)=cdfnc("PQ",Xi,m*ones(Xi),n*ones(Xi),nc*ones(Xi))  
    end  
end  
end  
endfunction  
  
//-----  
function Y=cdfCV2(X,n,cv)//to obtain the cdf of CV  
//-----  
[argout,argin]=argn()  
if nargin~=3  
    error("incorrect number of arguments")  
end  
if (n<=0)|(n~=floor(n))  
    error("argument "n" must be an integer >= 1")  
end  
if cv<=0  
    error("argument "cv" must be > 0")  
end  
Y=zeros(X)  
i=(X>0)  
if or(i)
```

```

    Y(i)=1-cdffisher(n./X(i),1,n-1,n/cv^2)
end
endfunction

```

```

//-----
function [mu,sigma]=musigmaCV2(n,cv)//to compute the mean and standard deviation
of the in-control CV
//-----
[argout,argin]=argn()
if argin~=2
    error("incorrect number of arguments")
end
if (n<=0)|(n~=floor(n))
    error("argument "n" must be an integer >= 1")
end
if cv<=0
    error("argument "cv" must be > 0")
end
cv2=cv^2
mu=cv2*(1-3*cv2/n)
sigma=sqrt(cv2^2*(2/(n-1)+cv2*(4/n+20/(n*(n-1))+75*cv2/n^2))-(mu-cv2)^2)
endfunction

```

```

//-----
function [LCL,UCL]=complmt(n,K,lam,cv0)//to compute LCL and UCL
//-----
[mu0CV2,sigma0CV2]=musigmaCV2(n,cv0)
UCL=mu0CV2+K*sqrt(lam/(2-lam))*sigma0CV2
LCL=mu0CV2
endfunction

```

```

//-----
function [Q,q]=Qewmacv2u(n,K,lam,cv0,cv1)//to calculate the transition probability
matrix and initial probability vector
//-----
[argout,argin]=argn()
if (argin<4)|(argin>5)
    error("incorrect number of arguments")
end
if (n<=1)|(n~=floor(n))
    error("argument "n" must be an integer >= 2")
end
if K<=0
    error("argument "K" must be > 0")
end
if (lam<=0)|(lam>1)
    error("argument "lam" must be in (0,1]")
end
if cv0<=0

```

```

    error("argument "cv0" must be > 0")
end
if nargin==4
    cv1=cv0
end
if cv1<=0
    error("argument "cv1" must be > 0")
end
[mu0CV2,sigma0CV2]=musigmaCV2(n,cv0)
UCL=mu0CV2+K*sqrt(lam/(2-lam))*sigma0CV2
LCL=mu0CV2
p=10
d=(UCL-LCL)/(2*p)
h=[LCL,LCL+d:2*d:UCL-d]
Hj=ones(p+1,1)*h
Hi=Hj'
Q1=(Hj+d-(1-lam)*Hi)/lam
Q2=(Hj-d-(1-lam)*Hi)/lam
Q=cdfCV2(Q1,n,cv1)-cdfCV2(Q2,n,cv1)
Q0=(mu0CV2-(1-lam)*h)/lam
Q(:,1)=cdfCV2(Q0,n,cv1)
q=zeros(p+1,1)
q(1)=1
endfunction

```

```

//-----
function [mu,sd,sk,ku]=momdphase(Q,q)
//-----
[argout,argin]=argn()
if nargin~=2
    error("incorrect number of arguments")
end
q=q(:)'
W=inv(eye(Q)-Q)
z=q*W
nu1=sum(z)
mu=nu1
if argout>=2
    WQ=W*Q
    z=z*WQ
    nu2=2*sum(z)
    sd=sqrt(nu2-nu1^2+nu1)
end
if argout>=3
    z=z*WQ
    nu3=6*sum(z)
    mu3=nu3+3*(1-nu1)*nu2+2*nu1^3-3*nu1^2+nu1
    sk=mu3/sd^3
end
if argout>=4
    z=z*WQ

```

```

nu4=24*sum(z)
mu4=nu4+6*nu3+nu1*(1-4*nu3)+(6*nu1^2-12*nu1+7)*nu2-3*nu1^4+6*nu1^3-
4*nu1^2
ku=mu4/sd^4-3
end
endfunction

```

```

//-----
function f=Kewmacv2u(K,lam,n,cv0)//to obtain f
//-----
if K<=0
    f=%inf
else
    ARL=rlewmacv2u(n,K,lam,cv0,cv0)
    f=(370.4-ARL)/370.4
end
endfunction

```

```

//-----
function ARL=lamewmacv2u(lam,n,cv0,cv1)//to obtain ARL
//-----
if (lam>1)|(lam<0)
    ARL=1e4
else
    global K0
    K=fsolve(K0,list(Kewmacv2u,lam,n,cv0),tol=1e-4)
    ARL0=rlewmacv2u(n,K,lam,cv0,cv0)
    ARL=rlewmacv2u(n,K,lam,cv0,cv1)
    mprintf("lam=%6.4f K=%6.4f ARL=%5.1f ARL0=%5.1f\n",lam,K,ARL,ARL0)
end
endfunction

```

```

//-----
function [lam,K,ARL,SDRL,ARL0]=lamKewmacv2u(n,cv0,cv1)//to calculate the
optimal chart parameters, ARL, SDRL and ARL0
//-----
[argout,argin]=argn()
if argin~=3
    error("incorrect number of arguments")
end
if (n<=1)|(n~=floor(n))
    error("argument \"n\" must be an integer >= 2")
end
if cv0<=0
    error("argument \"cv0\" must be > 0")
end
if cv1<=0
    error("argument \"cv1\" must be > 0")
end
end

```

```

global K0
K0=3
lam0=0.05
[ARL,lam]=optim(list(NDcost,lamewmacv2u,n,cv0,cv1),lam0,"ar",100,100,1e-4)
K=fsolve(K0,list(Kewmacv2u,lam,n,cv0),tol=1e-4)
[ARL,SDRL]=rlewmacv2u(n,K,lam,cv0,cv1)
ARL0=rlewmacv2u(n,K,lam,cv0,cv0)
endfunction

```

```

//-----
function [x,w]=quadlegendre(n,a,b)
//-----
[argout,argin]=argn()
if (argin<1)|(argin>3)
    error("incorrect number of arguments")
end
if argout~=2
    error("incorrect number of output arguments")
end
if ~exists("a","local")
    a=-1
end
if ~exists("b","local")
    b=+1
end
if a>=b
    error("argument "a" must be < argument "b"")
end
x=[2.01194093997434522301e-1;
    3.94151347077563369897e-1;
    5.70972172608538847537e-1;
    7.24417731360170047416e-1;
    8.48206583410427216201e-1;
    9.37273392400705904308e-1;
    9.87992518020485428490e-1]
w=[2.02578241925561272881e-1;
    1.98431485327111576456e-1;
    1.86161000015562211027e-1;
    1.66269205816993933553e-1;
    1.39570677926154314447e-1;
    1.07159220467171935012e-1;
    7.03660474881081247100e-2;
    3.07532419961172683551e-2]
x=(-x((n-1)/2:-1:1);0;x)*(b-a)+a+b)/2
w=[w((n+1)/2:-1:2);w]*(b-a)/2
endfunction

```

```

//-----
function EARL=erlewmacv2u(n,lam,cv0)//to calculate EARL
//-----
[xi,wi]=quadlegendre(15,1.03,2)
EARL=0
for il=1:15
    xil=xi(il)
    wil=wi(il)
    cv1=xil*cv0
    ARL=lamewmacv2u(lam,n,cv0,cv1)
    EARL=EARL+ARL.*wil
end

EARL=EARL/(2-1.03)
endfunction

//-----
function [opK,oplam,opEARL]=optewmacvE(n,cv0)//to calculate the optimal chart
parameters and EARL
//-----
[argout,argin]=argn()
if argin~=2
    error("incorrect number of arguments")
end
if (n<=1)|(n~=floor(n))
    error("argument "n" must be an integer >= 2")
end
if cv0<=0
    error("argument "cv0" must be > 0")
end

opEARL=%inf
global K0
for lam=0.01:0.01:1
    K0=3
    EARL=erlewmacv2u(n,lam,cv0)
    K=fsolve(K0,list(Kewmacv2u,lam,n,cv0),tol=1e-4)
    if EARL<opEARL
        opK=K
        oplam=lam
        opEARL=EARL
    else opEARL=opEARL
end
end
endfunction

```

APPENDIX H: COMPUTER PROGRAMMING FOR MRL AND EMRL-BASED

DESIGNS OF EWMA- γ^2 CHART

```
//-----  
function Y=cdfCV2(X,n,cv)//to obtain cdf of CV  
//-----  
[argout,argin]=argn()  
if nargin~=3  
    error("incorrect number of arguments")  
end  
if (n<=0)|(n~=floor(n))  
    error("argument "n" must be an integer >= 1")  
end  
if cv<=0  
    error("argument "cv" must be > 0")  
end  
Y=zeros(X)  
i=(X>0)  
if or(i)  
    Y(i)=1-cdfstudent(sqrt(n)./sqrt(X(i)),n-1,sqrt(n)/cv)  
end  
endfunction  
  
//-----  
function X=idfCV2(Y,n,cv)//to obtain idf of CV  
//-----  
[argout,argin]=argn()  
if nargin~=3  
    error("incorrect number of arguments")  
end  
if or((Y<=0)|(Y>=1))  
    error("all elements of argument "Y" must be in (0,1)")  
end  
if (n<=0)|(n~=floor(n))  
    error("argument "n" must be an integer >= 1")  
end  
if cv<=0  
    error("argument "cv" must be > 0")  
end  
X=n./(idfstudent(1-Y,n-1,sqrt(n)/cv)).^2  
endfunction  
  
//-----  
function [mu,sigma]=musigmaCV2(n,cv)//to compute the mean and standard deviation  
of the in-control sample CV  
//-----  
[argout,argin]=argn()  
if nargin~=2
```

```

    error("incorrect number of arguments")
end
if (n<=0)|(n~=floor(n))
    error("argument "n" must be an integer >= 1")
end
if cv<=0
    error("argument "cv" must be > 0")
end
cv2=cv^2
mu=cv2*(1-3*cv2/n)
sigma=sqrt(cv2^2*(2/(n-1)+cv2*(4/n+20/(n*(n-1))+75*cv2/n^2))-(mu-cv2)^2)
endfunction

```

```

//-----
function [LCL,UCL]=complmt(n,K,lam,cv0)//to obtain LCL and UCL
//-----
[mu0CV2,sigma0CV2]=musigmaCV2(n,cv0)
UCL=mu0CV2+K*sqrt(lam/(2-lam))*sigma0CV2
LCL=mu0CV2
endfunction

```

```

//-----
function [Q,q]=Qewmacv2u(n,K,lam,cv0,cv1)//to compute the transition probability
matrix and initial probability vector
//-----
[argout,argin]=argn()
if (argin<4)|(argin>5)
    error("incorrect number of arguments")
end
if (n<=1)|(n~=floor(n))
    error("argument "n" must be an integer >= 2")
end
if K<=0
    error("argument "K" must be > 0")
end
if (lam<=0)|(lam>1)
    error("argument "lam" must be in (0,1]")
end
if cv0<=0
    error("argument "cv0" must be > 0")
end
if argin==4
    cv1=cv0
end
if cv1<=0
    error("argument "cv1" must be > 0")
end
[mu0CV2,sigma0CV2]=musigmaCV2(n,cv0)
UCL=mu0CV2+K*sqrt(lam/(2-lam))*sigma0CV2
LCL=mu0CV2

```

```

p=100
d=(UCL-LCL)/(2*p)
h=[LCL,LCL+d:2*d:UCL-d]
Hj=ones(p+1,1)*h
Hi=Hj'
Q1=(Hj+d-(1-lam)*Hi)/lam
Q2=(Hj-d-(1-lam)*Hi)/lam
Q=cdfCV2(Q1,n,cv1)-cdfCV2(Q2,n,cv1)
Q0=(mu0CV2-(1-lam)*h)/lam
Q(:,1)=cdfCV2(Q0,n,cv1)
q=zeros(p+1,1)
q(1)=1
endfunction

//-----
function MRL=rlewmacv2u(n,K,lam,mrlini,mrl0,cv0,cv1)//to find MRL
//-----
[argout,argin]=argn()
if (argin<6)|(argin>7)
    error("incorrect number of arguments")
end
if (n<=1)|(n~=floor(n))
    error("argument "n" must be an integer >= 2")
end
if K<=0
    error("argument "K" must be > 0")
end
if (lam<=0)|(lam>1)
    error("argument "lam" must be in (0,1]")
end
if cv0<=0
    error("argument "cv0" must be > 0")
end
if argin==6
    cv1=cv0
elseif cv1<=0
    error("argument "cv1" must be > 0")
end
if mrlini<=0
    error("argument "mrlini" must be > 0")
end
[Q,q]=Qewmacv2u(n,K,lam,cv0,cv1)
q=q(:)'
for MRL=mrlini:mrl0+5
    W=eye(Q)-Q^MRL
    z=q*W
    probmed=sum(z)
    if probmed>=0.5
        break
    end
end
end

```

endfunction

```
//-----  
function percentile=prlewmacv2u(n,K,lam,percini,probperc,cv0,cv1)//to calculate the  
percentile  
//-----  
[argout,argin]=argn()  
if (argin<6)|(argin>7)  
    error("incorrect number of arguments")  
end  
if (n<=1)|(n~=floor(n))  
    error("argument \"n\" must be an integer >= 2")  
end  
if K<=0  
    error("argument \"K\" must be > 0")  
end  
if (lam<=0)|(lam>1)  
    error("argument \"lam\" must be in (0,1]")  
end  
if cv0<=0  
    error("argument \"cv0\" must be > 0")  
end  
if argin==6  
    cv1=cv0  
elseif cv1<=0  
    error("argument \"cv1\" must be > 0")  
end  
if percini<=0  
    error("argument \"percini\" must be > 0")  
end  
[Q,q]=Qewmacv2u(n,K,lam,cv0,cv1)  
q=q(:)  
for percentile=percini:5000  
    W=eye(Q)-Q^percentile  
    z=q*W  
    probmed=sum(z)  
    if probmed>=probperc  
        break  
    end  
end  
end  
endfunction
```

```
//-----  
function f=Kewmacv2u(K,lam,n,mrl0,cv0)  
//-----  
if K<=0  
    f=%inf  
else  
    [Q,q]=Qewmacv2u(n,K,lam,cv0,cv0)  
    q=q(:)
```

```

W=eye(Q)-Q^mrl0
z=q*W
f=0.5001-sum(z)
end
endfunction

```

```

//-----
function mrl=lamewmacv2u(lam,n,mrl0,cv0,cv1)//to find MRL
//-----
if (lam<=0)|(lam>1)
    mrl=%inf
else
    global K0
    K=fsolve(K0,list(Kewmacv2u,lam,n,mrl0,cv0),tol=1e-4)
    mrl=rlewmacv2u(n,K,lam,1,mrl0,cv0,cv1)
    if mrl<0
        mrl=%inf
    end
    mprintf("lam=%6.4f K=%6.4f mrl=%3d mrl0=%4d\n",[lam,K,mrl,mrl0])
end
endfunction

```

```

//-----
function [lam,K,PRL5,MRL,PRL95,MRL0]=lamKewmacv2u(n,mrl0,cv0,cv1)//to
calculate the optimal chart parameters, and the 5th, 50th and 95th percentiles of the run
length
//-----
[argout,argin]=argn()
if argin~=4
    error("incorrect number of arguments")
end
if (n<=1)|(n~=floor(n))
    error("argument "n" must be an integer >= 2")
end
if cv0<=0
    error("argument "cv0" must be > 0")
end
if cv1<=0
    error("argument "cv1" must be > 0")
end
if mrl0<0
    error("argument "mrl0" must be >0")
end
global K0
K0=3
lam0=0.05
lam=neldermead(lam0,lamewmacv2u,list(n,mrl0,cv0,cv1),tol=1e-4,opt="min")
K=fsolve(K0,list(Kewmacv2u,lam,n,mrl0,cv0),tol=1e-4)
PRL5=prlewmacv2u(n,K,lam,1,0.05,cv0,cv1)
MRL=rlewmacv2u(n,K,lam,PRL5,mrl0,cv0,cv1)

```

```

PRL95=prlewmacv2u(n,K,lam,MRL,0.95,cv0,cv1)
MRL0=rlewmacv2u(n,K,lam,mrl0-5,mrl0,cv0,cv0)
mprintf("%5.3f,          %5.3f)          (%2d,          %3d,          %4d,
%1d)%4d\n",[lam,K,PRL5,MRL,PRL95,n,MRL0])
endfunction

```

```

//-----
function [x,w]=quadlegendre(n,a,b)//to obtain Gauss-Legendre Quadrature
//-----

```

```

[argout,argin]=argn()
if (argin<1)|(argin>3)
    error("incorrect number of arguments")
end
if argout~=2
    error("incorrect number of output arguments")
end
if ~exists("a","local")
    a=-1
end
if ~exists("b","local")
    b=+1
end
if a>=b
    error("argument "a" must be < argument "b"")
end
x=[2.01194093997434522301e-1;
3.94151347077563369897e-1;
5.70972172608538847537e-1;
7.24417731360170047416e-1;
8.48206583410427216201e-1;
9.37273392400705904308e-1;
9.87992518020485428490e-1]
w=[2.02578241925561272881e-1;
1.98431485327111576456e-1;
1.86161000015562211027e-1;
1.66269205816993933553e-1;
1.39570677926154314447e-1;
1.07159220467171935012e-1;
7.03660474881081247100e-2;
3.07532419961172683551e-2]
x=(-x((n-1)/2:-1:1);0;x)*(b-a)+a+b)/2
w=[w((n+1)/2:-1:2);w]*(b-a)/2
endfunction

```

```

//-----
function eprl=eprlewmacv2u(n,K,lam,percini,probperc,cv0,deltamin,deltamax)//to find
EPRL
//-----

```

```

[xi,wi]=quadlegendre(15,deltamin,deltamax)
eprl=0

```

```

for il=1:15
    xil=xi(il)
    wil=wi(il)
    cv1=xil*cv0
    prl=prlewmacv2u(n,K,lam,percini,probperc,cv0,cv1)
    eprl=eprl+prl.*wil
end
eprl=eprl/(deltamax-deltamin)
endfunction

//-----
function EMRL=emrlewmacv2u(deltamin,deltamax,n,K,lam,cv0,mrl0)//to find EMRL
//-----
[xi,wi]=quadlegendre(15,deltamin,deltamax)
EMRL=0
for il=1:15
    xil=xi(il)
    wil=wi(il)
    cv1=xil*cv0
    MRL=rlewmacv2u(n,K,lam,1,mrl0,cv0,cv1)
    EMRL=EMRL+MRL.*wil
end
EMRL=EMRL/(deltamax-deltamin)
endfunction

//-----
function xsol=simplexolve(x0,fun,extra,tol)//to obtain K
//-----
[argout,argin]=argn()
if (argin<2)|(argin>4)
    error("incorrect number of arguments")
end
[j,p]=size(x0)
if j~=1
    error("argument "x0" must be a row vector")
end
if ~exists("extra","local")
    extra=list()
end
if ~exists("tol","local")
    tol=1e-12
end
if typeof(fun)~="function"
    error("argument "fun" must be a function")
end
if typeof(extra)~="list"
    error("argument "extra" must be a list")
end
if tol<=0
    error("argument "tol" must be > 0")

```

```

end
r=1
while %t
  X=simplex(x0,r)
  for i=1:p+1
    f(i)=norm(fun(X(i,:),extra(:)))
  end
  if and(isinf(f))
    r=r/2
  else
    break
  end
end
onesp1=ones(p+1,1)
while %t
  [f,j]=sort(f)
  X=X(j,:)
  fsol=f(p+1)
  xsol=X(p+1,:)
  fw=f(1)
  xw=X(1,:)
  xm=mean(X(2:p+1,:),"r")
  if sqrt(sum((xw-xm).^2))<=tol
    break
  end
  d=xm-xw
  xr=xw+2*d
  fr=norm(fun(xr,extra(:)))
  if fr<fsol
    xe=xr+d
    fe=norm(fun(xe,extra(:)))
    if fe<fr
      f(1)=fe
      X(1,:)=xe
    else
      f(1)=fr
      X(1,:)=xr
    end
  else
    xc=xw+0.5*d
    fc=norm(fun(xc,extra(:)))
    if fc<fsol
      f(1)=fc
      X(1,:)=xc
    else
      X=0.5*(X+onesp1*xsol)
      for i=1:p
        f(i)=norm(fun(X(i,:),extra(:)))
      end
    end
  end
end
end
end
end

```

```

endfunction

//-----
function EMRL=lamemrlewmacv2u(lam,deltamin,deltamax,n,mrl0,cv0)//to find EMRL
//-----
if (lam<=0)|(lam>1)
    EMRL=1e4
else
    global K0
    K=simplexolve(K0,Kewmacv2u,list(lam,n,mrl0,cv0),tol=1e-4)
    //K=fsolve(K0,list(Kewmacv2u,lam,n,mrl0,cv0),tol=1e-4)
    MRL0=rlewmacv2u(n,K,lam,mrl0-5,mrl0,cv0,cv0)
    EMRL=emrlewmacv2u(deltamin,deltamax,n,K,lam,cv0)
end
endfunction

//-----
function
[lam,K,QE05,EMRL,QE95,MRL0]=emrLEWMAxoptimecv2u(deltamin,deltamax,n,mrl0
,cv0)//to calculate the optimal chart parameters, and the 5th, 50th and 95th percentiles of
the run length
//-----
[argout,argin]=argn()
if argin~=5
    error("incorrect number of arguments")
end
if (n<=0)|(n~=floor(n))
    error("argument "n" must be an integer >= 1")
end
if mrl0<0
    error("argument "mrl0" must be > 0")
end
if cv0<=0
    error("argument "cv0" must be >0")
end
global K0
K0=3
lam0=0.05
lam=neldermead(lam0,lamemrlewmacv2u,list(deltamin,deltamax,n,mrl0,cv0),tol=1e-
4,opt="min")
K=simplexolve(K0,Kewmacv2u,list(lam,n,mrl0,cv0),tol=1e-4)
//K=fsolve(K0,list(Kewmacv2u,lam,n,mrl0,cv0),tol=1e-4)
MRL0=rlewmacv2u(n,K,lam,mrl0-5,mrl0,cv0,cv0)
QE05=eprlewmacv2u(n,K,lam,1,0.05,cv0,deltamin,deltamax)
EMRL=emrlewmacv2u(deltamin,deltamax,n,K,lam,cv0)
QE95=eprlewmacv2u(n,K,lam,1,0.95,cv0,deltamin,deltamax)
mprintf("(%6.4f,      %6.4f)      (%6.2f      %6.2f      %6.2f      %6.2f      %6.2f      %1d)
%4d\n",[lam,K,QE05,EMRL,QE95,n,MRL0])
endfunction

```